ROYAL SOCIETY
—— OF ——
CHEMISTRY

The
Analyst

A monthly international journal dealing with all branches of the theory and practice of

analytical chemistry, including instrumentation and sensors, and physical, biochemical,

clinical, pharmaceutical, biological, environmental, automatic and computer-based methods

The Analyst

The Analytical Journal of The Royal Society of Chemistry

Information for Authors

Full details of how to submit material for publication in *The Analyst* are given in the Instructions to Authors in the January issue. Separate copies are available on request.

The Analyst publishes papers on all aspects of the theory and practice of analytical chemistry, fundamental and applied, inorganic and organic, including chemical, physical, biochemical, clinical, pharmaceutical, biological, environmental, automatic and computer-based methods. Papers on new approaches to existing methods, new techniques and instrumentation, detectors and sensors, and new areas of application with due attention to overcoming limitations and to underlying principles are all equally welcome. There is no page charge.

The following types of papers will be considered:

Full papers, describing original work.

Short papers: the criteria regarding originality are the same as for full papers, but short papers generally report less extensive investigations or are of limited breadth of subject matter

Communications, which must be on an urgent matter and be of obvious scientific importance. Rapidity of publication is enhanced if diagrams are omitted, but tables and formulae can be included. Communications receive priority and are usually published within 5–8 weeks of receipt. They are intended for brief descriptions of work that has progressed to a stage at which it is likely to be valuable to workers faced with similar problems. A fuller paper may be offered subsequently, if justified by later work.

Reviews, which must be a critical evaluation of the existing state of knowledge on a particular facet of analytical chemistry.

Every paper (except Communications) will be submitted to at least two referees, by whose advice the Editorial Board of *The Analyst* will be guided as to its acceptance or rejection. Papers that are accepted must not be published elsewhere except by permission. Submission of a manuscript will be regarded as an undertaking that the same material is not being considered for publication by another journal.

Regional Advisory Editors. For the benefit of potential contributors outside the United Kingdom, a Panel of Regional Advisory Editors exists. Requests for help or advice on any matter related to the preparation of papers and their submission for publication in *The Analyst* can be sent to the nearest member of the Panel. Currently serving Regional Advisory Editors are listed in each issue of *The Analyst.*

Manuscripts (three copies typed in double spacing) should be addressed to:
The Editor, *The Analyst,*
Royal Society of Chemistry,
Thomas Graham House,
Science Park,
Milton Road,
CAMBRIDGE CB4 4WF, UK

Particular attention should be paid to the use of standard methods of literature citation, including the journal abbreviations defined in Chemical Abstracts Service Source Index. Wherever possible, the nomenclature employed should follow IUPAC recommendations, and units and symbols should be those associated with SI.

All queries relating to the presentation and submission of papers, and any correspondence regarding accepted papers and proofs, should be directed to the Editor, *The Analyst* (address as above). Members of the Analytical Editorial Board (who may be contacted directly or via the Editorial Office) would welcome comments, suggestions and advice on general policy matters concerning *The Analyst.*

Fifty reprints of each published contribution are supplied free of charge, and further copies can be purchased.

Editorial

Conference Report:
1989 Pittsburgh Conference and Exposition on Analytical Chemistry and Applied Spectroscopy
March 6th–10th 1989, Atlanta, Georgia, USA

The Pittsburgh Conference, or to give the full title "The Pittsburgh Conference and Exposition on Analytical Chemistry and Applied Spectroscopy" (Pittcon), which celebrated its 40th birthday in March 1989, is truly among the premier international meetings for the analytical chemist. In recent years it has been recognised by the Royal Society of Chemistry as one of the "key" meeting points for academics, industrial and instrumentation scientists and efforts have been made to have a strong presence there, to "fly the flag" of RSC Analytical Chemistry. In my role as United States Regional advisory Editor for *The Analyst*, it provides an opportunity to spend time with the UK editorial staff and also those from the RSC Information Services who nobly staff the "RSC booth" for four long days (and long they certainly are!). This year Atlanta, Georgia (the conference last met in Pittsburgh more than 20 years ago), provided an excellent venue to initiate Janet Dean, Editor of *The Analyst,* into the "delights" of contemporary US life. She had able tuition in this respect from Judith Egan, Editorial Manager of the Analytical Journals. They and other RSC staff hosted the highly regarded "RSC Reception" at which more than 250 guests and friends spent a very pleasant evening. Many now rate this as one of the "highlight" events of the conference and it is certainly an excellent advertisement for the Society!

In many ways, the Pittsburgh Conference typifies the average British view of US scientific events; certainly it is a gigantic enterprise and no place for the faint-hearted or those in awe of crowds! However, to mitigate the sheer size, it is universally agreed that this is among the best organised exhibition/conference event anywhere (it really has to be so!). It is organised by volunteers, consisting of members of the two co-sponsoring groups, The Society for Analytical Chemists of Pittsburgh (SACP) and the Spectroscopy Society of Pittsburgh (SSP). Many other organisations stand in awe of their accumulated experience. Pittcon is many different things to different people. It is *The* analytical instrumentation show having in 1989, 850 exhibitors and 2556 booth spaces. The wise know the frustration in attempting to contact people in the instrumentation business in the weeks before the meeting as they work, often frenetically, to prepare for the show, particularly when new instruments are due to be unveiled. It regularly draws the highest number of conferees (26 741 this year) for any chemistry meeting in the USA and in recent years it has become increasingly recognised for technical presentations (1324 papers and 210 posters in 1989). While many papers are presented by instrument manufacturers, the scientific committee takes care to minimise the commercial nature of these and to ensure sound scientific content; this is often, although not always, successful. The quality of the technical sessions was emphasised this year by no less than 37 "Invited Speaker" symposia. Of course, the sheer magnitude of the programme can be daunting. At one time this year there were 17 simultaneous technical sessions in progress. The conferee must learn to be very selective, to attend just those papers that are of major interest, and most importantly to plan their sequence so that they can be reached in time (the Georgia World Conference Center covers a total of 15 acres).

There is always a range of high-quality panel discussions, special seminars, etc., encompassing topics of wider interest. This year the annual ACS-sponsored conference breakfast discussion featured the Biopharmaceutical Industry in the 1990s. A special luncheon seminar and discussion held in collaboration with the US National Science Foundation (NSF) focused on the continuing under-representation of women in the science and engineering disciplines. The importance of a wider outreach was stressed as the week of the Conference was made "Science Week" in Atlanta and the state of Georgia and days were set aside as "Science Teachers" and "Science Students" days at the secondary school level. The conference always has good media news coverage wherever it is located. The conference also provides a flourishing "employment agency," to match job candidates and employer representatives. This year there were more than 850 each of candidates and openings.

There can be little doubt of the international stature of Pittcon. This year there were 2518 overseas visitors. In addition to technical participants, many of these were associated with exhibitors from instrument companies. For some years, the British Consulate-General has co-ordinated exhibition facilities for smaller to medium sized British companies who wish to exhibit at Pittcon; this year some 20 such availed themselves of this facility and formed a "UK aisle" in the Exhibition Hall. In contrast, some UK companies are now firmly established in the US marketplace with subsidiary enterprises or major North American marketing commitments. Pittcon is certainly the strongest opportunity for them in the analytical chemical market place.

There was a time when academic analytical chemists tended to downrate Pittcon as merely an instrument show. Today, it is much more than this. We encourage our graduate (postgraduate) students to attend and often to present papers. For them the experience of the conference is extremely valuable. They can emulate their academic mentors and "cover" the exhibition, wishing for all of the instrumentation that is unlikely ever to find its way into academic laboratories for purely economic reasons. Manufacturers know however that this is their next generation of customers and advisedly recognise them as such! Pittcon is now one of the best "advanced academic teaching tools that exist." Academic analytical chemistry is in a "holding pattern" in colleges and universities during Pittcon, with a high proportion of faculty members and staff at the meeting. However, the return on the educational investment involved is very high.

To pick out specific features of the instrumentation exhibition as being of exceptional general interest is virtually impossible; individuals must be biased by their own interests. Some major companies have exhibits covering 40–50 booth spaces, but sometimes the small entrepreneur can create as much personal excitement. To me the areas of major interest ranged from the introduction of a major GC - microwave plasma emission spectral detector system and a viable HPLC/FID instrument (by a UK company), to the rapidly developing field of capillary zone electrophoresis; and also from the increased sophistication and availability of LC - MS

instrumentation to the burgeoning fields of bioanalysis and biotechnology. One thing is certain, there is something for everyone and usually in a competitive sense as well.

Scientific meetings and symposia of all kinds and sizes are a part of life in our expansive discipline. They provide a forum for broadening our contacts in all aspects of science; meetings such as Pittcon take a large amount of energy just to survive, but the effort is definitely worthwhile. To those in Europe who have not experienced it, I have this advice: if you ever have the opportunity to attend Pittcon, take it!

Peter C. Uden
US Regional Advisory Editor
University of Massachusetts
Amherst, MA, USA

Denuder Tubes for Sampling of Gaseous Species

A Review

Zulfiqur Ali, C. L. Paul Thomas and John F. Alder
Department of Instrumentation and Analytical Science, UMIST, P.O. Box 88, Manchester M60 1QD, UK

Summary of Contents

Keywords: *Denuder tubes; atmospheric acidity; environmental monitoring; gaseous sampling*

Introduction

Denuder tubes were first considered on a theoretical basis in the 1890s during a study on the diffusion of ions into gases.[1] Later, in the 1930s, studies of atmospheric condensation nuclei revealed significant particulate losses from gas flows in sample pipelines and, consequently, the diffusional removal of particulates in both cylindrical and rectangular section pipelines was considered.[2] Subsequent measurements of the diffusional properties of micro-particulates were made with multi-tubular assemblies and diffusion batteries, consisting of several flat plates with narrow gaps between them.[3] In an appendix to this work, a mathematical treatment was presented of the diffusion from a stream flowing through a thin rectangular tube.

Diffusion measurements based on these methods continued, and in 1949 Gormley and Kennedy[4] derived a solution describing diffusion from a stream flowing through a cylindrical tube, originally proposed by Townsend.[1] Diffusion coefficients for sulphur trioxide and ammonia were determined by trapping these gases chemically in a glass tube lined with oleic acid or copper sulphate impregnated paper, respectively.[5] Laminar flow subduction zones were incorporated at the inlet to these devices, and the diffusion coefficients of sulphur trioxide and ammonia were measured by determining the mixing ratios of these gases within the tubing.

A study undertaken in the early 1960s was concerned with the effects of fluorides in the atmosphere.[6] An annular unit was used to separate gaseous fluoride species from their particulate counterparts. The unit consisted of three concentric cylinders coated with sodium hydrogen carbonate or aluminium. No theoretical basis was given for this design, and annular systems were not studied again until the early 1980s. Following on from this, an analytical technique using an "aerosol-passing gas adsorber" was described.[7] Fabricated from a series of glass tubes lined with potassium hydroxide and magnesium perchlorate, it was employed to remove water vapour from an aerosol sampling system for a hydrogen flame chemiluminescence detector used for aqueous sulphate ion determination. The removal of sulphur dioxide from a laminar flow gas stream by a diffusion denuder coated with lead(IV) oxide was shown to conform to the Gormley - Kennedy equation.[8] Sulphur dioxide at a concentration of 1.5 p.p.m. in air was passed through the tube, which was then cut into 0.5-in sections and analysed radiochemically. The diffusion coefficients for sulphur dioxide at 1 atm were found to be 0.117, 0.132 and 0.146 cm^2 s^{-1} at 0, 20 and 37 °C, respectively. Lead-based sulphur dioxide denuders were then used to remove sulphur-containing gaseous interferences quantitatively for measurements of the sulphate ion content in airborne aerosols.[9–12] The use of a heated sample tube to effect thermochemical changes in incoming sampled ammonium sulphates was first reported in 1978.[12] Other gases, notably ammonia, were removed from environmental gas samples by arrays of denuder systems,[13] which allowed the use of higher gas flow-rates than previously encountered. However, it was not until 1979 that the role of the denuder tube was reversed and it was used as a gas collection device rather than an instrument to denude a sample of certain gaseous components.[14] In this work, Ferm achieved a detection limit of 0.4 nmol m^{-3} of ammonia in air (0.01 p.p.b.) after a 24-h sample period. Interference from particulate ammonium salts at "extremely high" (400 nmol m^{-3}) concentrations was of the same order as the detection limit.

Description of Operation

For a denuder tube to function, a series of criteria must be met.

The removal of the analyte must have no global effect on the sample, the gas flow must be stable and laminar and the viscosity and temperature distribution within the gas flow must be homogeneous. Any axial diffusion of the sampled gas must be insignificant in comparison to the sample flow, and the collection surfaces should behave as infinitely large and perfect sinks towards the analyte. Adsorbate species should be neither created nor destroyed in the gas phase within the denuder tube. Schematic diagrams of the two types of denuder unit in common use are shown in Fig. 1.

Air is drawn through either the centre of the tube, or the annulus, at a rate such that its flow is laminar [Reynold's number $(Re) < 2100$].[15] Laminar flow is achieved a short distance from the inlet. In a tube of diameter d, the length of this subduction zone can be calculated as follows:

$$l = 0.07dRe \quad \ldots \quad \ldots \quad \ldots \quad (1)$$

where l is the length of the laminar flow subduction zone.

The establishment of laminar flow is important as this ensures that radial mixing can only take place via diffusion-based processes. It is essential that areas of collection surfaces where turbulent flow exists, and particulates therefore impinge on, do not contribute towards the analysis. Often a PTFE former or inlet is used to establish laminar flow prior to the collection surfaces. Molecular species diffuse through the laminar flow to the active collection surfaces, where they undergo irreversible adsorption or chemical bonding and are removed from the gas stream. Particulates with their much lower diffusion velocities cannot migrate to the walls during their residence time within the unit and hence, provided the above conditions are met, do not contribute to the final measurement. The deposition of particulates as a result of gravitational sedimentation would disrupt the performance of the unit. This problem is negated by using the tube in a vertical orientation, and employing cyclones and virtual impactors to remove large pieces of airborne detritus from the sample also ensures the effectiveness of this method.

Theory

Cylindrical Systems

The behaviour of trace amounts of gases in a denuder system can be described in terms of Fickian diffusion. The expression in common usage was derived by Gormley and Kennedy.[4] For a cylindrical denuder, their solution can be summarised as follows.

For a laminar flow, the velocity of the gas at any point in the denuder tube (Fig. 1) is given by

$$V = F(R^2 - r^2)/2\pi R^4 \quad \ldots \quad \ldots \quad \ldots \quad (2)$$
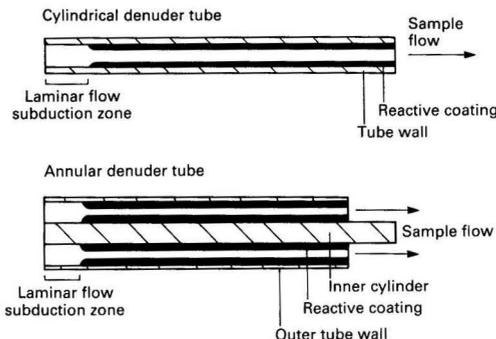
Fig. 1. Schematic diagrams of the cylindrical and annular denuder tubes

where V is the velocity of the gas flow at a radial displacement r from the axis, F is the sampled gas flow-rate and R is the radius of the tube.

The diffusive motion of the gaseous analyte within the unit is resolved into its cartesian components. The equations of motion that describe the transport of analyte parallel to the laminar flow and the denuder axis contain the appropriate correction:

$$dP_aD/dx = -P_au \quad \ldots \quad \ldots \quad \ldots \quad (3)$$
$$dP_aD/dy = -P_av \quad \ldots \quad \ldots \quad \ldots \quad (4)$$
$$dP_aD/dz = -P_a(w - V) \quad \ldots \quad \ldots \quad (5)$$

where D is the diffusion coefficient of the analyte, P_a is the partial pressure of the analyte and u, v and w are the diffusive velocities of the analyte with respect to the x, y and z axes, respectively.

The parameters u, v and w are then substituted into the continuity equation

$$\frac{d}{dx}(P_au) + \frac{d}{dy}(P_av) + \frac{d}{dz}(P_aw) = 0 \quad \ldots \quad \ldots \quad (6)$$

giving

$$\nabla P_a - \frac{1}{D} \cdot \frac{d}{dz}(P_aV) = 0 \quad \ldots \quad \ldots \quad \ldots \quad (7)$$

where

$$\nabla = \frac{du}{dx} + \frac{dv}{dy} + \frac{dw}{dz}$$

A transfer from cartesian to cylindrical co-ordinates provides the following expression:

$$\frac{1}{r} \cdot \frac{d}{dr}\left(r\frac{dP_a}{dr}\right) + \frac{1}{r^2} \cdot \frac{d^2P_a}{d\theta^2} + \frac{d^2P_a}{dz^2} - \frac{1}{D} \cdot \frac{d}{dz}(P_aV) = 0 \quad \ldots \quad (8)$$

where θ is the angle of displacement from the x axis in the x - y plane.

It is then assumed that $dP_a/d\theta = 0$ for reasons of symmetry and $d^2P_a/dz^2 = 0$ for $V \gg w$. The resulting equation forms the basis of the Gormley - Kennedy solution

$$\frac{d^2P_a}{dr^2} + \frac{1}{r} \frac{dP_a}{dr} - \frac{2F}{\pi R^4D} \cdot (R^2 - r^2) \cdot \frac{dP_a}{dz} = 0 \quad \ldots \quad (9)$$

for which the boundary condition is set such that

$$P_{a|R} = 0 \quad \ldots \quad \ldots \quad \ldots \quad \ldots \quad (10)$$

The mean radial concentration $\bar{c}$ at a length Z along the tube axis is proportional to

$$_0\!\int^R P_a2\pi Vr.dr \quad \ldots \quad \ldots \quad \ldots \quad (11)$$

The mixing ratio of the analyte at length Z can be expressed as

$$\bar{c}/c_0 = [4/(R^4P_{a0})] \,_0\!\int^R P_a(R^2 - r^2)r.dr \quad \ldots \quad (12)$$

where P_a is the solution to equation (9), P_{a0} the ambient vapour pressure of the analyte, c_0 the ambient concentration of the analyte and $\bar{c}$ the mean radial concentration of the analyte. Gormley and Kennedy provided the solution to equation (12) as a series:

$$\bar{c}/c_0 = 0.819\exp(-7.314\Delta_c) + 0.0975\exp(-44.6\Delta_c) + 0.0325\exp(-212\Delta_c) \quad \ldots \quad \ldots \quad (13)$$

where, at standard temperature and pressure,

$$\Delta_c = \pi D_0Z/2F \quad \ldots \quad \ldots \quad \ldots \quad (14)$$

(subscript c refers to the cylindrical system). For most sampling applications, where $\Delta_c \leqslant 0.05$, only the first term of this series will be significant and equation (13) can be approximated to

$$\bar{c}/c_0 = 0.82\exp(-7.3\Delta_c) \quad \ldots \quad \ldots \quad (15)$$

From these expressions it can be seen that the collection efficiency of a denuder tube increases with length, and also

with increasing values for the diffusion coefficient of the analyte. The collection efficiency is enhanced further by decreasing the radius of the tube and reducing the mean axial velocity of the sampled gas. Davies[16] has indicated that low values for the kinematic viscosity of the sample also lead to increased sampling efficiency; this is underlined further by Ferm's[14] treatment of the Gormley - Kennedy solution. The performance of a denuder tube can be seen to be affected by variables such as pressure, temperature and relative humidity. Such detail is often not reported in experimental studies, and no mention has been made of procedures that enable data obtained under different environmental conditions to be corrected. In some situations (*i.e.*, at high altitude) these factors will become significant.

Diffusion Coefficients

A number of studies involved analysis of the contents of segmented denuder tubes to determine the diffusion coefficient of the analyte, see Fig. 2. The sampling efficiency of each segment is defined by

$$E = \text{number of moles adsorbed/} \\ \text{number of moles sampled} \quad .. \quad .. \quad (16)$$

For the first segment

$$E = a/c \quad .. \quad .. \quad .. \quad .. \quad (17)$$

and for the second segment

$$E = b/(c - a) \quad .. \quad .. \quad .. \quad (18)$$

where c is the number of moles sampled, a the number of moles adsorbed in the first segment and b the number of moles adsorbed in the second segment. Combining equations (17) and (18) gives

$$E = (a - b)/a \quad .. \quad .. \quad .. \quad (19)$$

hence

$$c/c_0 = b/a \quad .. \quad .. \quad .. \quad (20)$$

Repeating this analysis for further segments yields a series of values for Δ_c with increasing values of Z. Then a plot of Δ_c against Z is a straight line of slope $\pi D_0/2F$. Hence the diffusion coefficient D_0 can be determined. The values obtained for the diffusion coefficient then allow elucidation of the analyte form in the sampled gas. Hence the diffusive mechanism of the sampling process can be verified, and information about any hydration or other molecular aggregation of the analyte obtained.

Annular Systems

The Gormley - Kennedy solution discussed here [equation (13)] does not apply to annular systems. Possanzini *et al.*[17] proposed an empirically modified form:

$$c/c_0 = A\exp(-\alpha\Delta_a) \quad .. \quad .. \quad (21)$$

where A and α are experimentally determined constants.
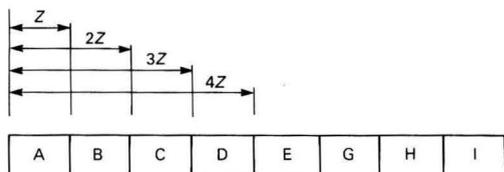
Fig. 2. Schematic diagram showing the denuder divided into a series of equal sections for the measurement of diffusion coefficients. $\bar{c}/c_0 = b/a = c/b = \ldots . = i/h$, where a = number of moles in section A, b = number of moles in section B, etc. Finally, $\bar{c}/c_0 = (i + h + g + e)/(a + b + c + d)$ and $\bar{c}/c_0 = 0.82\exp(-7.3\Delta_c)$, $\Delta_c = D_0\pi Z/2F$

The form of Δ_a (subscript a refers to the annular system) was also modified to incorporate the equivalent diameter of the annular channel. This was defined as four times the hydraulic radius, which in its turn was defined as the ratio of the cross-sectional area of the annular channel to its perimeter. The final form of Δ_a was given as

$$\Delta_a = \frac{\pi D_0 Z}{2F}\left(\frac{d_1 + d_2}{d_1 - d_2}\right) \quad .. \quad .. \quad (22)$$

where d_1 is the internal diameter of the external cylinder and d_2 the external diameter of the internal cylinder.

Values for A and α were calculated by determining Δ_a and the mixing ratio for three denuder tubes of different sizes, hence giving the following expression:

$$\bar{c}/c_0 = 0.82 \pm 0.1\exp[(-11.27 \pm 0.61)\Delta_a] \quad .. \quad (23)$$

The parameters A and α were determined with test atmospheres in the range 0.29–1.45 mg m^{-3} of sulphur dioxide in air and the relative humidity between 60 and 80%. The sampling rate ranged from 0.072 to 2.4 m^3 h^{-1}; the temperature at which these experiments were run was not given. The determination of A and α could have been accomplished by sectional analysis of the denuder units, but no indication was given as to why such an approach was not adopted, despite its inherent precision. It should be noted that the reliability of the results obtained by this method is dependent on the accuracy of the value assigned to the diffusion coefficient of the analyte under study.

As the hydraulic radius of the annular system increased, the velocity profile of the sampled gas tended towards that obtained between two infinite parallel sheets, *i.e.*, A and α tended towards the limiting values of a parallel-plate system as the hydraulic radius increased. No reference was made to previous work, which investigated diffusional deposition in rectangular channels.[3] A comparison between equations (15) and (23) revealed the advantages of the annular design over its cylindrical counterpart. For an equivalent sampling efficiency the annular system could be shorter and more compact, operate at higher sample flow-rates and have a larger sampling capacity, or a combination of any of these factors. These claims were subsequently verified in a comparative study,[18] which concluded that annular units were a substantial improvement over all other denuder tube designs.

Development of the Gormley - Kennedy Solution

Some of the assumptions underlying the Gormley - Kennedy solution have been challenged, and, subsequently, alterations to equation (13) have been proposed.

Braman *et al.*[19] pointed out that the surfaces of a denuder tube would be depleted with increasing sample volume. The corollary to this was that the effective length of the denuder tube decreased with increasing sample volume. If the denuder was being operated at a constant sampling rate, then the collection efficiency would decrease with increasing sampling time. By assuming pseudo-first-order adsorption kinetics, it was proposed that the effective length of a denuder tube at any time after the commencement of sampling could be described by

$$Z_t = Z_0\exp(-kt) \quad .. \quad .. \quad .. \quad (24)$$

where Z_t is the effective length of the denuder at time t, Z_0 the length of the denuder at $t = 0$, k the depletion constant (feed rate/tube capacity) and t the sample time. The sample size dependency of the length of the denuder was incorporated in the original expression, equation (15), which was modified to

$$\bar{c}/c_0 = 0.82\exp\left[-7.31 \cdot \frac{\pi D_0}{2F} \cdot Z_0\exp(-kt)\right] \quad .. \quad (25)$$

The significance of the increased precision obtained by this approach is dependent on the experimental conditions. Large depletion rate constants, due to high analyte concentrations or low surface capacities, would result in measurable reductions in the effective length of the denuder. High analyte concentrations do not require long sampling times however, and an appropriate choice of reagent for the tube coating ensures an adequate surface capacity. For the analysis of sulphur dioxide in air using a denuder tube,[20] the prediction given by equation (25) for the concentration of sulphur dioxide in the tube exhaust, after sampling for 17 h (a sample volume of 0.683 m³) is 0.32 $\mu g \ m^{-3}$. This can be compared to the value of 0.29 $\mu g \ m^{-3}$ obtained from equation (15). The measured analyte concentration was 30.5 $\mu g \ m^{-3}$ and the difference between the two predictions is not significant. Measurements of the diffusion coefficients of gaseous species obtained by the denuder tube method would be more accurate if equation (25) were applied, but the practical advantages that could be carried over to the trace analysis of gas are limited.

Other modifications to the Gormley - Kennedy equation have been suggested by Murphy and Fahey.[21] The perfect sink criterion was challenged and the boundary condition that arises from it [equation (10)] was shown to be an approximation. Instead, a constant reaction probability γ was proposed. This alternative treatment, based in part on previous work concerning haemodialysis,[22] resulted in a new equation for the mixing ratio:

$$\bar{c}/c_0 = \sum_{n=1}^{n=\infty} B_n \exp(-\Lambda_n^2 Z^*) \quad \dots \quad \dots \quad (26)$$

where Z^* is a function of Z [see equation (30)]. As for its predecessors, equation (26) can be approximated to the first term:

$$\bar{c}/c_0 = B_1 \exp(-\Lambda_1^2 Z^*) \quad \dots \quad \dots \quad (27)$$

The constants B_n and Λ_n are eigenvalues that arise out of the solution to the revised differential equation, which incorporates the new boundary condition. These two constants are also functions of a new dimensionless parameter the Sherwood number (N_{shw}), which can be likened to the Nusselt number used in heat-transfer theory. It is approximated by the following equation:

$$N_{shw} \approx 36 \left(\frac{T}{m}\right)^{\frac{1}{2}} \left(\frac{T_0}{T}\right)^{\beta} \frac{RP}{D_0} \cdot \frac{\gamma}{1-(\gamma/2)} \quad \dots \quad (28)$$

where T is the temperature (K), m the relative molecular mass of the analyte, T_0 the standard temperature (K), R the radius of the tube (cm) and P the pressure (kPa). The exponent β is derived from the expression describing the variation of the diffusional coefficient with temperature and pressure:

$$D = D_0 \left(\frac{T}{T_0}\right)^{\beta} \left(\frac{P_0}{P}\right) \quad \dots \quad \dots \quad (29)$$

where P_0 is the standard pressure. The term Z^* is given by the expression

$$Z^* = Z \cdot \frac{\pi}{2} \cdot \frac{D_0}{F} \left(\frac{T}{T_0}\right)^{\beta-1} \quad \dots \quad \dots \quad (30)$$

Murphy and Fahey[21] produced a table with values of B and Λ for a range of Sherwood numbers.

This treatment models the physical processes that take place in a denuder tube more exactly than the Gormley - Kennedy approach, and hence can be seen as an improvement. The introduction of the Sherwood number enables parameters such as temperature and pressure to be incorporated in the denuder unit design. Murphy and Fahey demonstrated that at low pressures, where the Gormley - Kennedy solution fails, this new approach yielded data that fitted the experimental results with significantly greater precision. This method demands *a priori* knowledge of the reaction probability factor and the diffusional behaviour of the analyte. To obtain such information may require extensive experimental work. The assumption of a constant reaction probability over the entire collection surface is not necessarily valid. The point made by Braman *et al.*,[19] that the effective length decreases with increasing sample volume, is not included in this treatment. Such an approach would require that the reaction probability factor be expressed as a sample size dependent variable. As the Sherwood number approaches infinity, equation (27) tends towards a limiting value, that given by the Gormley - Kennedy solution. Under normal sampling conditions the differences between this approach and the Gormley - Kennedy expression are not significant and the usefulness of this method in the analysis of trace amounts of gas has yet to be established.

Assessment of the Empirically Derived Annular Equations

Based on previous work,[4,14] Possanzini *et al.*[17] derived an expression describing diffusion in an annular system. The exponent term Δ was redefined in terms of the Reynolds number (Re) and the equivalent diameter of the system:

$$\Delta = \frac{2D_0 Z}{\gamma Re \delta} \quad \dots \quad \dots \quad \dots \quad (31)$$

where γ is the kinematic viscosity, δ the equivalent diameter (defined under Annular Systems) and $Re = \bar{V}\delta/\gamma$, where $\bar{V}$ is the mean axial velocity of the gas. For a cylindrical system

$$\delta = 4(\pi R^2 / 2\pi R) = d$$

and

$$\bar{V} = 4F/\pi d^2$$

therefore

$$Re = 4F/\pi d\gamma$$

and hence

$$\Delta = \pi D_0 Z/2F = \Delta_c$$

from equation (14).

For an annular system the equivalent diameter changes:

$$\delta_a = 4 \left[\frac{\pi}{4} \cdot (d_1^2 - d_2^2) \cdot \frac{1}{\pi(d_1 + d_2)}\right] = d_1 - d_2 \quad \dots \quad (32)$$

and

$$\bar{V}_a = \frac{4F}{\pi(d_1^2 - d_2^2)^{-2}} \quad \dots \quad \dots \quad \dots \quad (33)$$

therefore

$$\Delta = \frac{\pi D_0 Z}{2F} \cdot \frac{(d_1 + d_2)}{(d_1 - d_2)} = \Delta_a \quad \dots \quad \dots \quad (22)$$

Gormley produced an expression describing diffusion through a laminar flow in a rectangular section pipeline (*i.e.*, between infinite parallel planes[3]). The rectangular section had a width of $2a$ and a height of $2b$, where $b \gg a$. A treatment similar to that for the cylindrical system yielded the expression

$$\bar{c}/c_0 \approx 0.91 \exp\left(-3.77 \cdot \frac{b}{a} \cdot \frac{D_0 Z}{F}\right) \dots \quad \dots \quad (34)$$

Equations (34) and (23) may be compared, for an annulus can be considered to be a distorted rectangle (see Fig. 3). To a first approximation the two sections are equivalent with respect to gas flow behaviour within them. The centroid of the annulus is assigned to the height of the rectangle ($2b$) and the annulus gap to its width ($2a$).

$$b_a = \pi(d_1 + d_2)/4 \quad \dots \quad \dots \quad \dots \quad (35)$$

$$a_a = (d_1 - d_2)/4 \quad \dots \quad \dots \quad \dots \quad (36)$$

where subscript a refers to the annular system.
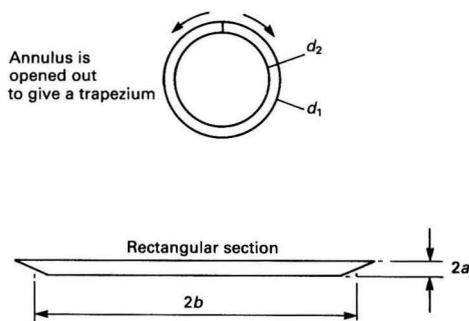
Fig. 3. Schematic diagram of a section of the annulus and its corresponding rectangular section

Substitution of equations (35) and (36) into equation (34) gives

$$\bar{c}/c_0 \approx 0.91 \exp\left[\frac{-3.77\pi D_0 Z}{F}\left(\frac{d_1 + d_2}{d_1 - d_2}\right)\right] \quad \cdot \cdot \text{ (37)}$$

Equation (37) only differs from equation (23) in the values of the numerical coefficients used.

The data obtained by Possanzini *et al.*[17] have been used to generate graphs of collection efficiency *versus* length using equations (23) and (37), Fig. 4. In a later study by the same group, nitrogen dioxide was removed from a gas sample by an annular denuder coated with potassium iodide in a Carbowax matrix.[23] The procedure for deriving the empirical constants A and α was repeated and another expression for the mixing ratio resulted:

$$\bar{c}/c_0 \approx 0.82 \exp\left[\frac{-1.125\pi D_0 Z}{F}\left(\frac{d_1 + d_2}{d_1 - d_2}\right)\right] \quad \cdot \cdot \text{ (38)}$$

Graphs are also shown in Fig. 4(*b*) comparing the efficiencies predicted from equations (38) and (37) and based on the data supplied by Possanzini *et al.*[23] The large difference between the two empirically derived expressions [equations (38) and (23)] emphasises the drawbacks to such an approach. The explanation given by Possanzini *et al.* for this difference was the occurrence of non-quantitative adsorption of nitrogen dioxide on the potassium iodide impregnated Carbowax. This is a feasible explanation when the nature of the adsorbing surface is considered, but no other experimental evidence was offered.

The distorted-rectangle approach produces an expression with an apparently large disparity between it and that derived empirically. The numerical constants in the exponent terms are -3.77 and -5.633 for equations (37) and (23), respectively. The difference between the two solutions is illustrated in Fig. 4. The divergence between the predicted collection efficiencies after a length of 20 cm is not significant, and is generally less than the experimental errors associated with the measurement of low gas concentrations. No work has been published that reproduces the result of Possanzini *et al.*,[17] however, it would appear that their result is valid, provided quantitative or near quantitative adsorption takes place. An expression based on a solution to equation (9) for an annular system would provide an interesting result. However, in the context of gas sampling the derivation of such an expression would make little material difference.

Applications to Analysis

Organic Atmospheric Species

Comparatively few results have been published on the collection of volatile organic compounds with denuder systems. Most of the work in this area has been concerned with species originating in automobile exhaust emissions. Annular denuders have been used to collect formaldehyde[24] and, using
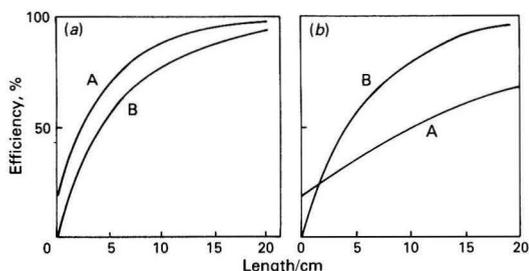
Fig. 4. Graphs of predicted collection efficiency *versus* denuder length. A, Possanzini equation; B, Gormley equation. (*a*) Sulphur dioxide; (*b*) nitrogen dioxide

a sodium hydrogen sulphate - triethanolamine coating, test atmospheres of 0.4 mg m^{-3} of formaldehyde in air were determined. A detection limit of 0.3 μg m^{-3} of formaldehyde in air was calculated for a sample time of 24 h and a flow-rate of 0.15 m^3 h^{-1}, although no supporting data were given to validate this claim. The analysis involved leaching the collection surfaces with water and using the chromotropic acid spectrophotometric technique[24] to determine the formaldehyde content of the washings. Phenol was found to interfere with the analysis. A 10–20% loss in apparent formaldehyde was reported for a phenol to formaldehyde ratio of 1 : 2. The effects of humidity and temperature on the analysis were not reported. A study of ageing indicated that coated exposed and unexposed units underwent no significant change after being sealed for 4 weeks. The conditions under which they were stored were not described.

This work was subsequently extended to include other low boiling-point aldehydes, using high-performance liquid chromatographic (HPLC) techniques.[25] Annular denuders were coated with 1% 2,4-dinitrophenylhydrazine and phosphoric acid in acetonitrile. Sampled aldehydes underwent derivatisation on adsorption yielding the appropriate 2,4-dinitrophenylhydrazone derivative. The products were eluted with acetonitrile, separated using HPLC and detected by UV - visible absorbance measurements or voltammetry. Test atmospheres of 1.2 mg m^{-3} of propionaldehyde in air and 1.6 mg m^{-3} of acetaldehyde in air were determined from sample volumes in the range 0.015–0.095 m^3. Collection efficiencies observed for this system were significantly lower than predicted. Variations in solubility were advanced as an explanation, but no experimental evidence was given in support of such a mechanism. Variations in the stability and the kinetics of the derivatisation products and processes were not discussed, and the possibility of non-quantitative adsorption was not considered either. The effect of humidity on the system was investigated and relative humidity levels of 50–90% were found to have no effect on the collection efficiency. Lower humidity levels were not reported. Samples taken from cigarette smoke, diesel exhaust and rural air were presented, showing that a number of aldehydes had been collected including acrolein and propionaldehyde. No data were given as to the stability of the unit with time, nor to the effects of chemical interference.

Further studies with annular denuders resulted in gaseous organolead compounds being determined.[26] Tetraalkyllead compounds were trapped on an iodine monochloride coating, stabilised in a polyethylene glycol - Carbowax 600 matrix. Elution was performed manually by washing with acidified hydrogen peroxide and the resulting washings were analysed using atomic absorption spectrometry at the 283.3-nm lead absorption line. The initial characterisation of this system was based on tetraethyllead atmospheres. However, the experimental details reported were sparse, with few details of concentration, calibration, sample volume or sensitivity being supplied. Interference from chemical or physical sources was not considered, but a study of ageing revealed that exposed

tubes could be stored for 3 d prior to analysis without any significant effect on the final result. The storage conditions were not given. In initial field trials of this system, samples taken from underground garages were found to have concentrations of organic lead as high as 1.5 µg m^{-3} in air, which was claimed to comprise 27% of the total lead content of the atmosphere. The technique could not distinguish between different organic moieties and the determination of a specific organolead compound was not possible.

A glass tube coated to a depth of 0.1 µm with the soot from a benzene or toluene flame has been employed as a general purpose gas adsorber.[27] The system was interfaced directly to a gas chromatograph and sample transfer was effected by thermal desorption. A temperature of 270 °C was maintained for 2.5 min to ensure quantitative desorption of all the trapped compounds. No other information was given as to the construction or operation of the thermal desorption unit. Diffusion coefficients calculated on the basis of the Gormley - Kennedy equation[3] were presented. As non-quantitative adsorption was reported, the validity of this method is questionable, for the perfect sink criterion of the Gormley - Kennedy solution was not fulfilled. Vapour profiles arising from the headspace analysis of foodstuffs, and from shipboard atmospheres were presented. Distinct vapour patterns were clearly obtained, but neither high-volatility compounds, nor low-volatility compounds normally associated with the particulate phase, were retained. No calibration or sample volume data were presented and no claims were made as to the sensitivity of this technique.

Ammonia Species

Ammonia occurs at low concentrations in the atmosphere and is thought to control atmospheric acidity owing to the formation of ammonium salts, which results in acid removal.[28,29] The equilibrium between ammonia and its salts is complicated due to the large number of precursors and reaction products involved. The model may be simplified by considering ammonia in the vapour phase to be in equilibrium only with ammonium nitrate.[30] Sampling using filtration techniques has led to the introduction of artifacts in the measurement of this equilibrium. The analyte might be overestimated by the release of ammonia from ammonium nitrate; alternatively, particle - particle reactions of ammonium salts with alkaline particles may result in the release of gaseous ammonia. The ammonia concentration might be underestimated as a result of the reaction of gaseous ammonia with acids deposited on the filter. It is important, therefore, to employ a sampling strategy that separates gaseous and particulate species.

Ferm[14] first reported the use of a denuder system for the measurement of ambient ammonia. The separation of gaseous ammonia from its particulate phase was achieved by employing a cylindrical denuder tube (l = 50 cm, i.d. = 3 mm) coated with oxalic acid. The analysis was achieved by dissolution of the sorption layer with 2 cm^3 of 0.1 M NaOH solution and the ammonium ions were determined by an ion-selective electrode with a detection limit of 8.5 mg m^{-3} of ammonia in air.

Collection efficiency studies[14] were carried out for ammonia in air in the concentration range 8.5–51 µg m^{-3}, with a sampling time of 24 h and a flow-rate of 2.9 l min^{-1}; collection efficiencies of 90.6% were achieved. An experimental value of 2.47×10^{-5} m^2 s^{-1} was obtained for the diffusion coefficient of ammonia, in agreement with a value of 2.36×10^{-5} m^2 s^{-1} obtained by Coulson and Richardson[15] at 1 atm and 25 °C. Ferm[14] also investigated particle deposition by sampling the ambient atmosphere with 1 m long uncoated tubes for a period of 2 weeks. The interference due to the particle phase was claimed to be of the same magnitude as the detection limit. The possibility of vaporisation of the ammonium ion, which may be significant with a sampling time of 2 weeks, was not considered.

Further studies of particulate deposition have been carried out by Dimmock and Marshall[31] using the technique described by Ferm. Ammonium nitrate aerosols were generated by an ultrasonic nebuliser and characterised by light scattering. Their results showed that 2.84 µg m^{-3} of ammonium nitrate in air contributed 0.2 µg m^{-3} to a measured free ammonia concentration of 22.45 µg m^{-3}. It was also reported that the concentration of ammonia recorded by this technique was dependent on the timing of the analytical procedure. Coated denuder units left to stand unsealed for 2.5 h prior to their analysis gave blank values ten times greater than normal. Similar units that were sealed before being left to stand showed no significant uptake of ammonia, even after 4 d. Further, exposed units that were sealed and stored before analysis gave elevated values for the ammonia concentration. The maximum increase in concentration reported was 20% relative to units analysed immediately after sampling. A 10-min period was sufficient to produce a measurable difference. The authors emphasised the importance of prompt analysis of exposed denuder samplers, although an explanation for these effects was not offered. The collection of ammonia by the unexposed tubes left open to the atmosphere can be explained by a passive diffusive process. Ammonia present in the air within the denuder tube is removed rapidly by the collection surfaces. The concentration gradient that results between the ammonia-free atmosphere in the denuder and the ambient air causes continuous transport of ammonia to the surface of the denuder. The diffusional pumping continues until the collection surfaces are saturated.

The reported increase of trapped ammonia in the sealed and exposed units can be attributed to the dissociation of trapped particulates within the sealed assembly. Particulate impaction occurs in the laminar flow subduction zone during sampling. Normally this region is excluded from the subsequent analysis; in a sealed denuder unit the natural equilibrium between these solids and free ammonia is disrupted, causing dissociation of the solids. The liberated ammonia is promptly trapped by the collection surfaces. These observations are important and any measurement technique for ammonia should take effects such as these into account.

Annular denuder tubes (l = 25 cm, annulus i.d. = 0.16 cm) coated with 1% oxalic acid in methanol have been used for sampling ammonia and ammonium ion species.[30] A flow-rate of 20 l min^{-1} and a sampling time of 30 min were used. Sampling artifacts were analysed by employing two denuders placed in series and separated by a filter and the concentration of gaseous ammonia was determined by analysing the contents of the first denuder. The ammonium ion concentration was determined as the sum of the ammonium in the filter and the ammonia released by the filter into the second denuder. The data showed that there was a significant release of free ammonia from the filter. In one instance 6.98 µg m^{-3} of free ammonia were measured in the second denuder. A second corresponding concentration of 7.9 µg m^{-3} of ammonium particulates was determined on a Gelman GA-4 type filter. The artifact appeared to vary not only with different types of filter but also with the same filter.

Dasgupta[32] has described a denuder tube with a thin cation-exchange membrane as the collecting element. Gaseous ammonia was collected on the perfluorosulphonate membrane as the ammonium ion, which diffused through the membrane and was carried off in a dilute acid stream for analysis by ion chromatography. The acidic solution also served to maintain the exchange sites in the H$^+$ form. Collection efficiencies of greater than 99% were obtained for ammonia concentrations from 15 ng m^{-3} to 1.2 µg m^{-3}, with flow-rates from 0.44 to 1.54 l min^{-1}. The cation-exchange membrane will allow a number of species to diffuse through; however, no interference studies were carried out. The gas phase limit of detection was predicted to be 45 ng m^{-3} of ammonia in air.

765

The use of two denuders in series separated by a filter, illustrates the extent of ammonia release associated with filters[30] and the importance of denuder tubes as sampling devices. The accurate determination of low levels of free ammonia in the atmosphere is made possible by the use of oxalic acid coated denuder tubes. However, immediate analysis of the oxalic acid coated denuder is required to avoid dissociation of ammonium particulates in the subduction zone. Particulate dissociation may be significant where long sampling times are required and, in addition, long sampling times do not permit diurnal studies. Annular denuder tubes, however, may be used to overcome many of these problems. The oxalic acid technique, although low-cost, is labour intensive and difficult to automate. The problem of ammonia adsorbing on to the uncoated glass sections of a denuder system has been neglected, despite the work of Dasgupta.[32] Until the results of such a study are known, the error associated with such processes is difficult to estimate.

Dasgupta's design of the denuder tube[32] is an important development in the technique. A variety of gaseous atmospheric species may be sampled by using the appropriate membrane material and scrubber solution. If the scrubber solution is used as part of a continuous flow analysis system, then spectrophotometric methods of detection can be employed, although in this mode the concentrating ability of the device is largely lost.

Nitrate Species

Nitric acid is an important acidic atmospheric species. Its measurement and that of its salts in the particulate phase enable the role of nitrogen oxide species in atmospheric chemistry to be elucidated.

Nitric acid and nitrate salts have been sampled using dual-filter techniques in which particulate nitrate was collected on the first filter and nitric acid on the second.[33,34] This method gives rise to positive and negative interferences arising from sampling artifacts. Nitric acid will be converted to the solid nitrate in the presence of sodium chloride or basic particulate species.[35] Conversely, the dissociation of ammonium nitrate, or its reaction with sulphuric acid, gives rise to elevated nitric acid levels within the sampling assembly, with an accompanying reduction in the nitrate-containing species.[36,37] Shaw et al.[38] overcame these problems with a denuder difference experiment. This method employs two sampling assemblies, both consisting of a nylon filter that collects both gaseous HNO_3 and particulate nitrate; in one of the assemblies the filter was preceded by a denuder tube coated with magnesium oxide. The difference between the amounts of nitrate collected in the two assemblies was due to the removal of gaseous nitric acid from the sample. Experiments run for 23 h at a flow-rate of 3.4 l min^{-1} showed that nitric acid concentrations exceeded those of particulate nitrates. Diurnal studies revealed that particulate nitrate concentrations remained fairly constant, whereas nitric acid levels increased during the day.

In a comparative study, particulate nitrate and nitric acid were measured by the penetration, denuder difference and dual-filter methods.[39] The sampler for the penetration method consisted of two nylon-lined denuder tubes ($l = 80$ and 18 cm) separated by a Teflon filter. Sampling was carried out at a flow-rate of 1.5 l min^{-1} with a sampling time of 24 h. Nitric acid and volatile particulate nitrates were analysed from the long upstream denuder. The short downstream denuder was used to collect the volatile particulate nitrate only. The denuder tube assembly used in the denuder difference technique allowed shorter sampling times. The assembly consisted of nine denuder tubes ($l = 50$ cm, i.d. = 3 mm) coated with sodium hydrogen carbonate.

The results of the two denuder methods and the dual-filter method for total inorganic nitrate agreed.[39] However, the dual-filter method gave a very high value (4.52 μg m^{-3}) for

nitric acid in air; this could be due to the dissociation of particulate ammonium nitrate. A nitric acid concentration of 3.75 μg m^{-3} was obtained by the penetration method compared with an average of 3.11 μg m^{-3} for the denuder difference method. This overestimation is thought to be due to turbulent flow caused by the intersection of the flow stream with the leading edge of the nylon filter. Alternatively, it has also been suggested that the collection efficiencies of the two methods are incorrect. The penetration method has a relatively poor sensitivity and requires time-consuming sample preparation and it appears to have no advantage over the denuder difference method, which has been shown to give precise experimental data.

The denuder tube methods described assume that the evaporation of particulate nitrates as they pass through the denuder tube is negligible. Larsen and Taylor[40] examined the artifacts that may arise from the sampling of ammonium nitrate aerosols. Gaseous ammonia and nitric acid were removed from the ammonium nitrate aerosol by means of a diffusion stripper employing sodium hydroxide and sulphuric acid chemical sinks. The rate of evaporation was measured by following the changes in size distribution of the aerosol with time.

Resistance to the transport of molecules across the vapour - liquid interface was small and sampling errors due to the evaporation of ammonium nitrate were calculated to be 2.5 and 1.8% for gaseous nitric acid and particulate ammonium nitrate, respectively. A number of factors will, however, cause these errors to decrease. Steady-state gas profiles in the denuder are not achieved instantaneously, hence in the time required to form steady-state profiles, the evaporation of particles would be less as a result of the higher concentration. Calculations performed by Stelson and Sienfeld[41] suggest that in the presence of ionic mixtures such as ammonium sulphate and ammonium nitrate the vapour pressures of ammonia and nitric acid would be lowered, and hence the sampling error would be lower.

Ferm and Sjodin[42] used a cylindrical denuder tube coated with sodium carbonate to sample nitrous acid. A flow-rate of 2 l min^{-1} yielded a collection efficiency of 95%. The sodium carbonate denuder was leached in water and the nitrite concentration was determined spectrophotometrically. A number of sampling artifacts exist including the formation of nitrous acid in the presence of nitrogen monoxide, nitrogen dioxide, water and peroxyacetylnitrate (PAN), the last of which is also partly adsorbed and hydrolysed to the nitrite. Corrections for interferences may be made by placing two denuder tubes in series. Assuming a 96% collection efficiency the ambient nitrous acid concentration may be calculated from the following equations:

$$I = 0.96[HNO_2] + \sigma_1 \qquad \ldots \quad \ldots \quad (39)$$

$$J = 0.0384[HNO_2] + \sigma_2 \qquad \ldots \quad \ldots \quad (40)$$

where I and J are the average nitrite contents in the denuders and σ_n denotes the fraction of nitrite not originating from ambient nitrous acid. As σ_1 and σ_2 are equal, solving equations (39) and (40) gives $[HNO_2] = 1.085(I - J)$. The applied corrections are not applicable where the concentrations of PAN are greater than those of nitrous acid. The method is therefore only useful in air close to NO_x sources, such as polluted urban air. It cannot be used to measure natural background levels of nitrous acid.

Automated monitoring of nitric acid and ammonia has been achieved by multi-stage selective thermal desorption from a tungsten(VI) oxide coated cylindrical denuder tube.[19,43] The analysis took 40 min with a sensitivity of sub-p.p.b. The adsorption of ammonia on tungstic acid is thought to be an acid - base reaction that is reversible at 350 °C

$$NH_3 + H_2WO_4 \underset{350\,°C}{\overset{}{\rightleftharpoons}} NH_4HWO_4$$
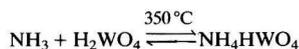
The mechanism for nitric acid adsorption is unclear, although it has been suggested that irreversible adsorption is involved. Nitric acid desorbs as nitrogen dioxide. The denuder tubes are coated by the vacuum deposition of tungsten wire. Blue tungsten(IV) oxide is oxidised to yellow tungsten(VI) oxide by heating at 500 °C. Alkylamines, nitrogen dioxide and PAN were all shown to interfere. The amount of ammonia adsorbed decreased in the presence of 100 p.p.b. of ozone. Diurnal studies of nitric acid and ammonia showed that in most instances higher nitric acid concentration maxima correlated with lower ammonia concentration maxima. Diffusion coefficients obtained by section analysis agreed with those reported by Wilke and Lee.[44] Braman et al.[19] concluded that, although the nitric acid may be associated with water or other compounds, hence decreasing the diffusion coefficient, ammonia existed in the non-associated form. These findings contradict those of a parallel study,[45] which showed that ammonia existed in its associated form. The tungstic acid denuder used in this study was prepared by coating six sections of tubing ($l = 15$ cm, i.d. $= 0.56$ cm) with a thin film of sodium hydroxide (0.5 M) - sodium tungstate [0.05 M in water - propan-2-ol (50 + 50 V/V)]. By rolling the tubes on a horizontal roller the coating was air dried. Sodium tungstate was converted to tungstic acid by passing hydrogen chloride through the tubes, which were then washed with water to remove sodium chloride and then heated at 500 °C in a furnace for 8 h. The sample capacity was shown to be much greater than that of the tube coated by vacuum deposition of tungsten wire although the vacuum deposition method did produce blank values that were 20 times lower. Both nitrate and ammonia were extracted quantitatively with three successive 3-cm³ portions of 1.0 mM LiOH solution at 90 °C and then the nitrate and ammonium ions in the extract solution were determined by ion chromatography.

The measurement of atmospheric nitric acid[46] was carried out in a comparative study of the tunable diode laser absorption, tungstic acid denuder tube and Teflon - nylon filter-pack methods. The laser method gave higher nitric acid concentrations than the other methods and quantitative agreement between these techniques was not obtained, although general trends in the variation of the nitric acid concentration could be identified. The tungstic acid method measured higher nitric acid concentrations than those using the filter pack, the difference being 5% for daytime measurements and a factor of two lower during the night. The difference could be due to the retention of nitric acid on the particulate matter of the filter.[47,48] The tungstic acid method also showed higher particulate nitrate concentrations than the filter-pack method and this may be due to the dissociation of particulates on the filter. Nitric acid concentrations were investigated in a further comparative study of the tungstic acid and filter-pack methods.[49] The former gave nitric acid concentrations three times higher than the latter and this difference was attributed to interference from organic nitrates in the denuder tube; however, no data were produced to confirm this. Interferences from nitrogen dioxide, PAN and propyl nitrate in the denuder tube were shown not to be significant.

A number of denuder tube techniques have been developed for the measurement of nitric acid with the tungstic acid denuder tube being the most widely reported for this purpose. Since its introduction, a number of studies have compared the tungstic acid method with measurements performed using other techniques, the result being a great deal of scatter in the inter-comparison. However, it was shown that the tungstic acid denuder tube produced larger apparent nitric acid mixing ratios than the filter-pack technique and the source of this difference has not yet been identified. The dissociation of particulate nitrates in the subduction zone of the denuder tube, which is particularly likely if the subduction zone is heated during the thermal desorption cycle, has not been considered. In a recent study Roberts et al.[50] concluded that tungstic acid coatings were subject to "slow evolutionary and occasionally catastrophic failure," indicating that tungstic acid coatings are not viable for long-term unattended use. There is a need for properly characterised adsorbing surfaces with high thermal stabilities and in this respect transition metal oxide surfaces may prove useful.

Hydrogen Chloride

Natural sources of hydrogen chloride include the reaction of marine-salt aerosols with atmospheric sulphuric and nitric acids, or volcanic emissions. The gas can also be released from refuse incineration plants and result from the combustion of certain types of coal.

Dimmock and Marshall[51] described a manual method for the determination of hydrogen chloride using a cylindrical denuder tube coated with sodium fluoride. The extraction was carried out using distilled water with detection by a chloride ion-selective electrode. Adsorption efficiencies >90% were obtained and the room air sampled was found to contain hydrogen chloride concentrations in the range 0.16–0.55 µg m⁻³. Interferences from particulate chloride, sulphur dioxide and nitrogen dioxide were found to be negligible.

Sulphur Species

Sulphur dioxide has been sampled with a cylindrical denuder tube coated with a mixture of sodium tetrachloromercurate(II) and malein buffer [the malein buffer was used to neutralise the hydrogen chloride produced during the reaction between tetrachloromercurate(II) and sulphur dioxide].[20] The cylindrical denuder tube was coated by injecting 0.4 cm³ of 0.1 M sodium tetrachloromercurate(II) - 0.1 M malein buffer in 1 + 1 methanol - water. The extraction was carried out using distilled water and the analysis by isotope dilution.

Sampling was performed in a polluted industrial atmosphere with a sampling time varying from 3 to 24 h with the relative humidity in all instances being >50%. Collection efficiencies of 90% were achieved except where the relative humidity approached 100%, and the results obtained for the collection of sulphur dioxide in denuders and on potassium hydroxide filters agreed.

Gas-phase concentrations of dimethyl sulphate and monomethyl hydrogen sulphate have been determined by collecting the species on cylindrical denuder tubes.[52] A paper-lined denuder tube was used for the collection of monomethyl hydrogen sulphate and a nylon denuder was used for sampling total gas-phase alkyl sulphates. Dimethyl sulphate was first collected on an XAD-2 resin bed and then determined by ion chromatography. The aqueous-extractable dimethyl sulphate hydrolyses to the monomethyl hydrogen sulphate and the increase in the monomethyl hydrogen sulphate concentration between the paper and the nylon denuder tubes was used as a measure of the dimethyl sulphate concentration.

Agreement between the expected and calculated diffusion coefficients supported the identification of dimethyl sulphate and monomethyl hydrogen sulphate as the species adsorbed on the denuder tubes. Laboratory studies did, however, show that up to 10% of the sulphur dioxide passing through the nylon denuder may be adsorbed on the walls, and a correction procedure was developed to overcome this interference effect. In field trials, this denuder approach did not yield results that agreed with those obtained from filter-based techniques. The authors[52] stated that the agreement was not good and they were unable to indicate which technique was the most reliable.

Ambient sulphuric acid aerosols have been sampled by means of a heated denuder tube coated with manganese and palladium oxides[53] with interferents being selectively removed from the sample by a series of pre-denuders. On completion of

sampling the denuder was placed in an oven and desorbed thermally at 800 °C into a convertor, which reduced any sulphur liberated to hydrogen sulphide, before being passed into a silver wool chemical pre-concentrator. Flash heating of the silver wool resulted in a concentrated injection of hydrogen sulphide into the gas chromatograph. A detection limit of 0.1 µg m^{-3} of sulphuric acid in air was obtained using this technique. A study of particulate dissociation at various denuder temperatures was undertaken and this underlined the possible dissociation of particulates in the subduction zone during thermal desorption. The results of this study indicated that dissociation of particulates trapped on the walls of the laminar flow subduction zone could occur during thermal desorption. Such findings[53] have important ramifications for the design criteria of automated denuder systems.

Multi-component Sampling

The criterion of laminar flow limits the sample flow-rate; therefore, in order to collect a measurable amount of analyte, long sampling times are required. To overcome this problem Stevens et al.[13] utilised 16 parallel tubes arranged in a circle to separate ammonia from ammonium salt particulates. No data relating to the amount of ammonia trapped were given in this report, and the problems of ensuring the reproducible handling of 16 tubes were not discussed. Forrest et al.[47] employed 48 sodium carbonate coated cylindrical tubes for sampling nitric acid, which allowed sampling flow-rates of 10–30 l min^{-1}. In this study, the unit was heated such that the relative humidity of the sample was lowered below the deliquescence point of sodium carbonate. The authors claimed that this did not significantly influence the results obtained, but the supporting data were not comprehensive. The results of a detailed study into such a procedure would establish whether heating the sample to permit better instrument operation is an acceptable practice in this area of application. Lewin and Hansen[54] described a diffusion denuder assembly, which, by means of a vacuum and a pressurised air system, allows the individual coating and extraction of 15 quartz glass tubes. This semi-automated method enabled denuder tube assemblies to be coated with a number of selective absorbents, decreasing the risk of contamination compared with manual methods.

Ammonia was sampled using tubes coated with 1.5% oxalic acid in ethanol[54] and acidic gases were sampled using tubes coated with 1 M potassium hydroxide in methanol. Automatic spectrophotometric methods were employed for sulphate, nitrate and chloride determinations and the indophenol method for the determination of ammonia. The data supplied for this system were sparse and few details on sensitivity, reproducibility and calibration procedures were given. However, the advantages of using the device described for batch-processing denuder tubes are self evident.

Liberti et al.[55] employed three annular denuders in series for the determination of sulphur dioxide, ammonia, nitric acid and hydrogen chloride. Sulphur dioxide was sampled using a sodium tetrachloromercurate(II) coated tube. Collection efficiencies >90% were obtained for sulphur dioxide with a sampling flow-rate of 20 l min^{-1}. Ammonia was sampled with an oxalic acid coated tube, and hydrogen chloride and nitric acid on a sodium fluoride coated tube. Little experimental detail was reported, but data obtained from the denuder assembly over a 7-month period indicated that ammonia and sulphur dioxide could be monitored with such a system. Nitric acid and hydrogen chloride were detected only intermittently by the unit. No explanation was given for this behaviour, and complementary data from other techniques would be required to support any conclusions drawn from their results regarding the presence, or lack of it, of hydrogen chloride and nitric acid in the sample.

A series of coated cylindrical denuder tubes operated at different temperatures was used to collect free ammonia and to distinguish nitric acid from ammonium nitrate and sulphuric acid from ammonium sulphate by their different thermal behaviour.[56] The tubes were extracted with doubly de-ionised water. Ammonium ions were detected by means of a gas-sensing membrane and nitrate and sulphate species were determined by ion chromatography.

The tubes were coated for collecting nitric acid, free ammonia and sulphur dioxide.[56] A tube operated between 390 and 410 K and coated with sodium fluoride was used for the collection of sulphuric acid and a sodium fluoride coated tube operated at 490–510 K was used to retain the sulphuric acid produced from the dissociation of ammonium sulphate and a further tube collected the liberated ammonia.

This last technique appears to be a simple and low-cost method for carrying out multi-component analysis. However, the dissociation of ammonium nitrate and sulphate before they reach their target tubes causes a degree of uncertainty and it was noted that at ammonium nitrate concentrations of 20 µg m^{-3}, half of the liberated nitric acid was found in the first tube.

The selective collection and determination of airborne sulphuric acid and ammonium sulphate has also been achieved using two copper(II) oxide coated denuder tubes at temperatures of 120 and 240 °C, respectively.[57] This method relies on the adsorption of sulphuric acid on copper - copper(II) oxide and the decomposition of ammonium sulphate at temperatures above 220 °C. The resulting copper sulphate was converted to sulphur dioxide by heating at 800 °C and then measured using a flame photometric detector. Interferences due to inorganic and organic sulphur species were avoided by passing the sample stream through potassium carbonate and active carbon-coated denuders.

The copper - copper(II) oxide was prepared by filling the tube with 3% m/V hydrated copper(II) nitrate in ethanol. The tube was emptied, dried first at room temperature and then at 200 °C to remove water of crystallisation. Nitrogen was passed through the tube at 400 °C for 5 min. Both ends of the tube were cleaned by inserting the tube in 1 M nitric acid and a black copper - copper(II) oxide coating was obtained after flushing with nitrogen and heating at 900 °C for 5 min. The technique employed two parallel copper - copper(II) oxide denuders. After completion of the sampling period in the first set of denuders, the sample flow was switched to the second set of denuders and the first set was analysed individually.

The data presented showed that very little ammonium sulphate was found in the first tube at the selected temperatures and at ammonium sulphate concentrations above 30 µg m^{-3}. No data were presented for possible dissociation artifacts at ammonium sulphate concentrations below 30 µg m^{-3}. This may be significant as the measured ambient ammonium sulphate concentrations were less than this value. Earlier work with the sodium fluoride manual method showed that dissociation of ammonium sulphate becomes significant at lower concentrations.[56] The copper - copper(II) oxide denuder tube has also been employed for the measurement of sulphur dioxide.[58] The effect of humidity on collection efficiencies and an investigation of sulphur-based interferents were carried out in the same study. A significant decrease in the collection efficiency with decreasing humidity was reported, but no explanations for the reasons were given. The interference from organic sources was stated as "not important" and data were presented that demonstrated agreement between results obtained from denuder systems and those produced through filter techniques insensitive to the presence of organic sulphur species. The reproducibility of the technique was claimed to be 3% and the available data showed the relative standard deviation to vary between 1.5 and 5%.

Slanina[59] have developed a "wet denuder" system for the sampling of ammonia, nitric acid, hydrochloric acid, sulphur dioxide and hydrogen peroxide. The wet denuder consisted of

an annular denuder coated with an aqueous layer, which was rotated about its axis to keep the surfaces wet. Two parallel wet denuders were employed. In one denuder the absorption solution contained formaldehyde and *p*-hydroxyphenylacetic acid to collect and stabilise sulphur dioxide and hydrogen peroxide. The absorption solution in the second denuder contained a formic acid buffer of pH 4 for the collection of ammonia, nitric acid and hydrochloric acid. After sampling, the absorption solutions were pumped out of the denuders into two sampling tubes. Hydrogen peroxide and sulphate were determined using fluorimetric and photometric detectors, ammonium ions by spectrophotometric measurement and nitrate and chloride ions by ion chromatography. A cyclone was used to reduce interferences from particulates. The effects of rotation of the collection surfaces and moving liquids within the denuder unit on laminar flow and particulate transmission efficiency were investigated; no significant perturbation of the system was reported. Clearly, the device described has other atmospheric monitoring applications and this approach may be expected to be extended to other areas of atmospheric analysis.

Conclusions

The determination of atmospheric species is fraught with problems; the dynamic equilibria between the various species make their determination particularly difficult. Separation of the gas and particulate phases by denuder tubes avoids the artifacts that may otherwise occur with filter-based methods. The denuder tube has the additional advantage of preconcentrating the gaseous analyte, which is not possible using conventional filters. Denuder tubes have proved to be an important development in atmospheric sampling, allowing the daily patterns and long-term trends of atmospheric species to be discerned.

The use of simple, cylindrical denuder tubes has several disadvantages. Their use is labour intensive, as both a coating procedure and extraction of the collected gases are involved and the low sampling flow-rates require long sampling times, hence causing a number of other artifacts. The introduction of the annular denuder tube allows much higher sampling flow-rates and hence shorter sampling times and the use of thermal desorption denuders eliminates the need for washing or re-coating. However, in this last method, the interference due to vaporisation of particulates in the subduction zone has not been clearly established. The wet denuder system has placed a much older sampling device, the bubbler, into a denuder tube context and may have wide application for the monitoring of thermally unstable species.

A degree of complexity has been introduced by the development of multi-component denuder tube systems. However, further fundamental work has to be carried out to realise the full potential of the technique. In particular, considerations have to be made about the nature and influence of non-adsorbing surfaces within the denuder tube. Considerations also have to be made about the employment of various sampling strategies such as the incorporation of iso-kinetic sampling from laminar gas flows.

The use of a wide range of denuder tube systems has been demonstrated, although they have been employed mainly for the measurement of species involved in atmospheric pollution and acid rain studies. Few applications have been reported for organic vapours in the atmosphere. It is most likely that the applications to which denuder tubes are employed will increase in the future, as they are attractive by virtue of their simplicity, ruggedness and ability to undergo long-term exposure to particle-laden atmospheres with minimal interference from the aerosol and particle content.

References

1. Townsend, J. A., *Philos. Trans. R. Soc. London, Ser. A*, 1900, **193**, 129.
2. Nolan, J. J., and Guerrini, V. H., *Proc. R. Ir. Acad., Sect. A*, 1935, **43**, 5.
3. Nolan, J. J., Nolan, P. J., and Gormley, P. G., *Proc. R. Ir. Acad., Sect. A*, 1938, **45**, 47.
4. Gormley, P. G., and Kennedy, M., *Proc. R. Ir. Acad., Sect. A*, 1949, **52**, 103.
5. Thomas, J. W., *J. Colloid Sci.*, 1955, **10**, 246.
6. Pack, M. R., Hill, A. C., Thomas, M. D., and Transtrum, L. G., *Am. Soc. Test. Mater. Spec. Tech. Publ.*, 1961, **281**, 27.
7. Crider, W. L., Barkley, N. P., Knott, M. J., and Slater, R. W., *Anal. Chim. Acta*, 1969, **47**, 237.
8. Fish, B. R., and Durham, J. L., *Environ. Lett.*, 1971, **2**, 13.
9. Durham, J. L., Wilson, W. E., and Bailey, E. B., *Atmos. Environ.*, 1978, **12**, 883.
10. Huntzicker, J. J., Hoffman, R. S., and Ling, C. S., *Atmos. Environ.*, 1978, **12**, 83.
11. Durham, J. L., Wilson, W. E., and Bailey, E. B., US Environmental Protection Agency Report No. EPA 600/3-76/088, Washington, DC, 1976.
12. Cobourn, W. G., Husar, J. D., and Husar, R. U., *Atmos. Environ.*, 1978, **12**, 89.
13. Stevens, R. K., Dzubay, T. G., Russwurm, G., and Rickel, D., *Atmos. Environ.*, 1978, **12**, 55.
14. Ferm, M., *Atmos. Environ.*, 1979, **13**, 1385.
15. Coulson, J. M., and Richardson, J. F., "Chemical Engineering," Volume 1, Second Edition, Revised, Pergamon Press, London, 1966.
16. Fuchs, N. A., *in* Davies, C. N., *Editor*, "The Mechanics of Aerosols," Pergamon Press, London, 1964.
17. Possanzini, M., Febo, A., and Liberti, A., *Atmos. Environ.*, 1983, **17**, 2605.
18. Liberti, A., *Acqua Aria*, 1986, **2**, 133.
19. Braman, R. S., Shelley, T. J., and McClenny, W. A., *Anal. Chem.*, 1982, **54**, 358.
20. Lewin, E. E., and Klokow, D., *Comm. Eur. Communities, Phys-Chem. Behav. Atmos. Pollut.*, L. Rep. Eur 7624, pp. 54–61.
21. Murphy, D. M., and Fahey, D. W., *Anal. Chem.*, 1987, **59**, 2753.
22. Cooney, D. C., Kim, S., and Davies, E. J., *J. Chem. Eng. Sci.*, 1974, **29**, 1731.
23. Possanzini, M., Febo, A., and Cecchini, F., *Anal. Lett.*, 1984, **17**, 887.
24. Cecchini, F., Febo, A., and Possanzini, M., *Anal. Lett.*, 1985, **18**, 681.
25. Possanzini, M., Ciccioli, P., Di Palo, V., and Draisel, R., *Chromatographia*, 1987, **23**, 829.
26. Febo, A., Di Palo, V., and Possanzini, M., *Sci. Total Environ.*, 1986, **48**, 187.
27. Cobb, G. P., Braman, R. S., and Hua, K. M., *Anal. Chem.*, 1986, **58**, 2213.
28. Gravehurst, G., and Bottger, A., *in* Versine, B., and Ott, H., *Editors*, "Proceedings of the 1st European Symposium on the Physico-Chemical Behaviour of Atmospheric Pollutants, Ispra, 16–18 October 1979," Reidel, Dordrecht, Holland, 1980, p. 383.
29. Georgii, H. W., and Muller, W. J., *Tellus*, 1974, **26**, 180.
30. Allegrini, I., Santis, F. D., Palo, V. D., and Liberti, A., *J. Aerosol Sci.*, 1984, **15**, 465.
31. Dimmock, N. A., and Marshall, G. B., *Anal. Chim. Acta*, 1986, **185**, 159.
32. Dasgupta, P. K., *Atmos. Environ.*, 1984, **18**, 1593.
33. Spicer, C. W., and Schumacher, P., *Atmos. Environ.*, 1977, **11**, 873.
34. Appel, B. R., Tokiwa, Y., and Haik, M., *Atmos. Environ.*, 1981, **15**, 283.
35. Appel, B. R., and Tokiwa, Y., *Atmos. Environ.*, 1980, **14**, 549.
36. Stelson, A. W., Friedlander, S. K., and Seinfeld, J. H., *Atmos. Environ.*, 1979, **13**, 369.

37. Harber, A. B., Richards, L. W., and Clarke, W. E., *Atmos. Environ.*, 1977, **11**, 87.
38. Shaw, R. W., Stevens, R. K., Bowermaster, J., Tesch, J. W., and Tew, E., *Atmos. Environ.*, 1982, **16**, 845.
39. Mulawa, M. A., and Cadle, S. H., *Atmos. Environ.*, 1985, **19**, 1317.
40. Larsen, T. V., and Taylor, G. S., *Atmos. Environ.*, 1983, **17**, 2489.
41. Stelson, A. W., and Sienfeld, J. H., *Atmos. Environ.*, 1982, **16**, 2507.
42. Ferm, M., and Sjodin, A., *Atmos. Environ.*, 1985, **19**, 979.
43. McClenny, W. A., Galley, P. C., Braman, R. S., and Shelley, T. J., *Anal. Chem.*, 1982, **54**, 365.
44. Wilke, C. R., and Lee, C. Y., *Ind. Eng. Chem.*, 1955, **47**, 1253.
45. Eatough, D. J., White, F. V., Hansen, L. D., Eatough, N. L., and Ellis, E. C., *Anal. Chem.*, 1985, **57**, 743.
46. Anlauf, K. G., Fellin, P., Wiebe, H. A., Schiff, H. I., Makay, G. I., Braman, R. S., and Gilbert, R., *Atmos. Environ.*, 1985, **19**, 325.
47. Forrest, J., Spandau, D. J., Tanner, R. L., and Newman, L., *Atmos. Environ.*, 1982, **16**, 1473.
48. Spicer, C. W., Howes, J. E., Jr., Bishop, T. A., Arnold, L. H., and Stevens, R. K., *Atmos. Environ.*, 1982, **16**, 1487.
49. Roberts, J. M., Norton, R. B., Goldan, P. D., and Fehsenfeld, F. C., *J. Atmos. Chem.*, 1987, **5**, 217.
50. Roberts, J. M., Longford, A. O., Golden, P. D., and Fehsenfeld, F. C., *J. Atmos. Chem.*, 1988, **7**, 137.
51. Dimmock, N. A., and Marshall, G. B., *Anal. Chim. Acta*, 1987, **202**, 49.
52. Eatough, D. J., Vernon, F. W., Hansen, L. D., Eatough, N. L., and Cheney, J. L., *Environ. Sci. Technol.*, 1986, **20**, 867.
53. Lindqvist, F., *Atmos. Environ.*, 1985, **19**, 1671.
54. Lewin, E. E., and Hansen, A. K., *Anal. Chem.*, 1984, **56**, 842.
55. Liberti, A., Allegrini, I., Febo, A., and Possanzini, M., *in* Irgolic, K. J., and Martell, A. E., *Editors,* "Environmental Inorganic Chemistry," VCH, Deerfield Beach, FL, 1985, pp. 419–430.
56. Slanina, J., Doornenbal, L. V. L., Lingerak, A. W., and Meilof, W., *Int. J. Environ. Anal. Chem.*, 1981, **9**, 59.
57. Slanina, J., Schoonebeck, C. A. M., Klockow, D., and Niessner, R., *Anal. Chem.*, 1985, **57**, 1955.
58. Slanina, J., Schoonebeek, C. A. M., and Keuken, M. P., *Anal. Chem.*, 1987, **59**, 2764.
59. Slanina, J., Report No. ECN-88- Verslag Van Project 4458 Droge-En Natte Depoisitie (Uitqebreide versie) door, Netherlands Energy Research Foundation, Petten, Netherlands, May 1988.

Prediction of Retention Behaviour on Modification of the Mobile Phase in High-performance Liquid Chromatography Using Metal Ions: 2-Aminophenol as a Model System

Roger M. Smith and Simon J. Bale*
Department of Chemistry, University of Technology, Loughborough, Leicestershire LE11 3TU, UK
Stephen G. Westcott and M. Martin-Smith
Glaxo Group Research, Ware, Hertfordshire SG12 0DJ, UK

A model has been developed for predicting the effect of transition metals as components of the mobile phase in high-performance liquid chromatography on the retention of an analyte containing a chelating group. It takes into account the secondary chemical equilibria in solution, including the formation constants of the complexes, the pH of the mobile phase and the concentration of the metal ions. The model was tested by comparison with data determined for the retention of 2-aminophenol on a porous polystyrene - divinylbenzene polymer column in the presence of metal ions.

Keywords: *High-performance liquid chromatography; transition metal ions; mobile phase additives; metal chelates; retention prediction*

Considerable use has been made of metal ions and complexes to alter the selectivity of separations carried out by high-performance liquid chromatography (HPLC).[1,2] Metal ions provide a useful means of modifying retention as only specific chemical groups and ligands will interact with a given metal and the extent of the interaction can usually be regulated by adjusting the pH of the mobile phase. In addition, steric properties are important because metals have fixed co-ordination sites and this may, under certain conditions, lead to stereoselectivity. The metal species used to effect a separation may be present as part of the stationary phase or, alternatively, may be incorporated in the mobile phase as a free ion or complex.

Metal ions may be introduced on to the stationary phase by impregnation on the silica surface or by bonding via a suitable ligand attached to the surface.[3–5] Previous workers have made use of the reversible charge-transfer complexation between silver ions and π-donors in argentation chromatography.[6–8] Columns loaded with ruthenium[9] and cadmium ions[10] have also been used for the separation of unsaturated compounds. Eiceman and Janecka[11] have used the binding properties of surface-active silanol groups on octadecylsilyl bonded silica to immobilise a range of transition metals, including copper(II), nickel(II), cobalt(II) and zinc(II). A mixture of aniline and substituted amines was used to demonstrate the different selectivities that could be achieved using these columns.

Metal ions may also be incorporated in the mobile phase and there are several advantages in using this approach. Specialised stationary phases are difficult to prepare reproducibly and in most instances are not stable due to leaching of the metal ions. Changing from one metal to another is difficult if not impossible. If metal ions are incorporated in the mobile phase, the change from one metal to another may be performed by washing the column with a few column volumes of the new mobile phase to give conditions for which the metal concentration is known. In general, when metal ions are present on the stationary phase analyte retentions are increased and the peaks are broad. However, when metal ions are present in the mobile phase, mass transfer is improved considerably and more efficient peaks are obtained. The complexes may also be either less or more polar depending on the charge and hence the retentions may either be increased or decreased. Selectivity is, in general, achieved through differences in the stabilities of the complexes formed between the analytes and the metal ions in the mobile phase and the hydrophobicities of the resulting species.

Metal chelates, such as nickel β-diketonates[12,13] and C_{12}-dien complexes,[5] have also been used as mobile phase additives in conjunction with reversed-phase columns. By using chiral metal chelates, enantioselectivity can also be achieved.[1,2,14]

With the exception of silver ions[15] relatively little use has been made of simple metal salts as mobile phase modifiers. Copper(II) ions have been used to modify the separation of the colchicines[16] and zinc(II) to increase the separation of the isomeric aminobenzoic acids.[17] Sternson and co-workers[18,19] found that the addition of nickel acetate to the mobile phase could be used to enhance the resolution of 2-aminophenol and its metabolites. We have recently extended this last study and have reported a detailed examination of the effects of a range of metal ions on the retention of 2-aminophenol.[20] The work was carried out using a polystyrene - divinylbenzene column so that interactions with silanols which occur on a silica-based column would not interfere with the interpretation of the results. The aim was to use 2-aminophenol as a model compound to gain a more detailed understanding of the retention modification caused by simple transition metal ions in the mobile phase. All the metal ions studied caused a reduction in retention due to the formation of a more polar 1:1 complex (ML+, L = ligand) between the ligand and the metal ions. The magnitudes of the changes were related to the metal ion concentration and depended on the pH of the mobile phase.

In this paper, we have developed a general model for the observed changes in the capacity factors of chelating groups in the presence of metal ions which takes into account the interactions taking place in these separations and involves the various equilibria present in solution. The model can be correlated with the effects of changing the metal ions and their concentrations and has been tested against the experimental results.

Experimental

Reagents

* Present address: Pfizer Central Research, Sandwich, Kent CT13 9NJ, UK.

Laboratory-reagent grade ammonium acetate, acetates of copper and nickel, and methanol (HPLC grade) were

obtained from FSA Laboratory Supplies (Loughborough, Leicestershire, UK). 2-Aminophenol (Aldrich, Gillingham, Dorset, UK) was recrystallised from water before use.

Apparatus

The liquid chromatograph consisted of a Pye Unicam PU 4010 pump, a Rheodyne 7125 injection valve fitted with a 20-μl sample loop and a Pye Unicam PU 4020 variable-wavelength UV detector set at 280 nm. Chromatograms were recorded on a Linseis chart recorder and a Hewlett-Packard 3390A integrator. The separations were carried out using Shandon stainless-steel columns (100 × 5 mm i.d.), which had been slurry-packed with PLRP-S (porous polystyrene - divinylbenzene copolymer, 5 μm; Polymer Laboratories, Church Stretton, UK). The temperature of the column was maintained at 30 °C with a thermostated water-jacket. The mobile phase flow-rate was 1 ml min^{-1}. Measurements of pH were made on a Pye Unicam 390 pH meter.

Sample and Mobile Phase Preparation

Solutions of 2-aminophenol were prepared fresh in methanol and diluted to the required concentrations with distilled water.

The mobile phase was prepared from a stock solution of 2.6 M ammonium acetate by dilution with methanol and water to give a final concentration of ammonium acetate that was 0.26 M in methanol - water (20 + 80 V/V). Metal ions were added as required by the inclusion of the appropriate volume of 0.2 M metal acetate solutions in the buffer. In each instance the measured pH was adjusted to 7.24 with concentrated hydrochloric acid or sodium hydroxide solution (4 M). The mobile phase was de-gassed under vacuum in an ultrasonic bath before use.

Procedure

Injections (20 μl) of solutions of 2-aminophenol were made on to the column and were eluted with mobile phases containing metal ions (0–0.07 M). The effect of the pH of the mobile phase was studied using the polymer column, in the pH range 4–13, with each metal ion at a concentration of 0.02 M except for copper (0.0001 M).

Data Analysis

Least-squares correlations were carried out on an Apple II computer using Curfit (Interactive Microware, State College, PA, USA) and non-linear least-squares using Genstat 4.03 from Lawes Agricultural Trust, Rothamsted Experimental Station, on a Honeywell Multics computer.

Results and Discussion

The use of metal ions as part of the mobile phase to alter selectively the chromatography of 2-aminophenol is an example of the use of secondary chemical equilibria in HPLC.[21] Such secondary equilibria are important in other modes of HPLC, such as ion-pair chromatography,[22] in which the influence of the pairing ion and counter ion on the equilibria in solution is used to alter the distribution of the analyte between the mobile and stationary phases. The effect of the pH of the mobile phase on the retention of ionisable compounds is another example of the way in which secondary chemical equilibria may be used to alter the selectivity of a separation. The equilibria involved in the HPLC of acids, bases and ampholytes have been discussed by Horvath et al.,[23] who proposed equations to predict the capacity factors of ionisable compounds with a varying mobile phase pH.
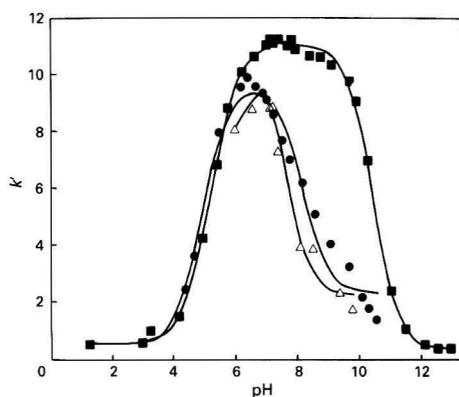
Fig. 1. Variation in the experimental capacity factor of 2-aminophenol with the mobile phase pH in: ■, the absence; and presence of nickel ions: ●, 0.01 M; and △, 0.02 M on a PLRP-S column. Solid lines are fitted curves from equations (32) and (35). Mobile phase, methanol - water (20 + 80 V/V) containing 0.26 M ammonium acetate

Secondary chemical equilibria have been reviewed by Karger et al.,[24] who looked at all uses of such equilibria in liquid chromatography. Vespalec et al.[25] have also discussed equilibria involving metal ions in HPLC but were concerned more with the separation of metal species than with the use of metal ions to modify retentions.

Retention Model

The use of metal ions to adjust retention will depend on the formation constants of the complex and the concentrations of the metal ions and ligand. If the latter is ionic its concentration will be dependent on the ionisation constant and the pH of the mobile phase. The over-all retention of the analyte will thus depend on a series of interconnected equilibria. Each species in the system will have a retention time which will be directly dependent on its distribution between the stationary and mobile phases. If the interchange between the species is rapid, the over-all retention time of the analyte should be represented by the ratio of the summation of the average time each of the species spends in the two phases. It should, therefore, be possible to generate a model of the chromatographic system which relates these different equilibria and which would be generally applicable to any metal - ligand combination. This model could then be used to predict the effects of using different metal ions or of changing the metal ion concentration or the pH of the mobile phase. The model should be capable of explaining the changes observed experimentally with 2-aminophenol and the equilibrium constants should have values that can be related to those obtained with non-chromatographic methods.

In developing a model based on the 2-aminophenol system it is first necessary to consider the situation in the absence of metal ions. 2-Aminophenol is an ampholyte in aqueous solution and can exist in three forms: the protonated amino cation (AH_2^+), the neutral molecule (AH) and the phenolate anion (A^-). In mobile phases with a low pH, 2-aminophenol will be present as a protonated amino cation and, as expected, a low retention is observed.[20] As the pH is increased the degree of protonation will decrease and an increase in retention is observed until at intermediate pH values (7–9) the analyte is mostly neutral and the retention reaches a maximum (Fig. 1). Finally, at higher pH values the phenol group will dissociate to give the negatively charged phenolate anion and again low retention times are observed. The well separated pK_a values for the two groups suggest that at the intermediate pH values 2-aminophenol will not be present as a zwitterion

$$[AH_2^+]_M \xrightleftharpoons{K_{a_1}} [AH]_M \xrightleftharpoons{K_{a_2}} [A^-]_M \xrightleftharpoons{K_1} [MA^+]_M \xrightleftharpoons{K_2} [MA_2]_M$$

Mobile phase

Stationary phase

$$[AH_2^+]_S \qquad [AH]_S \qquad [A^-]_S \qquad [MA^+]_S \qquad [MA_2]_S$$

Fig. 2. Equilibria involved in the HPLC of 2-aminophenol with metal ions in the mobile phase. M = mobile phase component; S = stationary phase component

and this can be confirmed by calculation. Hence the relative proportions of the three species are pH dependent and the equilibria between the three forms are governed by the dissociation constants of the amino and phenolic groups, K_{a1} and K_{a2}, respectively.

$$AH_2^+ \xrightleftharpoons{K_{a1}} AH + H^+ \quad .. \quad .. \quad .. \quad (1)$$

$$AH \xrightleftharpoons{K_{a2}} A^- + H^+ \quad .. \quad .. \quad .. \quad (2)$$
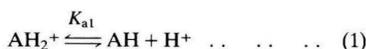
In the presence of metal ions (M^{2+}) the phenolate anion can form chelates and two further species are introduced into the over-all equilibrium, the 1 : 1 (MA^+) and the 2 : 1 (MA_2) chelates. The proportions of these two species are dependent on their respective formation constants, K_1 and K_2, and on the relative concentration of the anion $[A^-]$ to that of the metal ions $[M^{2+}]$.

$$A^- + M^{2+} \xrightleftharpoons{K_1} MA^+ \quad .. \quad .. \quad .. \quad (3)$$

$$MA^+ + A^- \xrightleftharpoons{K_2} MA_2 \quad .. \quad .. \quad .. \quad (4)$$
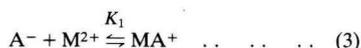
Because of complexation with the acetate buffer components at high pH, only a proportion of the added concentration of the metal ions will be available to complex with the anions. Hence the values of K_1 and K_2 will be the effective formation constants, which incorporate a factor for the acetate equilibria (which will be a constant at each pH and fixed acetate concentration), rather than the formation constants measured in aqueous solution.

The distribution of 2-aminophenol among the five possible species may be written as

$$AH_2^+ \xrightleftharpoons{K_{a1}} AH \xrightleftharpoons{K_{a2}} A^- \xrightleftharpoons{K_1} MA^+ \xrightleftharpoons{K_2} MA_2 \quad .. \quad (5)$$
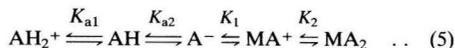
When 2-aminophenol is injected on to an HPLC column and eluted with an eluent containing metal ions, the same equilibria are set up in the mobile phase. Each of the species (X) present in the mobile phase is in turn in equilibrium with the stationary phase and is distributed between the mobile and stationary phases according to its distribution coefficient $(D_X = [X]_S/[X]_M)$ (Fig. 2).

As the separation occurs, each of the species will have its own individual capacity factor. However, as long as the exchange of the ligand between the different species is rapid, a single peak will be observed wit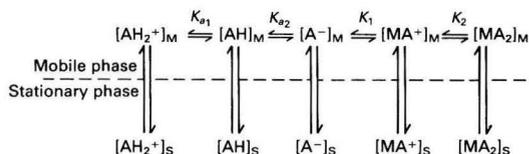h a capacity factor dependent on the over-all equilibrium of the analyte between the two phases. Hence the capacity factor under any set of conditions is dependent on the relative proportions of the individual

species and their individual capacity factors. At low pH the equilibrium shifts to the left and the observed capacity factor tends to that of the amino cation (AH_2^+). The introduction of metal ions, at above about pH 6, shifts the equilibrium to the right and the capacity factor tends to those of the chelates. Therefore, the capacity factor of 2-aminophenol may be controlled, and hence the selectivity of a separation of 2-aminophenol, by changing the position of the equilibrium by altering the pH, the metal ion concentration or by changing to a metal that forms either stronger or weaker chelates. Using these equilibria, a model that describes the retention can be generated.

The capacity factor (k') of a band of analyte passing through a column may be defined as

$$k' = \frac{\text{amount in stationary phase}}{\text{amount in mobile phase}} \quad .. \quad .. \quad (6)$$

The amount of the analyte in each phase will be equal to the concentration of each species multiplied by the volume of that phase. Hence, based on the equilibria for 2-aminophenol (Fig. 2), equation (6) may be written as

$$k' = \frac{[AH_2^+]_S V_S + [AH]_S V_S + [A^-]_S V_S + [MA^+]_S V_S + [MA_2]_S V_S}{[AH_2^+]_M V_M + [AH]_M V_M + [A^-]_M V_M + [MA^+]_M V_M + [MA_2]_M V_M} \quad (7)$$

If q is the phase ratio (V_S/V_M), i.e., the ratio of the volume of the stationary phase to that of the mobile phase, then

$$k' = q \left(\frac{[AH_2^+]_S + [AH]_S + [A^-]_S + [MA^+]_S + [MA_2]_S}{[AH_2^+]_M + [AH]_M + [A^-]_M + [MA^+]_M + [MA_2]_M} \right) (8)$$

The capacity factors of the individual species in the column may be defined as

$$\text{Protonated amine: } k'_b = \frac{q[AH_2^+]_S}{[AH_2^+]_M} \quad .. \quad (9)$$

$$\text{Neutral aminophenol: } k'_n = \frac{q[AH]_S}{[AH]_M} \quad .. \quad .. \quad (10)$$

$$\text{Phenolate anion: } k'_a = \frac{q[A^-]_S}{[A^-]_M} \quad .. \quad .. \quad (11)$$

$$1:1 \text{ chelate: } k'_{c1} = \frac{q[MA^+]_S}{[MA^+]_M} \quad .. \quad .. \quad (12)$$

$$2:1 \text{ chelate: } k'_{c2} = \frac{q[MA_2]_S}{[MA_2]_M} \quad .. \quad .. \quad (13)$$

By rearranging equations (9)–(13) to give expressions for the concentration of each species in the stationary phase, substituting these in equation (8) and cancelling the values for the phase ratio, equation (14) is obtained.

Dividing both top and bottom by $[AH]_M$ gives equation (15).

$$k' = \frac{k'_b[AH_2^+]_M + k'_n[AH]_M + k'_a[A^-]_M + k'_{c1}[MA^+]_M + k'_{c2}[MA_2]_M}{[AH_2^+]_M + [AH]_M + [A^-]_M + [MA^+]_M + [MA_2]_M} \quad .. \quad .. \quad .. \quad .. \quad (14)$$

$$k' = \frac{k'_b[AH_2^+]_M/[AH]_M + k'_n[AH]_M/[AH]_M + k'_a[A^-]_M/[AH]_M + k'_{c1}[MA^+]_M/[AH]_M + k'_{c2}[MA_2]_M/[AH]_M}{[AH_2^+]_M/[AH]_M + [AH]_M/[AH]_M + [A^-]_M/[AH]_M + [MA^+]_M/[AH]_M + [MA_2]_M/[AH]_M} \quad .. \quad .. \quad (15)$$

The equilibrium constant for each species in the mobile phase may be defined as

$$K_{a1} = \frac{[H^+]_M[AH]_M}{[AH_2^+]_M} \qquad \cdots \qquad \cdots \qquad \cdots \quad (16)$$

$$K_{a2} = \frac{[A^-]_M[H^+]_M}{[AH]_M} \qquad \cdots \qquad \cdots \qquad (17)$$

$$K_1 = \frac{[MA^+]_M}{[M^{2+}]_M[A^-]_M} \qquad \cdots \qquad \cdots \qquad (18)$$

$$K_2 = \frac{[MA_2]_M}{[MA^+]_M[A^-]_M} \qquad \cdots \qquad \cdots \qquad (19)$$

Each of these expressions may be rearranged to give an equation for the equilibrium concentration of the analyte species in the mobile phase divided by the concentration of the neutral aminophenol ([AH]$_M$).

Rearranging equation (16) gives

$$\frac{[AH_2^+]_M}{[AH]_M} = \frac{[H^+]_M}{K_{a1}} \qquad \cdots \qquad \cdots \qquad (20)$$

Rearranging equation (17) gives

$$\frac{[A^-]_M}{[AH]_M} = \frac{K_{a2}}{[H^+]_M} \qquad \cdots \qquad \cdots \qquad (21)$$

Rearranging equation (18) gives

$$[MA^+]_M = K_1[M^{2+}]_M[A^-]_M \qquad \cdots \qquad \cdots \qquad (22)$$

Rearranging equation (17) to give an expression for [A$^-$]$_M$, we obtain

$$[A^-]_M = \frac{K_{a2}[AH]_M}{[H^+]_M} \qquad \cdots \qquad \cdots \qquad (23)$$

Substituting in equation (22) for [A$^-$]$_M$ from equation (23) and rearranging gives

$$\frac{[MA^+]_M}{[AH]_M} = \frac{K_1K_{a2}[M^{2+}]_M}{[H^+]_M} \qquad \cdots \qquad (24)$$

Rearranging equation (19) gives

$$[MA_2]_M = K_2[MA^+]_M[A^-]_M \qquad \cdots \qquad \cdots \qquad (25)$$

Dividing both sides of equation (25) by [AH]$_M$ and substituting for [MA$^+$]$_M$/[AH]$_M$ from equation (24) gives

$$\frac{[MA_2]_M}{[AH]_M} = \frac{K_1K_2K_{a2}[M^{2+}]_M[A^-]_M}{[H^+]_M} \qquad \cdots \qquad (26)$$

By substituting equations (20), (21), (24) and (26) in equation (15), and cancelling the [AH]$_M$ terms, the capacity factor can be expressed in terms of the variables of pH and metal ion concentration [equation (27)]. We can assume that protons and free metal ions have a negligible distribution into the stationary phase so that [M^{2+}]$_M$ = [M^{2+}] and [H$^+$]$_M$ = [H$^+$] and is, therefore, directly related to the pH.

Equation (27) therefore describes the anticipated variation of the capacity factor of 2-aminophenol with the pH and metal ion concentration. It is a general model equation and could be applied to any similar metal ion - ligand system. For ligands that are not basic, the k'_b terms would be omitted. The equation also allows for the possibility that some of the 2:1 chelate may be formed during chromatography. However, this term contains an expression for the concentration of the

Table 1. Variation of the capacity factor of 2-aminophenol with the concentration of analyte and nickel ions. Mobile phase: methanol - water (20 + 80 V/V) containing 0.26 M ammonium acetate, pH 7.24. Column: PLRP-S

| | Capacity factor | | |
| 2-Aminophenol | Ni^{2+} concentration/M | | |
concentration/M	0	0.04	0.06
10^{-2}	11.70	7.02	4.05
10^{-3}	11.77	7.27	4.11
10^{-4}	11.73	7.33	4.11
10^{-5}	—	7.29	4.15
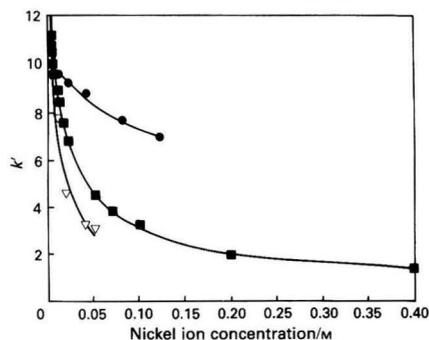
Fig. 3. Experimental and fitted data for the variation of the capacity factor (k') of 2-aminophenol with the nickel ion concentration on a PLRP-S column. Mobile phase, methanol - water (20 + 80 V/V) containing 0.26 M ammonium acetate. Experimental data at: ●, pH 6; ■, pH 7.24; and ▽, pH 8. The lines are fitted curves from equation (33)

anion [A$^-$]$_M$. As the anion concentration is dependent on the amount of analyte [AH] [equation (17)], the predicted retention would appear to be dependent on the sample size. However, in many instances K_2 is much smaller than K_1 so that the formation of any 2:1 chelate will be negligible. In addition, the metal ion concentration in the mobile phase (0.01–0.4 M) is in a large excess compared with the analyte concentration, which would be 0.001 M in the sample solution and will be diluted to 0.00001 M during elution, again favouring the 1:1 complex.

At the other extreme if the formation of the 2:1 complex is highly favoured, all the analyte may be converted to the complex, effectively giving on-column derivatisation and the retention is then that of the neutral ML$_2$ complex. This situation has been observed in the determination of dithiocarbamates with a mobile phase containing transition metal ions.[26]

In intermediate situations, when the formation of the neutral 2:1 complex is slightly preferred over the 1:1 complex, the over-all retention calculation would become more complex.

With 2-aminophenol it was found, in practice, that the retention was independent of the sample size provided that the analyte concentration was low (10^{-3} M or less, Table 1). In this instance the over-all equation may therefore be simplified by omitting the final terms relating to [MA$_2$] to give equation (28). In the absence of metal ions (i.e., when [M^{2+}] = 0) this equation may be reduced still further to an equation which

$$k' = \frac{k'_n + k'_b[H^+]_M/K_{a1} + k'_aK_{a2}/[H^+]_M + k'_{c1}K_{a2}K_1[M^{2+}]_M/[H^+]_M + k'_{c2}K_1K_2K_{a2}[M^{2+}]_M[A^-]_M/[H^+]_M}{1 + [H^+]_M/K_{a1} + K_{a2}/[H^+]_M + K_{a2}K_1[M^{2+}]_M/[H^+]_M + K_1K_2K_{a2}[M^{2+}]_M[A^-]_M/[H^+]_M} \qquad \cdots \qquad \cdots \quad (27)$$

$$k' = \frac{k'_n + k'_b[H^+]/K_{a1} + k'_aK_{a2}/[H^+] + k'_{c1}K_{a2}K_1[M^{2+}]/[H^+]}{1 + [H^+]/K_{a1} + K_{a2}/[H^+] + K_{a2}K_1[M^{2+}]/[H^+]} \qquad \cdots \qquad \cdots \qquad \cdots \qquad \cdots \quad (28)$$

describes the variation of the capacity factor of the ligand with pH [equation (29)].

$$k' = \frac{k'_n + k'_b[H^+]/K_{a1} + k'_a K_{a2}/[H^+]}{1 + [H^+]/K_{a1} + K_{a2}/[H^+]} \quad \cdot \cdot \text{ (29)}$$

Equation (29) is similar to that derived by Horvath et al.[23] for the effect of pH on an ampholyte or zwitterion and contains the two equations derived independently by Miyake et al.[27] and Horvath et al.[23] for the determination of dissociation constants by HPLC [equations (30) and (31)]. The derivation of these two equations was based on a similar but simpler model to give expressions for the variation of the capacity factor of a basic and an acidic compound with pH, respectively.

$$k' = \frac{k'_n + k'_a K_{a2}/[H^+]}{1 + K_{a2}/[H^+]} \quad \cdot \cdot \quad \cdot \cdot \quad \cdot \cdot \text{ (30)}$$

$$k' = \frac{k'_n + k'_a[H^+]/K_{a1}}{1 + [H^+]/K_{a1}} \quad \cdot \cdot \quad \cdot \cdot \text{ (31)}$$

These expressions describe sigmoidal curves (similar to those of pH titrations) as k' varies between the extremes of the neutral (k'_n) and fully ionised anionic (k'_a) forms.

Testing the Model Equation

Equations (28) and (29), derived for the variation of the capacity factor of 2-aminophenol with the pH and metal ion concentration, were tested by comparison with the experimental observations using a non-linear least-squares computer program. The program fitted simplified versions of the equations to the experimental data and reported values of the fitted capacity factor for the experimental conditions of variation of pH or metal ion concentration. The accuracy of the fitted data was then assessed by plotting graphs of fitted capacity factors versus experimental capacity factors and obtaining correlation coefficients by linear least-squares calculation.

In mobile phases free from metal ions equation (29) applies and can be expressed as

$$k' = \frac{A + Bx + C/x}{1 + Dx + E/x} \quad \cdot \cdot \quad \cdot \cdot \quad \cdot \cdot \text{ (32)}$$

where $x = [H^+]$ and A, B, C, D and E are constants related to those in equation (29). This relationship was fitted to the experimental data obtained for the variation of the capacity factor of 2-aminophenol with the mobile phase pH and a close correlation was found between the experimental values and the fitted curve (Fig. 1). A linear correlation of the fitted data versus experimental data gave a close relationship with an intercept of 0.00429 and a correlation coefficient of 0.998,
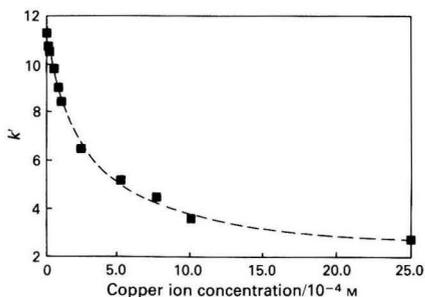
showing that equation (29) had accurately described the experimental measurements.

Using the values of $A-E$ from the regression, it was possible to determine the values for the ionisation constants; $pK_{a1} = 5.13$ and $pK_{a2} = 10.34$. These values agree with those obtained from a spectroscopic study of $pK_{a2} = 10.40$ in methanol - water and are similar to those for aqueous solutions, $pK_{a1} = 4.79$ and $pK_{a2} = 9.97$.[28]

The full model, equation (28), was then examined by considering the variation in the capacity factor of 2-aminophenol with the metal ion concentration at a constant pH. In a previous paper[20] we noted that the effect of the transition metal ions on the retention of 2-aminophenol depended directly on the metal ion concentration and also decreased in the order $Cu^{2+} >>> Ni^{2+} > Co^{2+} > Zn^{2+} > Cd^{2+} > Mn^{2+}$, which corresponded to the decrease in the magnitude of formation constants (K_1) for the 1 : 1 complexes.

If the pH of the mobile phase is kept constant, equation (28) can be simplified to give

$$k' = \frac{F + G[M^{2+}]}{1 + H[M^{2+}]} \quad \cdot \cdot \quad \cdot \cdot \quad \cdot \cdot \text{ (33)}$$

where F, G and H are constants related to the terms in equation (28). The formation constant, K_1, of the 1 : 1 chelate can be calculated from H if pK_{a1} and pK_{a2} are known. The capacity factor of the 1 : 1 chelate, k'_{c1}, can be calculated from

$$G/H = k'_{c1} \quad \cdot \cdot \quad \cdot \cdot \quad \cdot \cdot \text{ (34)}$$

Equation (33) was fitted to four sets of experimental data obtained previously for the changes in the capacity factor of 2-aminophenol with the metal ion concentration.[20] The correlations between the calculated values and the experimental values for Ni^{2+} at pH 6, 7.24 and 8, and for Cu^{2+} at pH 7.24 were all very close (Figs. 3 and 4 and Table 2). This showed that equation (28) was accurately describing the variation of k' with the metal ion concentration.

The formation constants, K_1, for the nickel and copper chelates were calculated from the constants (Table 3) using the pK_a value for the phenolic group obtained earlier ($pK_{a2} = 10.34$). The formation constants for nickel complexes at the different pH values were in reasonable agreement and the differences between them are probably due to the practical difficulties of obtaining values of k' approaching that of k'_{c1}.

However, although as expected the derived values for the formation constant of copper (log $K_1 = 6.69$ at pH 7.24) are relatively much greater than those for nickel (mean, log $K_1 = 4.59$), both these effective formation constants are considerably lower than those reported in the literature for aqueous solutions (Cu^{2+}, log $K_1 = 9.25$ and Ni^{2+}, log $K_1 = 6.10$).[29] These differences are probably due to the presence of methanol in the mobile phase and to an interaction of the

Fig. 4. Experimental data for the variation of the capacity factor (k') of 2-aminophenol with the copper ion concentration on a PLRP-S column. The broken line is the fitted curve. Mobile phase, methanol - water (20 + 80 V/V) containing 0.26 M ammonium acetate at pH 7.24

Table 2. Correlation of the calculated and experimental capacity factors of 2-aminophenol with changes in the metal ion concentration

Metal ion				pH	Slope	Intercept	Correlation coefficient
Ni^{2+}	..	..	..	6.0	0.973	0.229	0.994
Ni^{2+}	..	..	..	7.24	0.947	0.065	0.996
Ni^{2+}	..	..	..	8.0	0.990	0.073	0.995
Cu^{2+}	..	..	..	7.24	0.995	0.048	0.999

Table 3. Formation constants of 2-aminophenol chelates determined by HPLC

Metal ion				pH	$Log_{10} K_1$
Ni^{2+}	..	..	..	6.0	4.20
Ni^{2+}	..	..	..	7.24	4.67
Ni^{2+}	..	..	..	8.0	4.85
Cu^{2+}	..	..	..	7.24	6.69

metal ions with acetate ions in the mobile phase thus reducing their effective concentration.[30]

From the values of the empirical constants in equations (32) and (33) and the values of K_{a1}, K_{a2} and K_1, it is possible to determine the individual capacity factors; $k'_n = 11.08$, $k'_b = 0.58$, $k'_a = 0.22$; $k'_{c1}(Ni^{2+}) = 0.69$; and $k'_{c1}(Cu^{2+}) = 1.86$ [column, PLRP-S; mobile phase, methanol - water $(20 + 80$ $V/V)$ containing 0.26 M ammonium acetate; pH, 7.24]. As expected, the capacity factor of the neutral species (k'_n) was large whereas those of the ionised species (k'_b) and (k'_a) were low and corresponded to the values found experimentally (Fig. 1). The capacity factors of the ionised $1:1$ complexes were also small.

In a final comparison, the effect of changing the pH at a constant metal ion concentration was examined. Equation (28) can be simplified to give

$$k' = \frac{A + Bx + J/x}{1 + Dx + K/x} \ldots \ldots \ldots \ldots (35)$$

where A, B and C are the same constants as in equation (32) and J and K are constants which take into account the formation constant of the $1:1$ chelate and the metal ion concentration. The equation was fitted to data obtained for mobile phases containing 0.01 or 0.02 M Ni^{2+} (Fig. 1). However, the correlation was poorer than obtained previously and at high pH values the expression levelled out, suggesting higher values for k'_a of approximately 2. This anomaly probably arises because few experimental points could be obtained at pH values greater than 10 due to the insolubility of the nickel salts.

Conclusion

The model equation appears to give a good correlation between the experimental results and theory, suggesting that it correctly describes the experimental system. The values for the capacity factors and ionisation constants, which can be derived from the equation, agree well with those obtained by alternative techniques, but the formation constants of the complexes are much smaller than those reported for aqueous solutions, probably because of competing reactions from the buffer components and the presence of methanol in the mobile phase.

References

1. Davankov, V. A., *Adv. Chromatogr.*, 1980, **18**, 139.
2. Grushka, E., and Leshem, R., *Trends Anal. Chem.*, 1981, **1**, 95.
3. Chow, F. K., and Grushka, E., *Anal. Chem.*, 1977, **49**, 1756.
4. Chow, F. K., and Grushka, E., *Anal. Chem.*, 1978, **50**, 1346.
5. Cooke, N. H. C., Viavattene, R. L., Eksteen, R., Wong, W. S., Davies, G., and Karger, B. L., *J. Chromatogr.*, 1978, **149**, 391.
6. Vivilecchia, R., Thiébaud, M., and Frei, R. W., *J. Chromatogr. Sci.,* 1972, **10**, 411.
7. Aigner, R., Spitzy, H., and Frei, R. W., *Anal. Chem.*, 1976, **48**, 2.
8. Lam, S., and Grushka, E., *J. Chromatogr. Sci.*, 1977, **15**, 234.
9. Mikes, F., Schurig, V., and Gil-Av, E., *J. Chromatogr.*, 1973, **83**, 91.
10. Kunzru, D., and Frei, R. W., *J. Chromatogr. Sci.*, 1974, **12**, 191.
11. Eiceman, G. A., and Janecka, F. A., *J. Chromatogr. Sci.*, 1983, **21**, 555.
12. Lochmüller, C. H., and Hangac, H. H., *J. Chromatogr. Sci.*, 1982, **20**, 171.
13. Lochmüller, C. H., Hill, W. B., Porter, R. M., Hangac, H. H., Culberson, C. F., and Ryall, R. R., *J. Chromatogr. Sci.*, 1983, **21**, 70.
14. Lindner, W., LePage, J. N., Davies, G., Seitz, D. E., and Karger, B. L., *J. Chromatogr.*, 1979, **185**, 323.
15. Vonach, B., and Schomburg, G., *J. Chromatogr.*, 1978, **149**, 417.
16. Lacey, E., and Brady, R. L., *J. Chromatogr.*, 1984, **315**, 233.
17. Walters, V., and Raghavan, N. V., *J. Chromatogr.*, 1979, **176**, 47.
18. Sternson, L. A., and DeWitte, W. J., *J. Chromatogr.*, 1977, **137**, 305.
19. Sternson, L. A., Dixit, A. S., Riley, C. M., Siegler, R. W., and Schoech, D., *J. Pharm. Biomed. Anal.*, 1983, **1**, 105.
20. Smith, R. M., Bale, S. J., Westcott, S. G., and Martin-Smith, M., *Analyst*, 1987, **112**, 1209.
21. Foley, J. P., and May, W. E., *Anal. Chem.*, 1987, **59**, 102.
22. Hearn, M. J. W., *Editor*, "Ion-pair Chromatography," Chromatographic Science Series, Volume 31, Marcel Dekker, New York, 1985.
23. Horvath, C., Melander, W., and Molnar, I., *Anal. Chem.*, 1977, **49**, 142.
24. Karger, B. L., LePage, J. N., and Tanaka, N., *High-performance Liq. Chromatogr., Adv. Perspect.*, 1980, **1**, 113.
25. Vespalec, R., Vrchlabsky, M., and Cigankova, M., *J. Chromatogr.*, 1977, **141**, 313.
26. Smith, R. M., Morarji, R. L., and Salt, W. G., *Analyst*, 1981, **106**, 129.
27. Miyake, K., Okumura, K., and Terada, H., *Chem. Pharm. Bull.*, 1985, **33**, 769.
28. Albert, A., and Serjeant, E. P., "The Determination of Ionization Constants," Third Edition, Chapman and Hall, London, 1984.
29. Sims, P., *J. Chem. Soc.*, 1959, 3648.
30. Fuentes, R., Morgan, L. O., and Matwiyoff, N. A., *Inorg. Chem.*, 1975, **14**, 1837.

Design of a Computer-controlled Electroanalytical System

Richard M. Miller
Unilever Research Port Sunlight Laboratory, Quarry Road East, Bebington, Wirral, Merseyside L63 3JW, UK

Kathryn E. Thomas
Department of Instrumentation and Analytical Science, University of Manchester Institute of Science and Technology, P.O. Box 88, Manchester M60 1QD, UK

A dedicated high-level computer language has been written for use with a computer-controlled electroanalytical system. The language can be compiled to produce executable machine code modules, and provides considerable flexibility in the design of experiments. The compiled modules can be linked to programs in other high-level languages, allowing very complex strategies to be implemented. The language is sufficiently general to allow extension to the control of other types of analytical instrumentation.

Keywords: *Computer control; real-time control languages; electrochemistry*

The introduction of microprocessors and microcomputers over the last ten years has had an enormous impact on the design and use of analytical instrumentation.[1] Nearly all new commercial analytical instruments of any complexity now include a microprocessor or microcomputer for automatic control of the measurement process or manipulation of the data, or both. The impact of these developments in instrument control and data analysis on the work of an analytical scientist has been large, significantly changing the scientist's role from being a skilled manipulator of experimental apparatus to being a skilled designer and interpreter of experiments.

However, the design of many computer-controlled analytical instruments does not take full advantage of the flexibility available with computer control. Instead, effort has been concentrated on computerising existing experimental strategies and making the system accessible to the professional analytical scientist, without requiring any computer skills. This has led to the development of instruments that are close copies of earlier analogue or digital instrumentation. These systems are often "closed," in that they cannot easily be modified. As a result, the user is dependent on the skill of the designer in selecting the types and range of experiments that will be permitted, and prevented from adopting his traditional role in modifying, developing and improving experimental methodology. Instead of liberating the experimenter, computer control may lead to a situation where the user can devise an experiment which is physically possible using the equipment available, but which cannot be performed because of the limitations of the software.

To try and overcome these perceived difficulties, we have been exploring alternative control strategies in an attempt to find one that meets the practical requirements of the measurement scientist. As a model for a typical computer-controlled instrument, we have chosen an electroanalytical system. Analytical electrochemistry uses a very wide range of different perturbation experiments to characterise the system being studied and therefore requires a flexible control system. Many of the techniques involve the measurement of system responses to transient perturbations, requiring high speed and precisely timed interaction between the control system and the experiment. Further, as the inputs to and outputs from an electrochemical experiment are electrical, interfacing is not difficult and effort can be concentrated on the control system.

Design Criteria for a Control System

A computer control system for an analytical instrument should have the following characteristics. 1. Flexibility; it should be possible to specify any experimental protocol that the in-

strumentation is physically capable of carrying out. 2. Compatibility; once an experiment has been defined, it should be possible to execute the experiment from within another program. 3. Convenience; the system should have a good "human interface" which allows a wide variety of scientists to take advantage of the inherent flexibility.

The requirement for flexibility is paramount. All design choices place limits on what can be achieved within a particular system, but the constraints should be selected carefully to preserve flexibility. Without flexibility it is difficult to introduce new measurement methods and procedures, leading to stagnation and a reduction in innovation. Inappropriate methods may be used simply because it is too difficult to change the measurement system.

Compatibility is required to allow communication between the experimental system and other software, enabling a previously defined experiment to be executed from within another computer program. If this is possible, a much wider variety of experimental protocols can be used, significantly enhancing the flexibility of the system. For example, more sophisticated data analysis and interpretation procedures could be employed. A series of experiments could be carried out automatically using different experimental parameters to validate the data or further characterise the system. Pattern search techniques could be used to optimise the experimental conditions. Ideally, the defined experiment should exist as an executable module that may be called from within programs written in a wide range of languages and which can exchange data with the calling program.

Finally, the control software must be structured so that users with a wide variety of levels of computer skill should be able to use it. There is very little point in producing a system of high flexibility, which appears so complex to the users that they are unable to use it with confidence. If they do not trust the measurement system, they will not trust the results and will seek alternative methods to obtain the information required. This also implies that extensive error checking is required in the control software to ensure that the user is specifying a valid experiment.

The "human interface" between an operator and the control program of a laboratory computer has been studied by Ziegler[2] who considered that there were three possible approaches to communication between the operator and the computer program. 1. The user identifies a pre-defined "method" for which all required parameters have already been specified. 2. The program leads the user through a question and answer sequence to select the "method" and supply the required parameters. 3. The user defines the "method" and the required parameters by entering specific

commands taken from an application-oriented command language.

Each approach has distinct advantages and disadvantages. The use of pre-defined methods was thought to be convenient if a certain type of analysis with a given set of parameters were to be performed frequently, effectively a "turnkey" operation. However, if requirements change, this method of selection tends to reinforce the use of previously specified compromise "methods" which may not give optimum results in the new environment. This approach allows operation by very inexperienced users, but at the cost of a considerable reduction in flexibility.

Question and answer dialogues, or the use of "menus" from which selections are made, can be useful for the occasional user who can be guided through a hierarchical tree structure to select and define the method. This is the method most widely employed in commercial instrumentation, and has been used successfully for voltammetric measurements.[3-5] It offers a useful compromise between flexibility and user convenience. A wide range of options can be catered for, but the highly structured command sequence ensures that the inexperienced user can only choose compatible options and reasonable parameters for the experiment. However, every type of experiment to be performed must be included in the original design for the system, so that the appropriate menus and parameter validation can be included. To that extent it suffers the same disadvantages as the turnkey system; modification or extension of the system is difficult and unlikely to be a practical operation for the user. Software upgrades may be available from the manufacturer, but will only be produced to meet the common needs of a number of users, rather than the specific needs of an individual. It has also been noted that menu-driven systems can be irritating for experienced users because of the time-consuming nature of such dialogues and the amount of extraneous information which is displayed.[2]

Application-oriented command languages speed up communications with the computer, as only those parameters which actually need to be defined are referred to by the user. However, the system is more complex to use, as the operator must be familiar with the syntax and operation of all of the commands necessary for the correct operation of the instrumentation. Hence, the approach is more suited to the experienced daily user who is faced with the need to use a wider variety of experiments than can be accommodated in the turnkey approach. It is less appropriate for occasional users than the question and answer approach.

One such application-oriented command language is the problem oriented language (POL) devised by Finger[6-8] for data analysis. The use of an application-oriented command language enabled the programmer to develop a new language tailored to the specific problem. POL allowed a flexible order of entry for the input. More than one command could be placed on the same line and "filler" words could be included in the input line to aid understanding and give the language a more natural feel. These words would be ignored in processing. The POL system took these input lines and translated them into a series of calls to specific sub-routines to carry out the individual operations. Provision was also made for the system to use previously recorded command files and to be able to simulate a hierarchical question and answer user interface for less experienced users. One of the main disadvantages of POL was the large size of the program. The use of filler words and flexible input order meant that the part of the program dealing with input validation and keyword extraction was complex, large and slow. Although these features contributed to a flexible and comprehensible input format, there was a heavy price to pay in operational efficiency. A more concise form of input would simplify the translation process.

Prendergast et al.[9] have described the use of a general-purpose robot control language, using the plain language programming system SAVVY. The robot required programming in Tiny-BASIC, which is not very user friendly. SAVVY was used to produce/generate a control system which took commands in plain language and converted them into the appropriate instructions in Tiny-BASIC to program the robot. The system was able to determine the meaning of imprecise instructions so that it could deal with mis-spellings and alternative phraseologies. An important feature of this system was that all inputs were broken down into a series of primitive operations which could actually be executed by the robot. This is a key feature of robot and instrument control strategies and it is widely implemented in both commercial and experimental control systems.

ARTS is another robot control language, which was developed by Schlieper et al.[10] to control a ZYMATE 1 laboratory robot. Again, this language builds up a program to execute a given function from a series of elementary sub-operations. In this instance the language is designed to be used with programmable robots and laboratory instrumentation, and provides an interface for the user between the various programming languages and methods of different instruments, and a common descriptive system. When a program is executed, the operations specified are broken down into the appropriate coded instructions which must be sent to the particular device being addressed and then transmitted. The ARTS system is also programmed to translate messages and data from the instruments into the ARTS environment.

As each approach to the problem of the main-machine interface has specific applications, we decided to develop a control system which would be capable of generating application programs for each of the three approaches. This can be accomplished by producing a system based on an applications-oriented command language. Such a system would provide the desired flexibility and would meet the requirements of compatibility with other programs as the command list would be translated into an executable form which could be stored as a separate module and called from another executing program. Because experiments can be defined and stored in an executable form, it is relatively simple to provide a supervisor program which communicates with the user via a question and answer dialogue, selecting experiments from a library and passing the required parameters to the experiment module. Similarly, a turnkey system could be devised.

Having decided that an application-oriented command language is required, the question of programming environment must be faced. All computers execute programs in machine code; a series of primitive operations microprogrammed into the processor itself.[11] The microprogrammed instruction set is small and does not include many of the more complex operations which are useful in practical programming. Various high-level programming languages have, therefore, been created which allow the convenient development of complex programs, and which are then translated into machine code for execution by the computer.

An application-oriented command language would consist of a set of commands with associated parameters which cause certain specific operations to be carried out. As there will not be one to one mapping between the primitive operation required for the experiment and the primitive operations provided by the processor, it is clear that a translation step will be required. Machine code or assembler language would not be suitable for the creation of a control language, unless the microprogramming of the processor can be changed so that the required primitives are available. Specialist processors have been manufactured for a variety of applications, including sound generation and video display,[12,13] but they are only cost effective where a generic problem is involved, which can justify specialised fabrication. In the area of controllers for scientific instrumentation such generic solutions are not feasible, as the primitive operations are different in each

instance. Machine code and assembler language have been used successfully for the control of electrochemical experiments, but have been limited to simple turnkey systems where flexibility was not a requirement.[14,15] However, in order to achieve the goals set out above in a practical system, we feel that a high-level command must be developed, which will be translated into machine code.

There are three different ways in which a sequence of commands in a high-level language can be translated into a sequence of machine code instructions which can be executed. The program can be compiled as with FORTRAN, interpreted as with BASIC or compiled and interpreted as with threaded interpreted languages such as FORTH. In a compiled language the sequence of commands is translated, or compiled, as one operation to generate the machine code program. This is then linked with machine code sub-routines from a library to carry out any specialised primitive operations required by the language definition. The result of these operations is an executable machine code module. Error checking and input validation is carried out during the compilation step. The advantages of this approach are separation of translation and execution, and the reproducible generation of an executable module. It is possible to generate an exact mapping between the high-level commands and the corresponding machine code, which means that exact timing of operation can be achieved for real-time control. Disadvantages are the size and complexity of compilers, and the fact that unlike interpreters and threaded interpreted languages, they cannot readily be used for interactive program development.

In interpreted languages, command lines are translated and executed one at a time, following the logic flow defined in the program. Each line is checked for correct syntax and valid use of keywords and variable names. If there are any errors, an error message is generated and execution stops. If the line is valid, it is translated and executed. The next line is then interpreted in a similar way. This method has the advantages that interpreters are simpler and smaller programs than compilers, and that an interpreted language can be used interactively. However, because each instruction is validated and translated each time it is executed, interpreted languages are slow. Further, because of various housekeeping operations which occur in computers running interactively, it is impossible to predict the precise timing of the operations except under very limited circumstances.[5] One solution to this difficulty is to use machine code sub-routines for critically timed operations, called from supervisory programs written in an interpreted language. This approach has been used by Bond and co-workers[16,17] and Ploegmakers et al.[18] However, using experiment designs which call for a sequence of timed operations is difficult, as the uncertainty introduced by a series of calls from the high-level language means that extensive re-writing of the software may be required to reduce the number of calls needed. This inevitably makes the development of new methodologies time consuming, and requires considerable expertise on the part of the user.

Threaded interpreted languages (TILs) have found wide application for control of experimental equipment.[19] TILs differ from both compilers and interpreters in the method of execution of the program. The functional unit in TILs is the "word." Each word is defined in terms of a limited number of built-in primitive operations or other previously defined words. A threaded code interpreter produces a fully analysed internal form, consisting of a list of addresses of other previously defined words. The list is "threaded" together during the first, compilation stage. During the second stage the interpreter executes consecutive words with no further analysis or search being necessary. TILs normally have a wide range of primary internal operations, and the compilation mode allows great flexibility in the creation and definition of secondary words. Data are handled by last in first out stacks to conserve memory space and reverse polish notation is used to allow easy analysis of the instruction in terms of stack operations. TILs are superficially very attractive for this application. They are very compact, flexible and fast. However, their use of stacks and reverse polish notation makes them difficult for the novice user. In addition, the time taken to execute a particular secondary word depends on the way in which it is defined. Precise timing is difficult to establish. Finally, the enormous flexibility of TILs makes it difficult to ensure that only valid operations are carried out. TILs are therefore only likely to be of use to the experienced and competent user.

Despite the apparent problems, a microcomputer-controlled polarograph has been designed using FORTH as the programming language.[20] However, no rapid scan techniques were attempted so the accuracy and reliability of precisely timed sequences were not tested.

From discussions such as the foregoing, we concluded that the most appropriate choice of control system would be an application-oriented command language designed to be compiled into a directly executed machine code module. In the following sections the design and testing of a computer-controlled voltammetry system based on these principles are described.

Experimental

Instrumentation

A schematic diagram of the instrumentation used is shown in Fig. 1. A commercial microcomputer was chosen to control the instrumentation system and to act as the software development environment. A BBC Model B computer (Acorn Computers) with dual disk drives for data and program storage was used. A feature of the BBC microcomputer is the 1 MHz expansion bus, which can be used to control various peripheral devices. The various modules of the voltammetry system communicated with the BBC microcomputer through a local system bus, which was interfaced to the 1 MHz bus through a buffer card. The potentiostat was a standard three-amplifier design[21] modified to allow digital control of the current follower gain and connection/disconnection to the electrochemical cell. A schematic diagram of this system is shown in Fig. 2. The control voltage to the potentiostat was provided by a 12-bit digital to analogue converter interfaced to the system bus. The output from the current follower was passed to a 12-bit analogue to digital converter (ADC) card, which transferred digitised values to the computer. The electrode system was a static mercury drop electrode (Model 303, EG & G Instruments). A digital output
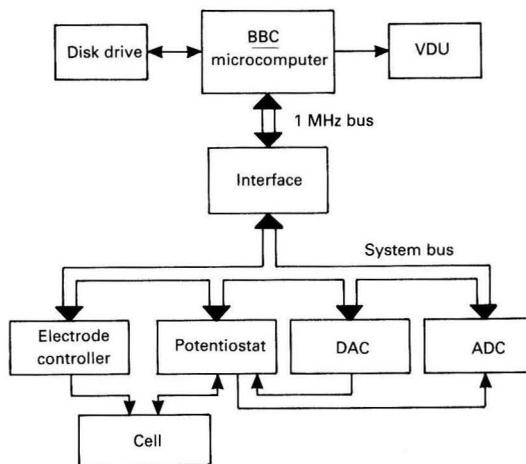

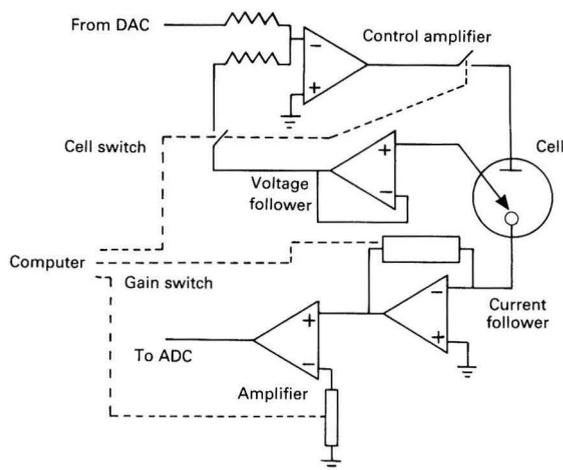**Fig. 1.** Schematic diagram of the experimental instrumentation

Fig. 2. Schematic diagram of the computer-controlled potentiostat

A: Initialise system
B: Set potential
C: Create new drop
D: Delay
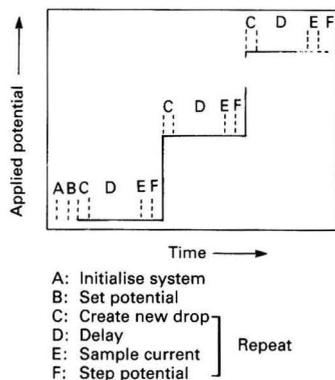E: Sample current
F: Step potential

Repeat

Fig. 3. Decomposition of a voltammetric experiment into primitive operations

card was provided to control the various functions of the static mercury drop electrode. Full details of this system will be published elsewhere.[22,23]

Software

In order to meet the requirement for a highly flexible and expandable system, it was necessary to identify the primitive operations, which would correspond to the various keywords of the high-level control language. A large number of existing voltammetric techniques were analysed to determine the minimum number of operations into which they could be decomposed. Fig. 3 shows how a typical voltammetric technique, in this instance staircase voltammetry, can be represented using a small group of operations. Common elements were identified across the set of techniques and from these the individual primitive operations were identified. In addition to the operations required for directly driving the potentiostat and for the data acquisition process, there were a number of program control operations. Specific operations were also required to control the electrode system. These latter primitive operations were specific to the particular instrumentation being used, whereas the others were more generic. Finally, primitive operations were also required for the storage and display of acquired data. A full list of the elementary operations used in this system is given in Table 1.

Table 1. Elementary operations required for the storage and display of acquired data

Keyword			Function
Start	..	..	Name control program
Purge	..	..	Toggle gas purge switch
Stir	..	..	Toggle stir switch
Drop	..	..	Initiate mercury drop dislodge/dispense and delay for 0.3 s
Delay	..	..	Initiate time delay
Set	..	..	Set applied potential (absolute value)
Step	..	..	Change applied potential (relative to existing value)
Loop	..	..	Mark start of repeating group of operations
End loop		..	Mark end of repeating group of operations
=	..	..	1. Set variables
			2. Manipulate data
Sample		..	Measure current
Display		..	Display results
Stop	..	..	Finish experiment

0	Start CSV	12	Delay 0.005
1	Purge	13	Sample A
2	Delay 100	14	Step −0.012
3	Purge	15	End loop
4	Set 0	16	Loop 100
5	Drop	17	Delay 0.005
6	Delay 1	18	Sample A
7	Drop	19	Step 0.012
8	Delay 1	20	End loop
9	Drop	21	Display A
10	Delay 5	22	Stop
11	Loop 100		

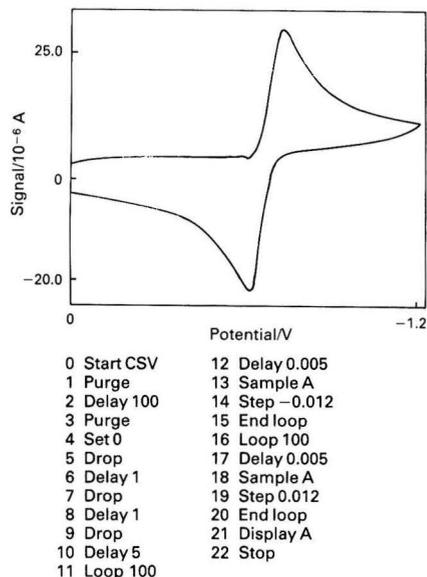**Fig. 4.** Cyclic staircase voltammetric determination of 100 p.p.m. of Cd^{2+} in 0.1 M nitric acid

In addition to these keywords, the language implements some mathematical operators and a limited form of variable storage. A total of 15 variables are available, labelled A–O. Variables A–E are data streams consisting of up to 256 two-byte words. These streams can be used with pointers and are intended to store data acquired during experiments. Hence, the expression "Sample C" in a program instructs the computer to read the current value on the input of the ADC and to store the result in the next available location in data stream C. Variables F–O are single values that may be used in programs for parameters which must be manipulated arithmetically during execution.

Mathematical operators for addition, subtraction, multiplication and division are provided. These can be applied to any variables including data streams; for example, in a differential technique, a result data stream can be calculated by subtracting two data streams representing pairs of data points collected at different positions on the perturbation cycle in an electrochemical experiment.

All of the primitive operations which generate an action were coded as machine code sub-routines in a run-time

library. The routines were optimised carefully for speed and the elapsed time for each operation was noted so that it could be allowed for in the compilation stage to preserve accurate timings. Where there was a parameter associated with the keyword for the primitive operation, indirect addressing was used to allow the parameters to be varied after compilation. This addressing scheme uses pointers embedded in the machine code which indicate specific memory locations where the current value of the parameter will be found. Primitive operations associated with program control were not coded as sub-routines, but formed part of the main program generated by compilation of the high-level control language.

The minimum data acquisition time for a single point in a sweep was 55 μs. This is equivalent to a data acquisition rate of 18 kHz. The maximum timing error for the acquisition of a single point at this acquisition rate was +4 μs. Owing to the way in which timing is carried out, the errors in timing are always positive and reflect the maximum time that may be taken to check various status flags. The minimum data acquisition rate was 2.3×10^{-4} Hz. The maximum timing error for a single point over all data acquisition rates was +8 μs.

Having defined the structure of the control language, a series of BASIC programs were written to provide a development and application environment. These programs covered the creation of a control program, its compilation and execution.

The module for creation of the control program allowed the user to enter the high-level code line by line. Parameter syntax and range were checked for each line as it was input and if any errors were detected the program forced the line to be re-entered. As soon as the final "stop" command was entered, marking the end of the control program, the entire program was checked for syntactical and logical errors. Completed programs were then saved on disk. Programs could be edited at any stage with the same level of error checking to allow easy modification.

The second module compiled the control programs into executable machine code. This was achieved by taking the primitive operations from the control program line by line and converting them into sub-routine calls to the appropriate machine code sub-routines from the run-time library. Parameters were also stored in the appropriate memory locations for each sub-routine. Programme control functions such as loops were converted into machine code operations within the calling machine code program. After compilation, the executable machine code program could be saved on disk for later execution.

The final module loaded the specified machine code program into memory, together with the run-time library, executed an initialisation machine code routine to set up the registers and instrumentation and transferred control to the machine code program to execute the experiment.

Results and Discussion

In order to test the usefulness of the completed system, a number of simple trial experiments were run. Fig. 4 shows the results obtained from a cyclic staircase voltammetry experiment carried out on a solution containing 100 p.p.m. of cadmium nitrate in 0.1 M nitric acid, together with the control program used. Note the two loops in lines 11–15 and 16–20 creating the forward and reverse scans, which are stored sequentially in data stream A. The system also records the potential at which each data point was recorded, allowing the "display" command simply to convert the sequential data set into the conventional display for a cyclic voltammogram. These results are broadly in agreement with those obtained by Bond et al.[24] The experiment was carried out at an effective sweep rate of 2.4 V s^{-1}.

A slightly more complicated example is the differential-pulse anodic stripping voltammetric analysis of laboratory tap
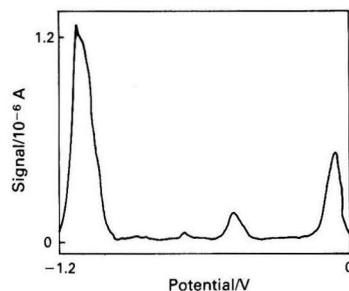
0	Start DPASV2	13	Delay 30
1	Purge	14	Loop 200
2	Delay 2	15	Delay 0.1
3	Purge	16	Sample A
4	Stir	17	Step 0.05
5	Set −1.2	18	Delay 0.1
6	Drop	19	Sample B
7	Delay 1	20	Step −0.045
8	Drop	21	End loop
9	Delay 1	22	D = B − A
10	Drop	23	Display D
11	Delay 150	24	Stop
12	Stir		

Fig. 5. Differential-pulse anodic stripping voltammetric analysis of laboratory tap water
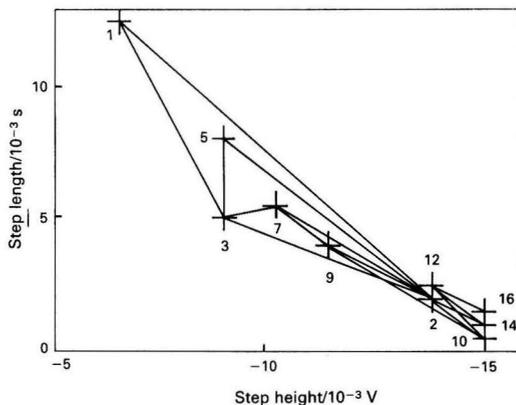

Fig. 6. Variations in step height and step length with vertex number during simplex optimisation of the staircase sweep voltammetric determination of 100 p.p.m. of Cd^{2+} in 0.1 M nitric acid

water. The results of this experiment are shown in Fig. 5 together with the control program. The main loop occurs between lines 14 and 21. Here the current is sampled either side of the differential pulse and stored in data streams A and B. The difference between the two data streams is obtained in line 22. As these arithmetic operators apply to the entire data stream, only one statement is required and this can be placed outside the main loop reducing the computational overhead. These results are comparable to those obtained for mixtures of various heavy metals.[25]

The signal to noise ratio obtained with this system is not good compared with conventional commercial instrumentation. This is largely due to electronic noise pick-up within the potentiostat and signal conversion electronics. However, despite the limitations of the experimental data, the results indicate the capabilities of the concept and demonstrate the use of the control language.

A large number of other simple voltammetric experiments have been programmed using this system including linear staircase voltammetry, sampled d.c. polarography, differential-pulse polarography and chronoamperometry.[23,26,27]
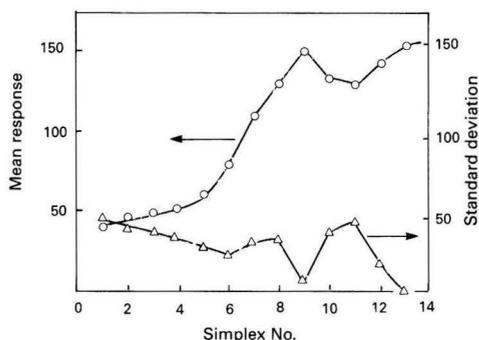
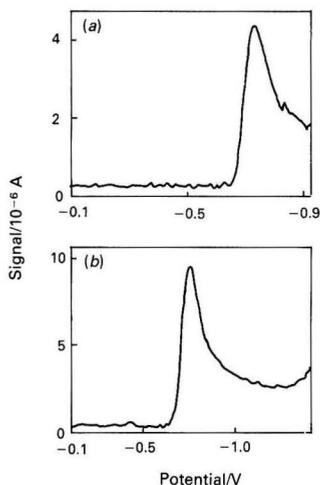**Fig. 7.** Change in the mean response and standard deviation with simplex number

Fig. 8. (a) Initial and (b) final results for optimising the signal to noise ratio in the staircase voltammetric determination of 100 p.p.m. of Cd^{2+} in 0.1 M nitric acid

The ability to execute a previously compiled experiment from within another program was regarded as being a very important feature of the system. If parameters could be passed from the supervisory program to the experiment, a high level of automation would be possible.

It has been widely recognised that automation of chemical analysis must extend beyond the unattended repetition of routine tasks to automatic method selection, development and optimisation. At present, setting up an analytical method often requires significant input from a highly trained analyst, even when the method is well established. The time spent in setting up the experiment is frequently less productive than other tasks the analyst might be engaged in, and, consequently, there is a high level of interest in the possibility of exploiting artificial intelligence and optimisation methodologies to minimise the involvement of trained scientists. The area where most work has been carried out is in the automation of chromatography, particularly liquid chromatography.[28,29] Because of the tedious nature of the multiple experiments necessary to optimise a separation, a variety of strategies have been adopted which range from simple stepwise searching of the available space, through directed search methods such as simplex optimisation, to the use of expert systems. Although fully automated method development is not yet available, all the necessary components now exist.

Automatic optimisation has also been applied to the field of flow injection (FI). Betteridge et al.[30] reported a computer-controlled system where the flow-rate of the various liquid streams was under software control. This allowed the determination of isoprenaline to be optimised by varying the pH, reagent concentration and flow-rate. All of the control software was written in Basic and no critical timing was required. The software was configured as a series of independent modules which could be linked flexibly to create the desired experimental structure. The strategy of passing parameters to an external routine from the calling program does not seem to have been exploited in this study. This may be due to the use of a single-language environment, which considerably simplifies communications between different components of the control system at the cost of greater limitations on the choice of language for the supervisory process. The system was able to operate unattended and the results obtained with the system were consistent with those obtained for manual optimisation.

In this study a linear sweep voltammetry experiment was set up using the control language and saved as an executable machine code program. A supervisory program was written in Basic to execute this experiment, calculate the peak signal to noise ratio and to use that result in the simplex optimisation of the experimental parameters. The step height and step length in the linear sweep experiment were specified in the control program as variables which would be modified by some other program. In effect, the control program was told that the values for the step height and step length would be found in specific memory locations which could be modified externally.

The simplex optimisation performed was the modified procedure of Nelder and Mead[31] with a variable step size. The experimental conditions for the three initial vertices of the simplex were selected randomly from within the experimental space that was available to this instrument. The Basic program calculated the conditions for each new experiment and called the machine code program that executed the experiment, passing the experimental parameters through the specified memory locations. After each experiment was performed, the results were displayed and the operator identified the voltammetric peak and a region over which the background root mean square noise could be calculated. The signal to noise ratio was then calculated and used as the experimental response to be optimised in the simplex procedure. A new simplex was calculated, generating a new experiment to be carried out. This continued until the optimisation criteria were met.

The optimisation was performed on the staircase sweep voltammetric determination of 100 p.p.m. of cadmium nitrate solution in 0.1 M nitric acid. Each linear sweep contained 100 steps. The step height was allowed to vary from -0.006 to -0.015 V with a precision of 1×10^{-3} V and the step length was allowed to vary from 0.001 to 0.020 s with a precision of 5 $\times 10^{-4}$ s. The optimisation process was set to terminate when the standard deviation of the response of the vertices of the simplex with respect to the mean response reduced to 1.0.

Fig. 6 shows the values of the variables selected for the optimisation procedure. Not all vertices are shown. If a reflection produced a vertex outside the experimental range, for example a vertex with a negative step length, the experiment was not performed. The vertex was instead allocated a zero response to force a contraction. These vertices have been omitted from the figure.

It has been suggested that an error exists in the implementation of the modified simplex algorithm that we use. We have been unable to find such an error, although it is possible that one exists. The simplex optimisation control program was written to test the usefulness of the compiled experiment code as a routine called from within a supervisory program and the feasibility of varying the experimental conditions by passing parameters from the supervisory program to the experimental

routine. As such, the simplex program was not tested as extensively as it would have been were it a key feature of the study. However, whether or not this program contains an error, the experiment was sufficiently successful to illustrate the usefulness of the approach.

Fig. 7 shows the change in mean response and standard deviation with increasing simplex number. The experimental results obtained under the optimum conditions are compared in Fig. 8 with those of experimental results obtained under the conditions of one of the initial vertices. In this experiment, there was operator intervention to determine the response factor for each set of experimental conditions; however, in experiments given elsewhere,[27] we have demonstrated that completely automatic operation is possible.

Conclusions

We have shown that it is possible to construct a computer-controlled instrument with a high degree of flexibility by creating a specialised high-level language. This concept is implemented through identification of the necessary primitive operations for the type of experiment to be carried out and the programming of these primitive operations in optimised machine code.

The system is not confined to existing experimental strategies; instead, any experiment that is physically possible with the available instrumentation can be programmed. A range of existing voltammetric experiments have been programmed successfully, requiring precise, high speed, real-time control.

We have also demonstrated that an experiment programmed using this high-level language can be saved as a single executable module which can be called from within another program. We have illustrated this by conducting a semi-automatic simplex optimisation of a linear sweep voltammetry experiment.

It is important to note that this approach is not limited to voltammetric experiments or this specific collection of instrumentation. For example, if it were necessary to use a different potentiostat and electrode combination, it would only be necessary to modify the appropriate machine code sub-routines that refer to the elementary operations controlling those parts of the system. Similarly, there is no reason why the same concept could not be extended to other kinds of instrumental experiment, for example many forms of spectroscopy. Each type of experiment will have different elementary operations, but the structure and concept of the language would be the same.

Finally, the system is in principle portable from computer to computer. In this instance there would be a need for a greater degree of conversion work, but the system would retain the same look and feel to the user. It would therefore represent a route by which a common user interface for a wide variety of computer-controlled instruments could be created.

Because of the ability to produce executable modules relatively simply, and to link these modules with other software structures, it is possible to create measurement systems with any degree of interaction that the user requires. The user may be allowed complete freedom to re-define the experiment, may be limited to the selection of a few parameters, for example through a menu system, or may be presented with a complete turnkey operation, which cannot be modified to any degree. All of these options can be achieved within the same environment, which allows the system developer considerable freedom and flexibility of approach.

References

1. Betteridge, D., and Goad, T. B., *Analyst*, 1981, **106**, 257.
2. Ziegler, E., *Anal. Chim. Acta*, 1980, **122**, 315.
3. Bruntlett, C. S., *Curr. Sep.*, 1983, **5**, 21.
4. He, P., Avery, J. P., and Faulkner, L. R., *Anal. Chem.*, 1982, **54**, 1313A.
5. He, P., and Faulkner, L. R., *J. Electroanal. Chem. Interfacial Electrochem.*, 1987, **224**, 277.
6. Finger, M., *Byte*, 1982, **7**(12), 314.
7. Finger, M., *Byte*, 1983, **8**(1), 254.
8. Finger, M., *Byte*, 1983, **8**(2), 314.
9. Prendergast, D., Slade, W., and Winkless, N., *Byte*, 1984, **9**(1), 122.
10. Schlieper, W. A., Isenhour, T. L., and Marshall, J. C., *J. Chem. Inf. Comput. Sci.*, 1987, **27**, 137.
11. Carter, L. R., and Huzan, E., "Computer Programming in BASIC," Hodder and Stoughton, London, 1981, p. 7.
12. Williams, G., Edwards, J., and Robinson, P., *Byte*, 1985, **10**(8), 83.
13. Nicholls, B., *Byte*, 1985, **10**(12), 169.
14. Gunasingham, H., *Anal. Chim. Acta*, 1985, **169**, 309.
15. Bond, A. M., and Norris, A., *Anal. Chem.*, 1980, **52**, 367.
16. Bond, A. M., Greenhill, H. B., Heritage, I. D., and Reust, J. B., *Anal. Chim. Acta*, 1984, **165**, 209.
17. Bond, A. M., Heritage, I. D., and Briggs, M. H., *Anal. Chem.*, 1984, **56**, 1222.
18. Ploegmakers, H. H. J. L., Mertens, M. J. M., and van Oort, W. J., *Anal. Chim. Acta*, 1985, **174**, 71.
19. Loeliger, R. G., "Threaded Interpretive Languages; Their Design and Implementation," BYTE Books, Peterborough, 1981.
20. Zollinger, D. Ph., Bos, M., van Veen-Blaaw, A. M. W., and van der Linden, W. E., *Anal. Chim. Acta*, 1985, **167**, 89.
21. Bond, A. M., "Modern Polarographic Methods in Analytical Chemistry," Marcel Dekker, New York, 1980, p. 178.
22. Miller, R. M., and Thomas, K. E., unpublished work.
23. Thomas, K. E., *PhD Thesis*, University of Manchester, 1986.
24. Bond, A. M., O'Halloran, R. J., Ruzic, I., and Smith, D. E., *Anal. Chem.*, 1978, **50**, 216.
25. Graneli, A., and Jagner, D., *Anal. Chim. Acta*, 1976, **83**, 19.
26. Dennis, H., *Masters Dissertation*, University of Manchester, 1984.
27. Oduoza, C. E., *PhD Thesis*, University of Manchester, 1987.
28. Berridge, J. C., *Anal. Chim. Acta*, 1986, **191**, 243.
29. Berridge, J. C., "Techniques for the Automated Optimisation of HPLC Separations," Wiley, Chichester, 1985.
30. Betteridge, D., Sly, T. J., Wade, A. P., and Porter, D. G., *Anal. Chem.*, 1986, **58**, 2258.
31. Nelder, J. A., and Mead, R., *Comput. J.*, 1965, **7**, 308.

Biosensing With Coated-wire Electrodes

Part 1. Glucose Sensors

Hashim M. Abdulla,* Gillian M. Greenway† and Albert E. Platt
Department of Science and Engineering, Humberside College of Higher Education, Cottingham Road, Hull HU6 7RT, UK

Peter R. Fielden
Department of Instrumentation and Analytical Science, UMIST, P.O. Box 88, Manchester M60 1QD, UK

Enzyme electrodes based on fluoride- and iodide-selective coated-wire electrodes are described for the determination of glucose. The electrodes consist of a homogeneous poly(vinyl chloride) membrane containing both the electroactive species and immobilised glucose oxidase. Two enzyme electrodes based on iodide were investigated. The first of these utilised an ammonium molybdate catalyst, yielded a sub-Nernstian calibration with a mean slope of 32 ± 1 mV decade^{-1} and had a lifetime of 4 d. The lifetime of the second electrode, for which peroxidase was also immobilised in the electrode membrane, was 6 d. A super-Nernstian calibration was obtained for this electrode with a mean slope of 79 ± 1 mV decade^{-1}. Finally, the enzyme electrode based on fluoride gave a calibration with a mean slope of 32 ± 1.5 mV decade^{-1}; this also had a lifetime of 6 d.
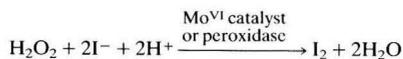
Keywords: *Coated-wire electrode; glucose sensor; glucose oxidase*

In recent years there has been considerable interest in the use of enzyme electrodes, based either on potentiometric or voltammetric measurements.[1,2] Such electrodes usually consist of a sensor electrode, which monitors the change in concentration of a reactant or product of a reaction catalysed by the chosen enzyme; this enzyme is immobilised next to the surface of the sensor. Although these systems have been employed in clinical analysis,[3] there is a need to develop a method that requires only small samples or one that can be utilised *in vitro*. The design of miniaturised ion-selective electrodes based on glass capillaries has been undertaken. These electrodes, however, are delicate and difficult to construct because they require an internal filling solution.[4] This paper describes an investigation into the possibility of using coated-wire electrodes that do not contain an internal reference solution to construct enzyme-based sensors. There are few instances of this type of electrode being utilised, although two urea electrodes based on pH measurements have been described. The basis of one was an antimony metal electrode[5] and the other an iridium oxide electrode.[6]
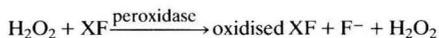
The coated-wire electrodes that we employed involved the use of ion exchangers as described by Helen *et al.*[7] Both iodide- and fluoride-selective coated-wire electrodes were used to produce the enzyme sensors. For both sensors the initial enzyme reaction is the same:

$$glucose + O_2 \xrightarrow{\substack{glucose \\ oxidase}} gluconic\ acid + H_2O_2 \quad .. \quad (1)$$

Then, either the depletion of iodide ions is sensed[8]

$$H_2O_2 + 2I^- + 2H^+ \xrightarrow{\substack{Mo^{VI}\ catalyst \\ or\ peroxidase}} I_2 + 2H_2O$$

or the production of fluoride ions is monitored[9]

$$H_2O_2 + XF \xrightarrow{peroxidase} oxidised\ XF + F^- + H_2O_2$$

where XF is an organofluorine compound.

---

* Present address: Department of Pure and Applied Chemistry, Strathclyde University, Glasgow G1 1XL, UK.

† To whom correspondence should be addressed. Present address: School of Chemistry, University of Hull, Cottingham Road, Hull HU6 7RX, UK.

Experimental

Reagents

Glucose oxidase (E.C. 1.1.3.4, 134 U mg^{-1}) purified from *Aspergillus niger* and peroxidase (E.C. 1.11.1.7, 330 U mg^{-1}) purified from Horseradish were obtained from Sigma (Poole, Dorset, UK). These were stored in a refrigerator at 4 °C. Aliquat 336 (tricaprylylmethylammonium chloride), dodecylamine, dioctyl phenylphosphonate and poly(vinyl chloride) (PVC) low relative molecular mass were obtained from Aldrich (Gillingham, Dorset, UK). The required ion-association complex was obtained by shaking a 60% V/V solution of Aliquat 336 in decan-1-ol with an aqueous solution (0.5–1 M) of the halide salt. The fluoride and iodide standards were prepared from stock solutions of the analytical-reagent grade sodium salts in phosphate buffer (0.1 M, pH 5). The glucose solutions were also prepared in phosphate buffer.

Electrode Preparation

The laboratory-manufactured electrodes consisted of platinum wire (7 × 1 mm o.d., grade 1, Johnson Matthey, Royston, UK), soldered to a copper connecting wire and enclosed in glass tubing (6 mm i.d.). The bottom of the tube was sealed with epoxy resin.

To construct the base electrodes (F$^-$ and I$^-$) a solution of PVC with dioctyl phenylphosphonate plasticiser (20% m/V PVC, 0.3% m/V plasticiser in cyclohexane) was prepared and the platinum wire was coated by dipping it in this solution. After allowing the electrode to dry for 40 min it was then dipped in the ion-association complex. The electrode was conditioned before use by soaking it for 15 min in a 100 mM halide solution. These electrodes were stored in air at room temperature and re-conditioned before use by repeating the conditioning process. Another fluoride electrode was prepared similarly, with dodecylamine in nitrobenzene as the ion exchanger.

The enzyme electrodes were prepared by physical immobilisation of the enzyme in PVC (see Table 1). Two enzyme electrode constructions were investigated. For membrane 1, the indicator electrode was constructed as described above, then dip-coated with a PVC layer (the same solution as for the base electrode in cyclohexane) and dry enzyme (*ca.* 3 mg of

Table 1. Construction and composition of membranes for coated-wire glucose sensors

| | Membrane No. | | | | | |
	1	2	3	4	5	6
Base electrode	←		I⁻		→	F⁻
Ion exchanger	←		Aliquat 336		→	Dodecylamine
Membrane design	Double layer	←	Homogeneous layer			→
Glucose oxidase/mg	3	3	3	6	1	3
Catalyst for H₂O₂ cleavage	Peroxidase	Ammonium molybdate	←	Peroxidase		→
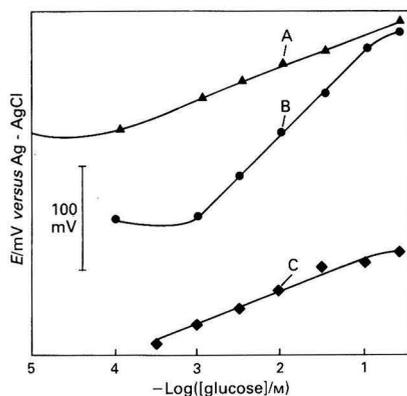
Fig. 1. Calibration graphs for membranes: A, 2; B, 3; and C, 6.

glucose oxidase and 1 mg of peroxidase for each base electrode) was pressed into the outer PVC layer before it hardened (typically 10 min after dip-coating). This resulted in an immobilised high-concentration layer of enzyme surrounding the base coated-wire ion-selective electrode.

In the second construction method (membranes 2–6), a homogeneous membrane was prepared. The electrode was first dipped into the PVC solution and allowed to dry for 10 min. The dry enzyme (1–6 mg of glucose oxidase) was then pressed into the soft PVC membrane to produce a single layer containing immobilised enzyme in contact with the platinum wire. After the PVC - enzyme coating had hardened the electrode was dipped into the ion-association complex as described previously. The electrodes were stored in pH 5 phosphate buffer solution at 4 °C. It was found that membrane permeation with the phosphate buffer solution was necessary for operation in order to ensure transportation of the species within the membrane. The electrodes consisting of both iodide and fluoride base electrodes were prepared in this manner.

Electrodes were also constructed in which peroxidase was co-immobilised with glucose oxidase by the described procedures (see Table 1). Peroxidase was essential for the fluoride-based electrode in order to catalyse the liberation of free fluoride ions by hydrogen peroxide.

Instrumentation and Measuring Procedure

Measurements were made with a high-impedance voltmeter (Corning, PT16) using a silver - silver chloride double-junction reference electrode (Radiometer, KZ01). Solutions were stirred at a constant rate while results were recorded on a chart recorder (BBC Georz SE-120). All measurements were made in a water-bath (Grant JB1) maintained at 25 °C and standard solutions were allowed to equilibrate for 1 h at this temperature, prior to use.

For glucose determinations using the electrode based on the measurement of iodide (membranes 1–5), sodium halide solution was added to each glucose standard (the optimum

iodide concentration was found to be 10^{-4} M, which is consistent with the results of other workers[6]). For glucose determinations based on the measurement of fluoride, 2 cm³ of H₂O₂ (20% *V/V*) and 5 cm³ of 4-fluorophenol solution (3 g in 10 cm³ of methanol made up to 100 cm³ with distilled water) were added to 25 cm³ of glucose standard solution.

Results and Discussion

Optimisation of the Indicator Electrode

Before preparing the enzyme electrodes it was essential to check the operation of the halide sensing (base) electrodes without enzyme. Of the base electrodes tested, the iodide-selective electrode was superior. This was found to have a near-Nernstian response for 0.1 mM– M iodide with a slope of 50 ± 1 mV decade⁻¹. This type of electrode had a response time of 1 min (the time taken to reach 1 mV from the equilibrium potential) and its sensitivity did not change significantly over a period of 3 months. The effect of changing the temperature of a 1 mM solution of iodide on the e.m.f. was also studied and the electrode was shown to be insensitive to temperature changes over the range 10–40 °C [slope = 0.08 mV decade⁻¹, relative standard deviation (RSD) = 0.6%].

The fluoride electrode based on Aliquat 336 was found to be unresponsive, having a sensitivity of 8 mV decade⁻¹. The electrode based on dodecylamine showed greater sensitivity (although well below the theoretical Nernstian response) for the range 1 mM– M with a slope of 32 ± 1 mV decade⁻¹. The deviation (from the log - linear relationship) at lower concentrations could be expected for the fluoride ion-exchange electrode as it is less selective than the iodide ion-exchange electrode according to the Hofmeister series.[10] The response time and lifetime were the same as those of the iodide electrode.

Optimisation of the Enzyme Electrode Membrane

The first type of enzyme electrode (membrane 1) had a very low sensitivity (6 ± 1.5 mV decade⁻¹), which suggested that there was insufficient mobility between the layers. An enzyme electrode was then constructed in which a "cocktail" of all the active species was trapped in one layer of PVC. This type of construction was found to be superior for all membranes (2–6) and these are discussed in more detail below.

The catalyst for the hydrogen peroxide cleavage of those sensors based on the iodide electrode was then studied by performing experiments on three electrodes. For the electrode with membrane 2, ammonium molybdate was used as the catalyst while oxygen was bubbled through the solution (Fig. 1). A sub-Nernstian calibration was obtained for this electrode in the range 0.1–100 mM glucose (slope, 32 ± 1 mV decade⁻¹). This electrode had a short lifetime of 4 d, a response time of 2–10 min and a recovery time of 2–30 min depending on the concentration (a 10-min response time and 30-min recovery time were needed only for very high concentrations, *i.e.*, 1 M).

787

Table 2. Characterisation of coated-wire glucose sensors

			Membrane 2	Membrane 3	Membrane 6
Linear range of glucose/mM	..	..	0.1–100	1–100	1–100
Mean of calibration slope/mV decade^{-1}		..	32 ± 1	79 ± 1	32 ± 1.5
Response time/min*	..	..	2–10	2–10	2–10
Wash time/min*	..	..	2–30	2–30	2–15
Lifetime/d	..	..	4	6	6

* Response and wash times increase with glucose concentration; the highest value quoted is for 1 M glucose solution.
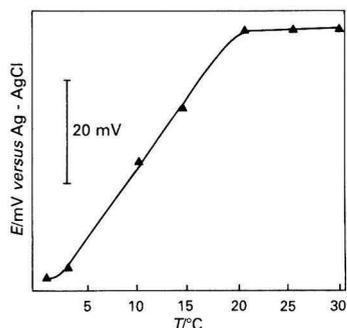
Fig. 2. Effect of temperature on the response of sensor 3. Glucose solution, 10 mM
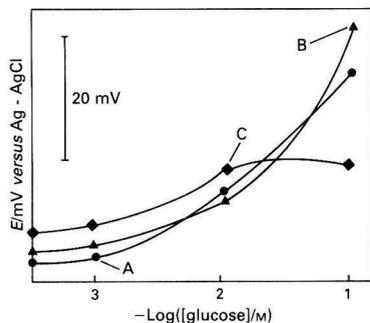
Fig. 3. Effect of lifetime on the iodide sensor, membrane 2. A, 4; B, 5; and C, 6 d

A glucose sensor was then prepared in which peroxidase was used as the catalyst (membrane 3). The peroxidase was co-immobilised with the glucose oxidase enzyme. With this design (Fig. 1) a super-Nernstian calibration was obtained over the range 1–100 mM (slope, 79 ± 1 mV decade^{-1}). The response time and recovery time of this electrode were the same as those of membrane 2 but the lifetime was 6 d. This enhanced sensitivity obtained with peroxidase was also observed by Al-Hitti *et al.*[8] Electrodes with peroxidase were used for all further studies owing to their higher sensitivities and longer lifetimes.

The optimum loading of the enzyme in the membranes was then investigated. Loadings of 1, 3 and 6 mg were investigated (membranes 3–5). The main effect of changing the concentration of the enzyme was found to be on the response time.

Membrane 3 (3 mg, 400 U of glucose oxidase) was found to be the most useful analytically having an acceptable sensitivity and a reasonable response time (discussed above). A micrometer, which was closed against the membrane until visual contact was observed, was used to calculate the thickness of membrane 3 (0.2–0.3 mm). It should be noted that the amount

of co-immobilised peroxidase was optimised in a similar manner and 1 mg (330 U) was used for all further studies.

The enzyme electrode based on the fluoride sensor (membrane 6) was prepared with 3 mg of glucose oxidase and 1 mg of peroxidase (Fig. 1). The electrode response was found to be sub-Nernstian for 1–100 mM glucose with a slope of 32 ± 1.5 mV decade^{-1}. The properties of sensors based on membranes 2, 3 and 6 are summarised in Table 2 with the results quoted as the mean for three replicates of each type.

Characterisation of the Sensors

Effect of sample temperature

The change in e.m.f. on altering the temperature of a 10 mM solution of glucose was investigated. As can be seen in Fig. 2, the e.m.f. increases with temperature up to 20 °C, at which point it begins to level off. If these results are compared with those obtained for the iodide base electrode the increase in the electrode sensitivity must be due to the enzyme. As the temperature increases, the enzyme activity increases up to 20 °C. Above this temperature a sharp levelling off is observed. Such behaviour is reproducible, but not yet understood.

Sensor selectivity

Interferences in enzyme electrodes can be caused by two types of interferent, those that affect the base electrode and those that can be acted on by the enzyme. The first type of interference was studied for both the iodide and fluoride electrodes. The iodide electrode was found to be very selective and did not respond to SO_4^{2-}, Cl^-, NO_3^- or Br^- at the 10 mM level. However, S^{2-} did interfere at a concentration of 50 mM. The fluoride electrode was found to be much less sensitive and, using the mixed solutions method, was found to have a selectivity ratio of 30 for hydroxide ions.

Glucose oxidase is not a completely specific enzyme and is known to affect sugars other than glucose.[11] Both the iodide- and fluoride-based glucose sensors were investigated by the mixed solutions method with respect to their selectivity for glucose over maltose. A selectivity ratio of 0.89 was calculated in both instances.

Sensor lifetime

Fig. 3 shows the decrease in sensitivity of membrane 2 over several days. As can be seen, the lifetime of this electrode is short and the sensitivity and linearity of the curves decrease as the age of the sensor increases. This was because the enzyme was only physically immobilised. After several days stored in buffer solution, the yellow colour of the glucose oxidase could clearly be seen in solution. The simplicity of construction and low cost of manufacture (if a metal other than platinum were to be utilised) mean that these electrodes could be designed to be disposable. Alternatively, the enzyme could be immobilised more permanently by using a chemical immobilisation technique (*e.g.*, cross-linking with glutaraldehyde).

Conclusions

This work has investigated the operation of coated-wire electrode-based enzyme sensors. The simplicity of construction, particularly with the homogeneous membranes containing both enzyme and ion sensor, offers the possibility of the mass production of low-cost disposable spot-test sensors for glucose. Although, in terms of over-all performance, these sensors offer no immediate advantage over other designs, they should not be discounted. Their small size and inherent robustness make them ideal for clinical sensing applications. Further work is necessary to ensure reproducible performance and methods to improve shelf lifetime should be investigated.

References

1. Vadgama, P., *in* Covington, A. K., *Editor*, "Ion-Selective Electrode Methodology," Volume II, CRC Press, FL, 1979, p. 23.
2. Albery, W. J., and Bartlett, P. N., *J. Electroanal. Chem.*, 1985, **194**, 211.
3. Home, P. D., and Alberti, K. G. M. M., *in* Turner, A. P. F., Karube, L., and Wilson, G. S., *Editors*, "Biosensors, Fundamentals and Applications," Oxford University Press, Oxford, 1987, p. 723.
4. Silver, I. A., *Philos. Trans. R. Soc. London, Ser. B*, 1987, **316**, 161.
5. Alexander, P. W., and Joseph, J. P., *Anal. Chim. Acta*, 1981, **131**, 103.
6. Ianniello, R. M., and Yacynych, A. M., *Anal. Chim. Acta*, 1983, **146**, 249.
7. Helen, J., Cormack, G., and Freiser, H., *Anal. Chem.*, 1972, **44**, 857.
8. Al-Hitti, I. K., Moody, G. J., and Thomas, J. D. R., *Analyst*, 1984, **109**, 1205.
9. Siddiqi, I. W., *Clin. Chem.*, 1982, **28**, 1962.
10. Buck, R. P., *Sensors Actuators*, 1981, **1**, 197.
11. Nagy, G., von Storp, L. M., and Guilbault, G. G., *Anal. Chim. Acta*, 1973, **66**, 443.

Nylon Tube *O*-Alkylation for Immobilisation of Covalent Enzymes

Francis N. Onyezili

Department of Foundation Studies, University of Agriculture, Private Mail Bag 2373, Makurdi, Nigeria

Nylon tube *O*-alkylation and its effects on the catalytic efficiency of urease (E.C. 3.5.1.5) immobilised on the tube were examined using dimethyl sulphate (DMS) and diethyl sulphate (DES) as alkylating agents on Nylon 6 of different wall thicknesses. Effective and easy control of the alkylation process was possible as both reagents scarcely reacted with nylon at room temperature (25 °C) and as high-temperature alkylation, at 100 °C, could be stopped rapidly by immersing the tube in an ice-bath. The optimum incubation times for alkylation with DMS and DES were 3 and 10 min, respectively. Diethyl sulphate, a less toxic reagent than DMS, caused less damage to the nylon tubes and produced more chemically stable *O*-alkylated derivatives. However, it was less efficient than DMS in creating reactive sites for covalent attachment of catalytically active urease on the tube. Although thick-walled nylon tubes immobilised more active enzyme, such tubes were less pliable than thin-walled tubes and could pose operational problems.

Keywords: *Nylon tube O-alkylation; urease immobilisation*

Nylon tubes, because of their mechanical strength, pliability and ease of incorporation in automated continuous-flow assay systems, are popular support matrices for immobilised enzymes.[1,2] However, this material is predominantly hydrophobic and essentially chemically inert except at the few amide linkages interspersed in its structure. Therefore, covalent coupling of an enzyme to a nylon tube is effected by modifying the tube to alter its chemistry and so provide a suitable environment for binding the enzyme without denaturing it. Partial hydrolysis of the tube with hydrochloric acid[3] and non-hydrolytic cleavage with dimethylaminopropylamine[4] have been employed for this purpose, but high temperature *O*-alkylation of the tube is often the method of choice because it yields the most catalytically active immobilised enzyme derivative.[5] However, little is known both about the process of nylon tube *O*-alkylation and the final effects of the process on the catalytic efficiency of the immobilised enzyme derivative. In this paper the process is examined further by using both dimethyl sulphate (DMS) and diethyl sulphate (DES) as alkylating agents and immobilising urease (E.C. 3.5.1.5) on two different sizes of Nylon 6 tubes.

Experimental

Thin-walled (1.0 mm i.d., 0.25 mm wall thickness) and thick-walled (1.0 mm i.d., 0.75 mm wall thickness) nylon tubes were obtained from Portex (Hythe, UK). Dimethyl sulphate and DES were supplied by BDH (Poole, UK) and stored at 25 °C over calcium hydride. Glutaraldehyde (25% *m/V* aqueous solution) was obtained from BDH and stored in small aliquots at −20 °C. When required, it was thawed out, diluted as appropriate and stored subsequently at 4 °C. Jack bean urease was obtained as a freeze-dried powder from Miles-Servac Laboratories (Maidenhead, UK) with a specific activity of 100 U mg⁻¹ at pH 7.0 and 25 °C. Unless indicated otherwise, all the other reagents were of analytical-reagent grade and were used without further purification.

Nylon Tube Alkylation

This procedure, because of the toxicity of the alkylating agents, was performed in a fume cupboard using gloved hands and protective eye glasses and with the utmost caution. A 1.0-m length of the tube was filled with either DMS or DES, using a syringe, and sealed tightly at both ends with steel clamps. After incubating at 100 °C in a boiling water-bath for the desired time, to allow alkylation to occur, the tube was immersed in an ice-bath for 10 min. The excess of alkylating

agent was then removed by perfusing the tube with 50 ml of re-distilled methanol at a flow-rate of 5 ml min⁻¹ using a peristaltic pump.

Determination of Cysteine Uptake by Alkylated Tubes

The alkylated tube was filled with a freshly prepared solution of 0.5 M cysteine (pH 9.0) containing 0.001 M EDTA and incubated at 25 °C for 5 h. Unreacted cysteine was recovered by perfusing the tube with 50 ml of 0.001 M EDTA containing 0.1 M KCl. The cysteine content of the effluent was determined with 5,5′-dithiobis(2-nitrobenzoic acid) (DTNB) as described by Eliman.[6] The uptake of cysteine by the alkylated tube was calculated from the difference between the cysteine concentration before and after incubation in the alkylated tube.

### Further Chemical Modification of Alkylated Tubes and Urease Immobilisation

Chemical modifications of the alkylated tube with 1,6-diaminohexane and glutaraldehyde were performed as described previously.[7] The *O*-alkylated tubes were reacted first with 0.2 M 1,6-diaminohexane in methanol for 3 h at 25 °C and then with 2% *m/V* glutaraldehyde in 0.2 M borate buffer (pH 9.0) for 8 min at 25 °C. Urease was immobilised by filling the modified tube with a solution containing 2 mg ml⁻¹ of the enzyme in 0.05 M EDTA buffer (pH 6.6) containing 0.001 M mercaptoethanol and incubating for 4 h at 4 °C. Unbound enzyme was removed by sequential perfusion with 1.0 M NaCl solution and distilled water.

Assay of Immobilised Urease

The immobilised urease activity was determined by measuring the ammonia in the effluent stream following perfusion of a solution of 0.05 M urea in 0.05 M EDTA (pH 6.6) through the immobilised enzyme tube at a flow-rate of 4 ml min⁻¹. The ammonia assay procedure has been described by Chaney and Marbach.[8]
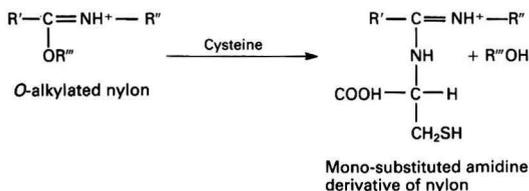
Results and Discussion

The esters resulting from *O*-alkylation of nylon tubes form mono-substituted amidines with cysteine, as follows:
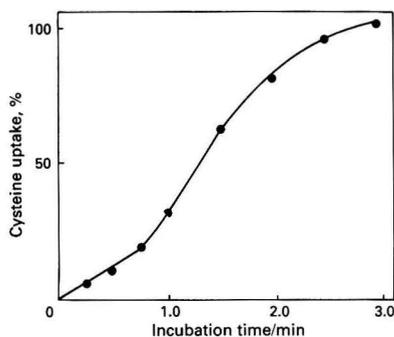
Fig. 1. Cysteine uptake in DMS alkylated thin-walled nylon tubes. All alkylations were performed at 100 °C on 1.0-m lengths of tube. Cysteine uptake was determined as described under Experimental; 100% uptake was equivalent to 0.086 µmol of cysteine bound per metre of tube
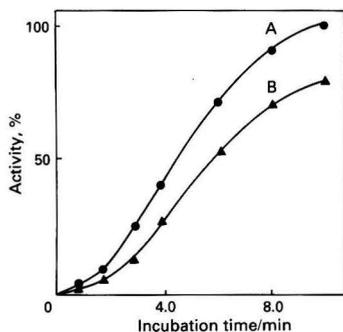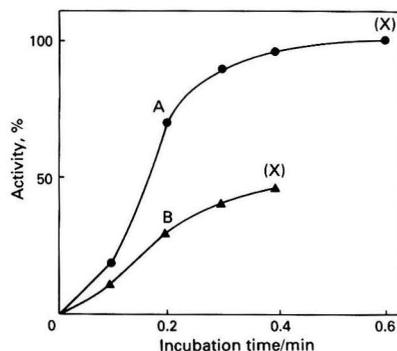

Fig. 2. Diethyl sulphate incubation time and the *O*-alkylation process. Alkylation with DES was performed at 100 °C on 1.0-m lengths of thin-walled nylon tube. A, Urease coupled directly to the alkylated tube; and B, tube modified further with 1,6-diaminohexane and glutaraldehyde before enzyme coupling. Urease activity was measured at 37 °C in the presence of 0.05 M urea in 0.05 M EDTA buffer (pH 6.6) perfused at a flow-rate of 4 ml min⁻¹; 100% activity produced 12 µmol of ammonia per minute per meter of tube

Fig. 3. Nylon tube wall thickness and the *O*-alkylation process. All alkylations were performed at 100 °C on 1.0-m lengths of tube with DMS. A, Thick-walled tubes; and B, thin-walled tubes, both modified (after alkylation) with 1,6-diaminohexane and glutaraldehyde before urease immobilisation. Urease activity was measured as described in Fig. 2; 100% activity produced 25 µmol of ammonia per minute per meter of tube [(×) = time at which disintegration of the tube was observed]

O-alkylated nylon

Mono-substituted amidine derivative of nylon

Hence, the uptake of cysteine by alkylated nylon tubes is a measure of the *O*-alkylation process itself.

Fig. 1 shows that the alkylation of thin-walled tubes with DMS at 100 °C was a fast process, with 80% of the maximum uptake of cysteine achieved after alkylating for 2 min. Thereafter, alkylation slowed down and, beyond 4 min, structural disintegration of the tube was observed. Esters such as those formed by alkylating nylon tubes have been reviewed[9] and are reported to be sufficiently hygroscopic to bring about their own decomposition, particularly in the absence of stabilising aromatic groups. Work reported recently[10] provides experimental evidence of such hydrolysis of alkylated nylon tubes, which would explain their disintegration on prolonged exposure to the alkylating agent.

As the reactive sites created by *O*-alkylation ultimately provided the basis for covalent enzyme binding on the tube, the efficiency of *O*-alkylation was monitored by exposing the

alkylated tube, either directly or after further chemical modification, to urease and measuring its catalytic activity. Also, DES, which is a milder alkylating agent than DMS, was used thus permitting the alkylation process to be observed for a longer period. The results of these investigations are shown in Fig. 2. The levels of enzymic activity in the tubes indicated that *O*-alkylation of thin-walled tubes with DES was slow for the first 2 min, then increased and continued for 10 min before structural disintegration began. Compared with alkylated tubes to which the enzyme was coupled directly, approximately 24% less urease activity was detected in tubes that had been alkylated for the same optimum period (10 min), but modified subsequently with 1,6-diaminohexane and glutaraldehyde before the enzyme was coupled. This finding (Fig. 2) is, presumably, an indication of the different chemistries governing urease immobilisation in each instance and suggests that subsequent modifications of *O*-alkylated nylon tubes reduce the number of active binding sites available to the enzyme. These subsequent modifications were introduced to create reactive sites for the enzyme away from the proximity of the hydrophobic nylon surface, which could cause unfolding (and denaturation) of the enzyme protein. However, as the results suggest, such modifications of the *O*-alkylated tube reduced its binding efficiency, at least with regard to catalytically active urease.

A comparison of DMS and DES alkylation of thin-walled nylon tubes was made by allowing the alkylation with each reagent to proceed for the same length of time (3 min) at 100 °C before the tubes, which had been similarly chemically modified,[7] were exposed to an enzyme coupling solution of urease (2 mg ml⁻¹) - mercaptoethanol (0.01 M) - EDTA pH 6.6 buffer (0.05 M). For the DMS - and DES - 1,6-diamonohexane - glutaraldehyde - urease tubes the urease activities were 9.6 and 0.9 U, respectively (the units of urease activity were equivalent to µmol of ammonia per minute per meter of the tube using the assay conditions described under Experimental). As DES alkylation could be performed for longer periods than alkylation with DMS, and as an increase in DES incubation time (within the limits beyond which disintegration of the tube occurred) resulted in a progressive increase in the activity of the final immobilised enzyme derivative (Fig. 2), it would appear that DES-alkylated tubes were more stable than those alkylated with DMS. This view is supported by a report[9] that at elevated temperatures a degradative "*O*" to "*N*" migration of alkyl groups may follow the alkylation process. This migration, which is analogous to the Chapman rearrangement,[11] would be less likely to occur in DES

alkylated tubes where the molecular size of the newly introduced alkyl group is larger.

The wall thickness of the nylon tube was a significant factor in the *O*-alkylation process as thick-walled tubes survived DMS alkylation for longer periods than did the thin-walled type (Fig. 3). Further, DMS alkylation for the same length of time (3 min) produced a three-fold higher urease activity in the thick-walled tube compared with that in the thin-walled tube (Fig. 3). The nylon tube matrix exists in various degrees of order and disorder[12] and has amorphous regions that are unsuitable for enzyme immobilisation.[3] A lower proportion of such amorphous regions in the thick-walled tubes could explain the higher activities observed in these tubes. This suggestion is merely speculative as the microstructure of the nylon matrix used in this study was not investigated. Also, a surface area effect in which the deeper nylon matrix of the thick-walled tubes binds more catalytically active urease could account for the higher enzyme activities in these tubes. Hence, from the results obtained, thick-walled tubes are to be preferred to thin-walled tubes. However, the former are less pliable and could pose operational problems in large-scale applications. Also, the problem of completely washing-out the reagents, which diffuse into the tube matrix, is greater for thick-walled tubes.

Conclusions

The optimum incubation times for the *O*-alkylation of thin-walled nylon tubes with DMS and DES were 3 and 10 min, respectively. Thick-walled tubes produced more active immobilised enzyme derivatives than did thin-walled tubes but were less pliable, which could pose operational problems. Effective and easy control of the alkylation process was possible with both DMS and DES as these reagents scarcely reacted with the tubes at room temperature (25 °C) and as their action could be stopped rapidly by immersing the tubes in an ice-bath. Tubes alkylated with DES appeared to be more chemically stable than those alkylated with DMS. Also, DES, which is a less toxic reagent than DMS, caused less damage to the nylon tubes. However, DES was less efficient than DMS in creating reactive sites for enzyme immobilisation and different alkylating conditions may be required to realise the full potential of the former.

References

1. Sundaram, P. V., *J. Solid-Phase Biochem.*, 1978, **3**, 185.
2. Werner, M., Mohrbacher, R. J., Riendeau, M., Murador, E., and Camblaghi, S., *Clin. Chem.*, 1979, **25**, 20.
3. Inman, D. J., and Hornby, W. E., *Biochem. J.*, 1972, **129**, 255.
4. Hornby, W. E., Inman, D. J., and McDonald, A., *FEBS Lett.*, 1972, **23**, 114.
5. Campbell, J., Hornby, W. E., and Morris, D. L., *Biochim. Biophys. Acta*, 1975, **384**, 307.
6. Eliman, G., *Arch. Biochem. Biophys.*, 1959, **82**, 70.
7. Onyezili, F. N., and Onitiri, A. C., *Anal. Biochem.*, 1981, **117**, 121.
8. Chaney, A. L., and Marbach, E. P., *Clin. Chem.*, 1962, **8**, 130.
9. Roger, R., and Neilson, D., *Chem. Rev.*, 1961, **61**, 179.
10. Onyezili, F. N., *Biotechnol. Bioeng.*, 1987, **29**, 399.
11. Orchin, M., Kaplan, F., Macomber, R. S., Wilson, R. M., and Zimmer, H., *in* "The Vocabulary of Organic Chemistry," Wiley, New York, 1980, p. 351.
12. Bawn, C. E., *in* "The Chemistry of High Polymers," Butterworths, London, 1948, p. 11.

1.5th-Differential Polarographic Determination of Trace Amounts of Selenium(IV) and Selenium(VI) in Natural Waters at a Dropping Mercury Electrode

Wu Dunhu*
Changchun Institute of Geography, Academia Sinica, Changchun, Jilin Province, People's Republic of China

Zhang Diyang†
Changchun Institute of Physics, Academia Sinica, Changchun, Jilin Province, People's Republic of China

Li Xiaoming
Changchun College of Geology, Changchun, Jilin Province, People's Republic of China

This paper describes a polarographic method for the determination of trace amounts of Se^{IV} and Se^{VI} in natural waters using a dropping mercury electrode. In an $HClO_4$ - Na_2SO_3 - NH_3 - NH_4Cl - $NH_2OH.HCl$ - KIO_3 system (pH 10), the selenium complex $SeSO_3^{2-}$ gave a peak potential at -0.57 V *versus* Ag. The peak current was directly proportional to Se in the concentration range 0.01–1 µg l^{-1}. The limit of detection was 10 ng l^{-1}. The proposed method is rapid, simple, sensitive and accurate. The recovery of Se from standard additions to samples of natural waters was between 93 and 105%.

Keywords: *Selenium; polarography; environmental chemistry; natural waters*

The role of Se as an important biological trace element in the human body has been investigated[1] and close correlations between Kaschin back disease, heart disease, Kasham disease and various cancers and the Se content of waters, soils, foods, animals and plants found in certain areas have been reported.[2,3] Owing to the presence of trace amounts of Se in the environment and in the human body, attempts were made to develop a method for its determination. A number of methods, including neutron activation analysis,[4] atomic absorption spectrometry,[5] fluorimetry,[6] gas chromatography,[7] polarography[8,9] and spectrophotometry[10] have been employed for the determination of trace amounts of Se in the human body and in hair. However, some of these methods require expensive instrumentation and strictly controlled experimental conditions while others are not sufficiently sensitive to satisfy the requirements for determining trace amounts of Se in water.

This paper describes a 1.5th-differential polarographic method for the determination of trace amounts of Se^{IV} and Se^{VI} in natural waters.[11] The Se is measured using a very sensitive catalytic wave which gives a detection limit of 10 ng l^{-1} in $HClO_4$ - Na_2SO_3 - NH_3 - NH_4Cl - $NH_2OH.HCl$ - KIO_3 using an XJP-821 Neopolarograph.

Experimental

Apparatus and Reagents

A laboratory-built XJP-821 Neopolarograph and an LZ3-100 recorder were used. In a three-electrode system, the dropping mercury electrode was the working electrode, an Ag electrode the reference and a Pt electrode the auxiliary.

Na_2SO_3 (10%), 0.8 M. Analytical-reagent grade anhydrous Na_2SO_3 (10 g) was dissolved in 100 ml of distilled water (freshly prepared every 3 d).

KIO_3 (4%), 0.2 M. Analytical-reagent grade KIO_3 (4 g) was dissolved in 100 ml of distilled water.

* Present address: Department of Applied Chemistry, Dalian Railway Institute, Dalian City, Liaoning Province, People's Republic of China.

† To whom correspondence should be addressed. Present address: Design and Research Institute of Petrochemical Industry of Jilin Province, 77 Stalin Street, Changchun, Jilin Province, People's Republic of China.

NH_3 - NH_4Cl buffer. Prepared by dissolving 50 g of NH_4Cl (analytical-reagent grade) in 190 ml of ammonia solution and diluting to 250 ml with distilled water (pH 10).

$NH_2OH.HCl$, 5%. Analytical-reagent grade $NH_2OH.HCl$ (5 g) was dissolved in 100 ml of water.

Standard solution of Se^{IV}, 1.0 mg ml^{-1}. Prepared by dissolving spectrometric grade SeO_2 (1.4053 g) in 1 l of 0.1 M HCl and then stored in a refrigerator. Solutions containing 0.01 and 0.001 µg ml^{-1} of Se^{IV} were prepared by appropriate dilution of the 1.0 mg ml^{-1} standard solution.

Standard solution of Se^{VI}, 1.0 mg ml^{-1}. Prepared by dissolving Na_2SeO_4 in distilled water. Stock solutions containing 0.01 and 0.001 µg ml^{-1} of Se^{VI} were prepared by appropriate dilution of the standard solution.

The water used throughout was distilled in a quartz still and the $HClO_4$, HNO_3 and HCl used were of super grade quality.

Procedures

Pipette 0.05, 0.10, 0.20, 0.30, 0.40 and 0.50 ml of Se^{IV} solution (0.001 µg ml^{-1}) into 10-ml electrolytic cells and to each cell,
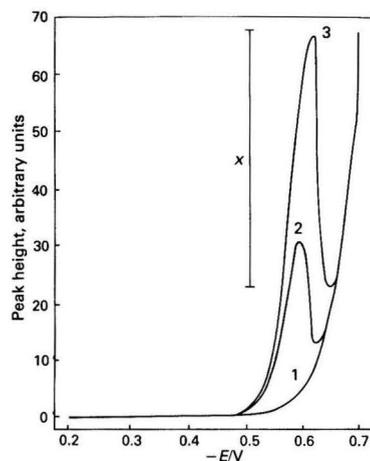

Fig. 1. Differential-pulse polarographic behaviour of Se^{IV}. 1, Solution blank; 2, 0.01; and 3, 0.05 µg l^{-1} of Se^{IV}. Measurement of the peak height is indicated by x

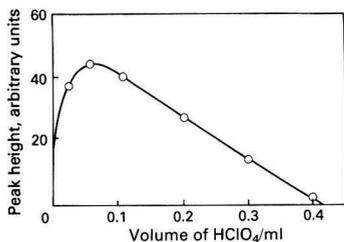**Fig. 2.** Effect of volume of $HClO_4$ added on the peak height of the solution containing Se^{IV}

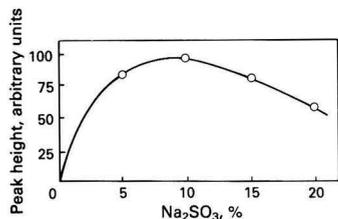**Fig. 3.** Effect of Na_2SO_3 concentration (%) on the peak height of the solution containing Se^{IV}

Fig. 4. Effect of the volume of NH_3 - NH_4Cl buffer added on the peak height of the solution containing Se^{IV}

Fig. 5. Effect of the volume of $NH_2OH.HCl$ added on the peak height of the solution containing Se^{IV}

Fig. 6. Effect of KIO_3 concentration (%) on the peak height of the solution containing Se^{IV}

including one blank, add 0.05 ml of $HClO_4$ and 1.0 ml of 10% Na_2SO_3. Leave the solutions to stand for 15 min after mixing, then add 1.0 ml of NH_3 - NH_4Cl buffer (pH 10), 0.25 ml of 5% $NH_2OH.HCl$ and 0.50 ml of 4% KIO_3 in sequence to each cell. After mixing, dilute the contents of each cell to 5.0 ml with distilled water and leave to stand for about 1 h before performing the determination.

Fig. 1 shows the 1.5th-differential polarographic curve of Se^{IV} obtained using the three-electrode system and scanning from -0.20 to -0.70 V. The peak occurred at -0.57 V.

The Se present in natural waters appears almost entirely in the polarogram as Se^{IV} and Se^{VI} does not make a contribution to the wave obtained in a catalytic system. Therefore, for an accurate determination of the total Se present, it is necessary to reduce any Se^{VI} to Se^{IV} by the addition of HCl.[12]

The following procedure is recommended for the reduction of Se^{VI} to Se^{IV}. Add 0.05 ml of $HClO_4$ and 0.05 ml of HCl, in sequence, to electrolytic cells containing 0, 0.10, 0.20, 0.30, 0.40 and 0.50 ml of the 0.001 µg ml^{-1} stock solution of Se^{VI}. Stand the cells on a hot-plate or in a sand-bath, allow the solution to evaporate slowly until fumes of $HClO_4$ appear, then cool the solution and add 1.0 ml of 10% Na_2SO_3 as reductant. The procedure for the determination of Se^{VI} is the same as that for Se^{IV}.

Results and Discussion

Selection of the Catalytic System

For the determination of Se^{IV}, various compositions for the catalytic system including the components Na_2SO_3, $HClO_4$, Na_2SO_4, $KHCO_3$, K_2CO_3, NH_3 - NH_4Cl, KIO_3 and $NH_2OH.HCl$ were studied. The $HClO_4$ - Na_2SO_3 - NH_3 - NH_4Cl - $NH_2OH.HCl$ - KIO_3 system was selected, having a high sensitivity for the Se^{IV} catalytic wave.

Effect of the amount of $HClO_4$ added

In order to convert Na_2SO_3 to H_2SO_3 for use in the catalytic system, $HClO_4$ was added. As Fig. 2 shows, the maximum peak height for Se^{IV} was achieved with the addition of 0.05 ml of $HClO_4$.

Selection of the Na_2SO_3 concentration

Fig. 3 shows the effect of the Na_2SO_3 concentration (as reductant in acid medium) on the peak height of Se^{IV}. The

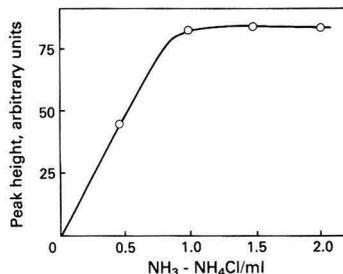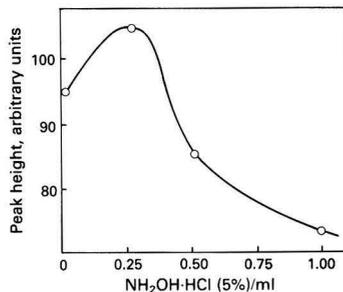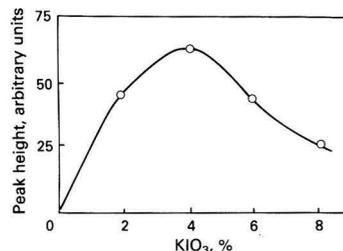peak maximum occurred with the addition of 1.0 ml of 10% Na_2SO_3 to the analytical system (final volume, 5 ml).

Effect of the amount of NH_3 - NH_4Cl buffer added

The effect of the amount of NH_3 - NH_4Cl buffer added on peak height is shown Fig. 4. The limiting value was reached when 1 ml of buffer solution was added.

Effect of the amount of $NH_2OH.HCl$ added

Fig. 5 shows the maximum peak height obtained when 0.25 ml of 5% $NH_2OH.HCl$ was added, in a total volume of 5.0 ml. The increase in the sensitivity of the Se peak height may be due to the presence of $NH_2OH.HCl$, which influences adsorption at the surface of the Hg drop, and the corresponding increase in the peak height caused by the catalytic reaction occurring at the electrode.[13]

Effect of the KIO_3 concentration

The Se peak height can be influenced considerably by a change in the concentration of KIO_3 (as a catalytic component). As shown in Fig. 6, the optimum choice was 0.5 ml of 4% KIO_3, in a total volume of 5.0 ml.

Based on these results, the optimum catalytic system consisted of 0.05 ml of $HClO_4$, 1.0 ml of 10% Na_2SO_3, 1.0 ml
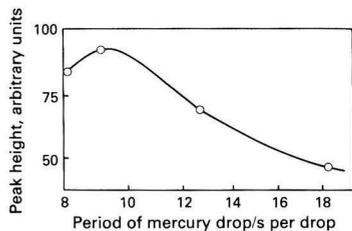
Fig. 7. Effect of the period of the mercury drop on the peak height. Sweep rate, 60 mV s^{-1}

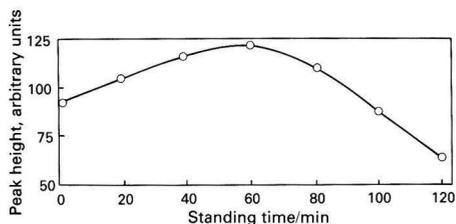**Fig. 9.** Effect of standing time on the peak height of the solution containing Se^{IV}

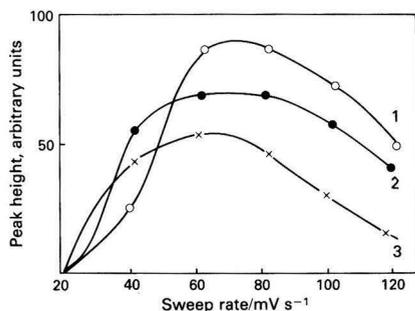**Fig. 8.** Effect of sweep rate on the peak height of the solution containing Se^{IV}. Period of mercury drop: 1, 9; 2, 11; and 3, 18 s per drop

of NH$_3$ - NH$_4$Cl (pH 10), 0.25 ml of 5% NH$_2$OH.HCl and 0.5 ml of 4% KIO$_3$, diluted to 5.0 ml with distilled water.

Optimisation of Instrumental Parameters

Effect of the period of the mercury drop on the peak current

The catalytic reaction at the electrode is influenced directly by the mercury flow-rate, hence the peak height was dependent on the length of the period of the mercury drop. The maximum peak height occurred with a 9-s period for a given sweep rate (Fig. 7).

Effect of sweep rate on the peak height

In order to obtain the maximum peak height, the sweep rate should be adjusted to fit the period of the mercury drop; 80 mV s^{-1} was chosen as the optimum sweep rate for a 9-s period (Fig. 8).

Initial voltage

The more positive was the initial voltage, the lower was the Se peak height. However, at potentials more negative than -0.4 V, the Se peak height was also influenced by the period of the mercury drop; therefore, an initial voltage of -0.2 V was chosen.

Effect of Standing Time

In order to obtain a stable result, the solution to be analysed was required to stand for some time. Fig. 9 indicates that 40–80 min was the optimum time; for times in the range 80 min–2 h, the peak height apparently decreased.

Effect of Interfering Ions

Generally, inorganic ions in natural waters do not interfere with the determination of Se^{IV}. From experiments, it was found that Ga^{3+}, Cu^{2+}, As^{3+} and Pb^{2+} (100 µg l^{-1}), Te^{4+} (50 µg l^{-1}), Ca^{2+}, Mg^{2+} and Mn^{2+} (20 mg l^{-1}), Fe^{3+}, NO$_3^-$ and
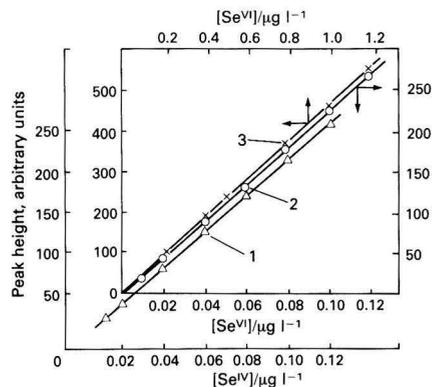
Fig. 10. Peak height plotted against [Se^{IV}] and [Se^{VI}]. Slope: 1, 100; 2, 100; and 3, 200
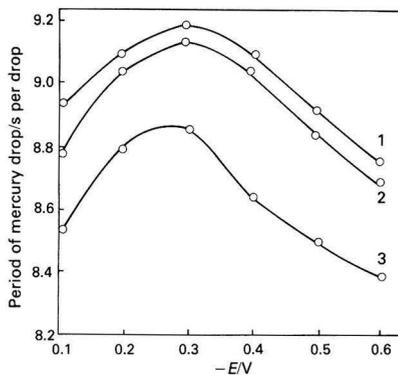
Fig. 11. Electrocapillary curves. 1, Without NH$_2$OH.HCl; 2, 0.25 ml of 5% NH$_2$OH.HCl added; and 3, 0.1 ml of 3% poly(vinyl alcohol) added
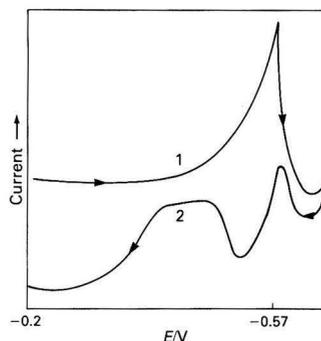

Fig. 12. Cyclic voltammetric curves: 1, cathodic sweep; and 2, anodic sweep

Table 1. Analytical results

Sample	Parameter	Mean value/ $\mu g \, l^{-1}$	No. of replicates	Standard deviation/ $\mu g \, l^{-1}$	Relative standard deviation,%	Standard added/$\mu g \, l^{-1}$	Recovery/ $\mu g \, l^{-1}$	Recovery,%
Water supply from								
Changchun city	Total Se	0.047	12	0.004	8.87	0.10	0.143	96
	Se^{IV}	0.014	12	0.002	14.3	0.04	0.054	100
	Se^{VI}	0.033	—	—	—	—	—	—
River water of the second								
Songhau river	Total Se	0.060	8	0.002	2.8	0.10	0.162	102
	Se^{IV}	0.037	8	0.003	6.98	—	—	—
	Se^{VI}	0.023	—	—	—	—	—	—
River water of Bing county								
(Shanxi province)	Total Se	0.284*	5	0.017	5.75	0.30	0.567	94
	Se^{IV}	0.009	5	—	—	—	—	—
	Se^{VI}	0.275	—	—	—	—	—	—
US Environmental Protection								
Agency Certified Values ..	Se^{IV}	0.227†	12	0.017	7.54	0.23	0.448	95

* Value determined by neutron activation analysis = 0.26 $\mu g \, l^{-1}$.
† Value given in US Environmental Protection Agency Manual, 600/4-79-020 = 0.231 $\mu g \, l^{-1}$.

SO_4^{2-} (5 mg l^{-1}), humic acid (10 mg l^{-1}) and 0.2 ml of 1% EDTA did not interfere. Mercury might interfere at levels greater than 25 $\mu g \, l^{-1}$; however, a better result can be obtained from the river water sample by nitration of the organic matter in it.

Relationship Between the Peak Current and the Concentrations of Se^{IV} and Se^{VI}

A linear relationship was obtained between the peak height and the Se concentration in the range 0.01–1.2 $\mu g \, l^{-1}$ under the optimum experimental conditions. As shown in Fig. 10, the graph for Se^{VI} (reduced in the presence of HCl) was consistent with that of Se^{IV}.

Study of the Behaviour of the Catalytic Wave of Se

Electrocapillary curve

The drop time is proportional to the surface tension of the dropping Hg. Therefore, as adsorption of $NH_2OH.HCl$ on the mercury surface would cause a decrease in the surface tension, the drop time should decrease correspondingly. Comparison of the curves shown in Fig. 11 clearly indicates adsorption of $NH_2OH.HCl$ on the mercury drop over a wide range (−0.1 to −0.7 V).

Effect of temperature on the peak current

The height of the catalytic wave increased with decreasing temperature. The temperature coefficients were −2.5% per °C (0–16 °C) and −6.8% per °C (16–32 °C), indicating the adsorptive behaviour of the catalytic wave.
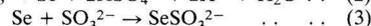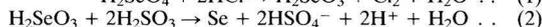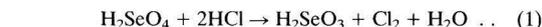
Effect of surface-active agent on the peak current

The adsorptive behaviour of the catalytic wave was also revealed by the experimental result that the peak height of the catalytic wave decreases and ultimately disappears with the addition of surface-active agents, such as poly(vinyl alcohol) and gelatin.

Cyclic voltammetric curve

The irreversibility of the reaction occurring at the electrode is shown clearly by the cyclic voltammetric curves in Fig. 12. Curve 1 indicates the adsorptive behaviour of the catalytic reaction; curve 2 shows two unsymmetrical peaks.

Catalytic mechanism

The behaviour of Se^{IV} in the catalytic reaction reported in the literature has been described as follows[14]:

$$H_2SeO_4 + 2HCl \rightarrow H_2SeO_3 + Cl_2 + H_2O \quad .. \quad (1)$$
$$H_2SeO_3 + 2H_2SO_3 \rightarrow Se + 2HSO_4^- + 2H^+ + H_2O \quad .. \quad (2)$$
$$Se + SO_3^{2-} \rightarrow SeSO_3^{2-} \quad .. \quad .. \quad (3)$$

The high sensitivity of the catalytic wave in Na_2SO_3 - NH_3 - NH_4Cl - KIO_3 (pH 10) results from the $SeSO_3^{2-}$ produced in the system. The reaction mechanism at the electrode is as follows:

$$SeSO_3^{2-} \xrightarrow[\quad IO_3^-, K_f \quad]{+2e^-} Se^{2-} + SO_3^{2-}$$
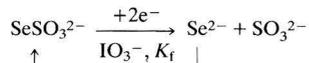
where K_f is the rate constant $(1.75 \times 10^9 \, l \, mol^{-1} \, s^{-1})$. The rate of the catalytic reaction is accelerated by the co-operative behaviour of $NH_2OH.HCl$ and KIO_3.

Analysis of Water Samples

Two 5.0- or 10.0-ml aliquots (depending on the Se content of the sample) of each water sample were transferred into electrical cells. These samples were then concentrated to half the original volume by heating gently on a hot-plate and 0.05–0.1 ml of $HClO_4$ and 0.2 ml of HNO_3 (concentrated) were added. One solution was evaporated to a volume of 0.2 ml (fumes appeared) and the other to a volume of 0.5 ml; to the latter was added 0.05 ml of HCl (concentrated), after which it was evaporated to a volume of 0.2 ml (white fumes appeared). To the two treated samples was then added 0.5 ml of 10% Na_2SO_3. After leaving the two solutions to stand for 20 min, 0.5 ml of NH_3 - NH_4Cl buffer, 0.1 ml of 5% $NH_2OH.HCl$, 0.25 ml of 4% KIO_3 and 1.0 ml of water were added to each solution in sequence. After shaking and allowing the mixtures to stand for 1 h, the total Se and Se^{IV} were determined. The reproducibility, accuracy and recovery of the experiment are indicated in Table 1.

Conclusion

Experimental results have demonstrated that the proposed 1.5th-differential polarographic method is simple, rapid, accurate and sensitive for the determination of Se in natural waters. The determination is carried out using the catalytic system $HClO_4$ - Na_2SO_3 - NH_3 - NH_4Cl - $NH_2OH.HCl$ - KIO_3 and suffers less interference from foreign ions under the selected conditions. The relationship between concentration and peak height (0.01–1.2 $\mu g \, l^{-1}$) is linear over a wide range with a correlation coefficient of 0.999, and the results are in good agreement with those achieved by neutron activation analysis and fluorimetry. Finally, the method can be applied to

the analysis of Se-containing water and soil samples from different regions.

References

1. Xu, H., "Biological Trace Elements—Selenium," Huazhong University of Science and Technology, Wu Han, Hu Ba Province, 1983, pp. 1–5.
2. "Selected Papers on Kasham Disease in China, Part I," Chinese Medical Academy, Beijing, 1977, pp. 53–56.
3. Schrauzer, G. N., *Bioinorg. Chem.*, 1975, **5**, 275.
4. Lieser, K. H., and Neitzert, V., *J. Radioanal. Chem.*, 1976, **31**, 397.
5. Ni, I., Terashina, S., and Ando, A., *Bunseki Kagaku*, 1984, **33**, 288.
6. Olson, O. E., *J. Assoc. Off. Anal. Chem.*, 1969, **52**, 627.
7. Wang, S., Xu, F., and Zhou, H., *Fenxi Huaxue*, 1980, **8**, 236.
8. Zhang, X., He, C., and Xu, C., "Acata Scientiarum Naturalium Universitatis Pekinesis," Beijing University Press, Beijing, 1985, No. 1.
9. Wu, D., *Fenxi Huaxue*, 1988, **16**, 159.
10. Kawashima, T., Kai, S., and Takashima, S., *Anal. Chim. Acta*, 1977, **89**, 65.
11. Goto, M., Hirano, T., and Ishii, D., *Bull. Chem. Soc. Jpn.*, 1978, **51**, 470.
12. "Proceedings of the 1984 Electroanalysis Meeting, Changchun, China, July 9th, 1984, Part I," 1984, p. 375.
13. Gao, X., and Yao, X., "The Catalytic Polarographic Wave of the Platinum Group," Scientific Press, Beijing, 1977.
14. Jiao, K., He, C., and Zhang, X., "Acata Scientiarum Naturalium Universitatis Pekinesis," Beijing University Press, Beijing, 1984, No. 5.

Simulation of Flow Injection Transients With Application to Amperometric Detector Response

Francis E. Powell

School of Food and Fisheries Studies, Humberside College of Higher Education, Grimsby DN34 5BQ, UK

Arnold G. Fogg

Department of Chemistry, Loughborough University of Technology, Loughborough, Leicestershire LE11 3TU, UK

An RC (resistance - capacitor) circuit has been built as an analogue simulator of the continuously stirred tank reactor model of the flow injection transport process. The analogue simulator was used as a fast-response time-calibration signal and to evaluate the fidelity of the time response of amperometric detection systems. Further uses of the device are discussed.

Keywords: *Flow injection; continuously stirred tank reactor; analogue simulator; amperometric detection*

The important parameters that describe the shape of a flow injection (FI) response curve are the peak height (*i.e.*, peak dispersion) and the peak variance (σ^2). The latter is made up of three contributions[1]:

$$\sigma_{peak}^2 = \sigma_{injection}^2 + \sigma_{transport}^2 + \sigma_{detection}^2 \quad .. \quad (1)$$

Excessive peak broadening due to the detector can present disadvantages in certain situations, *e.g.*, when limited transport dispersion is required in order to retain the original properties of the injected solution. Similar considerations apply in liquid chromatography, and here the detector variance has been divided further into a contribution due to the size and geometry of the detector cell, and contributions from the response times of the detector and recorder[2]:

$$\sigma_{detection}^2 = \sigma_{cell}^2 + \sigma_{electronic}^2 \quad .. \quad .. \quad (2)$$

Cell volume dispersion is usually studied by introducing a step change in the concentration of the signal-producing component and following the resulting response curve.[3–10] In this application it is important to have an estimate of the electronic time constants.

In this study, the fidelity of the responses of an amperometric detector and a recorder have been evaluated using a signal generator as an analogue simulator for the FI-pulse and concentration-step transport processes.

Continuous Stirred Tank Reactor (CSTR) Model of Transport Processes

The CSTR represents an idealised mixing stage in a transport process.[11] A solution containing a component of concentration c_0 flushes the solvent out of a mixing tank and the concentration rises with time t, given by the equation for the feed curve (*F*-curve)

$$c/c_0 = [1 - \exp(-t/\tau)] \quad .. \quad .. \quad .. \quad (3)$$

where τ is the residence time of the system. This response is symmetrically related to the curve [wash curve (*W*-curve)] obtained by washing out the vessel containing the solute at concentration c_0 with pure solvent[11]

$$F + W = 1 \quad .. \quad .. \quad .. \quad .. \quad (4)$$

This model is used frequently to describe the effect of detector volume on solute dispersion.[3–6]

The single-tank concept has also been adopted to model the FI process,[10] which in its simplest form consists of the transportation of the analyte from the point of injection to the detector without reaction [Fig. 1(*a*)]. In this model, the

dispersion in the transmission line is equivalent to the mixing process in a single CSTR stage [Fig. 1(*b*)]. The concentration of analyte in the sample is c_0. A small volume of this solution is injected into the carrier stream as a slug and on reaching the detector produces the idealised FI characteristic shown in Fig. 2. The leading edge of the slug initiates the *F*-curve response but when the following edge reaches the detector at t_p, a wash process takes over, producing a *W*-curve from the peak maximum at c_p. The shape of this characteristic can be decribed by the following parameters: residence time (τ); fraction of the peak signal (f) = c/c_p; dispersion (D) = c_0/c_p; and peak width (Δt) = $t_2 - t_1$.

The relationships existing between the parameters are obtained from the component *F*- and *W*-curves. The time t_1 is determined from the *F*-curve

$$c = c_0[1 - \exp(-t_1/\tau)] \quad .. \quad .. \quad .. \quad (5)$$

or, in parametric form,

$$t_1 = \tau \ln\left(\frac{D}{D - f}\right) \quad .. \quad .. \quad .. \quad (6)$$

At the peak maximum

$$t_p = \tau \ln\left(\frac{D}{D - 1}\right) \quad .. \quad .. \quad .. \quad (7)$$

The time t_2 is determined from the *W*-curve

$$c = c_p \exp[-(t_2 - t_p)/\tau] \quad .. \quad .. \quad .. \quad (8)$$

or, in parametric form,

$$t_2 = \tau \ln\left[\frac{D}{f(D - 1)}\right] \quad .. \quad .. \quad .. \quad (9)$$

Hence

$$\Delta t = \tau \ln\left[\frac{(D - f)}{f(D - 1)}\right] \quad .. \quad .. \quad .. \quad (10)$$

This final expression is equivalent to that obtained by Tyson.[12]

Principle of the Analogue Circuit

The *F*- and *W*-curves that form the basis of the mixing models described above are examples of first-order linear response functions, which have their counterparts in other physical systems.[13] In particular, RC (resistance - capacitor) electrical circuits can duplicate such behaviour and have been useful in the study of transport in a physiological context.[14] A schematic diagram of such a circuit, which can generate a full *F*-curve or the FI model characteristic, is shown in Fig. 3. The
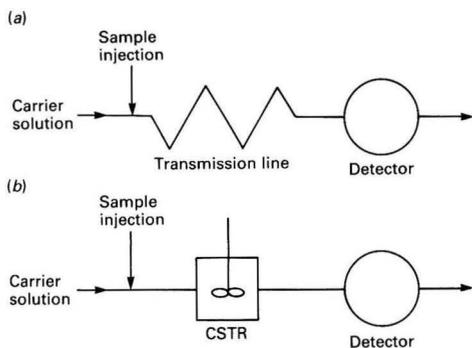
(a)

(b)

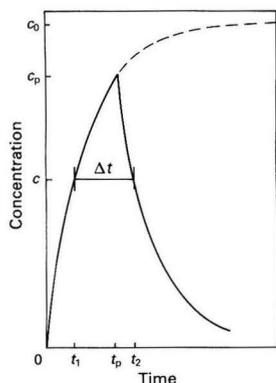**Fig. 1.** Schematic diagrams of (a) the single line FI manifold and (b) the hypothetical FI model system

Fig. 2. Idealised FI response characteristic: c_0, concentration of the injected sample; c_p, peak maximum concentration at time t_p; Δt, peak width at an arbitrary concentration at times t_1 and t_2

voltage developed at the output mimics the concentration from the CSTR. The RC circuit uses a resistance decade box and five calibrated 1-μF capacitors to provide RC charge time constants (equivalent to τ values) adjustable from 10 ms to 5 s. A fraction (0.21) of the input reference voltage is taken to a multiplier (actually a simple summing amplifier), which provides four equal steps from 0.21 to 0.84 and simulates the dispersion (D) in a reciprocal manner. Thus five dispersion values can be simulated. At the end of the charge cycle when the capacitor voltage (V_c) equals the comparator reference voltage, the comparator switches, thus triggering the bistable. The bistable controls the two ganged CMOS analogue switches, switching from the charge to the discharge cycle. The resistance and leakage effect of these switches is assumed to be negligible. The push-button resets the bistable and switches to charge and the start of another sweep. In addition to these fractional input voltages, there is a 1.05 option, which, when operational, ensures that the bistable cannot trigger; a full F-curve with a plateau at the input reference value is thus produced. High-input impedence operational amplifiers minimise errors due to shunt currents by buffering the input reference voltage to the control circuit and ensuring the accuracy of the output.

Apparatus and Experimental

Complete Assembly

The apparatus was centred around an electrochemical module that provided a voltage input to the cell or its analogue and also processed the response, which was in the form of a current flowing between the "test" input and a common virtual earth point within the module. This signal was converted internally into a voltage for display on the recorder (Fig. 4).

Electrochemical Module and Signal-matching Box

An EDT model ECP100 polarograph unit (EDT Analytical) was used. This instrument has an optional filtering time constant facility calibrated at 1.2 s. The output from the module was 1 V full scale and for interfacing purposes this was
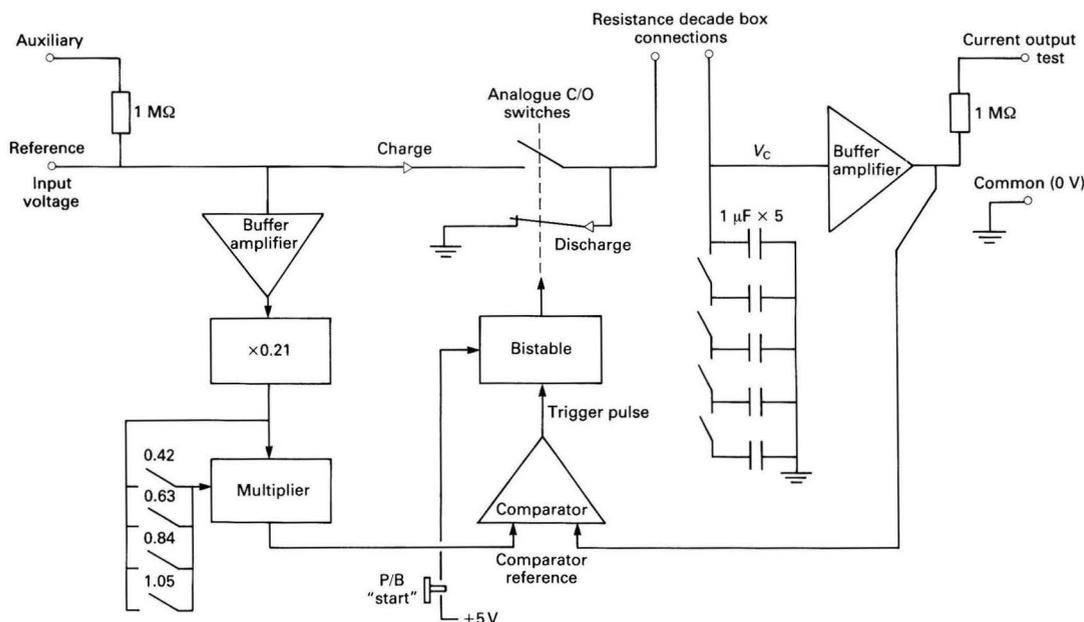

Fig. 3. Schematic diagram of the analogue circuit for the single-tank concentration step and the FI-pulse simulator
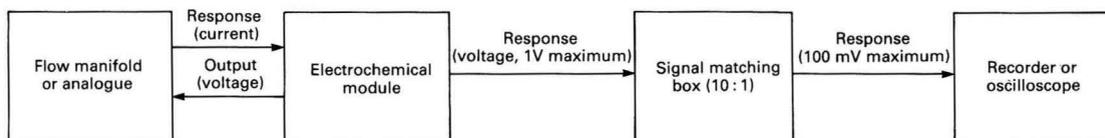
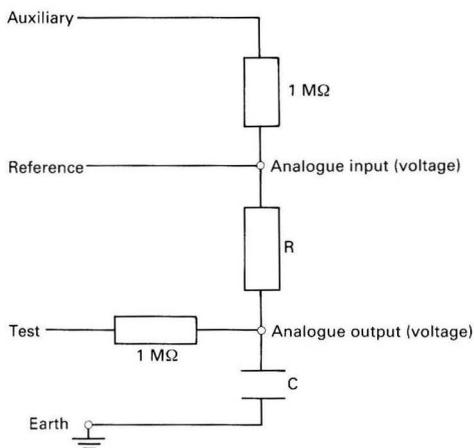**Fig. 4.** Schematic diagram of the assembly of response components

Fig. 5. Schematic diagram of the interface between flow analogue and EDT Model ECP100 polarograph. "Auxiliary," "reference" and "test" (or "working"), typically electrode connections from the polarograph to an electrochemical cell; R, resistance and C, capacitance components of the flow analogue circuit. C is connected to earth via the polarograph and "test" held to ground by the "virtual earth" of the current/voltage converter within the polarograph

Fig. 6. Pulse trace from the analogue obtained with the Howe YT1000 recorder. Chart speed, 10 mm s^{-1}. Analogue output: τ, 3 s; D, 1.359. Hatched lines joining experimental points ($\bigcirc$) represent peak width Δt values calculated from equation (10)

stepped down to 100 mV without loss of sensitivity via a laboratory-built operational amplifier signal impedance matching box.

Recording

Signals were recorded using either a Howe YT1000 pen recorder, a Telequipment DM64 storage oscilloscope or a Telequipment S51B oscilloscope (in conjunction with a Polaroid CR-9 camera and an appropriate Polaroid 667 black and white film).

Analogue

Although the analogue simulator as shown in Fig. 3 can be used with any suitable voltage source and voltage recorder, additional interfacing is required when using the analogue simulator in conjunction with the electrochemical module. "Auxiliary" and "reference" inputs were isolated by a 1 MΩ resistor functioning as the solution resistance. It was also necessary to convert the simulated voltage output into the current form using a voltage follower and a series 1-MΩ current-limiting resistor between the RC circuit and the "test" input. The voltage input from the electrochemical module was 1 V. These features are shown in Fig. 5. A full circuit diagram can be obtained from the authors.

Flow Manifold

A concentration-step input experiment was performed by injecting a 0.5-ml sample of 0.75 mM potassium hexacyanoferrate(II) in 1 M potassium chloride solution using a Rheodyne 5020 valve. The solution was presented horizontally to a glassy carbon wall-jet electrode. The construction and flow charac-
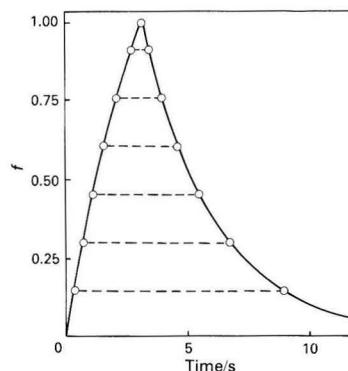
teristics of the laboratory-built wall-jet detector cell used have already been described.[15,16] In previous studies the carrier stream has been presented vertically upwards to the glassy carbon electrode, but in the work described here the detector unit was incorporated through a hole in the wall of a plastic beaker so that the carrier stream could be presented horizontally to the electrode. The detector unit was fixed (using epoxy resin) in place in the wall at the point where it had been clamped in previous applications.[15] The beaker contained 1 M potassium chloride solution in which was placed a silver - silver chloride reference electrode and a platinum auxiliary electrode to complete the three-electrode system. The potential of the working electrode was held at 0.70 V *versus* the reference to ensure diffusion-controlled electrolysis of the electroactive hexacyanoferrate(II) species. The transport line between the injection valve and the detection cell was 8 cm of PTFE tubing (i.d. 0.8 mm) and the solution was pumped by an Ismatec MS-4 Reglo/8 peristaltic pump. A pulse damper was placed between the pump and the injection valve.

Results and Discussion

FI Characteristics

Fig. 6 shows the display obtained with the pen recorder using $\tau = 3$ s and $D = 1.359$ from the RC analogue; the data points were calculated from equation (10). The trace demonstrates that accurate analogue signals can be generated and recorded under these conditions.

Polarographic Module Filter Time Constant

Many instruments have in-built exponential time constant circuitry to reduce high-frequency noise, but this can introduce over-all signal distortion. This effect can be demonstrated with the EDT module. The F-curves were obtained with and without operation of the filter circuit (Fig. 7). The convoluted arrangement used, *viz.*,

analogue function $(1 - e^{-t/\tau}, \tau = 1.2$ s$)$ * filter circuit

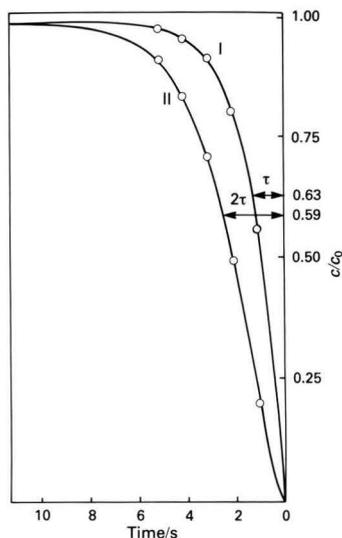response $(e^{-t/\tau}, \tau = 1.2$ s$)$

Fig. 7. *F*-curves obtained from the analogue to the EDT module. I, Without filter; II, with filter time constant $\tau = 1.2$ s in operation. The points shown were I, calculated from equation (3) and II, calculated from equation (11)
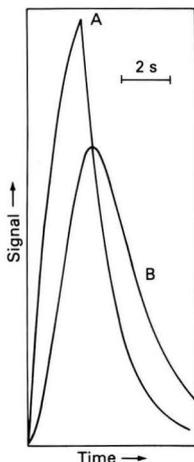

Fig. 8. Pulse signal ($\tau = 1.2$ s) through the EDT Model ECP100 polarograph. A, Without filtering; B, with filter time constant (1.2 s) in operation

corresponds in transport terms to the response from two tanks in series having equal volumes[17]:

$$c/c_0 = 1 - \exp(-t/\tau)(t/\tau + 1) \quad .. \quad .. \quad (11)$$

The experimental results agree well with this equation (Fig. 7), which also predicts that the total residence time (2τ) for the two mixing stages should occur at a c/c_0 value of 0.594; this is also confirmed experimentally in Fig. 7 where c/c_0 is seen to be located at 0.59 after 2.4 s. This value is significantly lower than the 0.632 fraction (based on a single tank) that is often used as an empirical measure of residence times in experimental situations[3-6]; hence such a practice should be viewed with some caution. When a simulated FI pulse ($\tau = 1.2$ s, $D = 1.19$) is passed through the same electronic path in the polarographic module as described, the output is modulated as shown in Fig. 8. The dispersion increases to 1.70 and the peak width broadens. In effect, the detection step introduces
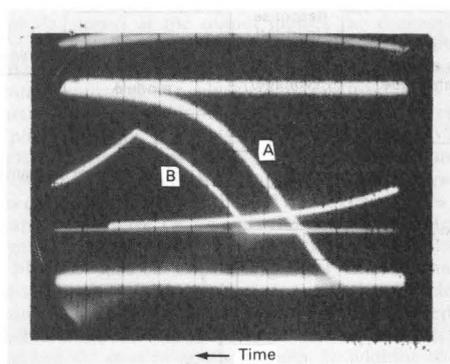

Fig. 9. Oscilloscope (Telequipment S51B) traces obtained. A, Experimental curve arising from the concentration step of 0 to 0.75 mm $K_4Fe(CN)_6$ in 1 m KCl in a glassy carbon wall-jet electrode detector cell. Flow manifold: 8 cm × 0.8 mm i.d.; flow-rate, 0.62 ml min^{-1}. B, Calibration curve from the analogue. RC = 1 s; peak maximum set at 0.63 full-scale response

an extra mixing stage into the total response. Actual FI curves reported extensively in the literature (*e.g.*, reference 18) bear a closer resemblance to the convoluted curve B than to curve A, suggesting that multi-mixing steps may more realistically represent actual manifold-detection systems than does the single mixing step. Another feature of the combined response is that the maximum occurs at the intersection with the original curve. In transport terms this follows from the mass balance on the second tank above, *viz.*, $\tau(dC_{out}/dt) = C_{in} - C_{out}$.

Here, C_{in} represents the signal from the RC analogue and C_{out} the combined response; τ is the effective residence time of the second stage (*i.e.*, in this instance, the filter time constant). Hence the output reaches a maximum ($dC_{out}/dt = 0$) when C_{in} equals C_{out}. A similar observation has been made on the effect of finite detector volume on Gaussian chromatographic elution curves.[19]

Recorder Calibration

The fidelity of the response through the polarograph module (with the filter circuit non-operational) and the signal-matching box was checked by sending an *F*-curve signal of known time constant (RC) from the analogue through the unit and measuring the response on a Telequipment DM64 storage oscilloscope, the time base of which was calibrated using mains frequency (50 Hz). A slow scan was used to establish the full-scale deflection and a fast scan was then employed to record the trace from which the experimental τ value was interpolated ($\tau = 0.632$ f.s.d.). Theoretical time constant values from 2 to 0.1 s were tried. At an RC value of 0.1 s, τ was found to be 0.101 ± 0.002 s (based on five replicates). However, when the pen recorder (Howe YT1000) was used in place of the oscilloscope and operated at its maximum chart speed (10 mm s^{-1}) the response to the analogue simulator was faithful only down to approximately $\tau = 1$ s. Thereafter, the response time of the pen was of the same order as the time constant of the transient signal and distortions of residence time and peak parameters appeared and became progressively worse as the τ value was reduced. As an independent check of this failure, the recorder response time was measured as 0.34 s, by a method based on the modulation in amplitude of standard sine waves.[20]

Transport transients with short residence times are therefore better captured with low-inertia recording. This is illustrated by the oscilloscope traces shown in Fig. 9, where the experimental *F*-curve (A) was generated by the step-wise change from 0 to 0.75 mm $K_4Fe(CN)_6$ (in 1 m KCl) when

presented to the electrochemical detector through the short transport line of the flow manifold. The time axis of the oscilloscope recorder was calibrated from the superimposed pulse trace (curve B), obtained by replacing the flow line by the analogue circuit. For this, using a peak-maximum voltage of 0.63 f.s.d., the peak time corresponded to the RC time constant (1 s) selected. Other experimental F-curves have been calibrated similarly using the versatility of the analogue device. This work is in progress.

Conclusion

Using an RC analogue circuit, the electronic components of an electrochemical detector have been shown to introduce negligible distortion to F-curve and FI peak transients down to residence times of 0.1 s unless the filter circuit is operational. However, a potentiometric pen recorder was found to be inadequate at residence times approximately three times the response time. Hence, in the recording of transport events having short residence times an oscilloscope or analogue to digital fast time capture microprocessor is essential. This is particularly relevant to response-curve studies of cell volume dispersion. The analogue circuit was also useful in the calibration of such a fast recording system.

References

1. Reijn, J. M., van der Linden, W. E., and Poppe, H., *Anal. Chim. Acta*, 1980, **114**, 105.
2. Scott, R. P. W., "Liquid Chromatography Detectors," Second Edition, Elsevier, Amsterdam, 1986, p. 27.
3. Forina, M., *Ann. Chim.*, 1973, **63**, 763.
4. Hanekamp, H. B., Bos, P., Brinkman, U. A. Th., and Frei, R. W., *Fresenius Z. Anal. Chem.*, 1979, **297**, 404.
5. Brunt, K., *Analyst*, 1982, **107**, 1261.
6. Stulik, K., and Pacakova, V., *Ann. Chim.*, 1986, **76**, 315.
7. Dieker, J. W., van der Linden, W. E., and Poppe, H., *Talanta*, 1979, **26**, 512.
8. Kutner, W., Debrowski, J., and Kemula, W., *J. Chromatogr.*, 1980, **191**, 47.
9. Kristensen, E. W., Wilson, R. L., and Wightman, R. M., *Anal. Chem.*, 1986, **58**, 986.
10. Tyson, J. F., and Idris, A. B., *Analyst*, 1981, **106**, 1125.
11. Nauman, E. B., and Buffham, B. A., "Mixing in Continuous Flow Systems," Wiley, New York, 1982, p. 6.
12. Tyson, J. F., *Analyst*, 1984, **109**, 319.
13. Pollard, A., "Process Control," Heinemann, London, 1971, p. 23.
14. Sheppard, C. W., "Basic Principles of the Tracer Method," Wiley, New York, 1962, pp. 89–113.
15. Fogg, A. G., and Summan, A. M., *Analyst*, 1984, **109**, 1029.
16. Powell, F. E., and Fogg, A. G., *Analyst*, 1988, **113**, 483.
17. Denbigh, K. G., and Turner, J. C. R., "Chemical Reactor Theory," Third Edition, Cambridge University Press, 1984, p. 86.
18. Valcarcel, M., and Luque De Castro, M. D., "Flow Injection Analysis," Wiley, New York, 1987, p. 81.
19. Vandenheuvel, F. A., *Anal. Chem.*, 1963, **35**, 1193.
20. McWilliam, I. G., and Bolton, H. G., *Anal. Chem.*, 1969, **41**, 1762.

Determination of Ethylenediaminetetraacetic Acid by Flame Atomic Absorption Spectrometry With a Chelating Ion-exchange Flow Injection Conversion System

Emil B. Milosavljević and Ljiljana Solujić

Institute of Chemistry, Faculty of Sciences, University of Belgrade, P.O. Box 550, 11001 Belgrade, Yugoslavia

James L. Hendrix and John H. Nelson

Departments of Chemistry and Chemical and Metallurgical Engineering, Mackay School of Mines, University of Nevada, Reno, NV 89557, USA

A flow injection method (FI) has been developed for the determination of ethylenediaminetetraacetic acid (EDTA) by flame atomic absorption spectrometry (FAAS). In the first step a copper(II) regenerant solution was injected on to an on-line column packed with Chelex-100 resin. The excess of copper ion, not retained on the column, was washed by an ammonia solution carrier. In the second step an EDTA sample was injected. The analyte displaced an equivalent amount of copper(II) from the chelating column. Eluted copper was determined by an FAA spectrometric detector positioned downstream. The signal obtained was proportional to the concentration of EDTA present in the injected sample. Using this FI-FAAS conversion method the detection limit was 0.1 μg ml^{-1}. The precision of the technique was better than a relative standard deviation of 1.5% at 0.50 μg ml^{-1} levels, with a throughput of 45 samples h^{-1}. The effect of sample volume and of ionic and organic ligand interferents on the FI-FAAS signals was studied. Only glycylglycine was found to interfere significantly.

Keywords: *Flow injection conversion method; flame atomic absorption spectrometry; chelating ion exchange; indirect ethylenediaminetetraacetic acid determination*

The on-line use of small chelating ion-exchange columns in flow injection (FI) combined with flame atomic absorption spectrometry (FAAS) is convenient for the pre-concentration, matrix isolation and subsequent determination of metal ions,[1–6] in addition to the speciation of different complexing[7] and oxidation[8] states of a given metal. Recently, an FI system was described[9] in which the analyte (sulphide) was precipitated on-line by cadmium(II) ions; the colloidal precipitate formed passed unhindered through the system and was detected by FAAS. A chelating ion-exchange material containing immobilised 8-quinolinol was utilised to retain the excess of cadmium(II) ions. The continuous flow non-chelating ion-exchange - FAAS system was used previously for the determination of free copper ion in solution.[10] To illustrate the precision and accuracy of this approach, the system was used to monitor the complexometric titration of copper(II) with ethylenediaminetetraacetic acid (EDTA).[10]

In this paper a different approach to an indirect determination of anions by an FI-FAAS system was developed. The method was tested for the determination of the disodium salt of EDTA, which in the FI manifold used displaces an equivalent amount of copper(II) ions from the chelating ion-exchange column in the copper form. The copper(II) liberated is determined by FAAS.

Experimental

Reagents and Materials

All chemicals were of analytical-reagent grade. The aqueous reagent and standard solutions were stored in polyethylene bottles. Re-distilled water was used throughout. Standard solutions of EDTA were prepared by suitable dilutions of a buffered 100 μg ml^{-1} EDTA solution. To all standards and samples was added a 2 M NH$_3$ - NH$_4$$^+$ buffer (pH 9.3) to a final concentration of 0.05 M. A slight modification of the manifold permits on-line addition of the buffer. However, the mixing coil and additional line that have to be added increase dispersion and lower the sensitivity of the method. The small column was made and packed with Chelex-100 resin (50–100

mesh, Sigma), which contains iminodiacetate functional groups, in a manner described earlier.[3,4] The resin in the column was changed from the sodium to the copper form as follows: 10 ml each of 2 M nitric acid, re-distilled water and concentrated copper(II) solution (1 g of CuSO$_4$.5H$_2$O in 50 ml of 2 M NH$_3$ - NH$_4$$^+$ pH 9.3 buffer) were pumped sequentially through the column at a flow-rate of 3.6 ml min^{-1}. The excess of copper was then washed from the column with 20 ml of re-distilled water. This procedure was repeated each day at the start-up. The regenerant solution was made up to be 50 μg ml^{-1} in copper(II) and 0.05 M in NH$_3$ - NH$_4$$^+$ pH 9.3 buffer.

Instrumentation and Apparatus

The flame atomic absorption spectrometer (Perkin-Elmer 2280), with an air - acetylene flame, was connected to a Honeywell Electronic 195 strip-chart recorder. The sample uptake of the nebuliser was adjusted to 3.6 ml min^{-1}. A copper hollow-cathode lamp (Perkin-Elmer) was used as the light source and the signals at 324.8 nm (0.7-nm spectral slit width) were recorded.

The two-valve FI manifold, which is illustrated in Fig. 1, was constructed from an FIAstar 5020 analyser (Tecator), equipped with two peristaltic pumps and an L-100-1 automatic sample volume injector. The other valve (Rheodyne, Model 5020) was used for regenerant injections. In the manifold illustrated in Fig. 2, a single laboratory-built eight-port valve, similar to that described earlier,[4] was used for the sequential injections of the sample and regenerant solutions. In both manifolds all connections were made of either 0.5 mm i.d. Microline or Tefzel tubing.

Results and Discussion

The feasibility of an indirect determination of EDTA anion by FAAS with a chelating ion-exchange flow injection conversion system was first tested using the simple manifold illustrated in Fig. 1. The analysis cycle was initiated [Fig. 1(a)]

(a)

(b)
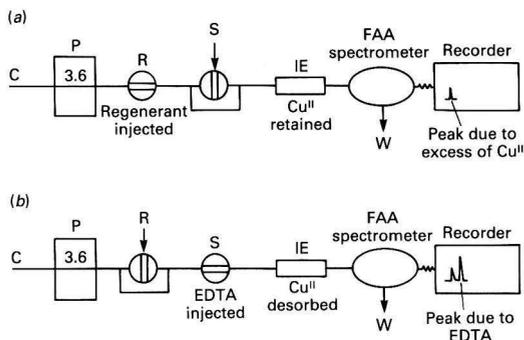
Fig. 1. Two-valve manifold used for the determination of EDTA. P, Peristaltic pump; R and S, regenerant and sample valves, respectively; IE, chelating ion-exchange column; and W, waste. The flow-rate of the carrier, C, is given in ml min^{-1}. (a) First step and (b) second step

(a)

(b)
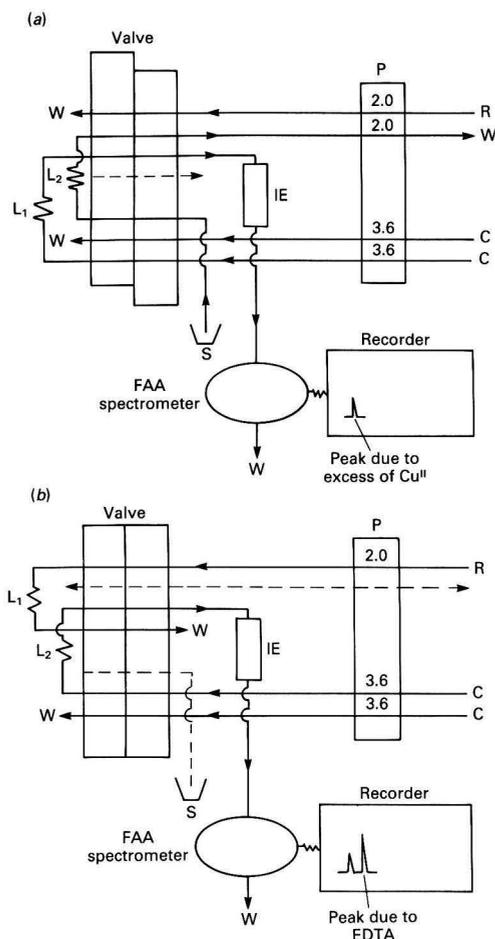
Fig. 2. Single-valve manifold used for the determination of EDTA. P, Peristaltic pump; R and C, regenerant and carriers, respectively; L_1 and L_2, regenerant and sample loops, respectively; IE, chelating ion-exchange column; S, sample; and W, waste. Flow-rates are given in ml min^{-1}. The description of the valve functions in positions (a) and (b) is given in the text

by injecting a pre-determined volume of a buffered copper(II) regenerant solution through valve R. The excess of copper(II) not retained on the column was washed by the carrier solution

Fig. 3. Rapid-scan response to two injections of a copper(II) regenerant (first signal in each pair) followed by a 40 µg ml^{-1} EDTA standard (valve switchings are indicated by the arrows)

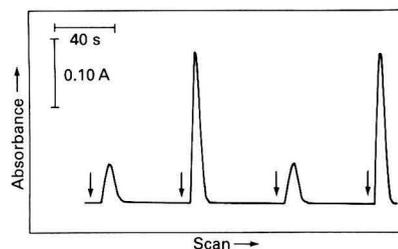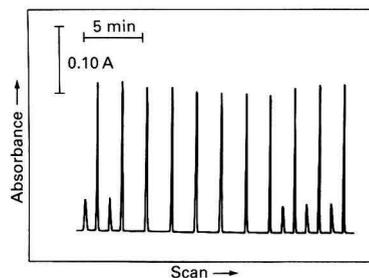**Fig. 4.** Effect of omitting the regeneration step after each analysis step (see text for details)

through to the FAA spectrometer where it was detected, and the corresponding peak recorded. In the second step [Fig. 1(b)], a buffered EDTA sample was injected through valve S. The EDTA eluted a nearly equivalent amount of copper(II) (see below) from the column to the FAA spectrometric detector where it was quantified. The corresponding peak recorded was proportional to the concentration of EDTA in the sample or standard injected.

In order to find the best carrier, several solutions were tested. With re-distilled water or 0.1 M NaCl carriers, it took an excessively long time (2.5–3 min) for the base line to be re-established after the injection of 250 µl of the copper(II) regenerant. A probable reason for this phenomenon was that after the copper(II) had filled all the chelating sites on the resin, some copper(II) ion was bound additionally by adsorption. Re-distilled water or 0.1 M NaCl only slowly eluted the adsorbed copper. A 0.02 M acetate buffer (pH 5.6) was found to be only slightly faster. However, the wash-out period for the excess of copper(II) regenerant was found to be very rapid with either a 0.05 M NH_3 - NH_4^+ buffer (pH 9.3) or a 0.2 M ammonia solution. With the latter as a carrier the copper(II) signal appeared 6 s after valve R was switched, and the base line was reached after only 25 s (Fig. 3). It was obvious that elution of the adsorbed (non-chelated) copper was much more rapid with a carrier that could form a relatively stable complex with copper(II). The signal due to eluted copper appeared 5 s after EDTA injection via valve S (200 µl) and the base line was reached after 17 s.

Fig. 4 illustrates an experiment in which a single EDTA standard was injected twice in the normal fashion (with the regeneration step), followed by six injections of the same standard without the regeneration step, and finally, three injections with re-introduced regeneration. As can be seen, the EDTA signal decreased steadily when the regeneration step was omitted. Also, it took three complete cycles to re-establish the previous signal value for a given EDTA standard.

After it had been established that an indirect FI-FAAS method for the quantification of EDTA was possible, the two-valve manifold was replaced by a single-valve manifold.
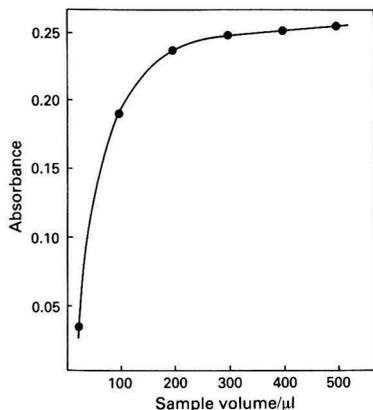
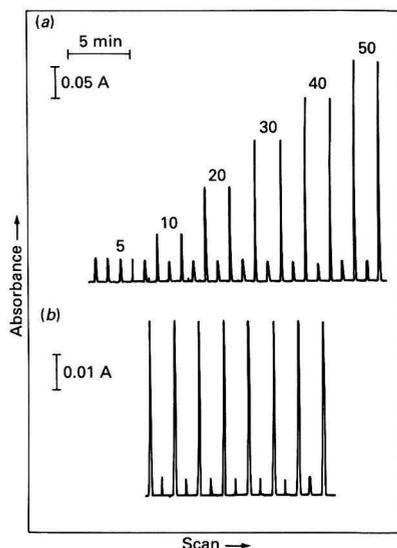**Fig. 5.** Variation of absorbance with injected volume

Table 1. Determination of EDTA in the presence of potential interferents (all samples contained 10 µg ml^{-1} of EDTA and 400 µg ml^{-1} of the salt)*

Salt				Molar concentration ratio Salt : EDTA	Change in absorbance,† %
NaCl	..	..	..	255	−0.9
Na$_2$CO$_3$		..	..	140	+5.2
NaNO$_3$		..	..	175	−3.6
NaBr	..	..	..	145	−2.0
Na$_2$SO$_3$		..	..	118	−0.9
NaNO$_2$		..	..	216	−2.3
Na$_3$PO$_4$		..	..	91	+2.3
Na$_2$B$_4$O$_7$		..	..	74	+3.1
KI	..	..	..	90	−3.3
KCl	..	..	..	200	−0.6
NH$_4$Cl	..		..	278	+0.7
Na$_2$SO$_4$		..	..	105	+0.4
KSCN	..	..	..	153	−3.2

* All samples contained a 0.05 M NH$_3$ - NH$_4^+$ buffer (pH 9.3).

† Signs + or − indicate an increase or decrease in absorbance relative to a pure EDTA standard, respectively.

Fig. 6. (a) Calibration run for EDTA in the concentration range 5–50 µg ml^{-1} (each standard was injected in duplicate) with the manifold depicted in Fig. 2. (b) Recordings of seven repetitive injections of a 0.50 µg ml^{-1} EDTA standard. The first peak in each pair corresponds to an excess of regenerant

This system, illustrated in Fig. 2, in which all the flow patterns required were regulated by a single eight-port rotary valve, simplified manipulation, eventual miniaturisation and full automation.

The analytical cycle commenced by switching the valve to position (a) (regeneration step). In this position an ammonia solution carrier washes the regenerant from the regenerant loop L$_1$ to the column IE. The copper(II) not retained on the column was washed to the FAA spectrometer and the peak due to the excess of regenerant was recorded. At the same time an EDTA sample or standard filled the sample loop L$_2$, while one carrier line and regenerant flowed to waste. In order to preserve the regenerant, the corresponding waste line could be connected back to the regenerant container. When the valve was switched to position (b) (analysis step), EDTA from loop L$_2$ eluted copper(II) from the column to the FAA spectrometer where the latter was detected. The peak obtained was proportional to the concentration of EDTA in

the sample. At the same time the regenerant filled the loop L$_1$ for a subsequent regeneration step. Repeating the cycle quantified EDTA in the next sample or standard.

The dispersion coefficient, defined previously,[11,12] for the FI conversion system needed to be determined indirectly, as it must be ensured that there is no interaction between the column material and the analyte. Also, in order to determine C^0 (the original concentration of a given standard solution) EDTA cannot be pumped through the system because this analyte is not quantified directly by the FAA spectrometric detector. In order to determine the dispersion coefficient for the system described, it was desirable to determine C^0, by pumping a copper(II) standard in 2 M nitric acid as a carrier, and to determine C^{max} (the concentration that corresponds to the apex of the FI signal), by injecting the same copper(II) standard using 2 M nitric acid as a carrier. Under these conditions (low pH) copper(II) was not retained (chelated) by the resin in the column. By comparing C^0 and C^{max} a value of only 1.16 was found for the dispersion coefficient for a single-valve manifold (volume of L$_1$ = 200 µl).

Experiments were carried out to determine an optimum sample loop volume. The results obtained when various sample volumes of a 40 µg ml^{-1} EDTA standard were injected are shown in Fig. 5. As can be seen, sample volumes greater than 200 µl did not increase the sensitivity of the system appreciably. For all the subsequent experiments (study of linearity, reproducibility and interferences), the sample and regenerant loop volumes were 200 and 250 µl, respectively.

The conversion efficiency[13] for this system could be calculated from the ratio of peak heights obtained when equivalent concentrations of EDTA and copper(II) were injected via the sample loop; an EDTA standard was injected using a 0.2 M ammonia solution carrier after the usual regeneration step, whereas a copper(II) standard was analysed using a 2 M nitric acid carrier [no retention of copper(II) by the resin; the set-up was identical with that used for the dispersion coefficient determination described earlier]. The conversion factor indicated how much of the EDTA injected was converted on-line to the corresponding copper complex in the FI manifold used. Assuming the expected 1 : 1 stoicheiometry, the conversion factor for the system investigated was found to be 0.96 (value of 1 indicates total conversion).

Fig. 6(a) illustrates a typical calibration run for the concentration interval 5–50 µg ml^{-1} of EDTA (each standard was injected in duplicate) for a single-valve manifold with the volume of L$_1$ = 250 µl and L$_2$ = 200 µl; linear calibration graphs were obtained in the interval 0.5–50 µg ml^{-1} of EDTA, with a slope and correlation coefficient of $(6.37 \pm 0.30) \times 10^{-3}$

Table 2. Study of potentially interfering organic ligands*

Compound†	Absorbance‡
Glycine	0.006
Glycylglycine	0.039
Imidazole	0.003
1,5-diphenylcarbazide§ ..	0.003
1,10-phenanthroline ..	0.005
Thiourea	0.003
Thioacetamide	0.002
Potassium oxalate	0.003
Citric acid	0.012
Potassium cyanide	0.011

* A 10^{-4} M EDTA standard gave an absorbance of 0.230.
† All samples contained a 0.05 M NH_3 - NH_4^+ buffer (pH 9.3).
‡ Average of three determinations.
§ 1% *V/V* acetone added.

A μg^{-1} ml and 0.9991, respectively. The detection limit, calculated according to a recent recommendation,[14] was 0.1 μg ml^{-1}. Fig. 6(*b*) shows that very good reproducibility was obtained even at low analyte concentrations of 0.5 μg ml^{-1} [relative standard deviation (RSD) = 1.4% for *n* = 7].

The study of potential interferents was divided into two parts. In the first part, common inorganic anions which form only weak complexes with copper(II) were investigated. This study was carried out in the following manner. To a 10 μg ml^{-1} EDTA standard a 40-fold excess (400 μg ml^{-1}) of a possible interferent was added and the change in absorbance relative to a standard containing only EDTA was determined. In the molar concentration comparisons, the excesses of the possible interferents were at levels from about 260- to 70-fold. Table 1 summarises this study. It can be seen that only Na_2CO_3 interfered at a level >5%. In the second part some organic ligands which form relatively stable complexes with copper(II) ion were tested. A series of possible interferents was studied at concentrations of 10^{-4} M. These solutions were injected via the sample loop L_2, and the absorbance values due to the copper eluted from the column were compared with the corresponding value obtained after the injection of an EDTA standard of the same concentration (10^{-4} M). The results are summarised in Table 2. From this table, at equivalent concentrations the only significant interferent was glycylglycine.

Conclusion

A technique for the indirect determination of disodium ethylenediaminetetraacetate by FAAS utilising an FI conver-

sion method has been described. Atomic absorption spectrometers have become ubiquitous in analytical laboratories, and this novel approach makes it possible to increase the number of species determinable with such spectrometers.

The potential of similar conversion techniques lies also in determining the chelating (complexing) ability of different natural samples. By selecting various chelating resin materials and metal ion regenerants, it should be possible to devise a systematic scheme for determining the complexing ability of a given sample in a complicated matrix. For example, these types of experiments may be important in following the fate of many metallic ion pollutants in the environment.

References

1. Olsen, S., Pessenda, L. C. R., Růžička, J., and Hansen, E. H., *Analyst*, 1983, **108**, 905.
2. Malamas, F., Bengston, M., and Johansson, G., *Anal. Chim. Acta*, 1984, **160**, 1.
3. Fang, Z., Xu, S., and Zhang, S., *Anal. Chim. Acta*, 1984, **164**, 41.
4. Fang, Z., Růžička, J., and Hansen, E. H., *Anal. Chim. Acta*, 1984, **164**, 23.
5. Fang, Z., Xu, S., and Zhang, S., *Fenxi Huaxue*, 1984, **12**, 997.
6. Bengston, M., Malamas, F., Torstensson, A., Regnell, O., and Johansson, G., *Mikrochim. Acta*, 1985, **III**, 209.
7. Milosavljević, E. B., Růžička, J., and Hansen, E. H., *Anal. Chim. Acta*, 1985, **169**, 321.
8. Milosavljević, E. B., Solujić, Lj., Nelson, J. H., and Hendrix, J. L., *Mikrochim. Acta*, 1985, **III**, 353.
9. Petersson, B. A., Fang, Z., Růžička, J., and Hansen, E. H., *Anal. Chim. Acta*, 1986, **184**, 165.
10. Treit, J., Nielsen, J. S., Kratochvil, B., and Cantwell, F. F., *Anal. Chem.*, 1983, **55**, 1650.
11. Růžička, J., and Hansen, E. H., *Anal. Chim. Acta*, 1978, **99**, 37.
12. Růžička, J., and Hansen, E. H., "Flow Injection Analysis," Second Edition, Wiley, New York, 1988, p. 24.
13. Haj-Hussein, A. T., Christian, G. D., and Růžička, J., *Anal. Chem.*, 1986, **58**, 38.
14. Analytical Methods Committee, *Analyst*, 1987, **112**, 199.

Indirect Determination of Zirconium in Microgranite Samples by Atomic Absorption Spectrometry

Debasis Chakraborty and Arabinda K. Das*

Department of Chemistry, University of Burdwan, Burdwan-713 104, India

An indirect method for the determination of zirconium in microgranite rock samples by atomic absorption spectrometry (AAS) is described. Zirconium forms a stable ion associate, $Zn^{2+}[ZrF_6]^{2-}$, in acidic solution that can be extracted into chloroform with an efficiency greater than 99.5%. The extract can be analysed for Zn (and hence indirectly for Zr) by AAS after stripping back into an aqueous phase containing 4 M HCl. The limit of detection by this method is 42 ng ml^{-1}, equivalent to a limit of determination in the rock of 1.1 µg g^{-1}. The calibration graph is linear up to 2.25 µg ml^{-1} of Zr. Large numbers of foreign ions do not interfere. The method was applied successfully to the determination of Zr in microgranite samples from Mayurbhanj (India).

Keywords: *Zirconium determination; solvent extraction; indirect atomic absorption spectrometry; microgranite analysis*

There are few reports on the direct determination of zirconium by atomic absorption spectrometry (AAS).[1-7] Direct methods for the determination of trace amounts of Zr by AAS with the higher temperature N_2O - C_2H_2 flame are not satisfactory because Zr forms refractory compounds that are difficult to vaporise and dissociate, resulting in low sensitivity with AAS.[1] Serious interferences[8] from various ions and compounds on the atomic absorption signal of Zr have also been observed. The sensitivity can be improved to some extent by solvent extraction of Zr with direct aspiration of the solvent[7] into an N_2O - C_2H_2 flame and by the addition of electrolytes such as $AlCl_3$,[1,2] $FeCl_3$[2] and NH_4Cl.[3] However, these techniques have not been studied fully for routine analysis. Aznarez *et al.*[9] reported a sensitive indirect AAS method for the determination of Zr that involves the formation of a heteropoly acid, molybdozirconophosphoric acid, in an acidic medium. This complex can be extracted into isobutyl methyl ketone (IBMK) and the Mo content determined by AAS using an N_2O - C_2H_2 flame. However, serious interferences may arise owing to co-extraction of other heteropolyacids, formed by Mo and other elements, into the same solvent. The most commonly used method for the determination of Zr in rock samples is X-ray fluorescence (XRF) spectrometry.[10,11] This is the preferred technique because of the large sample size and lack of sample preparation required, but the method is expensive.

In this paper, a rapid and sensitive indirect AAS method for the determination of Zr is described. The method is based on the fact that in acidic solution, Zr and fluoride ions form a stable complex with Zn, namely $Zn[ZrF_6]$, which can be extracted into chloroform. The Zn in the extract can be determined by flame AAS after stripping back into the aqueous phase with 4 M HCl. The amount of Zn is directly proportional to the concentration of Zr. The method was applied successfully to the determination of Zr in microgranite samples.

Experimental

Apparatus

Absorbance measurements were made with a Shimadzu atomic absorption spectrometer (Model 646) under the following instrumental conditions: Zn lamp current, 6 mA; wavelength, 213.9 nm; slit width, 0.38 nm; C_2H_2 flow-rate, 2.5 l min^{-1}; air flow-rate, 10 l min^{-1}; and burner height, 4 mm.

The pH values were measured with a Sambros digital pH meter (Model 335).

* To whom correspondence should be addressed.

Reagents

Zinc solution. A stock solution was prepared by dissolving $ZnSO_4.7H_2O$ (AnalaR, BDH, Bombay, India) in doubly distilled water and was standardised (1500 µg ml^{-1}) titrimetrically[12] with standard ethylenediaminetetraacetic acid (EDTA) solution. Working solutions were prepared from this stock solution by serial dilution with doubly distilled water.

Zirconium solution. A stock solution was prepared by dissolving $ZrOCl_2.8H_2O$ (guaranteed-reagent grade, Merck, Darmstadt, FRG) in 0.3 M HCl and was standardised (1250 µg ml^{-1}) gravimetrically[13] as ZrP_2O_7 and diluted with water as required. All other reagents used were of analytical-reagent or guaranteed-reagent grade.

Procedure

The following solutions were placed in a separating funnel in the order given: 1 ml of Zn^{2+} solution (200 µg ml^{-1}), 0.5 ml of 1.25% KF solution, 1 ml of the sample solution [for the blank, 1.0 ml of the process blank (see below) was used], 0.5 ml of pH 4.6 buffer (CH_3COONa - CH_3COOH solution) and 5 ml of chloroform. The funnel was shaken for 45 s and the mixture was allowed to stand for 3 min to establish the extraction equilibrium. The aqueous phase was discarded and the organic phase was washed twice with 2 ml of doubly distilled water and the washings were discarded. The organic phase was then treated with 5 ml of 4 M HCl and the volume of the aqueous phase was made up to 10 ml. Finally, the absorbance was measured by aspirating the aqueous phase into an air - C_2H_2 flame using doubly distilled water as the reference.

Preparation of the Rock Sample

The microgranite samples were collected from Mayurbhanj, India. Zirconium is known to be a difficult element to determine in granite rocks because it may not be distributed homogeneously, therefore presenting difficulties in sampling. Hence various parts of a microgranite rock were taken, finely ground and mixed well. A portion of this mixture was dried in an air-oven at 120 °C for 2 h and then kept in a desiccator for 1 h. A sample (0.5–1.1 g) was placed in a platinum crucible and treated[14] several times with 40% HF on a hot-plate to remove the silica. The residue was treated three times with 40% $HClO_4$ (5 ml each time) and the solution evaporated to dryness. The residue was taken into solution with 3 M HCl; any insoluble residue was fused with NaOH, taken into solution with 40% $HClO_4$ and mixed with the first acid-soluble fraction. Microgranites are likely to contain the acid insoluble
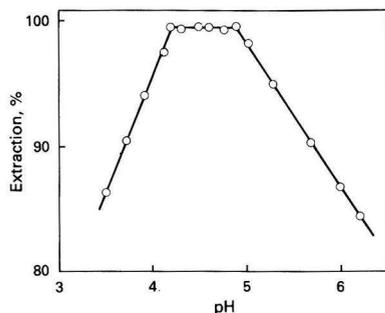
Fig. 1. Effect of pH on the extraction of Zr

Fig. 2. Decrease in absorbance of Zr ($1.25 \ \mu g \ ml^{-1}$) with time

mineral zircon, which may contain a large proportion of the Zr. Hence fusion with NaOH is important. Large amounts of Fe present in the microgranite sample solutions were removed by adding 1 ml of NH_4SCN solution ($4500 \ \mu g \ ml^{-1}$) and extracting the resulting $[Fe(SCN)]^{2+}$ complex into IBMK from 2 M HCl. The final volume of the solution was made up to 25 ml after adjusting the pH to 4.6.

Process Blank

For the preparation of the process blank, all the steps described above for sample preparation were followed (except for the addition of the rock powder) and the volume of the final solution was made up to 25 ml after adjusting the pH of the solution to 4.6, as above.

Results and Discussion

Shaking Time and Kinetics of Extraction

The extraction of the Zr complex into chloroform was investigated by shaking 5 ml of the solvent vigorously with the aqueous phase for various times. It was found that shaking for 30 s was sufficient for complete extraction. The time necessary to achieve the extraction equilibrium was tested with chloroform at pH 4.6. The extraction with this solvent proved to be very fast; the equilibrium was reached in about 3 min for both the known and unknown samples.

Effect of pH

The pH of the solution had a marked affect on the formation and extraction of the ion associate. As shown in Fig. 1 the percentage extraction was maximum and constant over the pH range 4.2–4.9. The working pH was fixed by using a CH_3COONa - CH_3COOH buffer of pH 4.6.

Choice of Solvent

Five different solvents were investigated as possible extractants of the ion associate (extraction efficiencies for Zr indicated in parentheses): chloroform (99.52%), carbon tetrachloride (58.36%), nitrobenzene (18.27%), butyl acetate (5.52%) and isoamyl acetate (3.31%). The results showed that the best solvent was chloroform because it was highly selective and gave the highest efficiency of extraction.

Choice of Stripping Agents

The $Zn^{2+}[ZrF_6]^{2-}$ ion associate was back-extracted from chloroform into the aqueous phase using a number of different acids, e.g., HCl, HNO_3, H_2SO_4 and $HClO_4$ of various strengths. Of these, HCl gave the highest sensitivity. Varying the strength of the HCl showed that complete back-extraction was achieved when the acid strength was 3 M or higher.
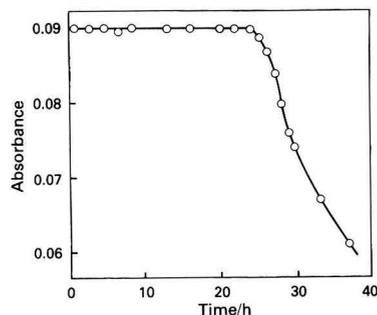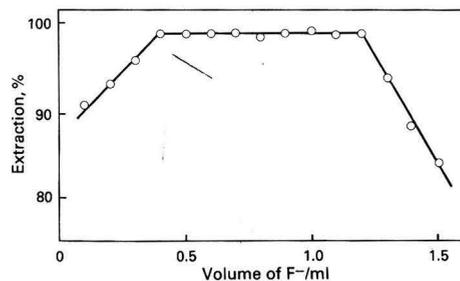

Fig. 3. Optimisation of the fluoride (1.25%) concentration

Variation of the Polarity of the Medium

The polarity of the aqueous phase was varied by the addition of different polar solvents, e.g., methanol, ethanol and 1,4-dioxane. However, the results indicated that the presence of these polar solvents caused a decrease in the extraction efficiency of the Zr complex. Hence, the use of these solvents was avoided in the procedure.

Stability of the Complex

The extracted complex was very stable, the absorbance remaining unchanged for 24 h. Thereafter, the absorbance decreased slowly owing to decomposition of the complex (Fig. 2).

Choice of the Metal

Five different divalent metal ions were used for the extraction of Zr from a fluoride medium. The extraction efficiency of the complex formed ($M^{2+}[ZrF_6]^{2-}$) was in the order, $Zn^{2+} >$ $Cu^{2+} > Cd^{2+} > Co^{2+} > Ni^{2+}$; hence the Zn^{2+} ion was used in the recommended procedure.

Choice of the Fluoride System

Using NH_4HF_2, KF and NaF, respectively, the $[ZrF_6]^{2-}$ ion was extracted into chloroform after complexing with Zn^{2+}. The results indicated that KF was the best system because it gave the highest extraction efficiency for a fixed amount of Zr ($1 \ \mu g \ ml^{-1}$).

Effect of Fluoride Concentration

As the concentration of KF in the aqueous phase was increased, the extraction efficiency of Zr also increased. However, it was found that the net extraction of Zr from the sample solution remained constant when the volume of KF

solution (1.25%) added was between 0.4 and 1.2 ml (Fig. 3). Hence a volume of 0.5 ml was used. The absorbance of the blank solution was unaffected by the addition of KF to the aqueous phase.

Effect of Foreign Ions

Experiments showed that it was possible to determine 10 μg of Zr^{4+} reliably (within an error of ±2%) in the presence of the following ions: NO_3^-, SO_3^{2-}, SCN^- and citrate (each at a 300-fold excess); $S_2O_3^{2-}$, $C_2O_4^{2-}$, CH_3COO^- and NO_2^- (each at a 200-fold excess); PO_4^{3-}, Br^-, I^- and $EDTA^{2-}$ (each at a 150-fold excess); Cl^-, WO_4^{2-}, AsO_4^{3-}, BrO_3^-, Ba^{2+}, SiO_3^{2-}, Co^{2+} and SeO_4^{2-} (each at a 120-fold excess); $B_4O_7^{2-}$, tartrate, SO_4^{2-}, IO_3^-, VO_3^-, Fe^{3+}, Al^{3+}, Ni^{2+}, Cd^{2+}, Mn^{2+} and Pt^{4+} (each at a 110-fold excess); Cu^{2+}, S^{2-}, La^{3+}, Mg^{2+} and Pb^{2+} (each at an 80-fold excess); Ti^{4+} (at a 60-fold excess); Ru^{3+} and Os^{3+} (each at a 40-fold excess); and Hf^{4+} (at a 15-fold excess). No serious interference effects are therefore expected for the determination of 10 μg of Zr. Moreover, the separation of Zr^{4+} and Hf^{4+}, which is normally a major problem in analytical chemistry, has been largely overcome using the proposed method.

Composition of the Complex

The composition of the complex was confirmed as being $Zn[ZrF_6]$ rather than $Zn_2[ZrF_8]$ or larger complexes by applying the molar ratio method to a series of solutions with fixed fluoride and Zr^{4+} concentrations and increasing Zn^{2+} concentrations. The molar ratio was determined to be 1.01, as expected for an extracted complex with the formula $Zn^{2+}[ZrF_6]^{2-}$.

Analytical Figures of Merit

The calibration graph is linear up to 2.25 μg ml⁻¹ of Zr. The limit of detection[15] (3σ) is 42 ng ml⁻¹, equivalent to a limit of determination in the rock of 1.1 μg g⁻¹. The sensitivity (the slope of the graph of absorbance *versus* concentration of Zr) of the method is 62 ml ng⁻¹ which is better than that of the direct AAS methods. The relative standard deviation (RSD) for ten determinations of 1.20 μg ml⁻¹ of Zr is 1.36% and for ten determinations of 1.10 μg ml⁻¹ of Zr in microgranite (A-2) solution the RSD is 1.85%.

Table 1. Determination of the Zr content in microgranite samples

Sample No.				Total Zr/μg g⁻¹	
				Present method	Spectrophotometric method
A-1	..	..	..	..	110.2	111.2
A-2	..	..	..	..	359.3	358.8
A-3	..	..	..	..	136.0	135.0
Bg-81	..	..	..	..	50.3	51.3
Bg-97	..	..	..	..	302.5	288.9
Bg-153	..	..	..	..	152.9	152.1

Table 2. Recovery of Zr from microgranite samples. Amount of sample solution taken: 1.0 ml in each instance

Sample No.			Zr added/μg	Zr found/μg	Recovery, %
A-1	..	..	0	4.6	—
			5.0	9.5	98
			7.0	11.8	103
A-3	..	..	0	5.4	—
			7.0	12.0	94
			9.0	14.3	99
Bg-153	..	..	0	4.2	—
			8.0	12.6	105
			10.0	13.9	97

Application

The results for the determination of Zr in various microgranite samples are shown in Table 1, and are compared with those given by a sensitive spectrophotometric method[16] using Alizarin S. To check the proposed method, three microgranite samples were also analysed by inductively coupled plasma atomic emission spectrometry (ICP-AES) at the Central Chemical Laboratory, Geological Survey of India, Calcutta. The results of the analyses were as follows: sample A-1, 112.0; sample Bg-97, 295.2; and sample Bg-153, 153.4 μg g⁻¹ of Zr. These values are comparable to those obtained with the proposed method and the spectrophotometric method. Apparent recoveries of 94–105% were obtained for the determination of Zr in three microgranite samples spiked with 5–10 μg of Zr (Table 2).

Conclusion

A solvent extraction method for the determination of Zr has been developed. The technique is based on the extraction of a Zn - Zr complex from an acidic solution into chloroform. The atomic absorption signal of Zn is then measured, which gives an indirect value for the Zr concentration. Owing to poor sensitivity, the direct determination of Zr by AAS is not widely used. High sensitivity was attained using the proposed indirect AAS method.

The indirect method described is highly sensitive, rapid and simple and is free from interferences from a large number of ions. The Zr in the microgranite samples can be determined accurately without using a masking agent and this is a particular advantage of the method. The procedure is suitable for the routine laboratory determination of Zr and provides an alternative to existing methods such as XRF[10,11] for the determination of Zr in geological samples.

References

1. Seymour, R. J., and Boss, C. B., *Anal. Chem.*, 1982, **54**, 1037.
2. Wallace, G. F., Lumas, B. K., Fernandez, F. J., and Barnett, W. B., *At. Spectrosc.*, 1981, **2**, 130.
3. Liu, J., and Zheng, Y., *Fenxi Huaxue*, 1982, **10**, 545.
4. Ermakov, V. S., Chekmarev, A. M., and Petrukhin, O. M., *Otkrytiya Izobret*, 1985, **4**, 126.
5. Yoshio, Y., and Kanji, I., *Bunseki Kagaku*, 1979, **28**, 733.
6. Hoare, J. L., and Ingham, P. E., *J. Text. Inst.*, 1979, **70**, 76.
7. Ermakov, V. S., Chekmarev, A. M., and Kuchkarev, E. A., *Zh. Anal. Khim.*, 1986, **41**, 1615.
8. Panday, V. K., *Anal. Chim. Acta*, 1971, **57**, 31.
9. Aznarez, J., Bellarra, M. A., and Bonilla, A., *Rev. Acad. Cienc. Exactas, Fis.-Quim. Nat. Zaragoza*, 1978, **33**, 133.
10. Liu, D., and Zhan, X., *Yankuang Ceshi*, 1987, **6**, 132.
11. Pascual, J., *Talanta*, 1987, **34**, 1027.
12. Bassett, J., Denney, R. C., Jeffery, G. H., and Mendham, J., "Vogel's Textbook of Quantitative Inorganic Analysis Including Elementary Instrumental Analysis," Fourth Edition, ELBS and Longman, New York, 1978, p. 325.
13. Wilson, C. L., and Wilson, D. W., "Comprehensive Analytical Chemistry," Elsevier, Amsterdam, 1962, p. 510.
14. Clearfield, A., and Stynes, J. A., *J. Inorg. Nucl. Chem.*, 1964, **26**, 117.
15. Long, G. L., and Winefordner, J. D., *Anal. Chem.*, 1983, **55**, 712A.
16. Sandell, E. B., "Colorimetric Determination of Traces of Metals," Third Edition, Interscience, London, 1959, p. 970.

Use of Dimethylglyoxime, Acenaphthenequinone Dioxime and Mixed Ligands of Dimethylglyoxime and Acenaphthenequinone Dioxime Supported on Naphthalene for the Pre-concentration and Determination of Nickel in Alloys, Tea and Water Samples Using Atomic Absorption Spectrometry

Masatada Satake and Jun'ichiro Miura
Faculty of Engineering, Fukui University, Fukui 910, Japan

Shiro Usami
Department of Industrial Chemistry, Faculty of Engineering, Toyama University, Toyama 930, Japan

Bal Krishan Puri
Department of Chemistry, Indian Institute of Technology, Hauz Khas, New Delhi-110 016, India

Solid chelating compounds such as dimethylglyoxime (DMG), acenaphthenequinone dioxime (ANDO) and their mixed ligands (DMG - ANDO) supported on naphthalene were found to provide a rapid and economical route to the pre-concentration of nickel in alloys and biological and natural water samples. Nickel formed chelates with DMG, ANDO and DMG - ANDO supported on microcrystalline naphthalene in a column at pH in the ranges 5.0–9.4, 6.1–11.0 and 7.1–11.0, respectively. The metal complex and naphthalene were dissolved out from the column using 3 ml of dimethylformamide - nitric acid and the absorbance was measured by an atomic absorption spectrometer at 232 nm. The calibration graphs obtained were linear over the concentration range 5–40 µg (for DMG) and 2–30 µg (for ANDO and DMG - ANDO) of nickel in 3 ml of the final solution. The precision and detection limits of the method were studied for DMG, ANDO and DMG - ANDO. The sensitivities for 1% absorption were 0.132, 0.104 and 0.100 µg ml^{-1} for DMG, ANDO and DMG - ANDO, respectively (0.153 µg ml^{-1} for the direct determination from the aqueous medium by atomic absorption spectrometry). The method was used for the determination of nickel in various standard reference materials and water samples from different natural sources.

Keywords: *Nickel determination; atomic absorption spectrometry; naphthalene column retention; dimethylglyoxime; acenaphthenequinone dioxime*

Vicinal α-dioximes such as dimethylglyoxime (DMG), α-furil dioxime, α-benzil dioxime, cyclohexane-1,2-dione dioxime (Nioxime) and cycloheptane-1,2-dione dioxime (heptoxime), have received considerable attention because of their high selectivity and sensitivity towards various metal ions. They have been used widely as reagents for the determination of transition metals, especially nickel and palladium, since the discovery of DMG by Tschugaeff.[1] Both nickel and palladium form stable water-insoluble complexes with all dioximes. They are co-ordinated to the functional group C(NOH)–C(NOH) of two dioxime molecules, forming a four-membered chelate ring of high stability.[2,3]

Recently, some adsorbents such as thiol cotton,[4] silanised glass beads,[5,6] C$_{18}$-bonded silica gel,[7] Amberlite XAD-4 resin,[8] cellulose,[9] silica gel[10] and a few metal oxides and hydroxides[11] have been reported for the pre-concentration of some metal ions. Although some of these are fairly effective, their preparation is sometimes lengthy and rigid control of conditions is required. Further, desorption of the metal complex is carried out by the slow process of elution; hence the procedure is even more time consuming.

This paper describes the analytical potential for the pre-concentration of nickel with DMG, acenaphthenequinone dioxime (ANDO) and their mixed ligands (DMG - ANDO) loaded with microcrystalline naphthalene. Dimethylglyoxime is very cheap and available commercially and ANDO can be synthesised easily in the laboratory by refluxing an ethanolic solution of acenaphthenequinone, hydroxylamine hydrochloride and anhydrous sodium acetate.[12]

Of the α-dioximes described above, DMG is the most studied and the most used reagent for the gravimetric determination of nickel. Nickel forms a characteristic pink precipitate with this reagent, especially in dilute solution (p.p.m. level); the precipitate is partially soluble in water.

Hence DMG is not suitable for the determination of trace metal ions in the p.p.b.–p.p.m. range. Acenaphthenequinone dioxime is insoluble in water and partially soluble in ethanol or acetone. Its complex is insoluble in water, ethanol and non-aqueous organic solvents such as benzene, toluene, xylene, chloroform and carbon tetrachloride.

We have previously reported a method involving solid - liquid separation after the adsorption of metal complexes on microcrystalline naphthalene and have applied it to the determination of several metal ions.[13–15] Recently, we have also observed that metal ions are adsorbed quantitatively together with the chelating agent on microcrystalline naphthalene in a column.[16,17] The method is very convenient (it does not involve filtration of the metal complex - naphthalene), rapid, economical and sensitive. The metal retained in the column is not eluted even after washing with water but can be dissolved out from the column together with the naphthalene using a suitable binary solvent; the metal can then be determined directly by atomic absorption spectrometry. In this work, various parameters were evaluated for the pre-concentration of nickel in various complex materials such as alloys and biological and environmental samples.

Experimental

Reagents

The standard nickel solution (6 p.p.m.) was prepared by diluting 6 ml of a 1000 p.p.m. atomic absorption standard nickel chloride solution to 1000 ml with doubly-distilled water. Buffer solutions were prepared by mixing the appropriate ratios of 1 M ammonia and 1 M ammonium acetate solutions. The dimethylformamide - HNO$_3$ (DMF - HNO$_3$) solution was prepared by mixing 3.5 ml of HNO$_3$ with 100 ml

of DMF. Naphthalene, DMG, DMF and all other reagents, unless specified otherwise, were of analytical-reagent grade. Doubly distilled water was used throughout.

Preparation of ANDO

In a 500-ml flask, 5.5 g of acenaphthenequinone were taken and mixed with 7 g of hydroxylamine hydrochloride, 10 g of sodium acetate, 250 ml of ethanol and 100 ml of water. This mixture was warmed with constant stirring and then refluxed for 12 h. The cooled filtrate was poured into ice - water. The dioxime compound was recrystallised twice from ethanol and dried (m.p., 222 ± 1 °C; yield, 3.1 g).[12]

Preparation of DMG, ANDO and DMG - ANDO loaded on naphthalene

Solutions of DMG (10 g) and ANDO (3 g) in acetone (170 and 80 ml, respectively) or an acetone solution (90 ml) of DMG (1.16 g, 0.01 mol) and ANDO (2.12 g, 0.01 mol) were stirred separately on a hot-plate stirrer arrangement at 35–40 °C; the solids were dissolved by adding 15–20 ml (for DMG) and 5–10 ml (for ANDO and DMG - ANDO) of distilled water. To the final solutions were added 10 g of naphthalene. The acetone solution of the chelating agent and naphthalene was added to 1600–2000 ml of distilled water with constant stirring at room temperature. The coprecipitated mixture was stirred for 3 h and allowed to stand for 12 h. The supernatant solution was aspirated using a siphon and then the mixture was washed twice with doubly distilled water. The resulting slurry of DMG, ANDO and DMG - ANDO on naphthalene in water was packed into the column by pushing the naphthalene with a flattened glass rod after slow aspiration of the column for DMG.

Apparatus

A Perkin-Elmer Model 403 atomic absorption spectrometer and a Toa-Dempa HM-5A pH meter were used. A hollow-cathode lamp for nickel was obtained from Hamamatsu Photonics. All absorption measurements were performed under the following operating conditions: wavelength, 232 nm; slit setting, 3 (7 A); current, 10 mA; acetylene flow setting, 35 (pressure, 0.6 kg cm^{-2}); and air flow setting, 57 (pressure 2.1 kg cm^{-2}). A funnel-tipped glass tube (60 × 6 mm i.d.) was used as the chromatographic column. All glassware and the columns were washed with 1 + 1 concentrated sulphuric acid - concentrated nitric acid prior to use. The column was plugged with cotton-wool and then filled with the naphthalene chelating agent to a height of 1.0–1.3 cm. The DMG - naphthalene was packed by lightly pushing it into the column with a flattened glass rod due to its bulky crystals and relatively low specific mass.

General Procedure

An aliquot of the nickel solution containing 5–40 μg (for DMG) or 2–30 μg (for ANDO and DMG - ANDO) of nickel was placed in a 20-ml beaker and to this were added approximately 0.5 ml of buffer and 1 M ammonia solution (pH 8.3–8.5). The sample solution was diluted to 15 ml with distilled water. Before this solution was passed through the column, packed with each of DMG, ANDO and DMG - ANDO, at a flow-rate of 0.3 ml min^{-1}, the column loaded with naphthalene chelating agent was conditioned to a suitable pH by passing through it 3–5 ml of the acetate buffer. After the sample solution had been passed through the column, the packing was washed with a small volume of distilled water and then aspirated strongly for about 10 min; the naphthalene material was pushed down with the flattened glass rod until naphthalene crystals no longer formed on dissolving the naphthalene which emerged from the column. The metal complex together with naphthalene was dissolved out with 3
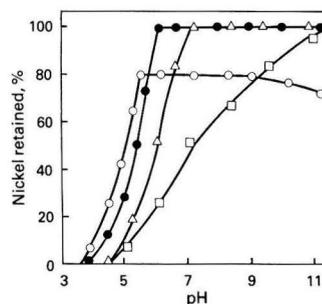

Fig. 1. Effect of pH on retention. Amount of Ni, 18 μg; solvent, DMF - HNO$_3$ (100 + 3.5); and reference, reagent blank. ○, DMG; ●, ANDO; △, 1 + 1 DMG - ANDO; and □, 2 + 1 DMG - ANDO

ml of DMF - HNO$_3$. This solution was aspirated into an air - acetylene flame and the absorbance was measured at 232 nm. Using the procedure described above, the absorbances for various amounts of nickel were measured for DMG, ANDO and DMG - ANDO and calibration graphs were constructed against reagent blanks prepared in a similar manner but without nickel.

Results and Discussion

Retention Characteristics of DMG, ANDO and DMG - ANDO

Each of the chelating agents has the functional group C(NOH)–C(NOH) of the dioxime molecule, which is co-ordinated with the metal. Hence, nickel forms the chelate with 2 mol of these dioxime molecules on the surface of micro-crystalline naphthalene after passing through the column. The amount of nickel retained is proportional to the amount of DMG, ANDO and DMG - ANDO. The coloured band of the chelate was clear when 4–6 g of DMG or 2–4 g of ANDO were used and the molar ratio of DMG to ANDO was 1 : 1 (Fig. 1).

Effect of pH

The retention of nickel was constant and at a maximum on the DMG, ANDO and DMG - ANDO naphthalene materials in the pH ranges 5.0–9.4, 6.1–11.0 and 7.1–11.0, respectively (Fig. 1). The retention of nickel in the column at pH 8.3–8.5 was 81, 99 and 100% for DMG, ANDO and DMG - ANDO, respectively. Less nickel was retained using DMG than using ANDO or DMG - ANDO because of the higher solubility of this chelate in water. This explanation is underlined by the fact that the retention of nickel decreases gradually with an increase in the volume of the aqueous phase. In subsequent work, the pH was adjusted to 8.3–8.5 with the various buffers and 1 M ammonia solution in all instances. The addition of 0.2–3.0 ml of the buffer with pH > 8.5 caused no variation in the retention of nickel, and 0.5 ml of this buffer was used in all further work.

Effect of Flow-rate

The flow-rate was varied from 0.2 to 10 ml min^{-1}. It was found that the retention of nickel was not affected by flow-rates up to 1.0 ml min^{-1} for DMG and 10 ml min^{-1} for both ANDO and DMG - ANDO, respectively. From the experimental results, the optimum flow-rate for DMG was found to be much lower than those for ANDO and DMG - ANDO. The clear pink band of the Ni - DMG chelate on naphthalene could be obtained by increasing the amount of DMG and the density of packing of naphthalene in the column. Hence it is necessary to adjust the packing to a suitable density of naphthalene material so that the clear band is obtained. In subsequent

Table 1. Precision and detection limits for DMG, ANDO and DMG - ANDO

| | Nickel taken*/μg | | | | | | | |
| | 6.00 | | 12.00 | | 18.00 | | 30.00 | |
Chelating agent	Mean value	Standard deviation	Mean value	Standard deviation	Mean value	Standard deviation	Mean value	Standard deviation
DMG	5.93	0.33	12.09	0.14	17.98	0.23	30.15	0.24
ANDO	6.03	0.06	11.92	0.12	18.05	0.17	29.81	0.18
DMG - ANDO	5.98	0.06	12.06	0.14	18.04	0.19	29.82	0.18

Chelating agent	Sensitivity for 1% absorption/ μg ml^{-1}	Mean absorbance of the reagent blank ($\bar{x}_B$)	Standard deviation of reagent blank (s_B)	Analytical sensitivity (S)†/ml μg^{-1}	Detection limit (c_L)‡/ μg ml^{-1}
DMG	0.132	0.001	0.00082	0.033$_3$	0.074
ANDO	0.104	0.001	0.00078	0.042$_7$	0.055
DMG - ANDO	0.100	0.001	0.00063	0.043$_3$	0.044

* $n = 5$.
† S, obtained from the slope of the calibration graph.
‡ $c_L = ks_B/S$; $k = 3$.[18,19]

work, the flow-rate was maintained at 0.3 ml min^{-1} for DMG and 1–2 ml min^{-1} for ANDO and DMG - ANDO for convenience.

Retention Capacity of the Chelating Agent Supported on Naphthalene

The retention capacities of the chelating agent supported on naphthalene were determined by the batch method. This experiment was performed by placing various amounts of nickel, 1–3 mg for DMG and 500 μg for ANDO and DMG - ANDO, 0.5 ml of the buffer and a suitable amount of naphthalene - chelating agent in a 100-ml separating funnel. This mixture was diluted to 30 ml, shaken by a mechanical shaker for 30 min and filtered through a filter-paper. The amount of nickel in the filtrate was determined directly by atomic absorption spectrometry (AAS). The naphthalene - chelating agent on the filter-paper was dried in the air and the solid mass was weighed on a balance. The retention capacity of nickel is proportional to the amount of DMG on naphthalene; hence various amounts (0.5–2.0 g) of DMG were coprecipitated with 10 g of naphthalene and the retention capacity was determined for 6.0 g of DMG by the extrapolation method. The maximum capacities were found to be 90, 4.0 and 3.5 mg g^{-1} of nickel for DMG, ANDO and DMG - ANDO, respectively.

Effect of Volume of the Aqueous Phase

The effect of the volume of the aqueous phase on the retention of nickel in the column was investigated for 10–1000 ml of aqueous phase. The retention remained constant and at a maximum for ANDO and DMG - ANDO even when the volume of the aqueous phase exceeded 800 ml, whereas it decreased gradually for DMG with increasing volume of the aqueous phase. Hence the volume of the aqueous phase must be kept constant. In subsequent work, 15 ml of the aqueous phase were used.

Choice of Solvent

An attempt was made to dissolve the nickel chelates of DMG, ANDO and DMG - ANDO together with naphthalene from the column. These solid masses were found to be insoluble in many non-aqueous and water-miscible organic solvents. The DMG complex dissolves in butylamine and binary solvents such as butylamine - DMF, HNO$_3$ - DMF and HCl - DMF. It is soluble in CHCl$_3$ but is not suitable for AAS. The ANDO and DMG - ANDO chelates are insoluble in non-aqueous and

water-miscible organic solvents but soluble in DMF containing small volumes of HNO$_3$, HCl, HClO$_4$ or butylamine. As the solid mass of nickel chelate and naphthalene is dissolved out from the column in a small volume (3 ml) of solvent, it is essential to select a solvent in which the chelate is highly soluble and which is also flammable for atomic absorption measurements. Hence various volume ratios of DMF and different acids were studied with respect to dissolution of the complex together with naphthalene. It was found that 100 + 3.5 DMF - HNO$_3$ was sufficient to dissolve the complex. In all instances, DMF - HNO$_3$ was the preferred solvent because of high solubility, sensitivity and stability of the chelate. It was also found that 2–3 ml of this solvent was sufficient to dissolve the mixture, enhancing the sensitivity of the method further. As only a small volume (3 ml) of solvent is required to dissolve the naphthalene - chelate, it was necessary to investigate the effect of the surplus water attached to the naphthalene. It was found that surplus water caused the absorbance to decrease and hence led to error in the determination. Therefore, it is necessary to eliminate the water attached to the naphthalene in the column completely by aspirating it. However, when more than 5 ml of solvent are used, 1–2 min of aspiration are sufficient.

Linearity, Sensitivity and Precision

Under the optimum conditions that have been described, calibration graphs for nickel were constructed at 232 nm. These were found to be linear over the concentration range 5–40 and 2–30 μg of nickel in 3 ml of DMF - HNO$_3$ solution for DMG and DMG - ANDO, respectively. The precision of the method for the determination of various amounts of nickel for DMG, ANDO and DMG - ANDO was studied together with the detection limits. The results are given in Table 1.

Effect of Foreign Ions

Different amounts of metal ions and alkali metal salts were added individually to a solution containing 18 μg of nickel, and the general procedure was applied. The tolerance limits (error < 3%) are given in Tables 2–5. Many of the salts can be tolerated in up to gram amounts. However, EDTA and KCN interfered in the determination. Of the metal ions tested, most metal ions did not interfere up to milligram levels. Although Cu^{II}, Co, Fe^{III} and Pd formed water-insoluble complexes with ANDO and DMG - ANDO and interfered seriously in the determination, they were easily masked by combinations of suitable masking agents and pH adjustment. In contrast, Fe^{III}, Co and Cu^{II} produced water-soluble complexes with DMG,

Table 2. Effect of various salts

Salt	Tolerance limit*		
	DMG	ANDO	DMG - ANDO
NaClO$_4$.H$_2$O	0.9†	0.9†	0.6
KNO$_3$	0.9†	0.9†	0.3
NaCl	0.9†	0.9†	0.3
CH$_3$COONa.3H$_2$O ..	0.9†	0.9†	0.6
NH$_4$Cl	0.9†	0.9†	0.3
KH$_2$PO$_4$	0.9†	0.5	0.1†
Na$_2$SO$_4$	0.9†	0.4†	0.3
Potassium sodium (K, Na) tartrate	0.8†	0.6	0.5, 0.8†‡
KI	0.5†	0.5†	0.1
KSCN	0.1	25 mg	0.5
Ammonium citrate ..	0.1	50 mg	4 mg
Na$_2$C$_2$O$_4$	0.15	0.1	0.5 mg
NH$_4$F	0.1	80 mg	50 mg
Thiourea	30 mg	1†	0.2
Disodium EDTA	100 µg	10 µg	5 µg
KCN	<1 µg	10 µg	10 µg
L-Ascorbic acid	0.4†‡	0.4†‡	0.4†‡

* Tolerance limit in g unless stated otherwise.
† Maximum value tested. Amount of Ni, 18 µg; pH, 8.3–8.5.
‡ Adjusted to pH 10.0.

Table 3. Effect of foreign metal ions for DMG

Metal ion	Tolerance limit*	Comment
Ca^{II} ..	0.15 g	
Mg^{II} ..	0.10 g	
Mo^{VI} ..	0.15 g	
Zn^{II} ..	0.10 g	Adjusted to pH 5.8 with 0.8 g of NH$_4$OAc
Mn^{II} ..	0.14 g	Adjusted to pH 6.1 with 0.8 g of NH$_4$OAc
Al^{III} ..	33 mg	Adjusted to pH 5.4 with 1 g of NH$_4$OAc
Fe^{III} ..	8 mg	Adjusted to pH 6.0 with 0.8 g of solid K,Na tartrate and ammonia solution or with 50 mg of KSCN and buffer
Fe^{II} ..	5 mg	Adjusted to pH 6.0 with 0.8 g of solid K,Na tartrate and ammonia solution or with 0.1 g of NH$_4$F and buffer
Pb^{II} ..	4 mg	Adjusted to pH 6.0 with 0.8 g of NH$_4$OAc or with 0.3 g of solid K,Na tartrate
Hg^{II} ..	4 mg	Adjusted to pH 6.0 with 0.5 g of solid K,Na tartrate and 0.4 g of NH$_4$OAc
V^V ..	5 mg	
Bi^{III} ..	4 mg	Adjusted to pH 6.2 with 0.8 g of solid K,Na tartrate and 0.4 g of NH$_4$OAc
Cd^{II} ..	4.5 mg	
W^{VI} ..	3 mg	
Cr^{VI} ..	5 mg	
Cr^{III} ..	5 mg	Adjusted to pH 6.4 with 0.4 g of K,Na tartrate and buffer
Co^{II} ..	3 mg	Adjusted to pH 7.4 with buffer and ammonia solution
Ag^I ..	1 mg	Adjusted to pH 8.8 with 0.8 g of K,Na tartrate and buffer
Ru^{III} ..	1 mg	Adjusted to pH 6.0 with 0.8 g of K,Na tartrate and buffer
Pt^{IV} ..	3.5 mg	Adjusted to pH 8.5 with 0.2 g of K,Na tartrate and buffer
Pd^{II} ..	1 mg	Adjusted to pH 7.9 with 0.1 g of NH$_4$F and buffer
Cu^{II} ..	3 mg	Adjusted to pH 6.2 with 30 mg of thiourea and buffer or with 50 mg of KSCN and buffer

* Maximum value tested. Amount of Ni, 18 µg; pH, 8.3–8.5.

which did not interfere in the determination of nickel. Metal ions precipitated as their hydroxides in neutral or alkaline solution could also be masked by adjusting the pH to a lower value or by the addition of K,Na tartrate and ammonium acetate (Tables 2–5). Hence, the method is highly selective and can be applied directly to the determination of nickel in various complex materials without any preliminary separation.

Table 4. Effect of foreign metal ions for ANDO

Metal ion	Tolerance limit	Comment
Ca^{II} ..	0.15 g*	
Mg^{II} ..	0.10 g*	
Mo^{VI} ..	0.20 g*	
Zn^{II} ..	0.15 g*	Adjusted to pH 10.7 with 0.4 g of K,Na tartrate and ammonia solution
Mn^{II} ..	0.15 g*	Adjusted to pH 6.7 with 1 M NH$_4$OAc
Al^{III} ..	20 mg	Adjusted to pH 11.2 with 1.5 ml of 20% triethanolamine and 1 M NaOH
Fe^{III} ..	2 mg	Adjusted to pH 11.0 with 2.5 ml of 20% triethanolamine and ammonia solution
Fe^{II} ..	2 mg	Adjusted to pH 10.7 with 2.0 ml of 20% triethanolamine and buffer
Pb^{II} ..	3 mg	Adjusted to pH 6.7 with 0.2 g of K,Na tartrate and buffer
Hg^{II} ..	3 mg*	Adjusted to pH 6.7 with buffer
V^V ..	4 mg	
Bi^{III} ..	2.5 mg	Adjusted to pH 9.0 with 0.4 g of K,Na tartrate and buffer
Cd^{II} ..	4.5 mg*	Adjusted to pH 6.5 with buffer
W^{VI} ..	3 mg*	
Cr^{VI} ..	4 mg	
Cr^{III} ..	2 mg	Adjusted to pH 6.5 with 0.3 g of K,Na tartrate and buffer
Co^{II} ..	600 µg	Adjusted to pH 10.7 with 0.2 g of K,Na tartrate, buffer and ammonia solution
Ag^I ..	2 mg*	Adjusted to pH 10 with buffer
Ru^{III} ..	2 mg	Adjusted to pH 10.8 with 0.2 g of K,Na tartrate, buffer and ammonia solution
Pt^{IV} ..	2 mg*	
Pd^{II} ..	2 mg*	
Cu^{II} ..	3 mg	Adjusted to pH 10.3 with 0.2 g of K,Na tartrate, 0.4 g of L-ascorbic acid and ammonia solution

* Maximum value tested. Amount of Ni, 18 µg; pH, 8.3–8.5.

Determination of Nickel in Standard Alloys

A 0.1–1.0-g amount of the standard alloy (Stainless Steel, Ni - Cr Steel, Al Alloy) was completely decomposed in 10–15 ml of 1 + 1 HCl by heating the mixture on a water-bath and 1.5–2 ml of H$_2$O$_2$ (30%) were added. The zinc alloy (2 g) was dissolved in 20 ml of 1 + 1 HCl, 2 ml of H$_2$O$_2$ and 1 ml of concentrated HNO$_3$. The magnesium alloy (5–6 g) was dissolved in 100 ml of 1 + 1 HCl and 1 ml of H$_2$O$_2$. In each instance the excess of H$_2$O$_2$ was decomposed by heating the solution on a water-bath. The solutions were cooled, filtered if necessary and diluted to 100 ml in a calibrated flask with distilled water. An aliquot of this sample solution was placed in a beaker, and to this were added K,Na tartrate (0.8 g) and the buffer. The pH of the solution was adjusted to 8.3–8.5 with 1 M ammonia solution and this solution analysed according to the general procedure. As Fe^{III}, Co and Cu^{II} formed water-soluble chelate ions which did not interfere in the determination, the procedure was found to be very selective and useful as a routine method of analysis. The results are given in Table 6.

Determination of Nickel in Tea Leaves and Pepperbush

Tea leaves (3–4 g) and pepperbush (3 g) were dissolved in 20–25 ml of concentrated HNO$_3$, 1 ml of concentrated HClO$_4$ and 1 ml of H$_2$O$_2$ in a Kjeldahl flask. The solution was cooled, filtered and diluted to 50 ml in a calibrated flask with distilled water. An aliquot of the resulting solution was placed in a beaker. To this were added 1 ml of 20% K,Na tartrate and 1 ml of 20% triethanolamine as the masking agents at pH 10.5. This solution was analysed by the general procedure. The results are given in Table 7. In the sodium diethyldithiocarbamate - isobutyl methyl ketone (DDTC - IBMK) method,[20]

Table 5. Effect of foreign metal ions for DMG - ANDO

Metal ion	Tolerance limit	Comment
Ca^{II}	0.15 g*	
Mg^{II}	0.10 g*	
Mo^{VI}	0.20 g*	
Zn^{II}	10 mg*	Adjusted to pH 10.5 with 0.5 g of K,Na tartrate and buffer
Mn^{II}	10 mg	Adjusted to pH 7.2 with ammonium acetate and ammonia solution
Al^{III}	4 mg	Adjusted to pH 10.5 with 1 to *ca.* 3 ml of 20% triethanolamine, 0.2 g of K,Na tartrate and buffer
Fe^{III}	6 mg*	Adjusted to pH 10.5 with 1 ml of 20% triethanolamine, 0.2 g of K,Na tartrate and buffer
Fe^{II}	2 mg	Adjusted to pH 10.5 with 3 ml of 20% triethanolamine and buffer
Pb^{II}	4 mg*	Adjusted to pH 8.5 with 0.5 g of K,Na tartrate and buffer
Hg^{II}	1 mg	Adjusted to pH 8.5 with 0.5 g of K,Na tartrate and buffer
V^{V}	5 mg*	
Bi^{III}	2 mg*	Adjusted to pH 10.5 with 0.7 g of K,Na tartrate and buffer
Cd^{II}	4.5 mg*	
W^{VI}	3 mg*	
Cr^{VI}	5 mg*	
Cr^{III}	3 mg*	Adjusted to pH 10.3 after oxidation of Cr^{III} to Cr^{VI} by heating with 3 ml of 30% H_2O_2 in alkaline solution
Co^{II}	1 mg	Adjusted to pH 10.8 with 0.02 g of DTCS,† 0.2 g of K, Na tartrate and buffer
Ag^{I}	1 mg	Adjusted to pH 8.5 with 0.5 g of K,Na tartrate and buffer
Ru^{III}	70 μg	Adjusted to pH 10.5 with 0.2 g of K,Na tartrate and buffer
Pt^{IV}	2 mg*	
Pd^{II}	1 mg*	
Cu^{II}	1.5 mg	Adjusted to pH 10.5 with 0.3 g of L-ascorbic acid, 0.4 g of K,Na tartrate and buffer, or with 0.1 to *ca.* 0.3 g of L-ascorbic acid, 0.2 to *ca.* 0.4 g of K,Na tartrate, 3 ml of 20% triethanolamine and buffer

* Maximum value tested. Amount of Ni, 18 μg; pH, 8.3–8.5.
† DTCS = *N*-(dithiocarboxy)sarcosine, diammonium salt.

IBMK is a useful solvent in which to perform atomic absorption measurements; sometimes, however, an emulsion forms in the two phases on shaking. Therefore the time for complete phase separation is increased considerably and the operation becomes troublesome. This causes error in the determination, whereas the proposed method makes the analysis easier and more accurate.

Determination of Nickel in Natural Water Samples

The proposed method was applied to the determination of nickel in river, lake and coastal water samples. An aliquot (500 ml) of the water sample was taken and adjusted to pH 1.5 with concentrated HNO_3. The sample was filtered in order to remove suspended material and was then analysed using the general procedure. Triethanolamine (20%, 4 ml) and K,Na tartrate (20%, 3 ml) were added to each water sample and the pH was adjusted to 10.7 for river water and hot spring water, and 8.2 for sea water to avoid the precipitation of Ca and Mg. The resulting solution was subjected to the general procedure. The DMG - naphthalene material is not suitable for the determination of nickel in water samples because the nickel chelates are fairly soluble in dilute solutions of nickel. On the other hand, ANDO and DMG - ANDO were employed successfully for various water samples; the results are given in Table 8. The solvent extraction step is simple and good recoveries are achieved; however, it is not suitable for the pre-concentration of trace amounts of nickel from larger volumes of aqueous phase (> 100 ml). Organic solvents are soluble in water to a certain extent. This leads to errors in the determination of nickel due to the change in volume of the organic solvent. Hence the sample must undergo a preliminary pre-concentration from the larger volume on an ion-exchange resin or by vacuum evaporation. However, the latter method cannot be applied to sea water because salts such as sodium chloride and potassium chloride crystallise on concentration of the sample. In the proposed method, naphthalene is used as the solid phase, the metal is retained as the chelate on naphthalene and the naphthalene is then dissolved in 2–3 ml of solvent. Hence the sensitivity is enhanced by pre-concentration of the nickel.

Conclusion

The combined use of the column and chelating agents such as DMG, ANDO and DMG - ANDO for the chromatographic

Table 6. Analysis of alloys for nickel using DMG

		Nickel, %	
Sample	Composition, %	Certified value	Found*
JSS 654-7 Stainless Steel†	C, 0.060; Cu, 0.028; Si, 1.29; Co, 0.45; Mn, 1.69; Cr, 24.84; P, 0.031; Mo, 0.016; N, 0.0258	20.33	20.37 ± 0.08
JSS 655-4 Stainless Steel	C, 0.055; S, 0.006; Cu, 0.088; Ta, 0.03; Si, 0.60; Co, 0.28; Mn, 1.58; Cr, 18.54; N, 0.024; P, 0.033; Mo, 0.051; Nb, 0.60	11.48	11.18 ± 0.05
JSS 503-4 Ni - Cr Steel	C, 0.33; S, 0.020; Cu, 0.084; Si, 0.27; V, 0.004; Mn, 0.63; Cr, 0.70; P, 0.029; Mo, 0.013; N, 0.0115	1.24	1.23 ± 0.01
NKK No. 916 Aluminium Alloy‡	Si, 0.41; Fe, 0.54; Cu, 0.27; Mn, 0.11; Mg, 0.10; Cr, 0.05; Zn, 0.30; Ti, 0.10; Sn, 0.05; Pb, 0.04; V, 0.02; Zr, 0.05; Bi, 0.03; Ga, 0.03; Co, 0.03; Sb, 0.01; Ca, 0.03; B, 0.0006	0.06	0.059 ± 0.001
Sumitomo 2011-4 Aluminium Alloy	Si, 0.030; Fe, 0.063; Cu, 6.58; Ti, 0.050; Mn, 0.003; Bi, 0.32; Pb, 0.30; Zn, 0.003	0.048	0.051 ± 0.003
NBS SRM 629 Zinc Alloy§	Cu, 1.50; Al, 5.15; Mg, 0.094; Fe, 0.017; Pb, 0.0135; Cd, 0.0155; Sn, 0.012; Cr, 0.0008; Mn, 0.0017; Si, 0.078	0.0075	0.00705 ± 0.00001
NBS SRM 171 Magnesium Alloy	Mn, 0.45; Si, 0.0118; Cu, 0.0112; Al, 2.98; Zn, 1.05; Pb, 0.0033; Fe, 0.0018	0.0009	0.0006 ± 0.0002

* Mean of four determinations. K,Na tartrate, 0.8 g; pH, 8.3–8.5.
† JSS = Japanese standards of iron and steel certificate of analysis (Tokyo).
‡ NKK = Nippon Keikinzoku Kogyo (Tokyo).
§ NBS SRM = National Bureau of Standards (Washington, D.C.) standard reference material.

Table 7. Determination of nickel in tea leaves and pepperbush

| Sample* | Nickel certified value/ $\mu g\,g^{-1}$ | Nickel content†/$\mu g\,g^{-1}$ | | |
		ANDO	DMG - ANDO	DDTC - IBMK‡
NIES No. 7, Tea Leaves (green tea of middle grade)§	6.5 ± 0.3	6.2 ± 0.1	6.3 ± 0.2	7.8 ± 0.4
A	—	6.25 ± 0.17	6.36 ± 0.14	5.28 ± 0.34
B	—	7.35 ± 0.21	7.42 ± 0.18	4.9 ± 0.4
C	—	5.25 ± 0.19	5.36 ± 0.18	6.57 ± 0.27
D	—	6.46 ± 0.39	6.38 ± 0.20	5.39 ± 0.25
E	—	7.76 ± 0.18	7.15 ± 0.21	8.48 ± 0.23
F	—	10.84 ± 0.25	10.11 ± 0.17	10.71 ± 0.20
G	—	3.89 ± 0.15	3.57 ± 0.33	3.30 ± 0.38
NIES No. 1 Pepperbush¶	8.7 ± 0.6	7.02 ± 0.15	7.15 ± 0.20	8.81 ± 0.32

* A–E, Green tea leaves of middle grade, commercial; F and G, green tea leaves of superior grade, commercial.

† Mean of four determinations. Potassium sodium tartrate (20%, 2 ml) and triethanolamine (20%, 1 ml) were added as masking agents at pH 10.5.

‡ Sodium citrate (2%, 3 ml) and DDTC solution (2%, 3 ml) were added to the solution at pH 8.0.

§ NIES (National Institute for Environmental Studies) No. 7 (values in parentheses are approximate and not certified) : K, 1.86 ± 0.07; Ca, 0.320 ± 0.012; Mg, 0.153 ± 0.006; and P, (0.37)%; Mn, 700 ± 25; Al, 775 ± 20; Zn, 33 ± 3; Ba, (5.7); Na, 15.5 ± 1.5; Sr, (3.7); Co, (0.12); Cu, 7.0 ± 0.3; Cd, 0.030 ± 0.003; Pb, 0.80 ± 0.03; Cr, (0.15); Cs, (0.022); Sc, (0.011); and Sb, (0.014) $\mu g\,g^{-1}$.

¶ NIES No. 1 (values in parentheses are approximate and not certified): K, 1.51 ± 0.06; Ca, 1.38 ± 0.07; Mg, 0.408 ± 0.020; and Mn, 0.203 ± 0.017%; Fe, 205 ± 17; Zn, 340 ± 20; Ba, 165 ± 10; Na, 106 ± 3; Rb, 75 ± 4; Sr, 36 ± 4; Co, 23 ± 3; Cu, 12 ± 1; Cd, 6.7 ± 0.5; Pb, 5.5 ± 0.8; As, 2.3 ± 0.3; P, (1100); Cr, (1.3); Cs, (1.2); Tl, (0.13); and Hg, (0.056) $\mu g\,g^{-1}$.

Table 8. Determination of nickel in natural waters

| Sample | Nickel found*/$\mu g\,l^{-1}$ | | |
	ANDO	DMG - ANDO	Alternative method†
River water, A	0.8 ± 0.1	0.7 ± 0.1	0.6 ± 0.2
River water, B	1.1 ± 0.1	1.0 ± 0.2	1.0 ± 0.1
River water, C	1.1 ± 0.2	1.0 ± 0.1	0.9 ± 0.2
River water, D	0.8 ± 0.2	0.8 ± 0.1	0.6 ± 0.3
River water, E	1.1 ± 0.1	1.1 ± 0.2	0.9 ± 0.3
Hot spring water, A‡	1.0 ± 0.2	0.7 ± 0.2	—
Hot spring water, B‡	1.2 ± 0.1	1.0 ± 0.2	—
Hot spring water, C‡	1.5 ± 0.2	1.3 ± 0.3	—
Coastal water (surface)‡	0.7 ± 0.1	0.7 ± 0.1	—
Lake water	0.9 ± 0.2	0.9 ± 0.2	0.7 ± 0.2

* Mean of three determinations.

† DDTC - IBMK extraction in the presence of sodium citrate (20%, 4 ml) after vacuum evaporation.

‡ Samples were adjusted to pH 8.2 to avoid precipitation of the hydroxides of Mg and Ca.

pre-concentration of metal ions offers many advantages. The main features of the method are the enhanced sensitivity for the determination of metal ions (as >300-fold concentration may be achieved), economy, only a small amount of naphthalene (0.1 g) is required, which itself can be dissolved in only 2–3 ml of organic solvent, and rapidity, the retained metal in the column is dissolved out by an organic solvent instead of being eluted. Further, although the DMG chelate is soluble in very dilute solutions of nickel, the use of mixed ligands of DMG and ANDO allowed the determination of nickel in very dilute solutions. The selectivity of the method may be improved further by using other optical and electro-analytical techniques of analysis. The column pre-concentration procedure that has proved effective for the determination of trace amounts of metals in alloys and biological samples relies on the chelation of metals with the dioxime ligands. The proposed method utilises a simple funnel or funnel-tipped column that is used efficiently and economically, 20–30 samples h^{-1} are pre-concentrated once and then trace amounts of metals are determined according to the general procedure. Finally, although for large-volume water samples many hours are required for their passage through the column, the operation itself is relatively simple and not necessarily tedious for the working load.

References

1. Tschugaeff, L. A., *Z. Anorg. Chem.*, 1905, **46**, 144.
2. Brunck, O., *Z. Angew. Chem.*, 1907, **20**, 1844.
3. Burger, K., Flaschka, H. A., and Barnard, A. J., Jr., "Chelates in Analytical Chemistry," Volume 2, Marcel Dekker, New York, 1969, p. 179.
4. Yu, M. Q., and Liu, G. Q., *Talanta*, 1983, **30**, 265.
5. Taguchi, S., and Goto, K., *Talanta*, 1980, **27**, 819.
6. Taguchi, S., Yai, T., Shimada, Y., and Goto, K., *Talanta*, 1983, **30**, 169.
7. Watanabe, H., Goto, K., Taguchi, S., McLaren, J. W., Berman, S. S., and Russell, D. S., *Anal. Chem.*, 1981, **53**, 738.
8. Sakai, Y., and Mori, N., *Talanta*, 1986, **33**, 161.
9. Burba, P., and Willmer, P. G., *Talanta*, 1983, **30**, 381.
10. Kubota, M., Matsumoto, K., and Terada, K., *Anal. Sci.*, 1987, **3**, 45.
11. Music, S., Gessner, M., and Wolf, R. H. H., *Mikrochim. Acta*, 1979, **I**, 94.
12. Chattopadhyay, P., and Majundar, S. K., *Mikrochim. Acta*, 1983, **III**, 213.
13. Nagahiro, T., Satake, M., Lin, J.-L., and Puri, B. K., *Analyst*, 1984, **109**, 163.
14. Satake, M., Katyal, M., and Puri, B. K., *Fresenius Z. Anal. Chem.*, 1985, **322**, 514.
15. Lin, J.-L., Satake, M., and Puri, B. K., *Analyst*, 1985, **110**, 1351.
16. Nagahiro, T., Uesugi, K., and Satake, M., *Analyst*, 1986, **111**, 1389.
17. Satake, M., Ishida, K., Puri, B. K., and Usami, S., *Anal. Chem.*, 1986, **58**, 2502.
18. Analytical Methods Committee, *Analyst*, 1987, **112**, 199.
19. Long, G. L., and Winefordner, J. D., *Anal. Chem.*, 1983, **55**, 712A.
20. Nagafuchi, Y., and Fukamachi, K., *Bunseki Kagaku*, 1980, **29**, T98.

Simultaneous Determination of Sodium Hydroxide, Sodium Carbonate and Sodium Chloride Concentrations in Aqueous Solutions by Near-infrared Spectrometry

Alexander Grant, Anthony M. C. Davies and Terry Bilverstone
AFRC, Institute of Food Research, Norwich Laboratory, Colney Lane, Norwich NR4 7UA, UK

The quantitative analysis of solutions containing various concentrations of sodium hydroxide, sodium chloride and sodium carbonate, over the range 0–15% *m/m*, has been carried out by near-infrared (NIR) spectrometry. Errors, caused by a high concentration of one salt when determining small amounts of another, have been investigated. The standard errors of the computed results from NIR measurements of each ion were: hydroxide, 0.12; carbonate, 0.34; and chloride, 0.52%. The measurements were made using a liquid sample cup in a fixed-filter NIR instrument and it was concluded that this was a practical system for continuous monitoring of the sodium hydroxide concentration in a process line even when contamination from hydrochloric acid and carbon dioxide occurred.

Keywords: *Sodium hydroxide determination; sodium carbonate determination; sodium chloride determination; near-infrared spectrometry*

Sodium hydroxide solutions are in common use in the food and chemical industries and it is often important that the concentration is maintained within certain limits. Our aim was to investigate the possibility of using near-infrared (NIR) spectrometry for the on-line analysis of sodium hydroxide solutions in a process where contamination from hydrochloric acid or carbon dioxide was possible. The initial concentration of sodium hydroxide in this process was 15% *m/m*.

As solid sodium hydroxide absorbs in the fundamental IR region of the spectrum, due to the stretching of the O–H bond, it may be expected that absorptions will also occur in the NIR region. However, these absorptions are likely to occur at wavelengths close to those of water, *i.e.*, in the 1440 and 1930 nm broad peak regions. In aqueous solution at the sodium hydroxide concentrations used, it is likely that the absorption due to OH$^-$ will be very small. Further, solutions of sodium carbonate and sodium chloride do not have absorptions in the NIR region and there would appear to be no theoretical basis for an NIR method of analysis. However, the NIR determination of sodium chloride in several foods has been reported.[1-3] Such an analysis is possible because of the variation in the shape and positions in the NIR spectrum of water.[4-8] We therefore decided that an investigation of the proposed use of NIR spectrometry was justified.

Watson and Baughman[9] have recently reported the possibility of the on-line analysis of caustic streams by NIR spectrometry. They identified several spectral regions for distinguishing between different concentrations of sodium hydroxide and found the choice of wavelengths restricted by the presence of chloride or carbonate ions. They were, however, unable to analyse solutions for their sodium hydroxide content when both chloride and carbonate ions were present. In the present work, it is shown that such NIR analysis is possible as is the determination of contaminating carbonate and chloride ions albeit with less accuracy.

Experimental

Solutions were prepared on a mass to mass basis using analytical-reagent grade chemicals and doubly distilled water. All possible solutions were prepared in which the sodium hydroxide, sodium carbonate and sodium chloride concentrations varied between 0 and 10% *m/m* in 2.5% *m/m* steps; however, no solution contained more than a total of 15% *m/m* of the sodium salts. This gave a total of 72 solutions.

The solutions were scanned using two spectrophotometers, a Neotec 6350 Mark 1 Research Composition Analyzer (Pacific Scientific, Gardner/Neotec Instrument Division, Buckinghamshire, UK) and a Technicon InfraAlyzer 400 [Technicon Industrial Systems, Bran + Luebbe (GB), Hampshire, UK]. Each spectrophotometer was fitted with the same ceramic liquid sample cell (Technicon, transflectance) and operated in a constant temperature room (23 ± 1 °C). The solutions were loaded into the cell using a syringe. The cell was emptied of the previous sample before it was rinsed and loaded with the next sample. A spectrum of each of two aliquots was taken per sample. The sample temperature was maintained at 20 °C by circulating coolant from a thermostatically controlled bath around the cooling coils of the cell.

Data from the Neotec 6350 instrument were recorded as the logarithm of the reciprocal of the reflectance (log $1/R$) at 2-nm intervals over the range 1100–2498 nm and stored on flexible disks using a Nova 4 computer. Each spectrum was an average of 50 scans. The InfraAlyzer, a fixed-filter spectrophotometer, carried out measurements at 19 wavelengths, ranging from 1445 to 2345 nm and the data were logged by an Apple computer before being stored on a flexible disk. All data were subsequently transferred to a Data General DG10 computer for analysis using a suite of programs originally written for a Nova 2/10 computer.[10]
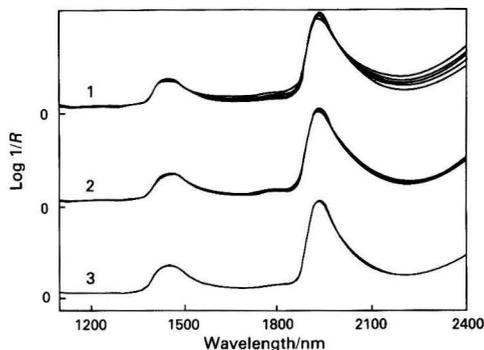

Fig. 1. Effect of increasing sodium salt concentrations (0–10% *m/m*) on the NIR absorption of aqueous solutions: 1, NaOH; 2, Na$_2$CO$_3$; and 3, NaCl (stacked spectra)

Results

Neotec 6350 Analysis

The log $1/R$ spectral data obtained from the Neotec 6350 instrument were used initially to examine the effect of increasing sodium salt concentration on the NIR absorption of water (Fig. 1). The data were also subjected to calibration analysis using a stepwise multi-linear regression (SMLR) technique, the concentration of each sodium salt being regressed against the log $1/R$ data at either two or four wavelengths (Figs. 2–4).
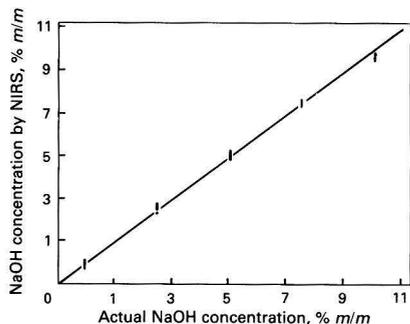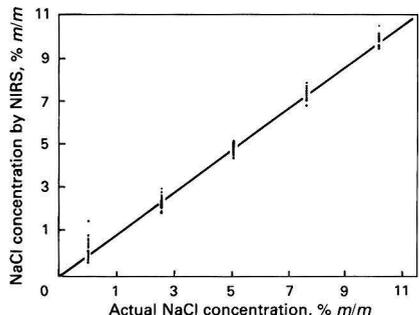

Fig. 2. Actual NaOH concentration (% *m/m*) *versus* NaOH concentration (% *m/m*) found by NIR spectrometry (calibration results from the Neotec 6350 data). Concentration = $-23.75 + 160.37\log(1/R)_1 - 132.15\log(1/R)_2$. 1 = 2296; 2 = 1860 nm. r^2 = 0.99; SEC = 0.12%
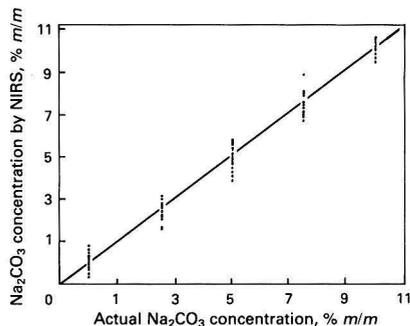
Fig. 3. Actual Na_2CO_3 concentration (% *m/m*) *versus* Na_2CO_3 concentration (% *m/m*) found by NIR spectrometry (calibration results from the Neotec 6350 data). Concentration = 11.68 − 975.74log$(1/R)_1$ + 517.37log$(1/R)_2$ + 1528.31log$(1/R)_3$ − 1586.98log$(1/R)_4$. 1 = 1414; 2 = 1906; 3 = 1178; 4 = 1380 nm. r^2 = 0.985; SEC = 0.39%

Fig. 4. Actual NaCl concentration (% *m/m*) *versus* NaCl concentration (% *m/m*) found by NIR spectrometry (calibration results from the Neotec 6350 data). Concentration = 44.96 − 592.18log$(1/R)_1$ − 573.97log$(1/R)_2$ + 615.32log$(1/R)_3$ + 238.72log$(1/R)_4$. 1 = 1502; 2 = 1408; 3 = 1396; 4 = 1982 nm. r^2 = 0.992; SEC = 0.29%

Technicon InfraAlyzer Analysis

Data from the Technicon InfraAlyzer were divided into two sub-sets each from one of two sample sub-groups. These sub-groups contained samples whose sodium salt concentration covered similar ranges. The first sub-set was used for calibration by regression analysis. The results of this analysis for sodium hydroxide, sodium carbonate and sodium chloride are given in Table 1.

These calibration results were used in equations of the following form:

$$c = k_0 + k_1\log(1/R)_1 + k_2\log(1/R)_2 + k_3\log(1/R)_3$$

where c is the concentration of the salt, k_0, k_1, k_2 and k_3 are calibration constants and $\log(1/R)_1$, $\log(1/R)_2$ and $\log(1/R)_3$ are data from wavelengths 1, 2 and 3, respectively. The validity of the calibration equations was tested on data from the second sub-set and the predicted results are plotted in Figs. 5–7.

Discussion

Many compounds are known to affect the NIR spectrum of the water in which they are dissolved. These compounds, commonly known as infrared shift reagents,[11] include many inorganic ions and cause measurable modifications to the absorption bands of water. One reason for these modifications is believed to be a change in the proportions of the various hydrogen-bonded species in the water "polymer." Polymer here refers to the dynamic collection of individual water molecules joined together by hydrogen bonds. It is the combinations and overtones of the fundamental absorptions of these individual hydrogen-bonded species that, by their

Table 1. Determination of sodium hydroxide, sodium carbonate and sodium chloride using the Technicon InfraAlyzer 400 (calibration data)

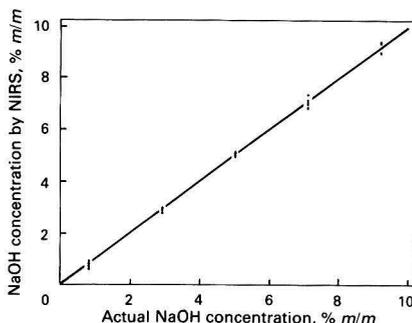|	Sodium salt		
	Hydroxide	Carbonate	Chloride
Wavelength—			
1	2310	1982	1982
2	1722	2336	1445
3	—	1818	2270
Constants—			
k_0	−32.004	276.407	−475.929
k_1	118.786	−268.504	674.984
k_2	−94.734	−253.351	−375.887
k_3	—	445.221	−55.643
r^2	0.999	0.995	0.972
SEC, %	0.090	0.223	0.504

Fig. 5. Actual NaOH concentration (% *m/m*) *versus* NaOH concentration (% *m/m*) found by NIR spectrometry (prediction results from InfraAlyzer data)

many overlapping absorptions, determine the resulting broad nature of the NIR spectrum of water. Some ions increase the amount of hydrogen bonding (structure making) whereas others decrease the bonding (structure breaking).

There are three types of hydrogen-bonded species within the water polymer that are largely responsible for the NIR absorption. These are water molecules with zero, one or two hydrogen bonds. The wavelength at which peak absorption occurs is different for each individual situation as is the value of each absorption coefficient. Non-hydrogen bonded water (or free water as it is sometimes called) absorbs at shorter wavelengths than the other two; as the amount of bonding within the water polymer decreases, the observed absorption maxima shift to shorter wavelengths.

As expected, sodium hydroxide, sodium carbonate and sodium chloride, in the concentrations added, all altered the NIR absorption of water. The different effects of these salts were best examined by using the second derivative of the log $1/R$ data (Fig. 8). Iwamoto et al.[8] showed that the derivative transformation of spectra was a useful method of separating the multiple absorptions which comprise the broad spectral peaks of water and used it to good effect in his studies on the state of water in food. Fig. 8 shows the considerable differences between the effect of either hydroxide or carbonate and chloride ions. The absorption in the 1400 and 1900 nm region in the sodium chloride solutions is much stronger than that of the other two compounds and may indicate that in chloride solutions there is a lower percentage of hydrogen bonds in the solvent. In contrast to sodium hydroxide and sodium carbonate, sodium chloride would therefore appear to be a structure-breaking reagent, a finding that is in agreement with reports in the literature.[6]
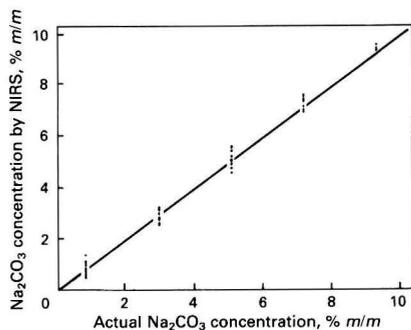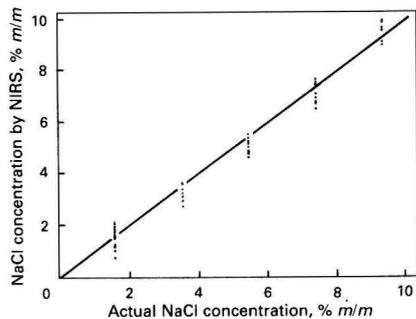
Fig. 1 indicates that for solutions containing only one salt, uniform variations in absorbance occurred at most wavelengths and many of these absorbances were highly correlated with the concentration of the salt. When all three salts were present there was no obvious correlation between absorptions and the concentration of a salt. However, regression analysis was successful in establishing relationships between absorptions at several wavelengths and the concentration of the salt.

The best results were obtained with sodium hydroxide solutions that required information from only two wavelengths (2296 and 1860 nm) for use in a calibration equation with a standard error of calibration (SEC) of 0.12%. These results are better than those of Watson and Baughman,[9] who found that in the presence of both sodium carbonate and sodium chloride interference occurred in the 2300 nm region. Both sodium carbonate and sodium chloride solutions required absorption values from four wavelengths in the calibration equations; the SEC values were 0.39 and 0.29%, respectively.

The results obtained with the Neotec 6350 instrument were encouraging and indicated that an NIR method of analysis for the concentration of the three sodium salts was possible, particularly for sodium hydroxide. However, manufacturing processes are unlikely to use expensive scanning spectrophotometers such as the Neotec 6350 instrument and must, therefore, utilise less sophisticated but possibly more robust instruments such as the Technicon InfraAlyzer. An InfraAlyzer 400, fitted with 19 fixed filters, was therefore used to examine the feasibility of the determinations with a reduced data set. The calibration equations developed (Table 1) were validated (Figs. 5–7) and the best results were again obtained for the determination of the sodium hydroxide concentration. This was probably assisted by the wavelengths available; the first wavelength chosen was 2310 nm, which was very close to the region of maximum change in the absorption. The InfraAlyzer wavelengths used for the calibration of sodium carbonate and sodium chloride were very different to those used in Neotec 6350 analysis but, despite this, the standard error of prediction (SEP) for the determination of the sodium carbonate content was slightly lower (0.34%). However, for sodium chloride, the SEP obtained from the InfraAlyzer data rose to 0.52%. Depending on the requirements of the manufacturer, these results may be adequate for the quality control of a product line. Better control may, however, be possible if filters were made available to provide wavelengths that were more suitable for the analysis.
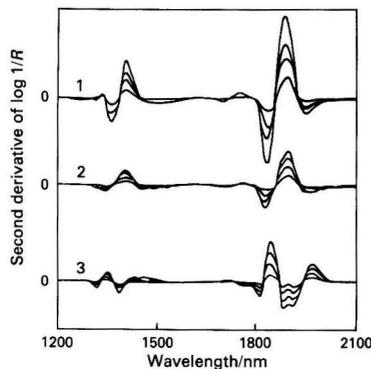

Fig. 6. Actual Na_2CO_3 concentration (% m/m) versus Na_2CO_3 concentration (% m/m) found by NIR spectrometry (prediction results from InfraAlyzer data)

Fig. 7. Actual NaCl concentration (% m/m) versus NaCl concentration (% m/m) found by NIR spectrometry (prediction results from InfraAlyzer data)

Fig. 8. Difference spectra obtained by subtracting second-derivative spectra (Neotec 6350, gap size 40 nm, segment size 10 nm) of distilled water from those of the aqueous sodium salt solutions (2.5–10% m/m). 1, NaOH; 2, Na_2CO_3; and 3, NaCl (stacked spectra). The maximum and minimum y-axis values were 0.14 and -0.07, respectively

Conclusions

The addition of sodium hydroxide, sodium carbonate and sodium chloride caused changes in the absorption spectrum of water which were used for the quantification of these salts. These changes occurred with sodium carbonate and sodium chloride even though these compounds themselves do not absorb in the NIR region. As the changes took place across the spectrum, it was possible to obtain calibrations using a robust filter instrument without optimising the wavelengths at which absorptions were measured. However, it is possible that errors in the determination of sodium chloride would be reduced if more suitable wavelengths were employed. It should be noted that this study was made at a constant temperature; changes of temperature also cause variations in the hydrogen bonding equilibrium.[12]

References

1. Hart, J. R., and Norris, K. M., *Cereal Chem.*, 1962, **39**, 94.
2. Honigs, D. E., Freelin, J. M., Hieftje, G. M., and Hirschfeld, T., *Appl. Spectrosc.*, 1983, **37**, 491.
3. Hed, Z., "Near Infrared Handbook," Sadtler, Philadelphia, 1981.
4. Hirschfeld, T., *Appl. Spectrosc.*, 1985, **39**, 740.
5. Buijs, K., and Choppin, G. R., *J. Chem. Phys.*, 1963, **39**, 2035.
6. Choppin, G. R., and Buijs, K., *J. Chem. Phys.*, 1963, **39**, 2042.
7. Choppin, G. R., and Violante, M. R., *J. Chem. Phys.*, 1972, **56**, 5890.
8. Iwamoto, M., Uozumi, J., and Nishinari, K., *in* Hollo, J., Kaffka, K. J., and Gonczy, J. L., *Editors*, "Proceedings of the International NIR/NIT Conference, Budapest, Hungary," Akademiai Kiado, Budapest, 1987, 3–1.
9. Watson, E., Jr., and Baughman, E. H., *Spectroscopy*, 1987, **2**, 44.
10. Hamid, A., and McClure, W. F., "Software for an On-line Computerized Spectrometer," NCARS Bulletin, North Carolina State University, Raleigh, 1978, No. 252.
11. Day, M. S., and Fearn, F. R. B., *Lab. Pract.*, 1982, **328**, 439.
12. Bonner, O. D., and Woolsey, G. B., *J. Phys. Chem.*, 1968, **72**, 899.

Quantitative Method for Determining the Concentration of Mercury(II) Sulphide in Soils and Sediments

Nathaniel W. Revis, Tanya R. Osborne, Dawn Sedgley and Adolf King
Oak Ridge Research Institute, Oak Ridge, TN 37830, USA

A method for extracting mercury from soil sequentially using HNO_3 and a saturated solution of sodium sulphide (ss-Na_2S) is described. Most chemical forms of mercury are soluble in HNO_3, with the exception of HgS. Because HgS is soluble in Na_2S solution, a sequential extraction procedure was developed to determine the distribution of HgS in soil. To determine the efficiency of this sequential extraction procedure, soil samples were spiked with either [203]HgS or [203]$HgCl_2$ and extracted sequentially with HNO_3 and ss-Na_2S. For samples spiked with [203]$HgCl_2$, HNO_3 extracted 95 and ss-Na_2S 1% of the added [203]$HgCl_2$. In contrast, for soil spiked with [203]HgS, HNO_3 extracted 1 and ss-Na_2S 98% of the added [203]HgS. When this sequential extraction procedure was applied to mercury-contaminated soil, the mercury concentrations in the combined HNO_3 and ss-Na_2S extracts accounted for 99% of the total mercury present. Further, of the total mercury present, 74–100% was HgS as determined by the concentration of mercury in the ss-Na_2S extract. These results suggest that the proposed sequential extraction procedure can selectively differentiate HgS from other species and compounds of mercury in soil.

Keywords: *Mercury(II) sulphide; quantitative method; extraction; soil*

Regulatory agencies frequently assess the potential environmental and human health risks of mercury by means of the concentration of mercury in soils and sediments. However, several studies have shown that the risk from mercury in the environment is determined by both the total concentration and the species of mercury. Hence there appears to be a need to establish allowable environmental concentrations of mercury after considering the total and relative concentrations of mercury species in soils and sediments.[1-3] To date, however, methods for the speciation of mercury in the environment have yet to be established.

Mercury can exist in soils and sediments in organic (*e.g.*, methylmercury), inorganic (*e.g.*, HgS) and elemental forms (*e.g.*, free mercury). Two factors determine the dominant species in soils and sediments: (1) existing chemical forms in the environment; and (2) the chemical form released into the environment and/or the chemical and biological reactions occurring in this environment. Several workers have reported the chemical and biological reduction of ionic mercury to elemental mercury, methylation of ionic mercury to methylmercury by aerobic and anaerobic bacteria and the conversion of ionic mercury to HgS by sulphate-reducing bacteria.[4-6]

The significance of these chemical and biological reactions on the relative concentrations of the different chemical forms of mercury in soils and sediments and the associated risk can be assessed by determining the chemical forms of mercury in the contaminated matrix. Several workers have described methods for extracting total mercury, elemental mercury and organic mercury from a variety of media.[7,8] However, methods have not yet been established for extracting HgS sequentially. This paper describes a quantitative procedure for extracting and determining HgS concentrations in soils and sediments. The method involves the sequential extraction of organic, inorganic and elemental mercury with HNO_3, followed by the extraction of HgS with Na_2S solution. Values for total mercury in soil were compared with levels of mercury extracted sequentially with HNO_3 and a saturated solution of Na_2S.

Experimental

Chemicals

The following chemicals were obtained from the sources indicated: HgS (Aldrich, St. Louis, MO, USA); Na_2S (Sigma, Milwaukee, WI, USA); ultra-pure HNO_3, H_2SO_4 and $HClO_4$

(J. T. Baker, Phillipsburg, NJ, USA); and [203]$HgCl_2$ (New England Nuclear, Boston, MA, USA). All other chemicals were of analytical-reagent grade.

Reagents

Sodium sulphide crystals were added to de-ionised water until saturation was reached. This saturated solution (ss-Na_2S) was used for dilution of the HgS standards, for extraction of HgS from soil and for the dilution of the soil extracts. A stock solution of HgS was prepared by adding 1 mg of HgS to 10 ml of ss-Na_2S. A working standard was prepared by mixing 1 ml of the stock HgS solution with 99 ml of ss-Na_2S to give a final mercury concentration of 1 μg ml^{-1}. A similar procedure was used to prepare an $HgCl_2$ standard except that 12 M HNO_3 was used to dissolve the $HgCl_2$ and to dilute the stock solutions.

Procedures

Soil samples were collected from areas known to be contaminated with mercury using a Jenkins sampler or as grab samples. The samples were mixed thoroughly, divided into three portions and processed. For one portion, dry mass was determined by allowing the sample to air-dry at room temperature for 72–96 h. Soil mass was determined at 24-h intervals and dry mass was assessed when the sample mass remained constant for 48 h. Dry mass was used for the calculation of mercury levels in soil. The other two portions were used for the extraction and digestion studies.

Mercury was extracted sequentially from the soil with a 12 M solution of ultra-pure HNO_3 and a saturated solution of Na_2S. A 1-g sample of soil (wet mass) was added to 4 ml of NHO_3 and the mixture shaken at room temperature overnight. The mixture was then centrifuged and the residue washed with 4 ml of HNO_3, re-centrifuged and the supernatants were combined. A 4-ml aliquot of ss-Na_2S was added to the soil residue and the sample shaken at room temperature overnight. The mixture was then centrifuged and the residue washed with 4 ml of Na_2S solution, re-centrifuged and the supernatants were combined. The supernatants from the HNO_3 and ss-Na_2S treatments were each filtered and analysed for mercury using the cold-vapour technique described by Lindstedt and Skare.[9] Mercury(II) sulphide and $HgCl_2$ standards were prepared as described above and used for the determination of mercury levels in the ss-Na_2S and HNO_3 extracts, respectively.

In some studies, radioactive mercury was added to sterilised

soil and extracted with water, HNO_3 and ss-Na_2S. For this, an aqueous solution of carrier-free $^{203}HgCl_2$ or ^{203}HgS (specific activity 7.4 mCi mg^{-1}) was diluted with de-ionised water, then 4 ml of the diluted radioactive solution were added to 1 g of sterilised soil (wet mass) and the mixture was shaken at room temperature for 5 d. The samples were then centrifuged and the supernatants removed and filtered. To each residue was added 4 ml of de-ionised water, HNO_3 and ss-Na_2S. After the addition of each extraction solution, the sample was shaken at room temperature overnight, then centrifuged and the supernatant removed. The residues were washed with the appropriate extraction solutions and the supernatants were combined, filtered and the radioactivity in the filtrate and residue was determined. The radioactivity in the filtrate after the 5-d period accounted for less than 1% of the total $^{203}HgCl_2$ and ^{203}HgS added.

In order to determine the total mercury concentrations in soil, the samples were digested according to the method of Feldman.[10] Briefly, a 1-g (wet mass) sample of soil was added to a 250-ml flask containing 5 ml of H_2SO_4 and 10 ml of HNO_3 (ultra-pure). An insulated condenser was attached to the top of the flask, the system was placed on a hot-plate and the temperature increased to 350 °C. The sample was heated for 4 h or until the HNO_3 had evaporated. A 10-ml aliquot of $HClO_4$ was added to the flask and the temperature increased to 450 °C. The sample was digested for 15 h (or until the $HClO_4$ had evaporated) and the mixture cooled before rinsing the condenser with de-ionised water. After the volume had been adjusted to 250 ml with de-ionised water, the mercury levels were determined as described above.

Results and Discussion

Calibration graphs for $HgCl_2$ and HgS were constructed by dissolving these compounds in HNO_3 and Na_2S solution, respectively. Replicate analyses of these standards were reproducible, with a variation between analyses of less than 8%. The correlation coefficient for each calibration graph was approximately 1.

In the extraction experiments described below, mercury concentrations were determined by reference to the calibration graph for mercury in the appropriate extractant. The solubility of pure HgS was measured in HNO_3 and ss-Na_2S; the results showed that HgS was completely soluble in ss-Na_2S and only 10–15% soluble in HNO_3. However, the levels of mercury in the HNO_3 extract were reduced to less than 1% when pure HgS was washed exhaustively with boiling, de-ionised water prior to extraction with HNO_3. To confirm this observation, HgS was added to soil and then extracted

with ss-Na_2S. The added HgS was completely recovered with ss-Na_2S (Table 1). Further, ss-Na_2S extracted 89–96% of the total endogenous mercury concentrations in this soil suggesting that mercury in the soil was predominantly in the HgS form.

Most chemical forms of mercury are soluble in HNO_3, with the exception of HgS.[11,12] To determine the specificity of HNO_3 and ss-Na_2S for extracting mercury from soil, $^{203}HgCl_2$ or ^{203}HgS was added to the soil and then extracted with HNO_3, followed by ss-Na_2S extraction. Nitric acid extracted

Table 2. Sequential extraction of ^{203}Hg from soil with de-ionised water, HNO_3 and Na_2S solution

| | | ^{203}Hg/disintegrations min^{-1} g^{-1} | | |
| | | Extracted | | |
Creek mile	Added	Water soluble*	HNO_3 soluble*	Na_2S soluble*
10.8	24 000†	240 (1.0%)	22 892 (95%)	316 (1.3%)
11.7	24 600†	256 (1.0%)	23 356 (95%)	232 (1.0%)
10.8	100 800‡	988 (1.0%)	1 067 (1.1%)	98 403 (98%)
11.7	98 300‡	1099 (1.1%)	1 508 (1.5%)	96 520 (98%)

* Mean of three experiments. The percentage extracted in each solvent is shown in parentheses.
† Added as $^{203}HgCl_2$.
‡ Added as ^{203}HgS.

Table 3. Extraction of mercury from soil with de-ionised water, HNO_3 or Na_2S solution

| | | | Hg/µg g^{-1} | | |
Creek mile	Soil depth/cm	Total mercury in soil digest	Water soluble*	HNO_3 soluble*	Na_2S soluble*
10.8 . .	5–20	1003	0.028 (988)	118 (896)	838 (101)
	20–35	1379	0.132 (1420)	186 (1111)	1140 (90)
11.7 . .	5–20	1716	0.120 (1801)	219 (1479)	1578 (101)
	20–35	1859	0.132 (1930)	244 (1699)	1656 (93)

* Results are the mean of three experiments. Results in parentheses refer to the total concentration of mercury remaining in the soil after extraction.

Table 4. Sequential extraction of mercury from soil using HNO_3 and Na_2S solution. Samples were taken from the same site but at different soil depths

| | | Hg/µg g^{-1}* | | |
Creek mile	First extraction with HNO_3	Second extraction with Na_2S solution	Total mercury extracted	Total mercury in the soil digest
10.6† . .	103 ± 15	325 ± 37	428 ± 53	443 ± 58

| | | Hg/µg g^{-1} | | |
Creek mile	First extraction with Na_2S solution	Second extraction with HNO_3	Total mercury extracted	Total mercury in the soil digest
10.6‡ . .	533 ± 57	65 ± 4	598 ± 61	621 ± 60

* Results are the mean ± standard deviation of three experiments.
† Soil depth, 0–10 cm.
‡ Soil depth, 20–30 cm.

Table 1. Recovery of HgS from soil

Creek mile	HgS added to soil/µg g^{-1}	Total mercury in Na_2S extract/ µg g^{-1}*	Recovery, %
10.8	0	1882 ± 47 (2050 ± 240)	0
	200	2180 ± 118	97
	400	2326 ± 109	95
	600	2792 ± 217	105
11.7	0	276 ± 11 (288 ± 37)	0
	200	526 ± 36	108
	400	785 ± 27	114
	600	1027 ± 72	116
13.7	0	66 ± 28 (74 ± 19)	0
	200	265 ± 38	97
	400	450 ± 68	95
	600	721 ± 23	107

* Results are the mean ± standard deviation for three experiments. Total mercury in each soil sample is shown in parentheses.

Table 5. Comparison of Na_2S extractable mercury in soil with mercury levels in a soil digest

Creek mile	Sample No.	Total mercury in soil digest/$\mu g\,g^{-1}$	Total mercury in Na_2S extract/$\mu g\,g^{-1}$	Amount extracted, %*
10.8 ..	1	170	135	79
	2	138	116	84
	3	158	148	94
	4	1097	885	81
	5	909	656	72
	6	1003	970	97
	7	1485	1228	83
	8	1273	1146	90
	9	1380	1052	76
	10	19	20	105
	11	641	622	97
	12	421	438	104
	13	460	495	108
	14	60	63	105
	15	2920	2970	102
				Mean: 92 ± 12
11.7 ..	1	116	115	99
	2	181	149	82
	3	114	130	114
	4	1410	1914	136
	5	2461	1680	68
	6	1289	1442	112
	7	2013	1273	63
	8	1996	2006	101
	9	1563	1306	84
	10	1685	1273	76
	11	2961	3030	102
	12	2200	2015	92
	13	98	122	124
	14	2562	2492	97
	15	3003	3772	126
				Mean: 98 ± 22
13.7 ..	1	45	40	89
	2	9	11	122
	3	43	39	91
	4	1.8	2.4	133
	5	2339	1757	75
	6	1797	1856	103
				Mean: 102 ± 22

* Results given as the mean ± standard deviation.

95 and Na_2S solution 1% of the added $^{203}HgCl_2$ (Table 2). In similar studies with ^{203}HgS, Na_2S solution extracted 98 and HNO_3 1%. These results show the specificity of ss-Na_2S for extracting HgS from soil. A further demonstration of this specificity is shown in Table 3. Mercury in soil taken from a site that had been contaminated in the late 1950s was extracted with water, HNO_3 and ss-Na_2S. The soil from this site was digested with acid (as described above) to determine the total concentration of mercury; the values obtained ranged from 0.5 to 3000 p.p.m. As shown in Table 3, the sum of the mercury concentrations in the different extracts accounted for 99.5% of the mercury concentrations observed in the soil digest. Further, in terms of the average percentage of the total mercury present in the soil digest, water extracted less than 0.1, HNO_3 13 and ss-Na_2S 87%.

The results in Table 3 suggest that complete extraction of mercury from soil can be achieved using both HNO_3 and ss-Na_2S. To confirm this observation, samples of soil were extracted sequentially with HNO_3 and ss-Na_2S (or the reverse). As shown in Table 4, the total mercury in the sequential extracts accounted for 97% of the total mercury in the soil digest. When soil samples were extracted first with HNO_3, then with ss-Na_2S, 23 and 73%, respectively, of the total mercury present in the sample was extracted. However, when soil samples were extracted first with ss-Na_2S, then with HNO_3, the amounts extracted were 86 and 10%, respectively.

The results in Table 4 are for soil samples collected at depths of 0–10 and 20–30 cm, respectively. The fact that the relative percentage of the total mercury extracted into ss-Na_2S was greater for the smaller soil depths suggests that the soil conditions at this depth favour the formation of HgS. At the greater depths, the soil conditions may not be as favourable for HgS formation and, therefore, the percentage of the total mercury extracted with HNO_3 would be greater.[6,13] This observation was, in part, confirmed following the measurement of the electrochemical potential of the soil at depths of 0–10 and 20–30 cm, respectively.

Table 5 shows the distribution of Na_2S-soluble mercury in soil samples collected from several locations at this contaminated site. The mean amount of the total mercury in soil from this site that was soluble in Na_2S ranged from 92 to 102%. This result suggests that more than 90% of the total mercury in this soil is in the HgS form.

These results are important for determining the potential environmental risk of mercury in soil at this site.[14,15] For example, a significant reduction in this risk should be observed with mercury species and compounds that are relatively insoluble in aqueous solution (i.e., the solubility of HgS in water is $1.1 \times 10^{-16}\,\mu g\,l^{-1}$). Hence, the method described here for extracting mercury from soil sequentially may be used to determine the potential environmental and human health risks associated with mercury in soils and sediments.

Conclusions

A method is described for extracting mercury from soil sequentially. The mercury is first extracted with HNO_3, then with a saturated solution of Na_2S. The HNO_3 extracts all forms of mercury, except HgS, whereas the Na_2S solution extracts only HgS. This extraction procedure provides a method for assessing the importance of chemical and biological reactions in soil and the potential environmental and human health risks of mercury-contaminated soil.

References

1. Friberg, L., and Vostal, J., "Mercury in the Environment,' CRC Press, Cleveland, OH, 1972, pp. 34–186.
2. D'Itri, F. M., "The Environmental Mercury Problem," Report to the Michigan House of Representatives Resulting from House Resolution 424 Great Lakes Contamination (Mercury) Committee, 1971.
3. Klein, D. H., *Environ. Sci. Technol.*, 1972, **6**, 560.
4. Robinson, J. B., and Tuovinen, O. H., *Microb. Rev.*, 1970, **48**, 95.
5. Jernelov, A., *Limnol. Oceanogr.*, 1970, **8**, 39.
6. Postgate, J. R., "The Sulphate-reducing Bacteria," Second Edition, Cambridge University Press, Cambridge, 1984.
7. Jacobs, L. W., and Keeney, D. R., *Environ. Sci. Technol.*, 1974, **8**, 267.
8. Ure, A. M., *Analyst*, 1977, **102**, 50.
9. Lindstedt, G., and Skare, I., *Analyst*, 1971, **96**, 223.
10. Feldman, C., *Anal. Chem.*, 1974, **46**, 1606.
11. Weast, R. C., Editor, "CRC Handbook of Chemistry and Physics," Sixty-sixth Edition, CRC Press, Boca Raton, FL, 1985, pp. B114–B116.
12. Meites, L., Editor, "Handbook of Analytical Chemistry," McGraw-Hill, New York, 1963, pp. 1–19.
13. Lawrence, A. W., and McCarty, P. L., *J. Water Pollut. Control Fed.*, 1965, **37**, 391.
14. "Environmental Health Criteria 1: Mercury," World Health Organization, Geneva, 1976.
15. Bashor, B. S., and Turri, P. A., *Arch. Environ. Contam. Toxicol.*, 1986, **15**, 435.

Inter-laboratory Determination of Bis(tributyltin) Oxide in Timber and Timber-treatment Solutions

Bernard S. W. Dawson, Nigel H. O. Cummins, Glenda F. Parker, Faye J. Cowan and Sung O. Hong
Forest Research Institute, Private Bag, Rotorua, New Zealand

Accurate analysis of timber preservatives in timber-treatment solutions and in treated timber is an essential aspect of quality control in the New Zealand wood preservation industry. The increasing use of light organic solvent preservatives in recent years has drawn attention to the need for dependable methods for the determination of bis(tributyltin) oxide (TBTO). As part of an on-going programme of timber preservative analyses at the Forest Research Institute the determination of TBTO was studied in detail by an inter-laboratory comparison between six laboratories. Significant differences between laboratories were found in the determination of TBTO (or tin) in timber preservative treatment solutions and preservative-treated timber. To rectify this situation, recommendations on the necessity to intensify quality assurance programmes are suggested.

Keywords: *Bis(tributyltin) oxide; quality assurance; inter-laboratory analysis*

Since the biocidal properties of bis(tributyltin) oxide (TBTO) were first described in 1954,[1] TBTO has been used as a fungicide. The determination of TBTO in a variety of samples can be achieved in several ways. The organotin compound can be decomposed and analysed for inorganic tin[2-6] or the sample can be analysed for inorganic tin *in situ* by X-ray fluorescence spectrometry.[7-9] The TBTO may also be determined without prior decomposition by atomic absorption spectrometry (AAS) or other methods.[4,10-16] Finally, species-specific methods of analysis, determining not only TBTO, but also any degradation tin products can be employed.[10,17-24] Only a few of the techniques cited are suited to the determination of TBTO in preservative-treated timber or timber-treatment solutions. In the timber preservation industry, tin is usually determined by extraction with ethanol - HCl followed by AAS,[6,10] by X-ray fluorescence spectrometry[7-9] or by acid digestion followed by AAS.[2-6] Timber-treatment solutions are analysed by titration[21] (for TBTO), acid digestion - AAS[2-6] and dilution with organic solvents followed by direct determination using AAS[4,10,11,15] (the AAS analyses are for inorganic tin, although the result is expressed as per cent. TBTO).

Quality assurance programmes are required if accuracy and precision in analytical determinations are to be achieved consistently over long periods of time.[25-27] This is especially so when different organisations and laboratories need to communicate meaningfully on the basis of the analytical results. There are two types of quality assurance assessment that are necessary to establish and maintain accuracy and precision within an area of analytical determination. They are intra-laboratory and inter-laboratory quality assurance. In the former, each laboratory establishes an experimental programme to provide statistical data to demonstrate and maintain the accuracy and precision of its experimental determinations. In the latter, one central organisation provides well characterised samples to other laboratories for analysis. On receipt of the participating laboratories' reports, the central organisation provides statistical data to these laboratories concerning the accuracy and precision of (1) the methods used, (2) the data obtained from various laboratories using the same method or (3) the data from different methods of analysis. Information on whether any laboratory gave markedly different results compared with group averages is also usually provided.

This paper describes the details and results of an inter-laboratory determination of tin or TBTO in timber and timber-treatment solutions from six laboratories in New Zealand. Emphasis is placed on the analysis of data for timber samples.

Experimental

Design of the Inter-laboratory Programme for the Determination of TBTO in Solutions and Tin in Timber

Six New Zealand laboratories were invited to participate in the programme. These laboratories, which included industrial and public analysts and a research institute, all perform determinations of TBTO in treatment solutions, and tin in treated timber on a regular basis. They were asked to analyse the samples, preferably by more than one method and to include duplication. The following samples were used. (1) Ten solution samples in kerosene, including a kerosene blank, to be analysed at the rate of 3 d⁻¹ for 3 d. Each day's samples were identical, except for the order of the samples. The TBTO concentrations were all in the range 1.90–2.10% *m/V*. (2) Thirty-seven timber samples (including a blank untreated timber) to be analysed over 3 d at the rate of 12 d⁻¹. Each day's samples were the same, but with random numbering. The levels of tin in the samples spanned the range 0.030–0.150% *m/m* with a large number of the samples straddling 0.080% *m/m* as this was the target retention level of Sn set by the New Zealand Timber Preservation Authority.[28]

Preparation of Solution and Timber Samples for Inter-laboratory Analyses

The samples were prepared using Fluka pract. grade (>92% TBTO) bis(tributyltin) oxide. The TBTO solution was analysed by the following procedures. (1) Titration with HBr in glacial acetic acid.[21] Various solutions, prepared by dilution of the stock solution, were analysed. (2) Digestion with 3 + 1 H_2O_2 - H_2SO_4 and analysis by AAS in a C_2H_2 - N_2O flame using aqueous standards made from BDH SpectrosoL 1000 p.p.m. Sn solutions.

The TBTO stock solution concentration was determined by the above analyses to be 95% *m/m* TBTO (coefficient of variation, 1.1%; number of results, 9).

The kerosene and ethanol (99%) used for sample preparation work were also analysed for TBTO/tin content. The kerosene was titrated with HBr in glacial acetic acid[21] and also analysed for Sn directly by AAS. The ethanol was analysed for Sn by AAS. Both solvents contained less than 0.01% *m/V* TBTO.

Solution samples

Three TBTO solutions, X, Y and Z, were prepared by weighing the previously analysed stock solution of TBTO and

a solvent (kerosene or ethanol) into a 1-l calibrated flask. Approximately 50-ml aliquots of each solution were transferred into polypropylene bottles for distribution. The stock TBTO solution and the prepared solutions X, Y and Z were stored at 4 °C in the dark (all participating laboratories were advised to follow this procedure).

Timber samples

The following procedure was used to treat timber with TBTO [owing to possible loss of TBTO from the timber on oven drying (see below for data) only nominal target values were calculated]. Two TBTO solutions, one in kerosene (10.006 g of TBTO per 100 ml) and one in ethanol (5.002 g of TBTO per 100 ml), were prepared. These were used to add a calculated amount of TBTO to 45.000-g amounts of oven-dried *Pinus radiata* sapwood (<2 mm particle size) in 500-ml beakers. After the samples had been oven-dried at 105 °C for 16 h the kerosene (K) samples still contained 7 g of kerosene, hence the timber was spread out in crystallising dishes (diameter 240 mm) and oven-dried at 105 °C for a further 4 h to constant mass. Ethanol evaporation for the ethanol (S) samples was complete after the initial drying period.

Following drying, each 45-g sample of TBTO-treated timber was ground in a large stainless-steel ring mill for about 120 s to produce a completely homogeneous timber flour (40

samples from one 45-g batch were analysed by ethanol - HCl extraction followed by AAS and were found to have a coefficient of variation of 2.5%). For the K3 and S3 samples (Table 1), which were prepared in two 45-g batches, each 45 g was ground in the ring mill separately and then combined and passed through a 12-channel riffle ten times. Samples (2 g) were distributed in screw-cap plastic vials.

The participating laboratories had no information on the TBTO/tin content of each sample except that the concentrations were of the order of those set out by the New Zealand Timber Preservation Authority.

Analytical Methods Used by Participating Laboratories

A brief description of the methods used by each laboratory for the determination of either TBTO or tin is given in Table 2.

Effect of oven drying on the TBTO content of timber

Different regimes for drying treated timber were investigated to assess the loss of TBTO from timber on oven drying. Two bulk samples (100 g) of oven-dried and milled *Pinus radiata* sapwood were treated with TBTO to produce concentrations of 0.102% *m/m* (ring-milled) and 0.111% *m/m* (Wiley-milled) TBTO. The treated samples were then air-dried separately for 24 h, milled again [either ring-milled (0.102% *m/m* TBTO) or Wiley-milled (0.111% *m/m* TBTO)] and riffled before being divided into 70 equal-sized portions.

Table 1. Concentrations of tin in timber (g of Sn per 100 g of oven-dried timber) from the various laboratories (A–I)*

Day	Sample					Laboratory					Nominal target value	Range
		A	B	C	D	E	F	G	H	I		
1	K1	0.035	0.031	0.042	0.025	0.021	0.033	0.032	0.032	0.047	0.030	0.021–0.047
	K2	0.049	0.053	0.059	0.048	0.046	0.052	0.058	0.053	0.079	0.050	0.046–0.079
	K3A	0.073	0.078	0.093	0.070	0.064	0.076	0.072	0.070	0.091	0.075	0.064–0.093
	K3B	0.073	0.078	0.093	0.065	0.060	0.074	0.077	0.069	0.105	0.075	0.060–0.105
	K4	0.091	0.150†	0.110	0.097	0.083	0.097	0.091	0.094	0.113	0.095	0.083–0.150
	K5	0.113	0.131	0.152	0.113	0.103	0.121	0.127	0.121	0.154	0.125	0.103–0.154
	S1	0.041	0.042	0.055	0.034	0.030	0.039	0.046	0.025	0.075	0.041	0.025–0.075
	S2	0.063	0.068	0.085	0.065	0.057	0.065	0.068	0.061	0.097	0.065	0.057–0.097
	S3A	0.082	0.087	0.104	0.078	0.070	0.083	0.087	0.094	0.112	0.085	0.070–0.112
	S3B	0.078	0.097	0.105	0.069	0.068	0.080	0.085	0.091	0.107	0.085	0.068–0.107
	S4	0.111	0.114	0.134	0.105	0.092	0.106	0.105	0.103	0.189†	0.110	0.092–0.189
	S5	0.145	0.158	0.169	0.162	0.125	0.146	0.144	0.155	0.187	0.151	0.125–0.187
2	K1	0.030	0.032	0.035	0.038	0.022	0.030	0.029	0.031	0.048	0.030	0.022–0.048
	K2	0.055	0.054	0.066	0.049	0.046	0.052	0.047	0.048	0.080	0.050	0.046–0.080
	K3A	0.071	0.074	0.090	0.088	0.064	0.070	0.070	0.065	0.096	0.075	0.064–0.096
	K3B	0.070	0.075	0.095	0.077	0.062	0.072	0.072	0.073	0.105	0.075	0.062–0.105
	K4	0.089	0.097	0.108	0.102	0.077	0.093	0.086	0.099	0.127	0.095	0.077–0.127
	K5	0.122	0.128	0.148	0.122	0.108	0.118	0.115	0.123	0.157	0.125	0.108–0.157
	S1	0.041	0.041	0.147‡	0.049	0.029	0.037	0.038	0.035	0.065	0.041	0.029–0.147
	S2	0.061	0.066	0.077	0.072	0.054	0.063	0.061	0.069	0.100	0.065	0.054–0.100
	S3A	0.082	0.083	0.094	0.087	0.073	0.078	0.073	0.087	0.118	0.085	0.073–0.118
	S3B	0.081	0.083	0.092	0.091	0.070	0.079	0.074	0.088	0.116	0.085	0.070–0.116
	S4	0.102	0.108	0.050‡	0.109	0.085	0.102	0.100	0.103	0.129	0.110	0.050–0.129
	S5	0.140	0.154	0.182	0.146	0.121	0.142	0.138	0.145	0.180	0.151	0.121–0.182
3	K1	0.031	0.030	0.041	0.031	0.022	0.034	0.031	0.020	0.045	0.030	0.020–0.045
	K2	0.051	0.052	0.061	0.055	0.043	0.046	0.044	0.044	0.063	0.050	0.043–0.063
	K3A	0.078	0.075	0.086	0.072	0.068	0.074	0.074	0.075	0.091	0.075	0.068–0.091
	K3B	0.075	0.075	0.084	0.066	0.063	0.076	0.070	0.065	0.093	0.075	0.063–0.093
	K4	0.092	0.101	0.117	0.082	0.081	0.091	0.089	0.092	0.114	0.095	0.081–0.119
	K5	0.124	0.131	0.165	0.106	0.109	0.127	0.118	0.123	0.140	0.125	0.106–0.165
	S1	0.043	0.039	0.050	0.046	0.031	0.042	0.034	0.026	0.064	0.041	0.026–0.064
	S2	0.065	0.064	0.078	0.065	0.057	0.067	0.060	0.064	0.084	0.065	0.057–0.084
	S3A	0.081	0.085	0.093	0.072	0.071	0.070	0.072	0.071	0.100	0.085	0.070–0.100
	S3B	0.083	0.087	0.094	0.075	0.075	0.080	0.071	0.077	0.102	0.085	0.071–0.102
	S4	0.107	0.117	0.135	0.094	0.095	0.106	0.101	0.103	0.125	0.110	0.095–0.135
	S5	0.143	0.162	0.198	0.122	0.136	0.147	0.143	0.147	0.177	0.151	0.122–0.198

* The nine result sets tabulated were obtained from six laboratories. At least two laboratories performed the analyses by different methods and submitted results for each method.

† Outliers identified by Cochran's Test, which were discarded for statistical analysis.

‡ Outliers identified by Cochran's Test, which were interchanged for statistical analysis.

Ten samples from each bulk sample were analysed by the BS method,[6] which employs air drying of the samples and a moisture-content determination on a separate sample. Ten further samples were freeze-dried before analysis and the final 50 samples were analysed after oven drying at 105 °C for periods ranging from 4 to 72 h.

Results

Statistical Analysis

The results of the determination of TBTO in solution and tin in timber are given in Tables 1 and 3. There were six sets of solution analyses and nine sets of timber analyses. Although only six laboratories participated in the programme at least two laboratories performed the timber analyses by more than one method. Accordingly, they submitted the appropriate number of result sets.

The data for solutions and timber samples were analysed for possible stragglers or statistical outliers using Cochran's test.[29] None were found for the solution data; however, for the timber data, two values were identified as stragglers (D, samples K3A and S5) and four points as outliers (B, K4; C, S1 and S4; and I, S4). The stragglers and outliers did not suggest any outlying laboratories and the straggler values were retained as data. The values of S1 and S4 for laboratory C were interchanged, as on the report returned to the co-ordinating laboratory, the values for S1 and S4 were consecutive in a table and clearly a transcription error had occurred. The remaining two outliers were discarded.

Analyses of solution and timber data were carried out on the actual data. The timber data required a variance stabilising transformation before an analysis of variance (ANOVA) was carried out as the data did not have a normal distribution with homogeneous variance. An appropriate transformation was found to be a square-root transformation.[30] When the F-value of an ANOVA was statistically significant ($p < 0.05$), a least significant difference (LSD) test was employed to compare the means, which are presented as non-transformed values in Table 4.

Solution Analyses

The ANOVA for the solution data showed significant differences (1% level) in both the performance of the laboratories and in the concentrations of TBTO in the samples. An LSD test, at the 1% level, was used to evaluate the differences in the laboratories' performance. Three classes of laboratory were found: D; B, F, E and H; and G (Table 5).

An ANOVA was also carried out to see if the chemical determinations by individual laboratories varied over 3 d. All laboratories were consistent over the three days of analysis except laboratory D which was highly inconsistent (Table 5).

When analytical data for each sample from all laboratories were combined, the coefficients of variation ranged from 5.2 to 6.4% (Table 6) for the three samples. The ranges of values for each sample were 25, 27 and 32% of the mean value for samples X, Y and Z, respectively. The confidence intervals for the three solutions are also given in Table 6.

Timber Analyses

An ANOVA showed significance in both the performance of the laboratories and in sample concentrations. The LSD tests were carried out to compare these differences (Table 5) and the results showed that there were five different classes of laboratory. Four groups contained one laboratory each, i.e., E, B, C and I and five, A, D, F, G and H, had similar means. The nominal target mean was 0.082.

The means of each sample (for all laboratories) and the 95% confidence limits are given in Table 6. The coefficients of variation, which were inversely proportional to the tin concentrations, were in the range 12.2–28.1%.

Table 2. Brief description of methods of analysis for each laboratory

Laboratory			Method
Solution samples—			
A, C, I	..		Not performed
B	..	..	BS 5666, Part 7, 1980 [dilution of solution sample with a reflux solution of methylated spirit without pyridine (MSWP) - 1.0% HCl - 612 p.p.m. of Li and analysis by AAS].[6] The AAS standards were prepared by digestion of 0.500 g of Sn metal with HCl - HNO₃ and diluted 1 + 1 with MSWP
D, F	..	..	In-house method. Solution sample diluted with kerosene. Analysed by AAS using standards prepared from TBTO using kerosene as solvent
E, H	..	..	Australian Standard 1607, 1974 (titration of TBTO with HBr in glacial acetic acid)[21]
G	..	..	In-house method. Sample solution digested with 3 + 1 H₂O₂ - H₂SO₄ plus HNO₃ as required to destroy organic matter. Made up to volume with water and analysed by AAS using BDH SpectrosoL 1000 p.p.m. Sn solution to prepare standards
Timber samples—			
A, F	..	..	Modification of BS 5666, Part 7, 1980 (samples were oven-dried).[6] Reflux 1 g of <2 mm oven-dried wood with 0.5% HCl + 1000 p.p.m. of lithium + 99% ethanol for 15 min, cool and filter. Analyse by AAS using TBTO solution diluted with the reflux solution
B, C, D	..		As per BS 5666, Part 7, 1980.[6] Reflux 1 g of sample in a solution of 1.0% HCl + 5000 p.p.m. of lithium in MSWP for 15 min, cool and filter. Analyse by AAS using standard preparation for laboratory B solution analysis
E	..	..	In-house method. Samples were refluxed with isobutyl methyl ketone (IBMK) containing ammonium pyrrolidine dithiocarbamate (APDC; 1 ml of solution used) prepared by dissolving 4 g of APDC in 100 ml of distilled water and washing with IBMK. Samples were filtered and analysed by AAS using standards prepared by IBMK extraction of aqueous tin from BDH SpectrosoL Sn solutions. Moisture contents were determined on a separate sample
G	..	..	In-house method. Oven-dried sample (1 g) digested with 3 + 1 H₂O₂ + H₂SO₄ plus HNO₃ as required to remove organic matter and made up to volume with distilled water. Analysed by AAS using aqueous standards prepared with BDH SpectrosoL Sn solutions
H	..	..	In-house method. Oven-dried samples were ground in a ring mill, pelleted and analysed by X-ray fluorescence spectrometry. The spectrometer was calibrated against standard pellets made after ring-milling AnalaR, oven-dried SnO₂ in cellulose
I	..	..	In-house method. Modification of BS 5666, Part 7, 1980.[6] Sample (1 g) was digested with 5 ml of H₂SO₄ and small amounts of H₂O₂, which were added by wash bottle. Digestion was taken to fuming over a hot-plate. The solution was made up to volume and analysed by AAS. The standards for AAS were prepared by digesting 0.500 g of oven-dried tin powder with 100 ml of HCl and 2.5 ml of HNO₃. No heating was required. The solution was diluted 1 + 1 with de-ionised water containing 6.12 g l⁻¹ of LiCl and 10% HCl

Table 3. Concentrations of TBTO in solution (g per 100 ml of solution)

Day	Sample	A	B	C	D	E	F	G	H	I	Nominal target value
					Laboratory						
1	X	—	2.24	—	2.20	2.13	2.18	1.95	2.07	—	2.01
	Y	—	2.06	—	2.24	2.03	2.05	1.90	1.97	—	1.90
	Z	—	2.12	—	2.28	2.12	2.07	1.74	2.06	—	2.00
2	X	—	2.18	—	2.48	2.20	2.07	2.03	2.09	—	2.01
	Y	—	2.03	—	2.45	2.00	2.04	1.92	1.99	—	1.90
	Z	—	2.12	—	2.40	2.08	2.13	1.94	2.06	—	2.00
3	X	—	2.17	—	2.14	2.12	2.13	2.03	2.09	—	2.01
	Y	—	2.12	—	1.99	2.02	2.01	2.00	1.98	—	1.90
	Z	—	2.10	—	2.05	2.07	2.13	1.97	2.10	—	2.00

Table 4. Mean of each day's analyses for solutions and timber samples together with the significance of the F-test for ANOVA for the daily variation of each laboratory

	No. of samples	A	B	C	D	E	F	G	H	I
					Laboratory						
					TBTO, % m/V						
Solutions—											
Day 1	3	—	2.14	—	2.24	2.09	2.10	1.86	2.03	—
Day 2	3	—	2.11	—	2.44	2.09	2.08	1.96	2.05	—
Day 3	3	—	2.13	—	2.06	2.07	2.09	2.00	2.06	—
Significance of F-test for ANOVA between days	—	—	NS*	—	†	NS	NS	NS	NS	—
					Sn, % m/m						
Timber—											
Day 1	12	0.080	0.091	0.100	0.078	0.068	0.081	0.083	0.081	0.113
Day 2	12	0.079	0.083	0.099	0.086	0.068	0.078	0.075	0.081	0.110
Day 3	12	0.081	0.085	0.100	0.074	0.071	0.080	0.076	0.076	0.100
Significance of F-test for ANOVA between days	—	NS	NS	NS	†	‡	NS	†	‡	†

* NS = not significant.
† Significant at the 1% level.
‡ Significant at the 5% level.

The intra-laboratory variation of analyses carried out over 3 d was assessed by ANOVA. Four laboratories, A, B, C and F, gave consistent results over 3 d (Table 4), while D, E, G, H and I were significantly different over a 3-d analysis period.

Discussion

The ranges of results for TBTO in solution for samples X, Y and Z were 25–32% of the mean values found for each sample. This spread of values is indicative of the need for more control at all stages of chemical and statistical analyses in the various laboratories.

The magnitude of the ranges, between laboratories, of tin concentrations in timber (Table 5) is disturbing. Laboratories E and I, with the lowest and highest grand mean values, respectively, contribute to the majority of the range end-points. These between-laboratory differences were obtained from laboratories conscientious enough to take part in this programme and which determine tin in timber routinely. Even with an awareness of the analytical problems, such wide ranges must be regarded as unsatisfactory.

The differences between laboratories are caused by the various methods employed at the operational level. For the solutions, the methods used by laboratories B, E and H were documented standard methods for the determination of TBTO[6,21] (BS 5666, Part 7, 1980 and AS 1607, 1974, respectively), known to be capable of producing accurate and reproducible results. These laboratories' results were consist-

ent over the 3-d analysis period. The other three laboratories (D, F and G) that returned solution analyses, used non-standard in-house methods. Of these laboratories, D performed poorly, being inconsistent over the analysis period, whereas laboratories F and G were consistent. Laboratory D also reported the highest results.

For timber analyses, laboratories B, C and D followed the BS method[6] while laboratories A, F and I used a modified form of the method. Laboratories A, B, C and F were consistent over the 3 d of analysis whereas laboratories D and I were inconsistent. The remaining three laboratories, E, G and H (all used in-house methods), performed poorly, producing inconsistent results over the 3 d of analyses. It therefore appears that the use of a standard method is more likely to produce consistent results than in-house methods. However, the performance of some laboratories using the standard method was still poor (inconsistent).

Effect of Oven Drying on the TBTO Content of Timber

The data for the drying experiment are presented in Table 7. Analysis of air-dried and freeze-dried samples produced mean TBTO values in agreement with the target values. The oven-dried ring-milled samples showed a 23% loss of TBTO in the first 4 h of drying, the loss increasing to 30% after 72 h, and the Wiley-milled samples suffered losses of TBTO of 16% (4 h) and 22% (72 h). The standard deviations for the analysis of the various batches of Wiley-milled samples were up to four

Table 5. LSD test for solution and timber samples

Solution samples—

Laboratory	Mean	LSD test at the 1% level*
D	2.25	|
B	2.13	|
F	2.09	|
E	2.09	|
H	2.05	|
G	1.94	|

LSD = 0.082

Timber samples—

Laboratory	Mean	LSD test at the 5% level*
I	0.106	|
C	0.100	|
B	0.085	|
A	0.080	|
F	0.080	|
D	0.080	|
H	0.079	|
G	0.078	|
E	0.069	|

LSD = 0.0038

Sample	Mean	LSD test at the 1% level*
S5	0.153	|
K5	0.127	|
S4	0.110	|
K4	0.097	|
S3B	0.085	|
S3A	0.085	|
K3A	0.077	|
K3B	0.076	|
S2	0.069	|
K2	0.054	|
S1	0.042	|
K1	0.033	|

LSD = 0.0058

* Means with a bar in the same column are not significantly different.

Table 6. Coefficients of variation (CVs) and 95% confidence limits (CLs) for each solution (TBTO, % m/V) and timber sample (Sn, % m/m) calculated using all data

Sample	No. of analyses per sample	Mean	CV, %	Range (min.–max.)	CL
Solution samples—					
X . .	18	2.14	5.2	1.95–2.48	2.08–2.20
Y . .	18	2.04	6.1	1.90–2.45	1.98–2.11
Z . .	18	2.09	6.4	1.74–2.40	2.02–2.15
Timber samples—					
K1 . .	27	0.033	22.8	0.020–0.048	0.030–0.036
K2 . .	27	0.054	17.6	0.043–0.080	0.050–0.058
K3A . .	27	0.077	12.2	0.064–0.096	0.073–0.080
K3B . .	27	0.076	15.9	0.060–0.105	0.071–0.081
K4 . .	26	0.097	12.6	0.077–0.127	0.092–0.102
K5 . .	27	0.127	12.9	0.103–0.165	0.120–0.133
S1 . .	27	0.042	28.1	0.025–0.075	0.038–0.047
S2 . .	27	0.069	16.6	0.050–0.100	0.064–0.073
S3A . .	27	0.085	15.1	0.070–0.118	0.080–0.090
S3B . .	27	0.085	14.6	0.068–0.116	0.080–0.090
S4 . .	26	0.110	13.2	0.092–0.129	0.103–0.115
S5 . .	27	0.153	12.8	0.121–0.198	0.144–0.160

times higher than those obtained for the ring-milled samples. The reduced loss of TBTO from the coarser Wiley-milled samples corresponds to a reduced surface area available for the loss of preservative and the increased standard deviation reflects a less homogeneous sample. It should be noted that this demonstrable loss of TBTO meant that only nominal

target values were assigned to the samples involved in the inter-laboratory programme.

Morgan and Purslow[31] studied the losses of volatile wood preservatives and quoted vapour pressure values for TBTO and white spirit of 1.1×10^{-5} mmHg (25 °C) and $1.5 - <0.1$ mmHg (20 °C), respectively. The values are for the pure chemicals only and do not take account of any interaction with the timber or solution mixtures. Particle, chip or board size and climatic factors such as temperature, humidity and winds, would all be important in service situations and, although solvent evaporation would greatly exceed that of TBTO, some loss of TBTO was envisaged. Higher temperatures would clearly accelerate such loss and the oven-drying experiment probably produced maximum losses.

An interesting point arising from the data in Table 5 is that the means for each timber sample were all found to be significantly different except for each of the two duplicate sets, which were the same. From Table 6 it can be seen that for the timber analysis the nominal target values all lay within the 95% confidence limits for each sample. This may imply that minimum amounts of TBTO were lost during sample preparation due to heating or it may be a coincidental consequence of averaging low and high values reported by the various laboratories. Clearly there was not a 20–30% loss of TBTO from the samples as indicated by the oven-drying experiments on milled timber.

Quality Assurance Programmes

In practical terms, accurate determinations of TBTO or tin in timber-treatment solutions or timber are essential to control and monitor timber treatment using that preservative. If there are contradictory analytical reports then the cost of action based on inaccurate analyses could be substantial. This is especially so in an industry where the threshold level (*i.e.*, 0.08% *m/m* Sn) is regarded as an adequate preservative level for timber protection.

Improvement in the determinations of TBTO or tin in timber industry related laboratories can be achieved by improved quality assurance of the entire analytical process. The following pertinent points demand constant attention.

1. Wherever possible, standard methods of analysis should be employed. Such methodology has been rigorously investigated and assessed so as to allow accurate and precise measurements to be made. One danger in modifying standard methods is that unless the modification is considered from every angle, ramifications of the change may not be known. In-house methods not relying on standard methods are likely to be flawed. Another advantage of using standard methods of analysis is that the performance of the method can be assessed separately from concerns that one may have about the methodology itself. This distinction between performance and methodology is a valuable tool in identifying sources of error in analyses.

2. The standard tin or TBTO compound should be of primary standard grade wherever possible.

3. The volatilisation of TBTO should be minimised by air drying (and not oven drying) samples prior to analysis.

4. As an adjunct to quality assurance, auditing the facilities of a laboratory and its methodology should be performed by national laboratory accreditation agencies such as the Testing Laboratory Registration Council (TELARC) (New Zealand) or the National Association of Testing Authorities (NATA) (Australia).

5. Mathematical calculations must be checked for accuracy. Probably as critical as the calculations themselves is the transcription of results. Results can easily be interchanged, integers in a number swapped and legibility of writing can also be problematical. Electronic data transfer has an advantage in this respect.

Table 7. Tin content (g of Sn per 100 g of oven-dried timber) of timber following air drying, freeze drying or oven drying

Drying treatment	Target value	Air-dried	Freeze-dried	Oven-dried/h				
				4	8	16	24	72
Mean $(n = 10)$	0.102*	0.099	0.098	0.079	0.077	0.073	0.072	0.071
Standard deviation	—	0.001	0.002	0.002	0.002	0.001	0.002	0.001
Tin content, % of target	—	97	96	77	75	72	71	70
Mean $(n = 10)$	0.111†	0.110	0.109	0.093	0.093	0.090	0.088	0.087
Standard deviation	—	0.004	0.004	0.004	0.004	0.002	0.004	0.004
Tin content, % of target	—	99	99	84	84	81	79	78

* Particle size of timber flour (ring-milled) estimated to be <250 μm.
† Particle size of sawdust (Wiley-milled) estimated to be >250 μm but <2 mm.

Table 8. Mean (m), repeatability (r) and reproducibility (R) values for duplicate timber samples (g of Sn per 100 g of timber)

	Day			Average over 3 d	Average over both samples
	1	2	3		
K3 sample—					
m	0.077	0.077	0.076	0.077	0.081
r	0.011	0.012	0.009	0.011	0.009
R	0.034	0.035	0.024	0.031	0.032
S3 sample—					
m	0.088	0.086	0.081	0.085	—
r	0.010	0.005	0.009	0.008	—
R	0.038	0.038	0.024	0.033	—

6. The ultimate goal is, however, to gain control of every facet of the laboratory and experiment through a comprehensive quality assurance programme.[27,32] Quality assurance programmes are required if accuracy and precision in analytical determinations are to be achieved consistently over long periods of time. Such a programme should include (a) calibration of all equipment on a roster system, with the calibration being traceable back to established primary standards, (b) working reference materials or standard reference materials in each batch of analyses (if the analysis of these materials shows any extreme values then the batch should be regarded as suspect and the analysis repeated), (c) the use of standard analytical methods and (d) full documentation of the entire quality assurance programme.

Determination of Repeatability and Reproducibility Values

Although a standard test method was not employed by the participating laboratories, there was still value in determining the repeatability and reproducibility values $(r$ and R, respectively, as defined in ISO 5725[29]) for the two sets of duplicate samples K3A and B and S3A and B. The duplicates were performed under repeatability conditions each day.[29]

The mean, m, r and R values for the duplicate samples are shown in Table 8. The data were finally averaged to give m, r and R values for 0.077–0.085% m/m Sn. The significance of the r value is that the difference between two single results on identical material by one operator using the same equipment in a short time interval will exceed 0.009% m/m Sn for 5% of the time. Further, single results on identical test material reported by two laboratories will differ by more than the value of R (0.032% m/m Sn) for 5% of the time. If a standard test method was employed the values of r and R would be expected to decrease substantially.

Conclusions

The intra-laboratory analyses for each participating laboratory showed that only one laboratory was inconsistent over 3 d of analyses for solutions, whereas only four were consistent over the 3 d for the timber sample analyses. This lack of

consistency was attributed to the use of non-standard methods of analysis. Standard methods should limit possible errors due to the methodology and hence promote better performance.

Inter-laboratory comparison of solution and timber samples has shown that the performance of the participating laboratories is not uniform. For the solution analyses three classes of laboratory were identified using ANOVA and LSD tests and five classes for the timber analyses. With coefficients of variation ranging from 12 to 28% for the timber analyses, many sources of variation are clearly present in the various laboratories' analyses. The adoption of standard analytical methods in conjunction with a thorough quality assurance programme are necessary steps to limit variations and improve analytical performance. The r and R values (0.009 and 0.032% m/m Sn, respectively) calculated for 0.077–0.085% m/m Sn would be expected to decrease considerably when the next inter-laboratory trial on TBTO in timber is performed.

Clearly there is a strong case for all laboratories to enhance and strengthen their current quality assurance programmes and to be more critical of the results they produce.

References

1. van der Kerk, G. J. M., and Luijten, J. G. A., *J. Appl. Chem.*, 1954, **4**, 301.
2. Engberg, Å., *Analyst*, 1973, **98**, 137.
3. Corbin, H. B., *J. Assoc. Off. Anal. Chem.*, 1970, **53**, 140.
4. Marr, I. L., *Talanta*, 1975, **22**, 387.
5. Ihnat, M., *in* Cantle, J. E., *Editor*, "Techniques and Instrumentation in Analytical Chemistry—Volume 5. Atomic Absorption Spectroscopy," Elsevier, Amsterdam, 1982.
6. British Standard 5666, Part 7, British Standards Institution, London, 1980.
7. Beaumont, A. G., and Mackay, C. A., *Int. Pest Control*, 1974, **16**, 8.
8. Ruddick, J. N. R., 10th Annual Meeting of the International Research Group on Wood Preservation, Working Group III, Preservatives and Methods of Treatment, Document No. IRG/WP/3125 Scotland, 1978.
9. Ishii, Y., Kawamura, H., and Yagi, S., *Bunseki Kagaku*, 1968, **17**, 3.
10. Williams, A. I., *Analyst*, 1973, **98**, 233.
11. Marr, I. L., and Anwar, J., *Analyst*, 1982, **107**, 260.
12. Gibson, J. H., Grossman, W. E. L., and Cooke, W. D., *Anal. Chem.*, 1963, **35**, 266.
13. Harrison, W. W., and Juliano, P. O., *Anal. Chem.*, 1969, **41**, 1016.
14. Headridge, J. B., and Sowerbutts, A., *Analyst*, 1972, **97**, 442.
15. Henshaw, B. G., and Williams, N., *J. Inst. Wood Sci.*, 1976, **7**, 18.
16. Freeland, G. N., and Hoskinson, R. M., *Analyst*, 1970, **95**, 579.
17. Plum, H., and Landsiedel, H., *Holz Roh Werkst.*, 1980, **38**, 461.
18. Herold, B., and Droege, K. H., *Fresenius Z. Anal. Chem.*, 1969, **245**, 295.

19. Henshaw, B. G., Morgan, J. W. W., and Williams, N. W., *J. Chromatogr.*, 1975, **110**, 37.
20. Ohlsson, S. V., and Hintze, W. W., *J. High Resolut. Chromatogr. Chromatogr. Commun.*, 1983, **6**, 89.
21. Australian Standard 1607, Standards Association of Australia, 1974.
22. Tonge, B. L., *J. Chromatogr.*, 1965, **19**, 182.
23. Kojima, S., *Analyst*, 1979, **104**, 660.
24. Williams, D. J., and Price, J. W., *Analyst*, 1964, **89**, 220.
25. Youden, W. J., "Statistical Methods for Chemists," Wiley, New York, 1951.
26. Mandel, J., "Statistical Analysis of Experimental Data," Wiley, New York, 1964.
27. Uriano, G. A., and Gravatt, C. C., *CRC Crit. Rev. Anal. Chem.*, 1977, **6**, 361.
28. New Zealand Timber Preservation Authority Specifications, New Zealand Forest Service, New Zealand, 1986.
29. International Organisation for Standardisation 5725 1986(E). Precision of Test Methods—Determination of Repeatability and Reproducibility for a Standard Test Method by Interlaboratory Tests.
30. Box, G. E. P., Hunter, W. G., and Hunter, J. S., "Statistics for Experimenters," Wiley, New York, 1978, pp. 232–235.
31. Morgan, J. W. W., and Purslow, D. F., *Rec. Ann. Conv. Br. Wood Preserv. Assoc.*, 1973, 173.
32. Dux, J. P., "Handbook of Quality Assurance for the Analytical Chemistry Laboratory," Van Nostrand Reinhold, New York, 1986.

Time-resolved Fluorimetric Detection of Terbium-labelled Deoxyribonucleic Acid Separated by Gel Electrophoresis

Steven S. Saavedra* and Enrico G. Picozza

Perkin-Elmer Corporation, 761 Main Avenue, Norwalk, CT 06859, USA

Deoxyribonucleic acid (DNA) was reacted with a strong chelating agent and labelled with terbium, yielding a highly fluorescent conjugate with a lifetime of 1.5 ms. When a pulsed source and gated detection electronics were employed, the long-lived decay allowed effective discrimination against background fluorescence and scattered excitation. Detection limits should therefore be signifcantly improved in comparison with covalent labels with fluorescence lifetimes in the nanosecond regime or stains such as ethidium bromide. The conjugate is very stable, remaining fluorescent on dilution and in an electric field at elevated temperatures (60 °C), conditions typically encountered during polyacrylamide gel electrophoresis. As an enhancement solution is not required to develop the fluorescence, this system could be utilised in situations where on-line detection is desirable. Although only DNA was labelled, the method is equally applicable to ribonucleic acid.

Keywords: *Time-resolved fluorescence; gel electrophoresis; nucleic acids; deoxyribonucleic acid detection; terbium chelate*

The detection of nucleic acids at trace levels is required in many areas of biotechnology and is performed conventionally using radioisotopes. However, the problems associated with the cost, instability, handling and disposal of ^{32}P-labelled reagents have created an interest in alternative detection strategies. Enzyme-catalysed colour development is one such alternative.[1–4] However, this group of methods cannot rival assays employing radioactively labelled probes in either sensitivity or ease of performance.

A number of methods for detecting nucleic acids based on fluorescence emission have been developed.[5–9] Several of the most widely used involve staining with a dye such as ethidium bromide[5]; however, the detection limits cannot approach those of autoradiography due to background emission from the unbound dye. Elimination of the background problem due to free dye can be achieved by covalent modification of the nucleic acid with a fluorescent tag followed by separation of the unreacted label. With an appropriate choice of fluorophore and optimisation of the optical train, sensitivities comparable to those of radioisotopic detection are possible. Several workers[10–14] have employed this approach for the on-line detection of deoxyribonucleic acid (DNA) sequences during polyacrylamide gel electrophoresis (PAGE). A drawback of this application is that the gel is a source of significant scattering and background fluorescence.

An alternative detection scheme which is theoretically more sensitive than autoradiography is time-resolved fluorimetry.[15–17] In this method, a chelated lanthanide metal with a long radiative lifetime is attached to the molecule of interest; pulsed excitation combined with a gated detection system allows for effective discrimination against short-lived background emission. Syvanen et al.[18] have demonstrated the utility of this approach for quantifying DNA hybrids via a europium-labelled antibody. In another paper, biotinylated DNA was measured in microtitre wells using Eu-labelled strepavidin.[19] A disadvantage of these types of assay is that the label must be washed from the probe and its fluorescence developed in a non-aqueous "enhancement" solution. The requirement for an enhancement solution prevents the use of this approach in situations where on-line detection is desirable.

We have developed an alternative means of detecting nucleic acids using time-resolved fluorimetry. Deoxyribonu-

cleic acid is reacted with a strong chelating agent and labelled with terbium, yielding a highly fluorescent conjugate with a long radiative lifetime. The conjugate is very stable and remains fluorescent on dilution and during gel electrophoresis. As an enhancement solution is not required to develop the fluorescence, this system could be utilised for on-line detection during PAGE.

Experimental

All materials and reagents were obtained from standard commercial sources. Plasmid pBR322 was purified by centrifugation on a caesium chloride - ethidium bromide gradient. The plasmid was then cleaved with *Hin*fI restriction enzyme following standard procedures.[20] The labelling adduct was prepared by reacting diethylenetriaminepentaacetic acid dianhydride (DTPAA) with *p*-aminosalicylate (pAS) according to the method of Bailey et al.[21] Briefly, sodium *p*-aminosalicylate dihydrate was dried overnight at 110 °C. Solutions of each of the reagents were prepared in dry dimethyl sulphoxide at 0.1 M; equimolar triethylamine was added to the DTPAA solution to facilitate dissolution. An equal volume of the pAS solution was added dropwise to the DTPAA solution followed by stirring for 60 min.

A 7-µl volume of the adduct reaction mixture was added to 150 µl of the plasmid digest (0.145 g l^{-1} of cleaved pBR322) and stirred at room temperature for 60 min. After storage overnight at 4 °C, 6.8 µl of 0.05 M TbCl₃ were added and the mixture was shaken and allowed to stand for 30 min. Excess of hydrolysed chelate was separated from the DNA - chelate conjugate by passing the mixture twice through a 16 × 1 cm column packed with Sephadex G25-150. The eluent buffer was 10 mM morpholine-4-propanesulphonic acid, pH 7.0. After each purification, the DNA-containing fractions were pooled and evaporated to dryness under vacuum.

The DNA concentration was determined by the measurement of the absorbance at 260 nm. The label concentration was determined by comparing the fluorescence of the purified conjugate with that of diethylenetriaminetetraacetic acid *p*-aminosalicylate (DTTA-pAS) complexed with Tb. The assumption inherent in this method is that the quantum yield of the conjugated label is equal to that of the free chelate. Correction for pAS absorption at 260 nm when measuring the DNA concentration was not necessary owing to the low pAS to base ratio. Spectral measurements were performed with a Perkin-Elmer 3840 UV - visible spectrophotometer and a

---

* Present address: Department of Biomedical Engineering, Duke University, Durham, NC 27706, USA.

Perkin-Elmer LS-5 spectrofluorimeter; the latter employed a pulsed source and gated detection electronics, permitting selective observation of the delayed emission. Unless stated otherwise, samples were excited at 260 nm and detected at 545 nm using 10-nm slits; the delay between excitation and detection was 0.1 ms while the gate was 6 ms.

The quantum yield of the free chelate was calculated using the relationship

$$\frac{Q_c}{Q_{qs}} = \frac{F_c A_c}{F_{qs} A_{qs}} \cdot P$$

where Q_c and Q_{qs} are the quantum yields of the free chelate and quinine sulphate, respectively, F_c and F_{qs} are the areas under the corrected emission spectra and A_c and A_{qs} are the absorbances at the respective excitation wavelengths. The value of Q_{qs} was taken to be 0.59 for excitation at 347 nm.[22] The quinine sulphate fluorescence was measured conventionally while the chelate emission was measured with the delay and gate settings given above. Multiplication by the phosphorimeter factor, P, corrects for measurement of the standard and sample emissions under different instrumental conditions.[23]

Lifetimes were determined by measuring the emission intensity as a function of the time delay between excitation and detection, keeping the gate constant. The data were fitted to the best single exponential of the form $I = I_0 e^{-kt}$.

Labelled restriction fragments were electrophoresed on a 1.5 mm × 16 cm strip of 5% polyacrylamide gel in 89 mM Tris - borate buffer, pH 8.0. The system was run at 8 V cm^{-1} until the tracking dye (Bromophenol Blue) was approximately 2 cm from the bottom of the gel. The gel was then removed from the apparatus and transilluminated (Fotodyne, Model 3-3000) to locate the labelled DNA fragments. The portions of the gel containing the DTTA-pAS - Tb-labelled DNA (identified by the characteristic green emission) were cut out and placed individually in centrifuge tubes with 1 ml of de-ionised water. After storage at 4 °C for 6 d, the supernatants were separated from the gel fragments, diluted to a final volume of 1.5 ml and assayed for chelate emission.

Results

The preparation of a chelating adduct by the reaction of DTPAA with pAS was first described by Bailey et al.[21] Performing the reaction under anhydrous conditions with an equimolar ratio of DTPAA to pAS allowed the adduct to be conjugated subsequently to a second amine-containing molecule (in this instance, human serum albumin) via the remaining unreacted anhydride moiety. The protein - chelate conjugate exhibited a strong affinity for Tb, with which it formed a highly fluorescent energy-transfer complex.

In a similar fashion, we reacted diethylenetriaminetetraacetic acid monoanhydride p-aminosalicylate (DTTAA-pAS) sequentially with the HinfI digest of the pBR322 plasmid, then with TbCl$_3$. The product exhibited a bright green emission on UV illumination which could not be eliminated by exhaustive dialysis. The HinfI digestion of pBR322 generates staggered ends on ten fragments ranging
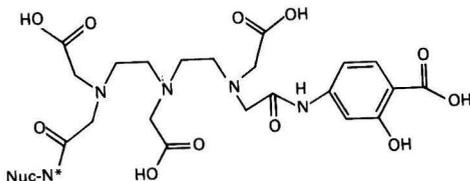
from 75 to 1631 base pairs in size; the sequence of single-stranded bases at each end is ANT, where N denotes any nucleotide and A and T are adenine- and guanine-containing nucleotides, respectively. We believe that the exocyclic amines on the exposed bases provide sites for attack by the monoanhydride adduct, forming an amide linkage. The expected structure is shown in Fig. 1.

Fluorescence excitation and emission spectra of the purified product are presented in Fig. 2. The emission spectrum is characteristic of the Tb^{3+} ion, with the maximum intensity occurring at 545 nm.[24] The excitation spectrum closely matches the absorption spectrum of pAS (also shown in Fig. 2); this is consistent with the contention that the Tb emission is not excited directly but is due to energy transfer from the salicylate group.[21,24] At these concentrations, the Tb fluorescence could not be detected in the absence of DTTA-pAS. Detection was also not possible in the presence of pAS and diethylenetriaminepentaacetic acid (DTPA), demonstrating that adduct formation is essential. Although single-stranded DNA (ssDNA) itself binds Tb and forms a fluorescent complex, this is not expected to contribute to the emission shown in Fig. 2 for the following reasons: (1) more than 99% of the DNA reacted with the adduct was double-stranded, which does not enhance the Tb fluorescence;(2) Tb is the limiting reagent in the synthesis, and the formation constant for ssDNA - Tb is approximately 10^6,[8,25] considerably less than that expected for either the DNA - chelate conjugate of the hydrolysed adduct (see below). This means that, essentially, none of the Tb should be available for complexation by the single-stranded portions of the cleaved pBR322; (3) the excitation spectrum of the ssDNA - Tb complex is very different to that shown in Fig. 2.[8,26]

The extent of the incorporation of the chelate in the purified conjugate was calculated to be 6.3 pmol per microgram of DNA. From a knowledge of the base composition of the pBR322 cleavage sites,[27] and assuming complete cleavage, the degree of substitution at the exposed bases was calculated to be 48%.

The quantum yield of the free chelate was calculated to be 0.10 at room temperature, which is appreciable for such a long-lived fluorophore; the molar absorptivity is 17 900 l mol^{-1} cm^{-1} at 260 nm and 7900 l mol^{-1} cm^{-1} at 310 nm. We predict that the spectral properties of the chelate coupled to DNA will be similar. Time-resolved emission measurements of the free chelate and the DNA - chelate conjugate yielded fluorescence lifetimes of 1.7 and 1.5 ms, respectively. Hence, when gated electronics were employed to discriminate against short-lived scattering and background fluorescence, detection of the chelate was possible at very low levels. An emission scan (2 nm s^{-1}) of a 500 pM solution of the free chelate using the standard conditions given above gave a signal to noise ratio of 10 at 545 nm.

Fig. 1. Schematic diagram of the presumed structure of the product formed from the reaction of the diethylenetriaminetetraacetic acid monoanhydride p-aminosalicylate adduct (DTTAA-pAS) with ssDNA; the amide linkage on the left is formed with an exocyclic amine (N*) on deoxyribonucleotides containing adenine, guanine or cytosine
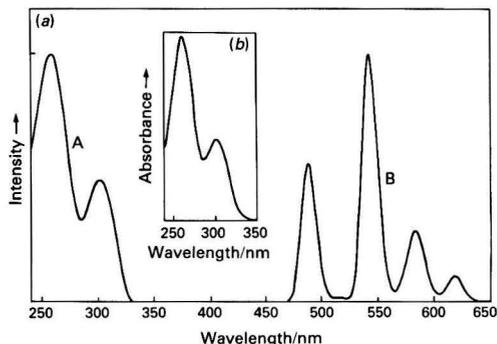
Fig. 2. (a) Fluorescence spectra of labelled pBR322 restriction fragments: A, excitation spectrum; B, emission spectrum. Instrumental parameters are given in the text. (b) Absorption spectrum of pAS shown for comparison

The stability constant for the complex formed between DTPA and Tb^{3+} is approximately 10^{23}.[28] The stability constants for the DTTA-pAS - Tb complex and the DNA - chelate conjugate are expected to be smaller, owing to the loss of one and two carboxyl groups, respectively in the formation of the amide linkages.[29] This was confirmed by measuring the conditional stability constant of the DTTA-pAS - Tb complex at pH 8.5 by a competitive exchange method.[30] A value of 10^{17} was obtained. Although the affinity of the DNA - chelate conjugate for Tb^{3+} is expected to be less, it is probably greater than 10^{10} because the metal could not be removed by exhaustive dialysis.

The Tb-labelled restriction fragments were subjected to PAGE to determine whether the integrity of the complex could be maintained at elevated temperatures in an electric field. Transillumination of the gel at room temperature after PAGE permitted detection of the characteristic green emission of the conjugated DNA. The DNA bands were extracted from the gel as described above and the chelate content was quantified by time-resolved fluorimetry. The total fluorescence recovered from the gel corresponded to 75 pmol of chelate (12 µg of DNA), representing 58% of the amount applied to the gel.

The effect of temperature on the quantum efficiency of the free chelate was examined in a separate experiment. The DTTA-pAS - Tb complex was added to an 8% polyacrylamide gel before polymerisation; cross-linking was allowed to take place in a standard 1-cm quartz cuvette. Fluorescence spectra acquired with the cuvette thermostated at 25 and 60 °C showed that the fluorescence intensity of the free chelate decreased by approximately 80% for this temperature increase.

Discussion

The objective of this work was to demonstrate the feasibility of detecting DNA on-line during PAGE by time-resolved fluorimetry using a lanthanide metal tag. Terbium chloride has been employed previously as a stain for identifying ssDNA, single-stranded ribonucleic acid (ssRNA) and double-stranded (ds) RNA in gels after electrophoresis.[8,9] Terbium is bound by the phosphate moieties in the nucleic acids and forms an energy-transfer complex with the base. The fluorescence lifetimes of these complexes are of the order of milliseconds (data not given), but the conditional stability constants are reported to be approximately 10^{6}.[6,8,25] small enough to require that the metal be present in excess. We have found that an excess of Tb^{3+} associates with weakly absorbing components in polyacrylamide gels, resulting in low levels of background fluorescence. In addition, a large (millimolar) excess of $TbCl_3$ added to the gel before electrophoresis causes the DNA fragments to clump at the top of the gel, retarding migration. These conditions prevent the use of $TbCl_3$ for on-line detection of trace amounts of nucleic acids. Hence we sought to label DNA covalently with a fluorescent Tb chelate having a high association constant so that the background problem caused by unbound Tb would be eliminated. The chelate described by Bailey et al.[21] exhibits the desired properties and was used in this work.

The DNA - chelate conjugate prepared here has a fluorescence lifetime similar to those of the complexes formed between Tb^{3+} and nucleic acids, but exhibits a much higher affinity for the metal. Although only DNA was labelled, the method is equally applicable to RNA. When a pulsed source and gated detection electronics are employed, the long-lived decay permits effective discrimination against the short-lived background. The high stability of the conjugate complex eliminates the long-lived background caused by unbound Tb^{3+}. Detection limits for this label should therefore be significantly improved in comparison with covalent labels with fluorescence lifetimes in the nanosecond regime[15] or stains

such as ethidium bromide or $TbCl_3$.[5,8] In fact, a study by Wieder[15] has shown that the sensitivity of time-resolved fluorescence techniques rivals, and potentially exceeds, that of radioisotopic detection methods.

The high affinity of the DNA - chelate conjugate for Tb^{3+} is maintained in an electric field at elevated temperatures (60 °C), conditions typically encountered during PAGE. The Tb label could therefore be employed for on-line detection of DNA or RNA during PAGE. Current on-line detection methods for nucleic acids based on covalent fluorescent labels have the disadvantage that the gel is a source of significant scattering and background fluorescence, necessitating the use of laser sources and sophisticated optical trains.[10-14] The use of the Tb label described here would largely overcome this disadvantage, resulting in equivalent or lower detection limits at reduced cost.

Finally, we do not consider the procedure described here to be a practical method for detecting restriction fragments and would not recommend its use as a general analytical method. It was employed solely to demonstrate the feasibility of detecting DNA fragments by time-resolved fluorimetry during PAGE. In view of this, we have not reported detection limits for actual samples. The measurement of meaningful detection limits requires the construction of an apparatus for on-line time-resolved fluorimetry and this will be the subject of a future paper.

References

1. Langer, P. R., Waldrop, A. A., and Ward, D. C., *Proc. Natl. Acad. Sci. USA*, 1981, **78**, 6633.
2. Leary, J. J., Brigati, D. J., and Ward, D. C., *Proc. Natl. Acad. Sci USA*, 1983, **80**, 4045.
3. Tchen, P., Fuchs, R. P. P., Sage, E., and Leng, M., *Proc. Natl. Acad. Sci. USA*, 1984, **81**, 3466.
4. Renz, M., and Kurz, C., *Nucleic Acids Res.*, 1984, **12**, 3435.
5. Le Pecq, J.-B., and Paoletti, C., *Anal. Biochem.*, 1966, **17**, 100.
6. Kapuscinski, J., and Skoczylas, B., *Anal. Biochem.*, 1977, **83**, 252.
7. Labarca, C., and Paigen, K., *Anal. Biochem.*, 1980, **102**, 344.
8. Topal, M. D., and Fresco, J. R., *Biochemistry*, 1980, **19**, 5531.
9. Al-Hakeem, M., and Sommer, S. S., *Anal. Biochem.*, 1987, **163**, 433.
10. Smith, L. M., Fung, S., Hunkapillar, M. W., Hunkapillar, T. J., and Hood, L. E., *Nucleic Acids Res.*, 1985, **13**, 2399.
11. Smith, L. M., Sanders, J. Z., Kaiser, R. J., Hughes, P., Dodd, C., Connel, C. R., Heiner, C., Kent, S. B. H., and Hood, L. E., *Nature (London)*, 1986, **321**, 674.
12. Ansorge, W., Sproat, B. S., Stegemann, J., and Schwager, C., *J. Biochem. Biophys Methods*, 1986, **13**, 315.
13. Ansorge, W., Sproat, B. S., Stegemann, J., Schwager, C., and Zenke, M., *Nucleic Acids Res.*, 1987, **15**, 4593.
14. Prober, J. M., Trainor, G. L., Dam, R. J., Hobbs, F. W., Robertson, C. W., Zagursky, R. J., Cocuzza, A. J., Jensen, M. A., and Baumeister, K., *Science*, 1987, **238**, 336.
15. Weider, I., in Knapp, W., Holubar, K., and Wick, G., Editors, "Immunofluorescence and Related Staining Techniques," Elsevier Biomedical Press, Amsterdam, 1978, p. 67.
16. Soini, E., and Kojola, H., *Clin. Chem.*, 1983, **29**, 65.
17. Ekins, R. P., and Dakubu, S., *Pure Appl. Chem.*, 1985, **57**, 473.
18. Syvanen, A.-C., Tchen, P., Ranki, M., and Soderlund, H., *Nucleic Acids Res.*, 1986, **14**, 1017.
19. Dahlen, P., *Anal. Biochem.*, 1987, **164**, 78.
20. Maniatis, T., Fritsch, E. F., and Sambrook, J., "Molecular Cloning: A Laboratory Manual," Cold Spring Harbor Laboratory, Cold Spring Harbor, New York, 1982, p. 100.
21. Bailey, M. P., Rocks, B. F., and Riley, C., *Analyst*, 1984, **109**, 1449.
22. Rhys Williams, A. T., Winfield, S. A., and Miller, J. N., *Analyst*, 1983, **108**, 1067.
23. Parker, C. A., "Photoluminescence of Solutions," Elsevier, Amsterdam, 1968, p. 272.

24. Sinha, A. P. B., *Spectrosc. Inorg. Chem.*, 1971, **2**, 255.
25. Haertle, T., Augustynika, J., and Guschlbauer, W., *Nucleic Acids Res.*, 1981, **9**, 6191.
26. Yonuschot, G., and Mushrush, G. W., *Biochemistry*, 1975, **14**, 1677.
27. Maniatis, T., Fristch, E. F., and Sambrook, J., "Molecular Cloning: A Laboratory Manual," Cold Spring Harbor Laboratory, Cold Spring Harbor, New York, 1982, p. 499.
28. Harder, R. and Chaberek, S., *J. Inorg. Nucl. Chem.*, 1959, **11**, 197.
29. Brechbield, M. W., Gansow, O. A., Atcher, R. W., Schlom, J., Esteban, J., Simpson, D. E., and Colcher, D., *Inorg. Chem.*, 1986, **25**, 2772.
30. Saavedra, S. S., unpublished work.

Fluorimetric Determination of Aluminium in Serum

Yukio Suzuki

Environmental Pollution Control Center of Kobe City, 5-1-6, Kano-cho, Chuo-ku, Kobe-shi, Hyogo 650, Japan

Sakingo Imai and Teruo Kamiki

Public Health Research Institute of Kobe City, 6–4, Minatojimanakamachi, Chuo-ku, Kobe-shi, Hyogo 650, Japan

A convenient fluorimetric method for the routine determination of aluminium in serum has been developed using lumogallion [4-chloro-3-(2,4-dihydroxyphenylazo)-2-hydroxybenzene-1-sulphonic acid]. Losses of aluminium during deproteinisation of the serum were prevented by treatment with a combination of 20 or 30% m/V trichloroacetic acid (TCA) and 5% m/V TCA. Iron(III) was removed by extraction into chloroform with capriquat (methyltrioctylammonium chloride) as an Fe^{3+} - lumogallion - capriquat ternary complex. The interference from Cu^{2+} was eliminated by using thiosulphate as a masking agent. The detection limit was 3.6 ng ml^{-1} and the calibration graph was linear up to 1.4 µg ml^{-1} of aluminium. Using the proposed method, the average concentration of aluminium in the serum of healthy subjects was found to be 6.8 ng ml^{-1}, in agreement with values reported in the literature.

Keywords: *Serum; aluminium determination; fluorimetry; routine analysis*

The importance of monitoring aluminium concentrations in the blood of patients undergoing haemodialysis has been realised because of the suspicion that aluminium intoxication is responsible for encephalopathy, oesteopathy and Alzheimer's disease.[1-3] Graphite furnace atomic absorption spectrometry[4] and inductively coupled plasma atomic emission spectrometry,[5] which are excellent methods for the determination of aluminium in serum, are usually used. In the fluorimetric method, the serum has to be deproteinised and hence the analytical procedure is cumbersome. The method has, therefore, received little attention; also, the deproteinisation step increases the possibility of contamination and of a loss of precision. However, fluorimetry is a simple and sensitive technique and does not require expensive apparatus. In addition, it is not necessary to employ a skilled operator.

The aim of this work was to develop a fluorimetric method for the determination of aluminium that could be used for routine analysis in clinical laboratories. This paper describes a convenient method, using lumogallion [4-chloro-3-(2,4-dihydroxyphenylazo)-2-hydroxybenzene-1-sulphonic acid] as a reagent, which is highly sensitive to aluminium.

Experimental

Apparatus

An Hitachi Model 204 fluorescence spectrophotometer with a 150-W xenon lamp was used. The working conditions were as follows: excitation wavelength, 490 nm; emission wavelength, 570 nm; lamp current, 7 A; and sensitivity, ×1. An Hitachi Model 05P-21B centrifuge and a Simazuseisakusho Model U 240 spectrophotometer were also used.

Prevention of Contamination

Care was taken in sample storage, reagent preparation and pre-treatment of equipment in order to prevent contamination. Serum samples were stored in 10-ml calibrated polypropylene test-tubes and all reagent solutions were stored in polycarbonate vessels. The test-tubes and the vessels were washed with 20% V/V nitric acid and de-ionised, doubly distilled water.[6] Commercially available reagents, high-purity grade, were used as received. The blank value throughout the analytical procedure was equivalent to about 90 ng of aluminium. This high value was mainly due to contamination

by the reagents. However, the variation in the values was 1.8 ng as the standard deviation, which is small enough to permit the determination of aluminium at the nanogram level. When a new reagent solution is prepared, the blank value should be checked. Further, the blank value should be shown to be free from contamination by the equipment by determining the blank value again immediately before the analysis.

Procedure

One- and 2-ml volumes of serum are placed in separate test-tubes. To the former, 1 ml of 20% m/V trichloroacetic acid (TCA) is added and to the latter, 1 ml of 30% m/V TCA in order to deproteinise the serum. The mixture is stirred for 1 min with a vortex-type mixer, centrifuged for 5–10 min at 4000 rev min^{-1} and the supernatant transferred into another test-tube. One millilitre of 5% m/V TCA is then pipetted into the test-tube containing the precipitate. After stirring vigorously, the mixture is centrifuged for 10 min at 4000 rev min^{-1} and the supernatant thus obtained is combined with the first supernatant.

Two millilitres of 0.2 M potassium hydrogen phthalate are added to the supernatant as a buffering agent. When the volume of serum taken is 1 ml, 0.6 ml of 2 M sodium hydroxide solution is added and when it is 2 ml, 0.8 ml of the sodium hydroxide solution is added. The pH will then be in the range 3.8–4.8. These test solutions are mixed with 0.5 ml of 2.5% m/V sodium thiosulphate solution and the mixture is allowed to stand for 10 min, after which 0.5 ml of 0.1% m/V lumogallion solution is added. The volume is made up to 10 ml by the addition of doubly distilled water and the mixture is heated at 70 °C for 5 min. The reaction mixture is cooled with water and transferred into a 100-ml separating funnel. Excess of lumogallion and the Fe^{3+} - lumogallion complex are extracted with 10 ml of 1.25% m/V capriquat - chloroform. The aqueous layer is allowed to stand until it becomes clear and the sample is then analysed by the proposed method.

A control solution and a solution employed for constructing the calibration graph are prepared using an aluminium standard solution (1 µg ml^{-1}). When the volume of serum taken is 1 ml, 0.8 ml of 2 M sodium hydroxide solution is added and when it is 2 ml, 1.1 ml of the sodium hydroxide solution are added.
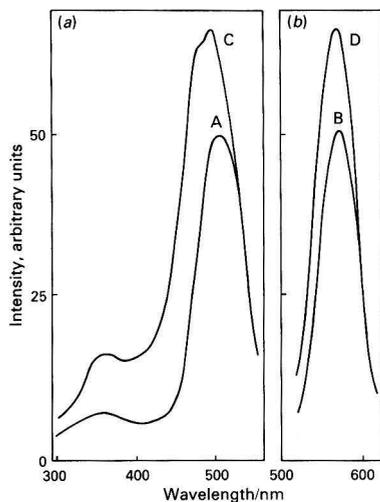
Fig. 1. (*a*) Excitation and (*b*) emission spectra. A and B, Reaction mixture of aluminium (1 μg ml^{-1}) and lumogallion; C and D, aluminium - lumogallion complex
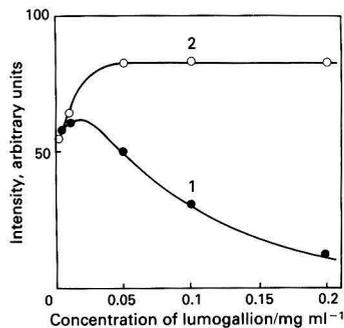
Fig. 2. Relationship between the concentration of lumogallion and the fluorescence intensity. 1, Reaction mixture of aluminium (1 μg ml^{-1}) and lumogallion; 2, aluminium - lumogallion complex. The fluorescence intensity of the reaction mixture was 50 at a lumogallion concentration of 0.05 mg ml^{-1}

Fig. 3. Extractability of the aluminium - lumogallion complex into capriquat - chloroform. 1, In the absence of TCA; and 2, [TCA] = 25 mg ml^{-1}. [Aluminium] = 1 μg ml^{-1}. For extraction with 100 mg of capriquat the recovery was set to 100%

Results and Discussion

Spectra of the Aluminium - Lumogallion Complex

The reaction mixture gave peaks at 500 and 575 nm in the excitation and emission spectra, respectively. The spectrum of the aluminium - lumogallion complex could be obtained by the ion-pair extraction of excess of lumogallion into capriquat - chloroform. The excitation and emission spectra of the chelate are shown in Fig. 1. The peak at 500 nm in the excitation spectrum of the reaction mixture was shifted to a shorter wavelength, 490 nm, in the corresponding spectrum of the aluminium - lumogallion complex. In addition, a discernible shoulder was present at 475 nm. The peak at 575 nm in the emission spectrum of the reaction mixture was also shifted to a shorter wavelength of 570 nm.

Amounts of Reagents Required

The final concentration of TCA in each sample was presumed to be different because of the consumption of TCA during the deproteinisation step. The concentration of TCA had no effect on the fluorescence intensity in the range 10–40 mg ml^{-1}

and hence the final concentration of TCA did not have to be kept constant prior to measurement.

The relationship between the concentration of lumogallion and the fluorescence intensity is shown in Fig. 2. The fluorescence intensity curve for the reaction mixture (curve 1) exhibited a maximum at a lumogallion concentration of *ca.* 0.01 mg ml^{-1}. Because of the absorption of exciting light by lumogallion itself, the fluorescence intensity decreased as the amount of lumogallion increased. The fluorescence intensity of the curve obtained by removing the excess of lumogallion with 125 mg of capriquat (curve 2) was greater than that of the reaction mixture. At a concentration of lumogallion greater than 0.05 mg ml^{-1}, the intensity of curve 2 reached a maximum and remained constant. Therefore, lumogallion should be used at a concentration of more than 0.05 mg ml^{-1}.

The ion-pair extraction with capriquat was carried out in order to remove excess of lumogallion and to eliminate the interference from Fe^{3+}. The aluminium - lumogallion complex must not be extracted into capriquat - chloroform. The curve for the extraction of the chelate is shown in Fig. 3. The presence of large amounts of anions such as trichloroacetate influenced the extractability of the aluminium - lumogallion complex; the complex was not extracted into chloroform containing up to 125 mg of capriquat in the absence of TCA. However, at a TCA concentration of 25 mg ml^{-1}, the chelate was not extracted into the chloroform layer even with 300 mg of capriquat. The formation of an ion-pair complex between the chelate and capriquat appears to be suppressed further with an increase in the concentration of TCA for a given amount of capriquat. As the final concentration of TCA was presumed to be different in each sample, 125 mg of capriquat should be used for the extraction. On the other hand, it was found that, irrespective of the TCA concentration in the reaction mixture, 0.5 mg of lumogallion was completely removed with 100 mg of capriquat in the pH range 2.2–6.4.

Reaction Conditions

The effect of temperature on the reaction of lumogallion with aluminium was investigated at 50 and 70 °C. About 20 min were required to obtain the maximum fluorescence intensity at 50 °C. At 70 °C, the fluorescence intensity reached a maximum and remained constant in less than 5 min.

The influence of pH on the fluorescence intensity of the aluminium - lumogallion complex is shown in Fig. 4. The fluorescence intensity reached a maximum and remained constant in the pH range 3.8–4.8. Changes in the TCA concentration in the sample had no influence on the fluorescence intensity. As the pH before and after the extraction with capriquat was very similar, it was not necessary to adjust the pH after the extraction.

Interferences

The proposed method was free from interferences from the principal ions found in human serum as shown in Table 1.
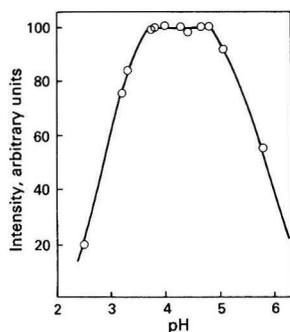
Fig. 4. Effect of pH on the fluorescence intensity of the aluminium - lumogallion complex. [Aluminium] = 1 µg ml^{-1}. The fluorescence intensity was 100 at pH 4.3

Table 1. Interference study

Ion				Added/ µg	Aluminium recovery ± SD, %*
Cr^{6+}	..	..	..	0.2	99.0 ± 3.5
Zn^{2+}	..	..	..	2	101.0 ± 1.8
Co^{2+}	..	..	..	0.2	98.4 ± 1.8
Ni^{2+}	..	..	..	0.2	100.3 ± 3.5
Ca^{2+}	..	..	..	400	100.0 ± 0.7
Na^{+}	..	..	..	7000	99.9 ± 2.0
P^{5+}	..	..	..	80	99.0 ± 0.5
V^{5+}	..	..	..	0.2	99.3 ± 0.9
Sn^{2+}	..	..	..	0.2	99.9 ± 2.1
Mg^{2+}	..	..	..	130	99.1 ± 3.5

* Four measurements were made on each set. 100 ng of aluminium were used. Values given are average recoveries ± standard deviation.
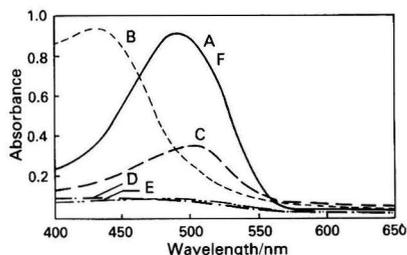
Fig. 5. Absorption spectra of the lumogallion complexes of aluminium, Fe^{3+} and Cu^{2+}. A, Aluminium - lumogallion; B, Fe^{3+} - lumogallion; C, Cu^{2+} - lumogallion; D, in the absence of Fe^{3+} - lumogallion; E, in the absence of Cu^{2+} - lumogallion; and F, aluminium - lumogallion solution treated with Na$_2$S$_2$O$_3$. [TCA] = 35 mg ml^{-1}

Iron(III) and Cu^{2+} formed coloured chelates with lumogallion having absorption maxima at 430 and 500 nm, respectively. Because these wavelengths were close to that of the aluminium - lumogallion complex (absorption maximum at 490 nm), the fluorescence intensity of the latter decreased due to the absorption of exciting light by the complexes of lumogallion with Fe^{3+} and Cu^{2+}. The chelation of Fe^{3+} increased markedly with decreasing acidity in the pH range 2–5. The Cu^{2+} - lumogallion complex formed readily in the pH range 3–5.

The Fe^{3+} - lumogallion complex was observed to form a ternary complex with capriquat easily. The extractability of the Fe^{3+} - lumogallion complex was not influenced by changes in the TCA concentration up to 35 mg ml^{-1}. A decrease in the extractability occurred with increasing acidity at a pH of less than 4.0. However, at a pH greater than 3.8, the Fe^{3+} -

Table 2. Interference from Fe^{3+} and Cu^{2+}

Ion		Added/ µg	Aluminium recovery(A), ± SD, %*	Aluminium recovery(B), ± SD, %*
Fe^{3+}	..	2.5	91.7 ± 2.1	100.4 ± 1.5
Fe^{3+}	..	5.0	82.2 ± 1.9	98.3 ± 1.1
Cu^{2+}	..	1.5	91.2 ± 1.7	100.7 ± 2.7
Cu^{2+}	..	3.0	86.8 ± 3.0	99.0 ± 3.1

* (A) Before the elimination of the interference; (B) after the elimination of the interference. 100 ng of aluminium were used. Four measurements were made on each set.

Table 3. Aluminium recovery

Aluminium added/ ng	Volume of serum/ ml	Aluminium found/ ng*	Recovery, %*	CV, %†
25	1.0	24.0	95.8	7.0
50	1.0	49.9	99.7	6.8
100	1.0	97.9	97.9	3.6
50	2.0	49.0	97.9	6.9
100	2.0	97.9	97.9	4.0

* Average of four measurements.
† Coefficient of variation of recovery.
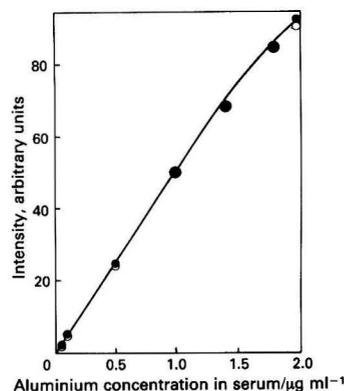
Fig. 6. Calibration graph. [TCA]: ○, 25; and ●, 35 mg ml^{-1}. The fluorescence intensity was 50 at an aluminium concentration of 0.1 µg ml^{-1}

lumogallion complex was extracted into the chloroform layer almost completely. Absorption spectra of the complexes of lumogallion with aluminium, Fe^{3+} and Cu^{2+}, the concentrations of which were 1 µg ml^{-1} in each sample, were obtained by extraction with capriquat. The results are shown in Fig. 5. The absorption spectrum of the aluminium - lumogallion complex was obtained by removing the excess of lumogallion with 125 mg of capriquat. The absorption spectrum of the Fe^{3+} - lumogallion solution containing a small amount of lumogallion was obtained by using 25 mg of capriquat. The Fe^{3+} - lumogallion complex was removed by using 125 mg of capriquat. The Cu^{2+} - lumogallion complex hardly formed an ion-pair complex with 125 mg of capriquat, cf. aluminium in the presence of large amounts of TCA.

The reaction of Cu^{2+} with S$_2$O$_3^{2-}$ in acidic solution was used to eliminate the interference from Cu^{2+}. The absorption due to the Cu^{2+} - lumogallion complex was decreased markedly by the addition of 0.5 ml of 2.5% m/V sodium thiosulphate solution in the pH range 3.8–4.8. The addition of 0.5 ml of 2.5% m/V thiosulphate solution had no influence on the formation of the aluminium - lumogallion complex. On the other hand, the interference from Fe^{3+} could not be eliminated by S$_2$O$_3^{2-}$.

Table 4. Measurement of serum aluminium in 15 healthy subjects

No.	Sex	Age/ years	Aluminium concentration/ $ng\ ml^{-1}$
1	M	49	7.5
2	F	58	6.6
3	M	49	3.8
4	M	59	3.8
5	F	58	5.1
6	F	52	7.5
7	F	48	8.1
8	F	54	7.2
9	M	48	6.4
10	F	18	4.2
11	F	18	11.1
12	F	18	3.8
13	F	48	5.1
14	F	38	9.4
15	M	38	13.2

Average: 6.8
Standard deviation: 2.8

Interferences from up to 5 µg of Fe^{3+} and 3 µg of Cu^{2+}, the average concentrations of which in human serum are now generally recognised to be 1.3 and 1.1 µg ml^{-1}, respectively,[7] could be eliminated completely as shown in Table 2.

Recovery

In order to prevent a decrease in the aluminium recovery caused by the deproteinisation step, the operating conditions were investigated. Centrifugation at 4000 rev min^{-1} for 5–10 min was found to be sufficient to remove all of the precipitate. The recovery of aluminium was determined by using 1 or 2 ml of serum to which 100 µl of an aluminium standard solution containing 1 µg of aluminium had been added. When 1 ml of 20% m/V TCA was used for the treatment of 1 ml of serum, the aluminium recovery was 79.4% ($n = 4$). When the precipitate obtained was washed further with 1 ml of 5% m/V TCA, the recovery increased to 95.8% ($n = 4$). Two washings with 5% m/V TCA only increased the recovery a little further [96.8% ($n = 4$)]. For the deproteinisation step, the treatment with a combination of 20 and 5% m/V TCA gave an aluminium recovery of about 80% for 2 ml of serum. When the TCA concentration was increased from 20 to 30% m/V, more than 95% of the aluminium could be recovered based on the addition of 100 ng of the metal. Recoveries for the addition of less than 100 ng of aluminium to 1 and 2 ml of serum are shown in Table 3.

Calibration Graph and Detection Limit

An example of a calibration graph is shown in Fig. 6. The calibration graph was linear for aluminium concentrations in serum ranging from 0 to 1.4 µg ml^{-1} regardless of the TCA concentration. The detection limit, calculated as the amount equivalent to twice the standard deviation of the blank, was 3.6 ng ml^{-1}.

Aluminium Concentration in Serum

One- and 2-ml volumes of pooled serum from a healthy subject were analysed using the proposed procedure in order to confirm the precision of the measurements. The concentrations of aluminium found were 7.0 ± 1.8 [1 ml of serum ($n = 5$)] and 7.1 ± 1.2 ng ml^{-1} [2 ml of serum ($n = 5$)]. The values show excellent agreement.

Two types of pooled serum from a healthy subject were also analysed. The aluminium concentrations were found to be 8.5 ± 1.5 (sample volume = 1 ml, $n = 10$) and 6.7 ± 0.9 ng ml^{-1} (sample volume = 2 ml, $n = 10$). These average concentrations are close to the normal values reported for aluminium in serum.[5,8,9]

The method was applied to the measurement of aluminium in the serum of healthy subjects and in the serum of patients with Alzheimer's disease and those undergoing haemodialysis. The concentrations of aluminium found were 6.8 ± 2.8 ($n = 15$), 25.8 ± 7.8 ($n = 10$) and 48.3 ± 44.2 ng ml^{-1} ($n = 35$), respectively. The results show that the average concentration of aluminium in the serum of patients with Alzheimer's disease and those undergoing haemodialysis is significantly higher than in healthy subjects. Table 4 gives the results for the measurement of serum aluminium in 15 healthy subjects. Using the proposed method, ten samples could be analysed in 2–3 h.

References

1. Robertson, J. A., Felsenfeld, A. J., Haygood, C. C., Wilson, P., Clarke, C., and Llach, F., *Kidney Int.*, 1983, **23**, 327.
2. Sideman, S., and Manor, D., *Nephron*, 1982, **31**, 1.
3. Mckinney, T. D., Basinger, M., Dawson, E., and Jones, M. M., *Nephron*, 1982, **32**, 53.
4. Brown, S., Bertholf, R. L., Wills, M. R., and Savory, J., *Clin. Chem.*, 1984, **30**, 1216.
5. Maurs, Y., and Allain, P., *Anal. Chem.*, 1985, **57**, 1706.
6. Iwasa, A., Yonemoto, T., Matsubara, I., and Nakagawa, K., *Bunseki Kagaku*, 1987, **36**, T113.
7. Kobori, K., Mise, Y., Takeda, H., Sakakibara, H., Maruyama, K., and Kobayashi, T., *Eisei Kensa*, 1983, **33**, 119.
8. Bertholf, R. L., Brown, S., Renoe, B. W., Wills, M. R., and Savory, J., *Clin. Chem.*, 1983, **29**, 1087.
9. Buratti, M., Caravelli, G., Calzaferri, G., and Colombi, A., *Clin. Chim. Acta*, 1984, **114**, 253.

Flow Injection Sample-to-standard Additions Method. Spectrophotometric Determination of Hydrochloric Acid and Orthophosphate

Yecheskel Israel and Ramon M. Barnes

Department of Chemistry, Lederle Graduate Research Center, University of Massachusetts, Amherst, MA 01003-0035, USA

Conventional flow injection (FI) has been utilised for the development of the sample-to-standard additions method as an alternative to the reverse FI standard additions method. An equation has been derived for the proposed method, allowing the calculation of sample concentration from two transient signals obtained from the injection of the sample solution and the blank, which must possess matched matrix composition. For these conditions the sample-to-standard additions method was as effective as the standard additions method. Two conventional FI methods for the determination of hydrochloric acid and orthophosphate in phosphate rock digests were examined by the sample-to-standard additions method. Satisfactorily accurate and precise results were demonstrated. Because the proposed method was operated in the conventional FI mode, an autosampler was incorporated to obtain a throughput of 80–100 samples h^{-1}.

Keywords: *Flow injection; sample-to-standard additions; spectrophotometry; hydrochloric acid; orthophosphate*

Betteridge and Fields[1] developed a pH gradient technique for the study of cation - ligand complexation behaviour. A basic or acidic solution was injected into a merged solution of the sample and a chelating agent. Hence, the conventional flow injection (FI) approach to inject the sample into a streaming carrier solution was reversed.

Tyson and co-workers[2–6] adopted the above sample introduction technique to develop a novel flow injection analogue of the standard additions method with atomic absorption spectrometric detection. Discrete volumes of the standard solution were injected into the analyte stream. Various applications were developed employing a graphical interpretation to compute the analyte concentration when the transient signal equalled zero.

For detectors operating in a linear dynamic concentration range, the analytical calculation of the standard additions method seemed more convenient and fitting to automation than the approach used by Tyson and co-workers.[2–6] For this reason reverse FI was exploited by Israel and Barnes,[7] who used a mathematical treatment for the development of a conventional standard additions method. This allowed a straightforward calculation of the analyte concentration requiring only two reverse FI discrete volume injections of the blank and a standard solution. Two transient measurements were obtained under the same dilution (see later). Fang *et al.*[8] tested the latter method[7] with a few standard reference materials and reported that the approach was simple and produced satisfactory results.

On-line process control with FI was employed in references 9–13. The potential application of the reverse FI standard additions method for on-line monitoring and control has been demonstrated recently by Frenzel.[14] His technique was based on the method of Tyson and co-workers[2–6] and used intermittent injection of standard solutions into a continuously flowing sample stream. Experimental conditions were given for spectrophotometric and potentiometric determinations with interpolative calibrations to determine the analyte concentration.

The feasibility of applying the reverse FI standard additions method to analytical problems seems promising. However, its implementation, particularly with an autosampler, would require a modification either of the flow configuration used conventionally with FI or the reverse FI standard additions method to make it compatible for automation.

The purpose of this paper is to demonstrate the analytical applicability of the sample-to-standard additions method as an alternative to the conventional FI standard additions method. In this approach the sample solutions are injected successively into a streaming standard solution (carrier). Hence, the FI is operated in the normal mode, and the sample-to-standard additions method can be achieved with an autosampler. For this purpose, two FI methods were modified and examined by this approach. The first is a recently developed acid - base spectrophotometric determination,[15] which employs acid - base indicators and yields a linear peak-height absorbance - concentration dependence. This analysis is applied to the determination of hydrochloric acid. The second method is the spectrophotometric determination of phosphate in rock samples by the formation of the yellow heteropolyanion 12-molybdophosphate.[16]

Theory

The main aspect of employing the classical standard additions method is to compensate for some matrix effects arising from the peculiar composition of the analyte. The detector response is measured for a diluted sample solution and a solution containing the same sample concentration to which a known amount of a standard solution has been added. Both measurements are obtained with identical sample dilution and as a result identical matrix composition. Therefore, calculating the sample concentration by the standard additions method is expected to be more accurate than calculating the same from measurements of standard solutions devoid of sample matrix composition.

The same principle must hold for the development of an FI standard additions method. Flow injection is unique in that the determination of the analyte concentration is made from a transient peak signal, I^p, defined by

$$I^p = kC^p_x = kC^0_x/D \quad .. \quad .. \quad .. \quad (1)$$

where D is the dispersion at peak height and k is the proportionality constant of a linear detector response to the analyte concentration at the transient peak, C^p_x. The dispersion at peak height is, in effect, a dilution factor which can be defined by

$$D = (V^p_x + V^p_c)/V^p_x \quad .. \quad .. \quad .. \quad (2)$$

where V^p_x and V^p_c are the hypothetical volumes of the sample and the carrier solution, respectively, prevailing instantaneously at the transient peak. Hence, the detector response relates to a diluted sample solution depending on the value of D.

The standard additions equation with reverse FI is

$$C^0_x = I^m C^0_s/(I^m - I^p) \quad .. \quad .. \quad .. \quad (3)$$

where I^p and I^m are the transient signals measured for the injection of discrete volumes of the standard and a blank solution, respectively, into the sample solution. The same relationship was derived previously.[7] The only difference between equation (3) and the equation derived previously is the sign of I^m. This has resulted from overlooking the fact that I^0_x, the steady-state signal obtained from streaming the sample solution, is the reference state for the measurement of I^m.

Both of the transients involved in the calculation of the analyte concentration [equation (3)] are obtained at the same dilution, D. The advantage of applying the FI standard additions method is that both the injected standard and the blank may be pure aqueous solutions, which need not have a composition matrix matched to the sample. However, in this method both I^0_x and I^m vary depending on the concentration of the sample (even when D is kept constant). This is a disadvantage as I^m must be determined for every sample. It was inferred previously that for reverse FI, $D = -I^0_x/I^m$.[15] Combining this relationship with equation (3) gives

$$C^0_x = C^0_s/(1 + DI^p/I^0_x) \quad .. \quad .. \quad (4)$$

Using equation (4), C^0_x can be determined from a single injection of the standard solution provided that both I^p and I^0_x are measured and that D is well established beforehand.

FI Sample-to-standard Additions Method

The FI sample-to-standard additions method is illustrated in Fig. 1. A standard solution with concentration C^0_s flows continuously to the detector to provide a steady-state response signal I^0_s:

$$I^0_s = kC^0_s + I_b \quad .. \quad .. \quad .. \quad (5)$$

where I_b is the background signal. A discrete volume, V_i, of a sample solution with initial concentration C^0_x is injected giving rise to an instantaneous response signal, I^t_{xs}, which relates to the whole concentration profile of the injected sample. Therefore, I^t_{xs} is the resulting signal associated with the dispersion of the injected sample solution into the standard solution and *vice versa* and is defined by

$$I^t_{xs} = I^t_s + I^t_x + I_b \quad .. \quad .. \quad .. \quad (6)$$
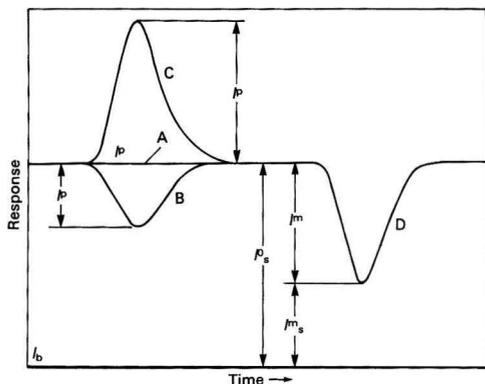
Fig. 1. Illustration of the FI sample-to-standard additions method responses (terms are defined in the text)

The detector response at peak height, I^p_{xs}, is given by

$$I^p_{xs} = k[C^0_s(D - 1) + C^0_x]/D + I_b \quad .. \quad (7)$$

I^0_s is the reference signal for the transient measurement of the injected sample solution, I^p, or $I^p = I^p_{xs} - I^0_s$ (Fig. 1). Another way of expressing equation (5) is given by

$$I^0_s = kC^0_s[(D - 1) + 1]/D + I_b \quad .. \quad .. \quad (8)$$

Subtracting equation (8) from equation (7) yields the transient signal obtained by the injection of the sample solution:

$$I^p = I^p_{xs} - I^0_s = k(C^0_x - C^0_s)/D \quad .. \quad .. \quad (9)$$

From equation (9) three conditions are obtained. (1) When $C^0_x = C^0_s$, then $I^p = 0$, and $I^p_{xs} = I^0_s$. No transient is displayed (Fig. 1, A). (2) When $C^0_x < C^0_s$, then $I^p < 0$, and a negative transient is present (Fig. 1, B). (3) When $C^0_x > C^0_s$, then $I^p > 0$, and a positive transient is obtained (Fig. 1, C).

Similarly to the injection of the sample solution, the injection of a discrete volume, V_i, of a blank solution into the streaming standard (carrier) solution yields a minimum transient signal, I^m (Fig. 1, D), and

$$I^m = I^m_s - I^0_s = -kC^0_s/D \quad .. \quad (10)$$

The value of I^m is always negative. Subtracting equation (10) from equation (9) gives

$$I^p - I^m = kC^0_x/D \quad .. \quad .. \quad .. \quad (11)$$

where $I^p - I^m$ is the peak-to-peak (inflection-to-inflection) signal between the two transient signals obtained by successive injection of the same volume of blank and sample solutions, respectively, into the streaming standard solution.

Combining equations (10) and (11) and rearranging yields the sample-to-standard additions method equation.

$$C^0_x = C^0_s(I^m - I^p)/I^m \quad .. \quad .. \quad (12)$$

To calculate the analyte concentration, C^0_x, two determinations are required to measure I^p from the sample injection and I^m from the blank solution injection. While a pure standard solution can be used as the carrier solution, the injected blank must have a matrix composition matched to the injected sample. This is the disadvantage of the FI sample-to-standard additions method. However, if this condition is satisfied, the approach exhibits the same advantages as the FI standard additions method. In addition, the concentration of the standard carrier solution used, C^0_s, will be constant throughout a series of sample analyses. This implies that both I^0_s and I^m remain constant for a constant D, and hence I^m need not be determined frequently. Re-injection of the blank solution is made to verify either the proper operation of the flow system or the stability of the detector. As the sample-to-standard additions method is operated in the conventional FI mode, an autosampler can be employed.

Differentiating equation (9) and for a constant C^0_s, yields

$$dI^p/dC^0_x = dI^p_{xs}/dC^0_x = k/D \quad .. \quad .. \quad (13)$$

A plot of I^p, or I^p_{xs}, *versus* C^0_x is linear for detectors operating within their linear dynamic range and yields a slope equal to k/D. As k is a constant, the slope and the sensitivity of the measurement are inversely proportional to D. By selecting a low value of D, the sensitivity is enhanced. Small values of D can be obtained by increasing the injection volume, increasing the flow-rate to the detector or decreasing the (reactor) volume between the injection port and the detector.

Experimental

Flow Injection Apparatus and Reagents

A complete FI system (Tecator FIAstar 5020) used with a spectrophotometric detector (Tecator FIAstar 5023) has been
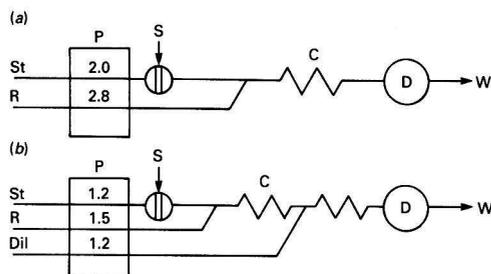
Fig. 2. Schematic diagrams of the flow systems for the sample-to-standard additions method. (*a*) Two-channel flow manifold for the determination of HCl: St, standard solution of HCl (carrier), 2.0 ml min⁻¹; R, reagent, 2.8 ml min⁻¹; P, peristaltic pump with constant speed motor; S, sample injection valve, loop volume 40 or 100 μl; C, coil (60 cm × 0.5 mm i.d.); D, spectrophotometric detector; W, waste. (*b*) Three-channel flow manifold for the determination of orthophosphate: St, standard solution of phosphate rock digests, 1.2 ml min⁻¹; R, reagent, 1.5 ml min⁻¹; C, coil (50 cm × 0.5 mm i.d.); Dil, diluent solution, distilled de-ionised water or dilute nitric acid (1 + 4 V/V) in distilled de-ionised water, 1.2 ml min⁻¹

described previously.[15] An external recorder was connected to the detector output, parallel to the connection of the analyser, to display replicate outputs of sample analyses. However, all the results were based on the data recorded by a printer (Tecator FIAstar 5021) and acquired by the detector controller (Tecator FIAstar 5032).

A schematic diagram of the flow system used for the determination of hydrochloric acid is depicted in Fig. 2(*a*). The main connections were made by Chemifold I (Tecator), a manifold with a single confluence junction.

The flow system used for the determination of orthophosphate in phosphate rock sample digests is depicted in Fig. 2(*b*). The main connections were made by Chemifold II (Tecator), a manifold with two confluence junctions.

The connection of coils, or tubes, was made using tapered PTFE tubes, O-rings and PVC tube unions (Tecator). Various coil sizes were used as indicated in Fig. 2, with coil dimensions expressed as length (cm) × i.d. (mm).

Analytical-reagent grade reagents and doubly distilled, de-ionised water were used throughout. Various aqueous solutions of HCl were prepared by dilution of a standard 1.0 M HCl solution with distilled, de-ionised water.

The reagent for the determination of HCl was 0.20 M sodium acetate - 50 mg l⁻¹ bromocresol green (BCG) - 0.002% m/V Triton X-100 (Rohm and Haas, Lot No. 2746) in distilled, de-ionised water.[15] Measurement of absorbance was carried out spectrophotometrically at 444 nm, which corresponded to the absorption peak of the acidic form of the BCG indicator.

The method of Basson *et al.*,[16] involving the formation of the yellow heteropolyanion 12-molybdophosphate is used routinely for the determination of phosphate in phosphate rock samples using an FI method. The alternative FI method for the determination of phosphate, *i.e.*, forming the reduced form of molybdophosphate (blue), is more sensitive, and therefore is inadequate when phosphate is the major constituent. In this work, the method of Basson *et al.*[16] was employed for the determination of orthophosphate in phosphate rock digests by the sample-to-standard additions method. However, the colour developing reagent used was less concentrated than the one proposed originally[16] to avoid precipitation upon standing. The reagent was prepared as follows. (a) Dissolve, with heating, 60 g of ammonium heptamolybdate, (NH₄)₆Mo₇O₂₄.4H₂O, in 200 ml of distilled, de-ionised water until a clear solution is obtained. Cool to room temperature. (b) Dissolve, with heating, 3 g of ammonium vanadate in 200 ml of distilled, de-ionised water. Cool to room temperature. (c) Dilute 320 ml of nitric acid (55%) with

200 ml of distilled, de-ionised water. (d) Add solution (b) to solution (c) while stirring. Slowly add solution (a) to the mixture of (b) and (c). Dilute to 1 l with distilled, de-ionised water and filter.

Preparation of the Standard Orthophosphate and Blank Solutions

Standard solutions of various concentrations were prepared from NBS phosphate rock samples (NBS SRM 120b Florida, 34.55% P₂O₅, and NBS SRM 56b Tennessee Brown, 31.55% P₂O₅). However, a low phosphate content rock was also used after grinding to 200 mesh and homogenising, for the preparation of a standardised solution. This sample digest was assayed, using replicate analyses, by a conventional yellow 12-molybdophosphate spectrophotometric method (3.10 ± 0.01% P₂O₅). Three standard solutions were prepared by weighing accurately *ca.* 0.5 g of each sample, followed by digestion with 50 ml of dilute nitric acid (1 + 4 V/V, with distilled, de-ionised water), which after cooling and filtration into a 500-ml calibrated flask, was diluted to volume with distilled, de-ionised water. Other standard solutions were prepared by the use of different volume ratios of the above solutions. This approach was adopted to achieve matrix-matching of the standard solutions as much as possible. Matrix-matching of the streaming standard solution with the sample solution is not required (*cf.*, Theory), therefore pure aqueous standard solutions can be used. However, in this work the matrix-matched solutions were also used as the streaming standard solutions.

The blank solution, which needs to match the sample solution matrix composition, was prepared by the dissolution of 0.32 g of CaCO₃ and 0.16 g of CaF₂ in 50 ml of dilute nitric acid (1 + 4 V/V) in distilled, de-ionised water. The solution was boiled for 10 min, cooled to room temperature and made up to volume in a 500-ml calibrated flask.

Spectrophotometric measurement of absorbance was performed at a range of wavelengths between 410 and 450 nm, none of which corresponded to the absorption peak of the yellow 12-molybdophosphate heteropolyanion. Usually, the absorption peak is not chosen for absorbance measurement in order to avoid matrix interference of the phosphate rock. In the range of wavelengths indicated above, the sensitivity of absorbance decreases as the wavelength is increased. Therefore, the sensitivity of measurement can be adapted to a considerable extent to the range of concentrations in the samples available by varying the wavelength.

Results and Discussion

Determination of Hydrochloric Acid by the FI Sample-to-standard Additions Method

Aqueous hydrochloric acid standard solutions were used both for the carrier streaming solution and for sample injection in order to investigate the sample-to-standard additions method approach in the absence of matrix effects. The flow system shown in Fig. 2(*a*) was used for continuously streaming a known concentration of a standard solution, C^0_s, which merged with a streaming reagent before reaching the detector. The reagent is composed mainly of sodium acetate solution, containing BCG acid - base indicator. The reaction of hydrochloric acid with an excess of sodium acetate gives an equivalent amount of acetic acid. In turn, the buffer formed (sodium acetate - acetic acid) establishes an equilibrium with BCG acid - base indicator. It was demonstrated previously[15] that FI under these conditions has linear peak-height absorbance dependence on the concentration of hydrochloric acid. Measurement of absorbance was carried out at a wavelength corresponding to the absorption peak of the acidic form of BCG. The same method was adopted for the determination of hydrochloric acid by the sample-to-standard additions
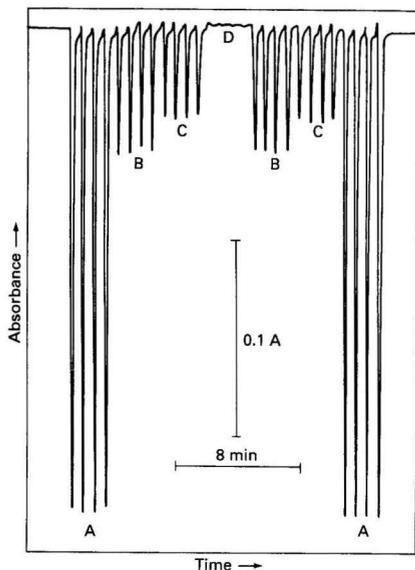
Fig. 3. Spectrophotometric determination of HCl by the sample-to-standard additions method at 444 nm. Concentration of HCl carrier solution, 0.15 M (1.2 ml min⁻¹). Reagent, 0.20 M sodium acetate - 50 mg l⁻¹ BCG - 0.002% m/V Triton X-100 (1.2 ml min⁻¹). Outputs of HCl samples (each) using a 40-µl injection volume: A, H₂O; B, 0.10; C, 0.11; and D, 0.14 M. The flow system of Fig. 2(a) was used. Sample throughput, 80 samples h⁻¹

Table 1. Spectrophotometric determination of standard hydrochloric acid solutions by the FI sample-to-standard additions method. Carrier solution: a standard solution of HCl in the range 0.10–0.16 M was chosen for each set of determinations. Reagent solution: 0.2 M sodium acetate - 50 mg l⁻¹ BCG - 0.002% m/V Triton X-100 in distilled water. Samples: standard solutions of 0.10–0.16 M HCl. Two coils, with dimensions given in parentheses [length (cm) × i.d. (mm)], were used. Sample throughput: 80–100 samples h⁻¹

Range of HCl/M	HCl standard carrier/M	Injection volume/µl	Intercept a	Slope $b/$ A l mol⁻¹	RSD, %
Coil (i) (20 × 0.5; 50 × 0.5)*—					
0.10–0.16	0.12	40	0.004	0.779	0.77
0.10–0.16	0.12	100	0.010	1.710	0.62
0.10–0.16	0.16	100	0.008	1.752	0.58
Coil (ii) (20 × 0.7; 50 × 0.7)†—					
0.10–0.14	0.10	100	−0.003	1.625	0.44
0.10–0.14	0.15	100	0.019	1.443	0.43
0.10–0.14	0.16	100	0.048	1.370	1.10

* $D = 4.0$ and $D_T = 9.6$, for 40-µl injection volume; $D = 1.8$ and $D_T = 4.3$, for 100-µl injection volume; D_T is the over-all dispersion, including dilution by the merging reagent stream, $D_T = D(U_c + U_r)/U_c$, where U_c and U_r are the flow-rates of the standard (carrier) and reagent solutions, respectively. A confluence junction is indicated in Fig. 2(a).

† $D = 2.4$ and $D_T = 5.8$, for 100-µl injection volume.

Fig. 4. Spectrophotometric determination of HCl by the sample-to-standard additions method at 444 nm. Concentration of HCl carrier solution, 0.12 M (2.0 ml min⁻¹). Reagent, 0.20 M sodium acetate - 13 mg l⁻¹ BCG - 0.002% m/V Triton X-100 (2.8 ml min⁻¹). Outputs of HCl samples (four each) using a 100-µl injection volume: A, H₂O; B, 0.10; C, 0.11; D, 0.13; E, 0.14; F, 0.15; and G, 0.16 M. The flow system of Fig. 2(a) was used. Sample throughput, 80 samples h⁻¹

Fig. 5. FI sample-to-standard additions method for the determination of orthophosphate in phosphate rock digests at 450 nm. Concentration of streaming standard orthophosphate solution, 163.8 mg l⁻¹ of P₂O₅. Solutions of orthophosphate digests, in mg l⁻¹ of P₂O₅, determined using a 40-µl injection volume (in four replicates): A, blank (cf., Experimental); B, 42.4; C, 62.0; D, 110.6, E, 116.0; F, 139.2; G, 242.0; H, 284.0; and I, 302.0. The flow system of Fig. 2(b) was used. Sample throughput, 100 samples h⁻¹

method. A set of hydrochloric acid standard solutions, and a blank, were injected successively into a standard solution and then merged continuously with the reagent. Each set of hydrochloric acid determinations was obtained using an autosampler.

Outputs (four determinations for each sample) using two sets of various concentrations of hydrochloric acid are depicted in Figs. 3 and 4. Negative transient peaks, I_P, were displayed when the concentration of the injected solution

(Fig. 3, peaks B–D) was lower than the concentration of the streaming standard solution. On the other hand, negative or positive transients were displayed when the injected solutions were either less or more concentrated than the streaming standard solution (Fig. 4, peaks B–G). In both Figs. 3 and 4, peaks A display the minimum transient, I^m, obtained by the injection of a distilled water blank into the streaming standard solution. Excellent reproducibility is obtained for replicates of each determination of the blank both for those that were injected initially or at the end of each set. Hence, the injection of the blank is required only when re-calibration becomes necessary.

Six series of acid determinations of various concentrations of standard solutions were carried out using two different coil dimensions. Also the injection volume was varied (40 or 100 μl) for two sets of determinations using the same coil dimensions. Both variables influence the dispersion of the injected solution in the streaming standard solution. The
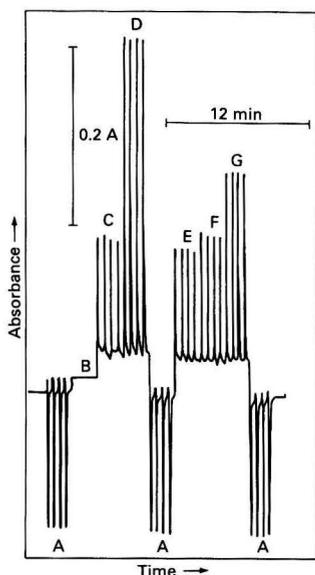
Fig. 6. FI sample-to-standard additions method for the determination of orthophosphate in phosphate rock digests at 410 nm. Concentration of streaming standard orthophosphate solution, 62.0 mg l^{-1} of P_2O_5. Solutions of orthophosphate digests, in mg l^{-1} of P_2O_5, determined using a 40-μl injection volume (in four replicates): A, blank (cf., Experimental); B, 62.0; C, 112.2; D, 206.0; E, sample 1 (110.0); F, sample 2 (113.3); and G, sample 3 (139.4). Samples 1–3, digests of phosphate rock. The flow system of Fig. 2(b) was used. Sample throughput, 100 samples h^{-1}

results obtained were treated using equation (12). To assess the linearity of the absorbance - concentration dependence, least-squares calculations from the average of four determinations were used to evaluate the slope [$b = k/D$, cf., equation (13) and following] and the relative standard deviation (RSD) (%) from the slope b of each series of experiments.

The results obtained for the determination of hydrochloric acid are listed in Table 1. From entries 1 and 2 of Table 1, the consequence of increasing the injection volume is an increase in the slope or an increase in sensitivity as was predicted by equation (13) for lower values of D. However, when the coil configuration (ii) was employed, having greater i.d.s than coil configuration (i), the slope decreased, also in agreement with equation (13). This resulted from the increase in D as the coil i.d. increased. A satisfactorily low RSD (%) was obtained for the first five entries of Table 1, although for the last entry, the result was 1.10%. This may be due in part to using a streaming standard solution concentration higher than the concentration of the injected solutions.

Determination of Orthophosphate in Phosphate Rock Digests by the FI Sample-to-standard Additions Method

Real phosphate rock acid digests were used. Throughout, two injection volumes (40 and 100 μl) were utilised with the flow system of Fig. 2(b). Similarly to the determination of hydrochloric acid, outputs of two series of determinations of orthophosphate are depicted in Figs. 5 and 6 (four replicates per sample solution). Excellent reproducibility is demonstrated in both figures for the sample injection and for the blank. Satisfactory results were obtained for three digests of phosphate rock samples (Fig. 6, peaks E–G). The results obtained were in excellent agreement with the average results obtained by conventional spectrophotometric analyses of the same digests.

The results were treated in the same way as for the hydrochloric acid determination and are listed in Table 2. Satisfactory results were demonstrated for all sets of determinations of orthophosphate in phosphate rock digests, yielding very low RSDs (%) from the slopes of absorbance - concentration dependence determined by least-squares calculations.

The influence of the choice of wavelength on the sensitivity of measurements is demonstrated in the first three entries of Table 2. The slope is highest for 410 nm and lowest for 450 nm. However, comparing the second entry with the last two demonstrates clearly the increase in slope resulting from the increase in injection volume. The importance of changing the sensitivity of measurement by the choice of instrumental parameters is valuable for instances requiring adaptation of the sensitivity to the range of concentration to be measured. The increase in the sensitivity using both approaches, which are indicated above, may be required for detecting small

Table 2. Spectrophotometric determination of orthophosphate in phosphate rock sample solutions by the FI sample-to-standard additions method. Carrier and samples: standard solution of phosphate rock digests in dilute nitric acid (see Experimental). Reagent: vanadomolybdate solution in dilute nitric acid (see Experimental). Blank: see Experimental. Diluent: distilled, de-ionised water, or dilute nitric acid (1 + 50 V/V). Sample throughput: 80–100 samples h^{-1}

P_2O_5 range/ mg l^{-1}	P_2O_5 carrier/mg l^{-1}	Diluent	Injection volume*/μl	Wave-length/nm	Intercept a	Slope b/ A l g^{-1}	RSD, %
62.0–206.6	206.6	H_2O	40	440	0.0034	1.330	0.72
62.0–206.6	260.0	H_2O	40	450	−0.0030	1.185	0.39
62.0–206.6	62.0	H_2O	40	410	−0.0056	3.112	0.30
62.0–300.6	110.6	H_2O	40	440	0.0054	1.504	0.55
62.0–300.6	141.2	H_2O	40	440	0.0066	1.525	0.20
41.2–139.4	163.8	HNO_3	100	450	0.0080	2.570	0.48
41.2–300.6	141.2	HNO_3	100	450	0.0120	2.350	0.68

* $D = 3.0$ and $D_T = 9.8$, for 100-μl injection volume; $D = 6.5$ and $D_T = 21.3$ for 40-μl injection volume. Two confluence junctions are represented in Fig. 2(b).

variations in the phosphate content. This is necessary, for example, when the phosphate content in phosphate rock must not be less than a specified value.

Printer readings of the base line can be used to follow the reproducibility of I^0_s resulting from the streaming of the standard solution for both methods. Irregular behaviour is an indication of improper flow or detector response as might result from a dirty spectrophotometric flow cell. A valuable indication of the proper operation of the entire system can be assessed from the reproducibility of I^0_s and I^m.

Conclusion

Two FI methods for the spectrophotometric determination of hydrochloric acid and orthophosphate in phosphate rock digests were adapted for determination by the FI sample-to-standard additions method. Satisfactory results were obtained for both methods with excellent reproducibility and accuracy. The latter is demonstrated by the low RSD (%) obtained from the slope of the absorbance - concentration dependence calculated by least-squares regression. The sample-to-standard additions method must be carried out with a blank matrix that matches the sample matrix. If this requirement is satisfied, the FI sample-to-standard additions method has the same advantages as the FI standard additions method. With an autosampler sample throughput was 80–100 samples h^{-1}. The use of equation (12) eliminates the need to inject standard solutions or to obtain a calibration graph as is commonly practiced in conventional FI determinations. However, the determination of one or two standards is often performed. Re-injection of a blank solution is required only when re-calibration is necessary. Continuous streaming of a standard solution using this method produces a steady-state signal between injections, which provides diagnostic information of inconsistencies in the functioning of the flow system and/or the detector.

References

1. Betteridge, D., and Fields, B., *Anal. Chim. Acta*, 1981, **132**, 139.
2. Tyson, J. F., *Anal. Proc.*, 1981, **18**, 542.
3. Tyson, J. F., and Idris, A. B., *Analyst*, 1981, **106**, 1125.
4. Tyson, J. F., Appleton, J. M. H., and Idris, A. B., *Analyst*, 1983, **108**, 153.
5. Tyson, J. F., Appleton, J. M. H., and Idris, A. B., *Anal. Chim. Acta*, 1983, **145**, 159.
6. Tyson, J. F., and Idris, A. B., *Analyst*, 1984, **109**, 23.
7. Israel, Y., and Barnes, R. M., *Anal. Chem.*, 1984, **56**, 1188
8. Fang, Z., Xu, S., Wang, X., and Zhang, S., *Anal. Chim. Acta*, 1986, **179**, 325.
9. van der Linden, W. E., *Anal. Chim. Acta*, 1986, **179**, 91.
10. Růžička, J., *Anal. Chim. Acta*, 1986, **190**, 155.
11. Gisin, M., and Thommen, C., *Anal. Chim. Acta*, 1987, **190**, 165
12. Růžička, J., *Fresenius Z. Anal. Chem.*, 1988, **329**, 653.
13. Thommen, C., Garn, M., and Gisin, M., *Fresenius Z. Anal. Chem.*, 1988, **329**, 678.
14. Frenzel, W., *Fresenius Z. Anal. Chem.*, 1988, **329**, 668.
15. Israel, Y., *Anal. Chim. Acta*, 1988, **206**, 313.
16. Basson, A. D., van Staden, J. F., and Cattin, P. M., *Fresenius Z. Anal. Chem.*, 1981, **307**, 373.

Micellar Systems in Flow Injection for the Spectrophotometric Determination of Neodymium in Glasses

José Luis Pérez Pavón, Bernardo Moreno Cordero,* Jesús Hernández Méndez and Jorge Cerdá Miralles
Department of Analytical Chemistry, Bromatology and Food Sciences, Faculty of Chemistry, University of Salamanca, Salamanca, Spain

Neodymium (0.03–21 µg ml^{-1}) can be determined at a sampling rate of 120 h^{-1} by injection at pH 2.7 in the presence of 0.4 M NaNO$_3$ into a carrier containing 1.6 × 10^{-3} M 1-(2-pyridylazo)-2-naphthol (PAN) (0.15 g of Triton X-100 plus 1 mg of PAN) buffered at pH 9.2 [HBO$_2$ + NaBO$_2$ (0.04 M)] and monitoring the absorbance at 560 nm. The influence of the presence of electrolytes in the matrix on peak height was studied. The interferences produced by heavy metals were eliminated by extracting their diethyldithiocarbamates into chloroform - ethyl actate (1 + 1). The method was applied to the determination of Nd in a commercial glass.

Keywords: *Neodymium determination; 1-(2-pyridylazo)-2-naphthol; micellar systems; flow injection; glasses*

Flow injection techniques[1-3] have been widely used in such fields as environmental and clinical chemistry and agricultural analysis because they permit the automated determination of analytes. In addition, the determination is often simpler and faster than with the batchwise method.

Organised molecular systems have found wide application in many analytical techniques, both in the determination of trace elements and in separations.[4-6] However, there are few reports describing the use of these systems in flow injection (FI).[2]

In a previous paper[7] we carried out a study on the neodymium - 1-(2-pyridylazo)-2-naphthol (PAN) system in micelles of Triton X-100 and proposed a spectrophotometric method for the determination of Nd in glasses. In this work a simple and rapid (120 samples h^{-1}) method is proposed for the determination of trace amounts of Nd in a micellar medium of Triton X-100 using an FI technique. The method was applied to the determination of Nd in a commercial glass.

Experimental

Reagents

Standard solutions of Nd were prepared as described previously.[7] Solutions of PAN were prepared by dissolving appropriate amounts of the solid product (Merck) in aqueous solutions of Triton X-100, taking advantage of the characteristics of non-ionic surfactants of producing phase separations on increasing the temperature (cloud point *ca.* 65 °C) in order to reduce the time necessary for dissolution of the chromophore and to avoid the formation of foam which subsequently hinders the accurate dilution to volume.

Apparatus

A Gilson Minipuls 2 (four channels) peristaltic pump was employed. The sample injector was a Rheodyne 2050 valve with interchangeable loops of different capacities. All pH measurements were made with a Radiometer PHM 51 pH meter. The absorbance was measured with a Coleman 55 spectrophotometer using a Hellma 178 12 QS flow cuvette with a path length of 1 cm and an internal volume of 18 µl.

All statistical parameters were obtained using the Statworks program on an Apple Macintosh computer.
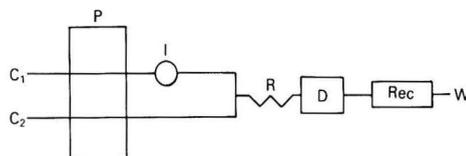
Fig. 1. Schematic diagram of the manifold used. P, Peristaltic pump; I, injection valve; D, detector; R, mixing coil; Rec, recorder; and W, waste

Manifold

For the study of the different variables a manifold constructed from PTFE tubes (0.5 mm i.d.) with two channels C$_1$ and C$_2$ and a T-junction was used (Fig. 1).

Procedure

The calibration graph was obtained by injecting 143 µl of the solution containing Nd in 0.4 M NaNO$_3$, pH 2.7 (HCl), through channel C$_1$ into a carrier containing 1.6 × 10^{-3} M PAN (0.15 g of Triton X-100 plus 1 mg of PAN) buffered at pH 9.2 (HBO$_2$ + NaBO$_2$) and monitoring the absorbance at 560 nm. A 50-cm reactor (R) was used and the flow-rate was 2.2 ml min^{-1} for each channel. We chose to introduce the same carrier solution through channel C$_2$ because both the stability of the base line and the reproducibility of the measurements were found to be better.

Results and Discussion

Influence of the Concentration of Triton X-100

The influence of the surfactant concentration on the shape of the FI diagram and the parameters that define it was studied by injecting 123 µl of carmoisine (40 p.p.m.) via a simple single-channel manifold (length, *l*, 50 cm; flow-rate, *Q*, 2.2 ml min^{-1}) into a stream of water in which the concentration of Triton X-100 was varied from 0.001 to 5%. No appreciable changes were observed in the FI diagrams obtained, hence any subsequent modifications could not be attributed to the presence of micelles in the system.

The peak height does not depend on the concentration of the surfactant in solution but rather on the Triton X-100 to PAN ratio, and decreases as this ratio increases; for values higher than 1.0 g of Triton X-100 to 1 mg of PAN the signal almost disappears. This behaviour of the system can be explained by the fact that on increasing the amount of surfactant in solution (for values higher than the critical

---

* To whom correspondence should be addressed.
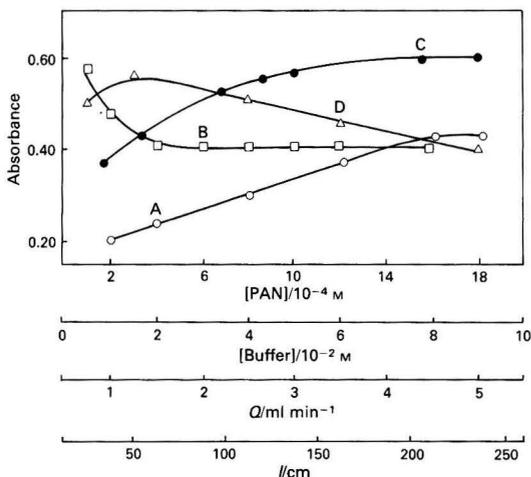
Fig. 2. Influence of A, PAN concentration; B, buffer concentration; C, flow-rate; and D length of reactor on peak height. Nd, 8.0×10^{-5} M; PAN, 1.6×10^{-3} M (0.15 g of Triton X-100 plus 1 mg of PAN); V_i, 143 µl; and pH, 9.2 ($HBO_2 + NaBO_2$)
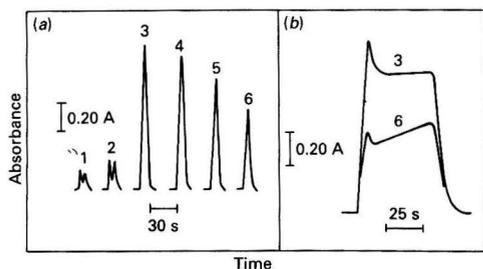
Fig. 3. (a) Influence of the pH of the sample injected on the signal. (b) Stopped-flow FI diagram. Nd, 8.0×10^{-5} M; PAN, 1.6×10^{-3} M (0.15 g of Triton X-100 plus 1 mg of PAN); V_i, 143 µl; l, 50 cm; Q_{total}, 4.4 ml min^{-1}; and pH, 9.2 [$HBO_2 + NaBO_2$ (0.04 M)]. Sample pH: 1, 1.9; 2, 2.1; 3, 2.7; 4, 2.9; 5, 3.3; and 6, 4.9

micellar concentration), only the number of micelles increases, the concentration of monomers in solution remains constant. This feature hinders the formation of the chelate as each atom of Nd has to co-ordinate three molecules of PAN. We chose 0.15 g of Triton X-100 to 1 mg of PAN as the most suitable Triton X-100 to PAN ratio; ratios lower than this gave irreproducible signals owing to the fact that the system studied was not totally solubilised.

Influence of PAN Concentration, Buffer Concentration, Flow-rate and Length of Reactor

Fig. 2 shows the influence of the PAN concentration, buffer concentration, flow-rate and length of the reactor on the peak height.

Influence of pH

One of the variables that most affects the development of the reaction, and hence the signal obtained, is the pH at which the sample is injected. The absorbance of the Nd - PAN- Triton X-100 system is at a maximum for pH values close to 9.2[7]; accordingly, this value was chosen as the optimum for the carrier and for measurement in the detector. However, the pH at which the sample containing Nd is to be injected should be between 2 and 3 in order to enhance the reaction kinetics so

Table 1. Determination of Nd in micelles of Triton X-100. Influence of electrolytes in solution. Nd, 8.0×10^{-5} M; PAN, 1.6×10^{-3} M (0.15 g of Triton X-100 plus 1 mg of PAN); V_i, 143 µl; l, 50 cm; Q_{total}, 4.4 ml min^{-1}; and pH, 9.2 [$HBO_2 + NaBO_2$ (0.04 M)]

Electrolyte added*	A_{560}/nm	
	pH 4.9	pH 2.7
None	0.58	1.08
NaNO$_3$	1.01	1.05
KNO$_3$	0.88	1.09
NaCl	0.91	1.03
NaClO$_4$	0.75	1.01
LiClO$_4$	0.30	1.02

* Final concentration, 0.40 M.
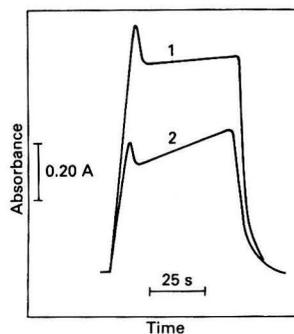
Fig. 4. Stopped-flow FI diagram in the presence and absence of NaNO$_3$. Nd, 8.0×10^{-5} M; PAN, 1.6×10^{-3} M (0.15 g of Triton X-100 plus 1 mg of PAN); V_i, 143 µl; l, 50 cm; Q_{total}, 4.4 ml min^{-1}; and pH, 9.2 [$HBO_2 + NaBO_2$ (0.04 M)]. 1, 0.04 M NaNO$_3$; and 2, no electrolyte present

that they will be sufficiently fast for the reaction to take place in the few seconds that elapse between mixing and arrival at the reactor (Fig. 3). If the sample is injected at a pH lower than 2, double peaks appear, which prevent accurate measurements owing to the inability of the buffer to maintain a pH of 9.2 in spite of the mixing at the T-junction. Values higher than 3 lead to a decrease in peak height because they decrease the kinetics of the reaction. This fact can be explained by bearing in mind that formation of the chelate is due to displacement of the hydroxide ions from the hydroxy complex by PAN molecules, as shown in the following reaction:

$$[Nd(OH)_n]^{3-n} + 3PANH \rightleftharpoons$$
$$Nd(PAN)_3 + H_2O + (n-3)OH^-$$
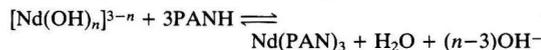
On increasing the concentration of OH$^-$ ions in the medium, formation of the hydroxy complex is favoured and the reaction rate decreases; this phenomenon is not observed if the reaction is performed under batch conditions as the measurement cannot be carried out in such a short time.[7] In order to corroborate these results, the FI diagrams corresponding to two different pH values were recorded, one at the optimum working pH of 2.7 and the other at pH 4.9, by stopping the flow after the bolus of the sample had passed through the detector (Fig. 3). It can be seen that at a pH of 4.9 the reaction continues to take place after the flow has been stopped; however, at the optimum pH the signal does not increase with time, which shows that the reaction has gone to completion.

Matrix Effect: Influence of Electrolytes in Solution

In most determinations it is necessary to dissolve or mineralise the sample prior to analysis, thus generating relatively high

Table 2. Determination of Nd in micelles of Triton X-100. Analytical parameters

Analytical parameter	In the absence of $NaNO_3$	In the presence of $NaNO_3$
Calibration graph . .	1.28×10^4 (Nd) + 0.08 ($r = 0.9993$)	1.32×10^4 (Nd) + 0.06 ($r = 0.9997$)
S, %*	0.57	0.68
Limit of detection, p.p.b.†	85	27

* Nd, 1.6×10^{-5} M (ten solutions).

† Obtained from the equation $(3S_B + x)/m$, where S_B is the standard deviation of ten measurements of the blank and m is the slope of the calibration graph

Table 3. Determination of Nd in a commercial glass

		Nd_2O_3, %		
Sample	Flow injection	X-ray fluorescence spectro-metry	Conventional spectro-photometry	Derivative spectro-photometry
1	0.037	0.05	0.037	0.037
2	0.036	0.05	0.036	0.037
3	0.037	0.05	0.037	0.036

amounts of electrolytes in the medium. It is known that the presence of electrolytes in solution can alter the shape and size of the micelles and that changes in the absorption spectra can occur; in some instances these changes have been attributed to ionic exchanges on the surface of the micelle. Moreover, the disruptive effect of the electrolytes with respect to the structure of the water molecules can alter the reaction rate significantly. In order to check the matrix effect produced by the presence of electrolytes in the reaction medium, a study was performed by injecting the sample at two pH values, 2.7 and 4.9, in the presence of different electrolytes. The results obtained (Table 1 and Fig. 4) indicate that when the pH at which the sample is injected is equal to 4.9 (the non-optimum pH), in all instances except for $LiClO_4$, the presence of electrolytes leads to an increase in the reaction rate, as shown by the corresponding stopped-flow FI diagrams, as expected. However, this effect is not observed when the sample is injected at pH 2.7 (the optimum pH).

Calibration Graph, Precision and Detection Limit

Under the experimental conditions chosen, $\lambda = 560$ nm, pH of the sample on injection = 2.7, volume of sample injected (V_i) = 143 µl, ratio of Triton X-100 to PAN = 0.15 g to 1 mg, $l = 50$ cm, pH of carrier = 9.2 [HBO_2 + $NaBO_2$ (0.04 M)] and Q_{total} = 4.4 ml min⁻¹, the calibration graph, the precision of the method and the limit of detection both in the absence and presence of 0.04 M $NaNO_3$ can be obtained. The results (Table 2) show that the presence of an electrolyte in solution improves the sensitivity and correlation coefficient; further, it decreases the limit of detection and increases the linearity range from 5.6×10^{-5} to 8.0×10^{-5} M.

Study of Interferences

All the heavy metals interfere with the determination of Nd as they form intensely coloured chelates with the chromophore. However, this interference can be eliminated by extracting the corresponding diethyldithiocarbamates into chloroform - ethyl acetate $(1 + 1)$. The interference produced by Ce^{IV}, which is not removed under the experimental conditions, can be eliminated by precipitating the basic salt formed with $KBrO_3$. Of the anions studied, citrate and phosphate are the main interferents; fluoride and tartrate only interfere at ratios higher than 100 : 1. All the other lanthanides interfere.

Determination of Nd in a Commercial Glass

A solution of the glass (approximately 0.25 g), obtained as described previously,[7] together with the washing liquids, is adjusted to pH 2.7 and a sufficient amount of $NaNO_3$ is added to give a final concentration of 0.4 M. The volume is then made up to 25.0 ml. A 143-µl aliquot is injected through channel C_1 (Fig. 1) into a carrier containing 1.6×10^{-3} M PAN (0.15 g of Triton X-100 plus 1 mg of PAN) buffered at pH 9.2 [HBO_2 + $NaBO_2$ (0.04 M)] and the absorbance is monitored at 560 nm. The results obtained with flow injection were compared with those obtained using X-ray fluorescence spectrometry, conventional spectrophotometry[7] and derivative spectrophotometry[7] (Table 3).

Conclusion

A rapid and sensitive FI method has been developed for the determination of Nd. The method was applied to the determination of Nd in a commercial glass.

References

1. Růžička, J., and Hansen, E. H., "Flow Injection Analysis," Wiley, New York, 1981.
2. Růžička, J., and Hansen, E. H., *Anal. Chim. Acta*, 1986, **179**, 1.
3. Valcárcel, M., and Luque de Castro, M. D., "Flow Injection Analysis. Principles and Applications," Ellis Horwood, Chichester, 1987.
4. Pelezzeti, E., and Pramauro, E., *Anal. Chim. Acta*, 1985, **169**, 1.
5. Armstrong, D. W., *Sep. Purif. Methods*, 1985, **14**, 212.
6. Hinze, W. L., in Hinze, W. L., and Armstrong, D. W., *Editors*, "Ordered Media in Chemical Separations," ACS Symposium Series 342, American Chemical Society, Washington, DC, 1987.
7. Hernández Méndez, J., Moreno Cordero, B., Pérez Pavón, J. L., and Cerdá Miralles, J., *Analyst*, 1988, **113**, 429.

Direct Spectrophotometric Determination of Trace Amounts of Mercury(II) in Aqueous Media as its Dithizonate Complex in the Presence of a Neutral Surfactant

Har Bhajan Singh, Brajesh Kumar and Rattan Lal Sharma
Department of Chemistry, University of Delhi, Delhi-110 007, India
Mohan Katyal
Department of Chemistry, St. Stephen's College, University of Delhi, Delhi-110 007, India

The spectrophotometric determination of mercury in aqueous solution as its dithizonate complex in the presence of Triton X-100, a neutral surfactant that renders both the ligand and the complex water soluble, is described. The molar absorptivity, specific absorptivity and Sandell sensitivity of the complex at the wavelength of maximum absorption (490 nm) were found to be 3.868×10^4 l mol^{-1} cm^{-1}, 192.8 l g^{-1} cm^{-1} and 5.2 ng cm^{-2}, respectively. Beer's law was obeyed between 1×10^{-6} and 2×10^{-5} M Hg^{2+}. The interference caused by the presence of a number of common cations and anions was studied and the method was applied successfully to the analysis of a mercury-based pesticide.

Keywords: *Mercury complex; dithizone; spectrophotometry; derivative spectrophotometry; surfactant*

Mercury in any form is a serious environmental pollutant.[1] This necessitates its detection and determination in many different matrices, particularly at trace levels. Mercury forms a pink - red complex with dithizone in acidic medium and this has formed the basis of a number of spectrophotometric methods[2–4] for the determination of microgram amounts of mercury(II). Most of these methods involve extraction of the mercury - dithizone complex into chloroform followed by measurement of its absorbance. Although these procedures are cumbersome, have inherent sources of error and are limited by the solubility of the ligand and the complex in aqueous medium and by the stability of the resulting solutions, dithizone remains the most commonly used reagent for the spectrophotometric determination of trace amounts of mercury.[2–7] Although the reaction is sensitive at the p.p.m. level, it lacks selectivity. Further, the insolubility of both the reagent and the mercury complex in water necessitates the use of a toxic organic solvent such as chloroform to extract the coloured complex for spectrophotometric measurements. These limitations have been overcome by the introduction of a micellar system, which is normally employed in phase-transfer reactions.[8–10] As both the ligand and the resulting complex are electrically neutral, a neutral surfactant, Triton X-100, was used to form the desired micellar system. The absorption studies were carried out in both the derivative and the zero-order (normal) modes. Derivative spectra were recorded in order to obtain information about the appropriate ligand to metal ratio necessary for quantitative work.

Experimental

Reagents

All chemicals used were of analytical-reagent grade. Aqueous solutions of mercury(II) (1.0×10^{-4} M), Triton X-100 (4% m/V) and hydroxylamine hydrochloride (5% m/V) were prepared by dissolving the appropriate amounts of mercury(II) chloride, Triton X-100 and hydroxylamine hydrochloride, respectively, in water. As dithizone is sparingly soluble in the Triton X-100 solution, the appropriate amount of dithizone required to give a 1×10^{-4} M solution was first dissolved in the minimum volume of 1 M NaOH solution and the 4% m/V Triton X-100 solution was then added. Finally, this solution was acidified with dilute H_2SO_4 to give a pH of 2.0–3.0. Dithizone in aqueous solution undergoes oxidation whereby the concentration of its solution changes. In order to

prevent this, hydroxylamine hydrochloride was added and the solutions were kept at <10 °C.

Instrumentation

Spectra were recorded on a Shimadzu 260 UV - visible recording spectrophotometer. An EC digital pH meter (Model PH 5662) was used to measure the pH of the solutions.

Preparation of Working Solutions

To study the effect of pH on complex formation, two series of solutions, one series being 1×10^{-4} M with respect to the metal ion and the other containing no metal ion, were prepared. In addition to the metal ion, each solution comprising the series contained dithizone (5×10^{-5} M), Triton X-100 (1.2% m/V) and hydroxylamine hydrochloride (0.25% m/V); the volume of each solution was made up to 10 ml. The pH of these solutions was adjusted to between 1.0 and 6.0.

To study the effect of varying the surfactant concentration on the absorbance of the mercury - dithizone - Triton X-100 system, a series of solutions containing increasing amounts of Triton X-100, 2×10^{-6} M Hg^{2+}, 5×10^{-5} M dithizone and 0.25% m/V hydroxylamine hydrochloride, at the pH of maximum complex formation, was prepared.

A series of solutions containing increasing amounts of mercury(II), under the optimum conditions for complex formation described above, was prepared in order to determine the concentration range over which Beer's law was obeyed by the system.

To study the effect of varying the dithizone concentration, solutions with increasing ligand concentrations were prepared under the conditions of maximum complex formation, keeping all the other variables constant.

The effect of the presence of interfering ions on the mercury - dithizone complex was studied by adding the ion to a solution of the complex and recording the change in the absorbance. A 1% change in the absorbance was taken as an indication of interference from the ion added.

Results and Discussion

Absorption Spectrum and Effect of pH on the Absorbance of the System

Visible spectra of the solutions containing the mercury - dithizone complex were recorded against water in the range

300–800 nm. The complex showed an absorption maximum at 490 nm. The ligand also absorbed in the visible region and had absorption maxima at 605 and 440 nm. As the ligand absorbed significantly at the absorption maximum of the complex, the relative increase in the absorbance of the complex was calculated and plotted against the pH of the solution. The maximum of this plot was at pH 2.4, which was taken as the pH of maximum complex formation.

Effect of Surfactant Concentration on the Absorbance of the System

The absorbance at 490 nm of solutions containing increasing amounts of Triton X-100 was found to be proportional to the surfactant concentration up to 1.2% m/V. A slight decrease, however, was observed above this concentration. In all the subsequent studies, the surfactant concentration was maintained at 1.2% m/V.

Effect of Dithizone Concentration on the Absorbance of the System

To investigate the effect of increasing dithizone concentrations, a series of solutions containing increasing amounts of dithizone and a fixed amount of the metal ion (2×10^{-6} M) and hydroxylamine hydrochloride was prepared. The absorbance of the solutions at 490 nm increased with an increase in the dithizone concentration and reached a maximum at a 7-fold excess. The absorbance (corrected) remained constant (in the range ±0.5%) for dithizone concentrations of 7.0×10^{-6}–3.5 $\times 10^{-5}$ M (a 7–35-fold excess of the ligand). In subsequent studies, therefore, the metal to ligand ratio was kept within this range.

Effect of Metal Ion Concentration on the Absorbance of the System

The absorbance of solutions containing increasing amounts of the metal ion and the ligand at 490 nm was plotted against the metal ion concentration in order to evaluate the range over which the absorbance was proportional to the metal ion concentration. Regression analysis gave the following relationship between the absorbance and concentration with a residual square of 0.9977:

$$c = 0.8994A - 0.2639$$

where c is the concentration ($\times 10^{-6}$ M) and A is the absorbance ($\times 10^{-1}$). As dithizone also absorbs in the visible region, the values of the corrected absorbance, $A_{\text{corr.}}$, were calculated from the equation

$$A_{\text{corr.}} = A_{490} - (A_{490}/A_{610})_L \times A_{610}$$

where A_{490} and A_{610} are the absorbances of the complex observed at 490 and 610 nm, respectively, and $(A_{490}/A_{610})_L$ is the ratio of the absorbance of the ligand at 490 nm to that at 610 nm. The corrected absorbance values were found to have the following relationship to the metal ion concentration with a residual square of 0.9991:

$$c = 1.6121A_{\text{corr.}} + 0.0783$$

The concentration range over which Beer's law was obeyed was found to be 1–20 μM of Hg^{2+}. The Sandell sensitivity (with respect to the metal ion) and molar absorptivity (at 490 nm) of the complex were found to be 5.2 ng cm^{-2} and 3.868×10^4 l mol^{-1} cm^{-1}, respectively.

Dithizone forms both primary and secondary dithizonates with mercury. These dithizonates have different molar absorptivities depending on the pH and the metal to ligand ratio.[11,12] This can be seen from the difference in the nature of the spectra of the system at different pH values and metal to ligand ratios. It is, therefore, imperative to ensure that the
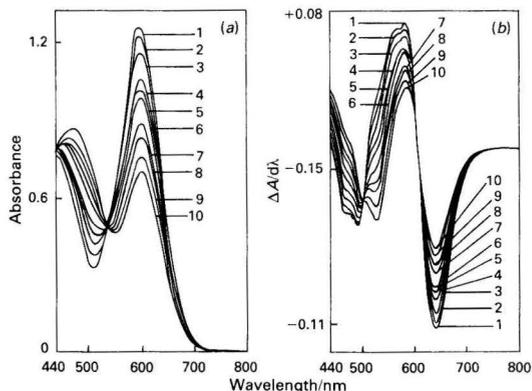
Fig. 1. (*a*) Zero-order and (*b*) first-derivative spectra of solutions containing 1, 2.5×10^{-4} M dithizone; and 2, 1.0×10^{-6}; 3, 2.0×10^{-6}; 4, 3.0×10^{-6}; 5, 4.0×10^{-6}; 6, 5.0×10^{-6}; 7, 6.0×10^{-6}; 8, 7.0×10^{-6}; 9; 8.0×10^{-6}; and 10, 9×10^{-6} M Hg^{2+} at pH 2.4

metal to ligand ratio is in the appropriate range. This can be monitored by studying the first-derivative spectra of the samples in the range 500–580 nm [Fig. 1(*b*)]; the zero-order (normal) spectra cannot be used for this purpose because they show only a minute shift in the maximum near the $\lambda_{\text{max.}}$ of the complex. The first-derivative spectra on the other hand show a trough at 525 nm if the ligand to metal ratio falls below 8; a clear trough in curve 8 (ligand to metal ratio = 7.1) and a shoulder (but no trough) in curve 6 (ligand to metal ratio = 8.3) can be seen in Fig. 1(*b*). It is, therefore, desirable to record the first-derivative spectra of the solutions in addition to the zero-order spectra when determining microgram amounts of mercury using dithizone.

Composition and Stability Constant of the Complex

From the plot obtained by Job's method of continuous variation, the Hg^{2+} to dithizone (H_2Dz) ratio forming the complex was found to be 1:2 at pH 2.4. The complex can, therefore, be represented as $Hg(HDz)_2$, which is in agreement with the reported composition in the organic phase.[2–4]

The conditional stability constant of the 1:2 ($Hg:H_2Dz$) complex was calculated, assuming the following equilibrium in the system:

$$Hg^{2+} + 2H_2Dz \rightleftharpoons Hg(HDz)_2 + 2H^+$$
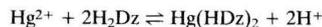
As the solutions are very dilute and a non-ionic surfactant was used, the concentrations were taken instead of the corresponding activities. The free ligand concentration was calculated from the absorbance of the ligand at 610 nm; at this wavelength, the absorbance of the complex was negligible.

Due care was taken to ensure that the chloride ion was not present when calculating the stability constant as it forms complexes with Hg^{2+}. The stability constant was found to be 1.411×10^6 (average of six values) with a coefficient of variation of 9.2%.

Influence of Foreign Ions on the Determination of Mercury

The effect of the presence of foreign ions on the determination of microgram amounts of mercury was investigated by studying the absorption spectra in both the zero-order and various derivative modes.

The interference was tested at 2×10^{-5} M, *i.e.*, the concentration of the interfering ion was ten times that of the Hg^{2+} ion. The cations investigated were Pb^{2+}, Zn^{2+}, Fe^{2+}, Fe^{3+}, Co^{2+}, Ni^{2+}, Cu^{2+}, Ag^+, Tl^+, Cd^{2+}, Cr^{3+} and VO^{2+}. Of these, Co^{2+}, Cu^{2+} and Ag^+ interfered seriously, even when present at the same concentration as Hg^{2+}, *i.e.*, at 2×10^{-6} M.

Zn^{2+} produced a significant interference when present at more than ten times the Hg^{2+} concentration. Examination of the spectra of the solutions containing the foreign ion showed that the interference could not be eliminated even by recording the spectra in various derivative modes.

The effect of the presence of complexing anions on the system was also investigated. Of the complexing anions studied, Cl^-, Br^-, I^-, CH_3COO^-, SCN^-, citrate and tartrate did not interfere when present at up to a 50-fold concentration; however, the presence of I^- masked the formation of the complex by 38% when present at a 500-fold excess with respect to the Hg^{2+} ion. Thiocyanate, citrate and tartrate showed a hyperchromic effect when present at a 500-fold excess over the metal ion. Thiourea, ethylenediamine-tetraacetic acid and ascorbic acid did not interfere at a 50-fold excess; however, thiourea interfered (showed a hyperchromic effect) at a 500-fold excess.

Applications

The proposed method was used to recover adulterated mercury from tap water and to determine the mercury content in the pesticide Emision-6, an ethoxy mercury(II) chloride based water-soluble pesticide. The results obtained were compared with those given by atomic absorption spectrometry (AAS). The method adopted is described below.

(*i*) Two series of solutions, one containing 1 ml of tap water and the other no tap water and both containing 0.2 ml (or 0.3 or 0.4 ml) of 10^{-4} M $HgCl_2$ solution, were prepared. To each solution 5 ml of 10^{-4} M dithizone solution, 3 ml of 4% *m/V* Triton X-100 and 0.5 ml of 5% *m/V* hydroxylamine hydrochloride were added. The pH was adjusted to 2.4, keeping the final volume at 10 ml. Absorption spectra were recorded and the corrected absorbance values at the $\lambda_{max.}$ of the complex were calculated. The concentration was then read from the calibration graph.

(*ii*) An aqueous solution (0.2 ml of a 2.0×10^{-5} M solution) of the pesticide was taken. To this, 5 ml of 10^{-4} M dithizone solution, 3 ml of 4% *m/V* Triton X-100 and 0.5 ml of 5% *m/V* hydroxylamine hydrochloride were added and the pH was adjusted to 2.4, maintaining the final volume at 10 ml. The absorption spectra of the solutions were recorded and the corrected absorbance values at 490 nm were calculated. The mercury content could be obtained from the calibration graph.

The results obtained are given in Tables 1 and 2.

Conclusion

It has been shown that the well known method for the determination of trace amounts of mercury(II) using dithizone can be employed directly in the aqueous phase without the need for an extraction step. The modified method is superior to the existing method.

Table 1. Results of recovery of Hg^{2+} from tap water

Amount of Hg added/ μM	Amount of Hg recovered/ μM	Error, %
2.00	1.98	−1.0
2.00	1.98	−1.0
2.00	2.02	1.0
2.00	1.99	−0.5
3.00	3.01	0.33
4.00	3.96	−1.0

Table 2. Results of the analysis of a pesticide solution containing mercury

Amount of Hg in the pesticide, p.p.m.	Amount of Hg found, p.p.m.		Error, %
	Dithizone - Triton X-100 method	AAS method	
14.84	14.73	14.86	−0.74
14.84	14.88	14.80	0.24
14.84	14.90	14.90	0.40
14.84	14.70	14.78	−0.94
14.84	14.80	14.89	−0.27
14.84	14.89	14.88	0.34

References

1. Friberg, L., Nordberg, G. F., and Vouk, V. B., *Editors*, "Handbook on the Toxicology of Metals," Elsevier/North Holland Biomedical Press, Amsterdam, 1979.
2. Melles, J. L., and de Bree, W., *Recl. Trav. Chim. Pays-Bas*, 1953, **72**, 576.
3. Friedberg, H., *Anal. Chem.*, 1955, **27**, 305.
4. Irving, H. M., Andrew, G., and Risdon, E. J., *J. Chem. Soc.*, 1949, 541.
5. Truhaut, R., and Boudene, C., *Bull. Soc. Chim. Fr.*, 1959, 1850.
6. Tiptsova, V. G., Andreichuk, A. M., and Bazhanova, L. A., *Zh. Anal. Khim.*, 1965, **20**, 1200.
7. Nabrazyski, M., and Kostrrewska, B., *Rocz. Panstw. Zakl. Hig.*, 1984, **35**, 125.
8. Watanabe, H., and Matsunage, H., *Bunseki Kagaku*, 1976, **25**, 35.
9. Hayashi, K., and Ito, K., *Bunseki Kagaku*, 1971, **20**, 1550.
10. Chen, X., Han, C., and Yan, Z., *Fenxi Huaxue*, 1984, **12**, 135.
11. Irving, H. M., and Nowicka-Jankowska, T., *Anal. Chim. Acta*, 1971, **54**, 55.
12. Kiwan, A. M., and Irving, H. M., *Anal. Chim. Acta*, 1971, **54**, 351.

SHORT PAPERS

Spectrophotometric Determination of Total Cyanide in Surface Waters Following Ultraviolet Induced Photodecomposition

Tsutomu Ohno

Department of Plant and Soil Sciences, University of Maine, Orono, ME 04469-0118, USA

A simple and sensitive spectrophotometric method for the determination of total cyanide in surface waters is described. Sodium hexacyanoferrate(II) can be found in surface waters owing to its use as an anti-caking agent in road de-icing salts. The method is based on the decomposition of complexed cyanide to free cyanide by exposure to short wave ultraviolet (UV) light. The sample is then analysed for free cyanide by a method based on the Konig reaction. The optimum sample UV irradiation time and the effect of NaCl on the spectrophotometric method were investigated. The method was applied to various surface water samples using standard additions to eliminate the interference from high salt concentrations and background sample colour in some surface water samples.

Keywords: *Total cyanide determination; hexacyanoferrate(II); water analysis; spectrophotometry; anti-caking agent*

In climates with significant snowfall, NaCl is used as a de-icing agent on roads. To ensure uniform spreading, road salts are treated with anti-caking agents such as sodium hexacyanoferrate(II) to prevent formation of large salt clumps.[1] Although the toxicity of hexacyanoferrate(II) salts is low,[2] exposure to sunlight can lead to decomposition to give free cyanide which is highly toxic to plant and animal life.[3]

The measurement of complexed cyanide in water using an ion-selective electrode to determine the free cyanide following the ultraviolet (UV) photodecomposition of complexed cyanide compounds has been reported.[4,5] The method described here uses a spectrophotometer instead of an ion-selective electrode to determine cyanide; improved detection limits and a saving in time were obtained.

Experimental

Apparatus

A Bauch and Lomb 20 spectrophotometer was used for all measurements. An UltraViolet Products R-52G lamp was used to irradiate samples contained in 25 × 100 mm quartz test-tubes.

Reagents

All chemicals were of analytical-reagent grade and were used without further purification. All solutions were prepared with de-ionised water and stored under refrigeration.

Cyanide stock solution. A 100 μg ml^{-1} stock solution of cyanide was prepared from KCN. Appropriate working cyanide solutions were prepared by dilution of the stock solution with de-ionised water.

Sodium hexacyanoferrate(II) stock solution. A 1 μg ml^{-1} stock solution of Na$_4$[Fe(CN)$_6$] was prepared with de-ionised water and stored in a glass bottle protected from light.

Barbituric acid reagent. Three grams of barbituric acid were wetted with de-ionised water and 15 ml of pyridine were added. De-ionised water was used to bring the volume to 50 ml while stirring the contents to aid dissolution of the barbituric acid.

N-chlorosuccinimide - succinimide reagent. One gram of succinimide was dissolved in 40 ml of de-ionised water. N-chlorosuccinimide (0.1 g) was added and the mixture was stirred to dissolve the solid. The volume was then made up to 100 ml.
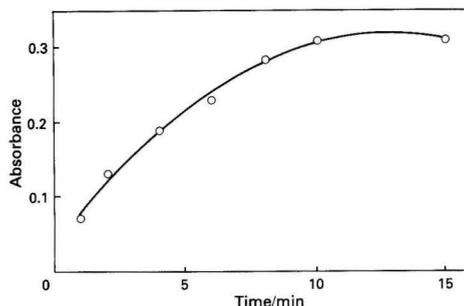
Fig. 1. Effect of UV irradiation time on the release of free cyanide from Na$_4$[Fe(CN)$_6$]

Procedure

Surface water samples were filtered through Whatman No. 40 filter-paper to remove any debris collected with the water sample. Quartz test-tubes were filled with 25 ml of water and placed within 2 cm of the UV lamp housing for 10 min. Immediately after the UV photodecomposition treatment, 4.5-ml aliquots were transferred into four test-tubes. For standard additions analysis the aliquots were spiked with 0, 0.05, 0.10 and 0.15 μg of cyanide. After shaking, 0.2 ml of the N-chlorosuccinimide - succinimide reagent was added and the contents of the test-tubes were mixed. After 1 min, 0.2 ml of the barbituric acid - pyridine reagent was added. The absorbance at 575 nm was read after 10 min.

Results and Discussion

The proposed spectrophotometric determination is based on the procedure developed by Lambert *et al.*[6] This method has good sensitivity down to approximately 5 μg l^{-1} of cyanide. The low concentrations of total cyanide found in surface waters necessitates a method with low detection limits.

Ultraviolet Photodecomposition

The effect of the duration of exposure to UV light on the decomposition of hexacyanoferrate(II) to free cyanide is
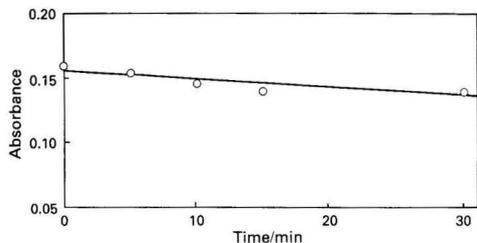
Fig. 2. Effect of time on the re-formation of the complexed cyanide after UV photodecomposition
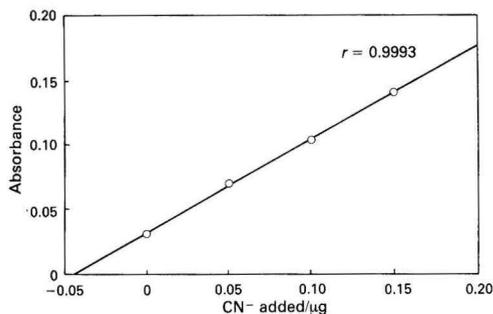
Fig. 3. Determination of total cyanide in a surface water sample using the standard additions method

Table 1. Effect of NaCl on the linear calibration equations for cyanide

NaCl/g l^{-1}	Regression equation	r
0	$A = 0.001 + 3.00[CN^-]$*	0.999
1	$A = -0.001 + 2.94[CN^-]$	0.998
5	$A = -0.002 + 2.90[CN^-]$	0.999
10	$A = -0.002 + 2.79[CN^-]$	0.999

* CN^- concentration from 0 to 0.1 μg ml^{-1}.

shown in Fig. 1. To ensure complete release of cyanide from the hexacyanoferrate(II) salt, 10 min were selected as the irradiation period with the lamp used here. A similar time course study should be run with each lamp to ensure complete decomposition of the complexed cyanide.

The rate of re-formation of the complexed cyanide after stopping the UV irradiation was monitored for 30 min (Fig. 2). There was a 3% decline in the absorbance reading after 5 min and a 12% decline after 30 min. This suggests that the analysis should be initiated as soon as possible after the UV irradiation step.

Effect of NaCl on the Calibration Graph for Cyanide

A calibration graph for cyanide was prepared using distilled water spiked with 0, 1, 5 and 10 g l^{-1} of NaCl in order to investigate the effect of NaCl on the proposed method for the

determination of cyanide (Table 1). The concentration of NaCl used was selected to cover the concentrations of NaCl found in waters adjacent to road-salt storage facilities.[7] The slopes of the linear regression lines were 3.00, 2.94, 2.90 and 2.79 A μg^{-1} ml for 0, 1, 5 and 10 g l^{-1} of NaCl added, respectively. The decrease in the slope coefficient with increasing NaCl concentrations indicates that NaCl interferes with the spectrophotometric procedure.

Standard Additions Procedure

The evidence for interference from background levels of NaCl prompted investigation of the use of the standard additions method for the determination of cyanide. In addition to the various levels of NaCl found in salt-affected surface waters, the colour of the samples also varies with the degree of dissolved organic carbon. The use of standard additions compensated for the interference found in surface water samples caused by high background NaCl levels and colour. Fig. 3 shows absorbance values for the analysis of a bog water using the method of standard additions. The linear regression line had a correlation coefficient (r) of 0.9993, indicating that a linear relationship existed between absorbance and concentration.

Conclusion

Surface waters can be affected by the run-off from road salt which often contains sodium hexacyanoferrate(II) as an anti-caking agent. The total cyanide concentration in these samples can be determined spectrophotometrically after decomposition of the complexed cyanide to free cyanide by exposure to UV light. The interference from high background levels of NaCl and colour can be avoided by the use of the standard additions method with the spectrophotometric analysis.

References

1. Tyler, D. R., *J. Chem. Educ.*, 1985, **62**, 1016.
2. "Merck Index," Ninth Edition, Merck, Rahway, New York, 1976, p. 1113.
3. Doudoroff, P., "Toxicity to Fish of Cyanides and Related Compounds. A Review," EPA 600/3-76-038, US Environmental Protection Agency, Duluth, MN, 1976.
4. Sekerka, I., and Lechner, J. F., *Water Res.*, 1976, **10**, 479.
5. Goulden, P. D., Afghan, B. K., and Brooksbank, P., *Anal. Chem.*, 1972, **44**, 1845.
6. Lambert, J. L., Ramasamy, J., and Paukstelis, J. V., *Anal. Chem.*, 1975, **47**, 916.
7. Hsu, M. T., Maine Department of Transportation Technical Paper 84-4, Bureau of Highways, Materials and Research Division, Maine, 1984.

Performance of the AMEL 430 Automated Polarographic Stand - Static Sessile Mercury Drop Electrode Apparatus at High Negative Potentials

Romano Andruzzi
Dipartimento di Chimica e Ingegneria Chimica dei Materiali, Università dell'Aquila, Via Sergi 4, 67100 L'Aquila, Italy

Lucio Cizza
AMEL, Instruments for Electrochemistry, Via Bolzano 30, 20127 Milan, Italy

Giancarlo Marrosu and Antonio Trazza*
Dipartimento di Ingegneria Chimica, Università "La Sapienza," Via del Castro Laurenziano 7, 00161 Rome, Italy

The performance of the AMEL 430 automated polarographic stand using static sessile mercury drop electrodes for various electrochemical techniques has been studied. N,N-Dimethylpyrrolidinium iodide [$E_{\frac{1}{2}} = -2.7$ V (SCE)] and p-methoxybenzaldehyde azine [$E_{\frac{1}{2}} = -2.0$ and -2.6 V (SCE)] were used as substrates with dimethylformamide as the solvent and tetrabutylammonium tetrafluoroborate (or iodide) as the electrolyte. The results obtained suggest that the AMEL 430 automated polarographic stand - static sessile mercury drop electrode device is particularly useful in situations where other commercial static hanging mercury drop electrodes fail to perform, for example, at high negative potentials or in the study of cathodic surface disrupting substrates.

Keywords: *Static sessile mercury drop electrode; polarography*

In 1978 EG & G Princeton Applied Research (PAR) developed a new type of mercury electrode: the static mercury drop electrode. This electrochemical device was the first to permit both hanging mercury drop and dropping mercury techniques with a single electrode assembly. Because the mercury drop is dispensed electromechanically, current-sampling operations such as those with differential-pulse polarography are performed on a renewable mercury electrode of constant surface area. Hence base-line distortions are reduced and the sensitivity is enhanced. However, neither the PAR model nor other commercial static mercury drop electrodes (Metrohm, Tacussel and more recently AMEL) perform at high negative potentials and/or in the study of mercury surface disrupting reactions.

As a long-lasting sessile mercury drop electrode was employed successfully in investigations of the electrochemical reduction of tetraalkylammonium cations,[1] which react with the cathode to form amalgams, and of the stripping analysis of natural and artificial matrices[2–5] it seemed possible that some of the difficulties encountered with the commercial static mercury electrodes could be eliminated by using a static sessile mercury drop electrode.

This paper describes the use of the AMEL 430 automated polarographic stand employing a static sessile mercury drop electrode for voltammetric studies of N,N-dimethylpyrrolidinium iodide, a reactant which disrupts the mercury surface,[6,7] and of p-methoxybenzaldehyde azine, which exhibits reduction steps at high negative potentials,[8] in dimethylformamide (DMF). The voltammetric curves obtained with static sessile mercury drop electrodes are shown to be highly reproducible even in situations where other static mercury electrodes fail to perform.

Experimental

N,N-Dimethylpyrrolidinium iodide and p-methoxybenzaldehyde azine were prepared as described previously.[6,8]

An AMEL 430 multi-polarograph analyser was used. The static sessile mercury drop electrode was prepared by drawing
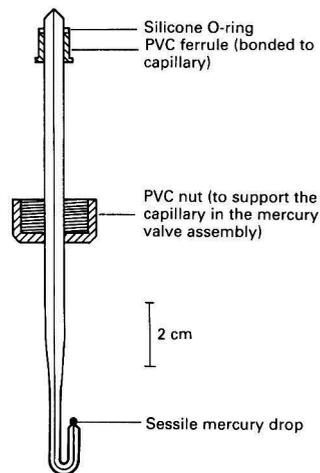
Fig. 1. Static sessile mercury drop electrode

a polarographic capillary and bending it in the shape of a hook (Fig. 1) as described previously.[2–5] The reference electrode was an aqueous SCE connected to the solution by a methylcellulose - DMF - tetrabutylammonium tetrafluoroborate NBu_4BF_4 [or iodide (NBu_4I)] bridge,[7] and all potentials are reported *versus* this electrode. A Pt wire served as the counter electrode.

Dimethylformamide (Merck, spectrophotometric grade) was purified[9] before use. Tetrabutylammonium tetrafluoroborate or iodide, as required, (Carlo Erba, RS grade for polarography) was vacuum-dried at 60 °C for 2 d and argon (99.99%) was used to de-oxygenate the solution. The solution was purified by elution through a column of molecular sieves (type 5A, Union Carbide - BDH) and then bubbled through a solution of the electrolyte prior to entering the polarographic cell.

---

* To whom correspondence should be addressed.
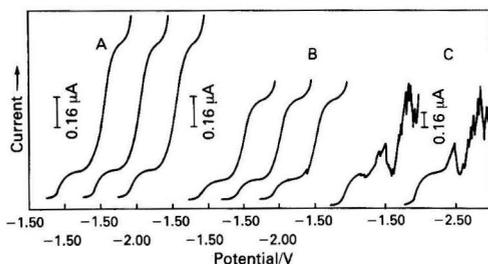
Fig. 2. Test polarograms of 6.1×10^{-4} M p-methoxybenzaldehyde azine in 0.1 M NBu$_4$I - DMF recorded using the AMEL 430 automated polarographic stand. A, Static sessile mercury drop electrode with drop time = 0.5 s and drop size 12; B, as A with drop time = 1.0 s; and C, static hanging mercury drop electrode with drop time = 1.0 s and drop size 5
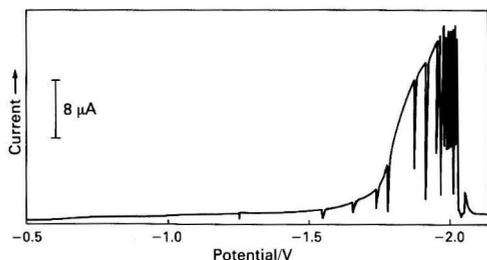
Fig. 3. Test polarogram of 6.0×10^{-4} M p-methoxybenzaldehyde azine in 0.1 M NBu$_4$I - DMF recorded using the PAR 174A polarographic analyser with the PAR 303 static mercury drop electrode. Drop size, small; sweep rate, 5 mV s^{-1}
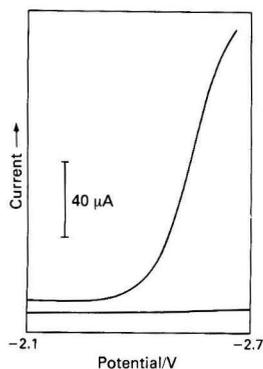
Fig. 4. Cyclic voltammogram of 2.8×10^{-3} M N,N-dimethylpyrrolidinium iodide in 0.1 M NBu$_4$BF$_4$ - DMF recorded using the PAR 174A polarographic analyser with the PAR 303 static mercury drop electrode. Drop size, small; sweep rate, 50 mV s^{-1}

In order to study the behaviour of the AMEL 430 analyser, voltammograms of the same compounds were recorded using both the AMEL 430 analyser and static sessile mercury drop electrode and the PAR 174A polarographic analyser equipped with a PAR 303 static hanging mercury drop electrode, an Ag - AgCl, KCl$_{std}$ reference electrode and a Pt wire counter electrode. The operating instructions of the PAR Model 303 electrode system were adhered to carefully and hence voltammograms were recorded soon after capillary cleaning.

Results and Discussion

The electroreduction of p-methoxybenzaldehyde azine and N,N-dimethylpyrrolidinium iodide was investigated using
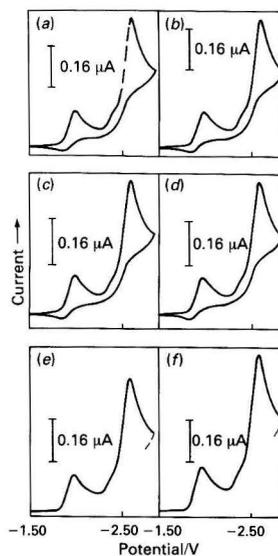
Fig. 5. (*a*)–(*d*) Cyclic and (*e*) and (*f*) cathodic voltammograms of 6.1×10^{-4} M p-methoxybenzaldehyde azine in 0.1 M NBu$_4$I - DMF recorded using the AMEL 430 automated polarographic stand with the static sessile mercury drop electrode. (*a*) Single scan, drop size 12; (*b*) five consecutive scans, drop size 12; (*c*) and (*d*) nine consecutive scans, drop size 12; (*e*) six consecutive scans, drop size 12; and (*f*) six consecutive scans, drop size 24. Sweep rate, 200 mV s^{-1}
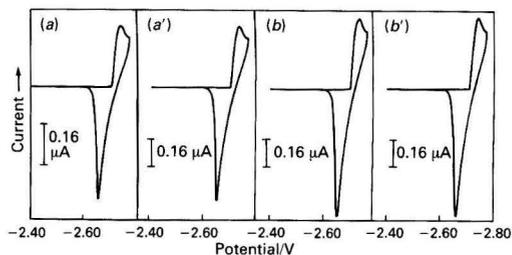
Fig. 6. Cyclic voltammograms of 1.5×10^{-3} M N,N-dimethyl-pyrrolidinium iodide in 0.1 M NBu$_4$BF$_4$ - DMF recorded using the AMEL 430 automated polarographic stand with a static sessile mercury drop electrode. Single scan; sweep rate, 50 mV s^{-1}. Drop size: (*a*) and (*a'*) 10; (*b*) and (*b'*) 20

various electrochemical techniques. Measurements obtained using static sessile mercury drop electrodes and other static mercury electrodes were compared.

Polarographic Techniques

Normal polarographic measurements with a static hanging mercury drop electrode (both AMEL 430 and PAR 303) could not be performed for either p-methoxybenzaldehyde azine or N,N-dimethylpyrrolidinium iodide. Indeed, with both substrates, the loss of drops was significant and mercury streamed off the capillary during recording of measurements; hence no reproducible currents could be recorded (Fig. 2, C and Fig. 3 for the AMEL 430 and PAR 303 systems, respectively). However, by using static sessile mercury drop electrodes these complications were overcome and highly reproducible, simple polarograms were obtained (Fig. 2, A). A similar improvement was observed in the differential-pulse polarogram when the static sessile mercury drop electrode was used in place of the static hanging mercury drop electrode.

Cyclic Voltammetry

Cyclic voltammetric measurements of *p*-methoxybenz-aldehyde azine or *N,N*-dimethylpyrrolidinium iodide using a static hanging mercury drop electrode (both AMEL 430 and PAR 303) were unreliable. The mercury drop fell off during the cathodic part of the measurement and an anodic peak could not be detected (Fig. 4). The use of a static sessile mercury drop electrode yielded highly reproducible and sharp peaks for both *p*-methoxybenzaldehyde azine (Fig. 5) and *N,N*-dimethylpyrrolidinium iodide (Fig. 6).

Conclusions

The experimental results reported here, together with those obtained with other sessile mercury drop electrodes or other polarographic techniques, suggest that the AMEL 430 automated polarographic stand employing a static sessile mercury drop electrode is particularly useful in situations where other static hanging mercury drop electrodes fail to perform, for example, at high negative potentials or in the study of surface disrupting substrates.

References

1. Andruzzi, R., Marrosu, G., Trazza, A., and Kariv-Miller, E., *Electrochim. Acta*, 1986, **31**, 163.
2. Andruzzi, R., Trazza, A., and Marrosu, G., *Talanta*, 1982, **29**, 751.
3. Andruzzi, R., Trazza, A., and Marrosu, G., *Anal. Lett.*, 1982, **15**, 1565.
4. Andruzzi, R., Trazza, A., and Marrosu, G., *Ann. Chim. (Rome)*, 1983, **73**, 321.
5. Andruzzi, R., Trazza, A., and Marrosu, G., *Anal. Lett.*, 1983, **16**, 853.
6. Kariv-Miller, E., Nanjundiah, C., Eaton, J., and Swenson, K. E., *J. Electroanal. Chem.*, 1984, **167**, 141.
7. Kariv-Miller, E., and Andruzzi, R., *J. Electroanal. Chem.*, 1985, **187**, 175.
8. Kitaev, Yu. P., Ivanova, V. Kh., Savin, V. I., and Trifonova, L. I., *Izv. Akad. Nauk SSSR, Ser. Khim.*, 1972, **10**, 2179.
9. Trazza, A., Andruzzi, R., and Carelli, I., *Electrochim. Acta*, 1982, **27**, 347.

BOOK REVIEWS

The Kinetics of Environmental Aquatic Photochemistry: Theory and Practice

Asa Leifer. *ACS Professional Reference Book Series.* Pp. xxx + 304. American Chemical Society. 1988. Price $59.95 (USA and Canada); $71.95 (Export). ISBN 0 8412 1464 6.

This book is directed to the environmental scientist and covers the topic of its title. The kinetics are focused on the determination of photochemical rate coefficients and half-lives in aqueous media in sunlight. The book is tightly printed and its narrative parallels this tightness without sacrificing most details in mathematical derivations. Developments of the last decade are summarised in this monograph.

The book has a preface, an introduction, 15 chapters, three appendices, an epilogue, a list of generously defined symbols and a very good index. Three main parts provide the structural framework of the book: theoretical concepts, experimental procedures and direct and indirect photoreaction test methods. The direct and indirect test methods are presented in flow-chart fashion in the overview given as an introduction. Later in the book, these methods are discussed in detail and illustrated with calculations for relevant examples. These examples and calculations occupy three chapters (Chapters 8, 11 and 15).

The theoretical treatment presents succinctly the transmission and absorption of light by aqueous solutions and the basic laws of photochemical efficiency (*e.g.*, Grotthus - Draper and Stark - Einstein laws). An equally succinct presentation of kinetic aspects in photochemistry follows. These presentations, in Chapter 1, serve as an introduction to a discussion of the absorption and transmission of solar radiation: (*a*) in the atmosphere (Chapter 2) and (*b*) in a body of natural water (Chapter 3). Chapter 4 is dedicated to rates of reaction and half-lives in natural water bodies in the environment. The theoretical aspects (covered in 90 pages) close with Chapter 5, which presents a generalised model of the kinetics of photochemical reactions in aquatic media. Instrumental parameters and physico-chemical interactions limiting the practicability of theoretical concepts are, however, not discussed. Their presentation would have added to the usefulness of the book.

The rest of the book, oriented to practical aspects, is a systematic and well organised account that takes the reader through (*a*) direct photoreaction screening tests (Chapters 6–8), (*b*) the determination of photoreaction quantum yields in aqueous solutions and sunlight photoreaction rates (Chapters 9–11) and (*c*) indirect photoreactions in humic waters (Chapters 12–15).

The readers for whom this book was written (environmental scientists and engineers) will appreciate the compactness of this volume, in which verbosity has been avoided. The book can be recommended to those for whom it is designed as it fulfills the task of a "Professional Reference Book."

Horacio A. Mottola

Crystal Chemistry and Refractivity

Howard W. Jaffe. Pp. x + 335. Cambridge University Press. 1989. Price $75 (hardback). ISBN 0 521 25505 8.

This is an important new book and essential reading for research workers and their graduate students who specialise, or would aspire to specialise in the structure, crystal chemistry and refractivity of minerals. Howard Jaffe of the University of

Massachusetts at Amherst has based his style of presentation in the text on over 40 years experience of teaching advanced mineralogy and crystal chemistry to first year graduate students who did not necessarily have the appropriate background in chemistry, physics, mathematics and elementary crystallography. Accordingly, the book is divided into two sections.

Part One (146 pages) covers the principles of crystal chemistry and refractivity and is sub-divided into 11 chapters covering the atomic and electronic structure of the elements, chemical bonding (covalent and ionic, as relevant to crystal chemistry), Pauling's rule of valency, crystal symmetry, crystal-field theory and structure, packing and distortion of crystalline materials, refractivity and polarisability.

Part Two (179 pages) has the title "Descriptive crystal chemistry" and is sub-divided into nine chapters. Chapter 12 reviews the classification and formulation of silicates and is followed by 8 chapters that detail the crystal chemistry of about 60 representative mineral types. Chapters 13–16 consider the crystal chemistry of the various categories of silicate minerals. Chapter 17 deals with borate minerals; Chapter 18, oxide and some fluoride minerals; Chapter 19, complex anions (sulphates, tungstates, phosphates, carbonates and fluorocarbonates) and the final Chapter 20, with sulphides, arsenides and related compounds. References to cited papers are included at the end of each chapter. The subject index is supplemented by a useful mineral index with over 250 entries. A notable feature of each chapter is the inclusion of both clear diagrams and photographs of atomic (ball or packing) models to elucidate mineral structures.

The importance of this book is clearly the way in which the basic principles (chemistry, physics and mathematical crystallography) are combined and integrated to give an authoritative introduction to the crystal chemistry of minerals. In developing this text, the author has successfully used a light and interesting style to describe what could otherwise become a somewhat esoteric subject. Hence the concept of crystal packing is related to the results of shaking a crate full of oranges and we are reminded that 50–75% of all known mineral species have either been found only once or have been found at only one locality.

This is a very readable book and highly recommended for those wisihing to specialise in the crystal chemistry of minerals.

P. J. Potts

Risk Assessment of Chemicals in the Environment

Edited by M. L. Richardson. Pp. ix + 579. Royal Society of Chemistry. 1988. Price £59.50. ISBN 0 85186 1180.

During the time I was reviewing this book, the daily newspapers were carrying stories such as the risks from pesticide residues in baby foods, the threat of a marine ecological disaster from the loss of a container of lindane at sea, problems of water quality and the risks to the "ozone layer" from chlorofluorocarbons. Such stories and the way they are presented have an important influence on public perceptions of chemicals and the risks associated with their use. As pointed out in the epilogue to the book, good evidence is essential to balance the distortions often made by the media, where there seems to be an insatiable appetite for disasters.

The aim of the book is to review the current status of risk assessment, a topic that has developed over many years to the extent that various approaches are now available. In addressing this aim, the contents of the book relate to the proceedings of the 3rd European Conference organised by the Royal Society of Chemistry on behalf of the Federation of European Chemical Societies' Working Party on chemicals in the

environment. The worldwide participation in the conference is reflected in the authorship of the chapters of the book, which relate to a diverse range of experiences from different countries.

In the many interesting and varied chapters will be found procedures appropriate to disasters such as that in Bhopal and to problems such as solvent abuse. Evidence will be found on decision making in the control of air pollution posing health risks, and an outline of a general selection procedure for identifying priority aqueous pollutants among the 100 000 chemicals in the European market. One chapter on the fate of chemicals, with particular reference to pesticides, points out that it is impossible to foresee all the potential hazards—a particularly apt comment in view of the recent loss of pesticide containers at sea!

It would be unfair to select merely a few of the topics covered in this worthwhile book, which provides a valuable introduction and overview to the many areas of risk from chemicals. The thirty chapters are divided into four sections of which the first gives a general overview. Technical and social issues including public awareness are raised, while the cultural and political conditioning of different approaches in different countries are considered. Other chapters take a global approach with contributions to international harmonisation, together with international efforts for preventing or mitigating injury from chemical disasters.

The second group of chapters consider toxicological approaches, including epidemiological- and physiological-based pharmacokinetic approaches, and also alternative procedures to traditional studies. The third section is concerned with incidental emissions to air and water, and includes issues such as modelling acid rain risks, international river pollution, radon and environmental impact analysis. The final section of the book considers practical issues of intentional emissions relating to substances such as pesticides, fine chemicals and pharmaceuticals. The book concludes with a useful glossary and list of addresses of organisations.

Most chapters are well referenced and provide useful introductions to the respective areas, although the value of two chapters, each of slightly over two pages in length, is not immediately apparent. This criticism apart, the book is a worthwhile compilation in which I have found useful information and from which I have gained pleasure in reading.

R. S. Barratt

Electron Capture Negative Ion Mass Spectra of Environmental Contaminants and Related Compounds
Elizabeth A. Stemmler and Ronald A. Hites. Pp. xvii + 390. VCH. 1988. Price DM128; £45. ISBN 0 89573 708 6 (VCH Publishers); 3 527 26904 5 (VCH Verlagsgesellschaft).

This book contains an interesting collection of negative ion mass spectra obtained with a quadrupole mass spectrometer operated in a quasi-chemical ionisation mode with methane as the reactant gas. The book consists of a short two and a half page preface, 361 pages upon each of which are graphic representations of the compound structure and the spectra obtained by the technique with the ion source at both 100 or 250 °C and 37 pages of indexes—compound name, molecular weight, spectral peaks at 100 °C and spectral peaks at 250 °C. Proof reading could have been more careful.

The title chosen for the book is discussed in the preface and is perhaps misleading as many of the spectra are not what might be expected from a simple "soft" electron capture mechanism. This is unfortunate, especially as the same authors have published papers, to which no reference is made in this book, using the terminology "methane enhanced negative ion mass spectra," which seems to fit the technique

used better. The title is also a little all-embracing as some well known environmental contaminants, such as 2,3,7,8-tetra-chlorodioxin are not included whereas other chlorinated dioxins are. What is the usefulness of the ECNIMS technique, when is it the preferred technique, is it more specific, what are the approximate molar sensitivities, etc? None of these points are discussed.

The presentation of the spectra is not uniform—some have identities assigned to peaks, others do not. Some of the assignments are wrong, *e.g.* that on page 89, where $(M-Cl)$ should be $(M-H)$. The mass axes for the 100 and 250 °C spectra differ on some pages, which is initially confusing. The format of page 40 differs from all of the other spectra pages. There is no attempt to propose mechanisms for the production of observed peaks, especially where there are peaks of higher mass, *e.g.* $M + 13$, which must be due to some ion - molecule reaction and not simple electron capture. Some halogenated aliphatic compounds produce "molecular ions," others just ions of the halogen—why? There are other interesting "anomalies" which go unexplained, for example 2-nitrobenzoic acid, methyl ester gives predominantly the molecular ion whereas the isomeric compound, 2-nitrophenol, acetyl derivative gives predominantly a peak at 59. With the corresponding 3-nitro compounds both the ester and the acetyl derivatives give the molecular ions. This lack of explanation, and lack of reference to previously published work, seriously undermines the value of the spectra presented and in fact one wonders if exactly the same technique has really been used for all of them.

Despite the deficiencies of presentation, this book could be a foundation data-base where this technique is found to have real advantages over other techniques for environmental monitoring.

D. F. Lee

Developments in Solvent Extraction
Edited by S. Alegret. *Ellis Horwood Series in Analytical Chemistry.* Pp. 221. Ellis Horwood. 1988. Price £30. ISBN 0 7458 0303 2.

This book, based on a school of solvent extraction held in Barcelona, edited by a Spanish analytical chemist and with contributions from two others, reflects the significant and increasing Spanish contribution to analytical chemistry in recent years.

Although the book is one of an analytical chemistry series, its scope extends far beyond the accepted definition of that subject. Solvent extraction itself is one of the most versatile chemical processes and its development has proceeded on a broad front with cross-fertilisation between applications ranging from micro to macro.

In the book's final chapter, which is both factual and readable, the valid claim is made that industrial use of solvent extraction was pioneered in the nuclear industry. It is fair to say that this industry was also responsible for the rapid growth of solvent extraction methods in analytical chemistry.

Of the twelve chapters, five are concerned with fundamentals such as thermodynamic aspects (Chapters 2 and 10). Chapter 3 describes the use of solvent extraction to study the kinetics of metal - chelate formation by means of a novel flow-through spectrophotometric detector which measures rates of transfer of solute. Speciation of solutes, especially amines, in a variety of two-phase systems is discussed in Chapters 4 and 5, with the emphasis on the computerised fitting of curves, derived from model systems, to experimental data.

Chapters 1 and 7 are of direct interest to the analyst, the latter particularly so, with a treatment of recent important

developments in flow analysis (continuous extraction, flow injection and high-performance liquid chromatography).

In a rather sparse chapter on industrial liquid-extraction equipment, centrifugal contactors are mentioned but not described. Two further chapters are concerned with industrial applications. In Chapter 8, a few reagents for extractive metallurgy are described and the question is asked "Are any more reagents needed or should the existing ones be consolidated?" Chapter 11 is an account of industrial applications to the separation and purification of non-ferrous metals and includes the speculation that supported liquid membranes might be used for these purposes. The theory of such membranes is outlined in Chapter 9.

The choice of topics is rather haphazard; hence the book resembles the proceedings of a conference as opposed to a structured work. Nevertheless, an overview of modern developments in solvent extraction is achieved. The generally high standard of the chapters concerned with analytical chemistry, and the analytical implications elsewhere in the book, justify its recommendation to analysts and others working in the field of solvent extraction.

There are some typographical and textual errors, *e.g.* "ligand - ligand extraction" (p. 141), Figures 5.2 and 5.3 where a caption should be transposed and Figure 7.6 where a caption is wrong.

The price is reasonable.

C. G. Taylor

Carbon-13 NMR Spectroscopy
H.-O. Kalinowski, S. Berger and S. Braun. Pp. 776. Wiley. 1988. Price £75. ISBN 0 4719 1306 5.

Carbon-13 NMR spectroscopy is a well established technique for structural and stereochemical analysis in solution. There is an extensive literature on the technique and its applications, and a number of standard texts exist. This book makes a welcome addition to the latter.

The book follows the general format of standard texts, covering the theoretical principles before discussing experimental methods, then correlations of NMR parameters with structure and moving on to include relaxation effects, dynamic NMR methods and a small number of applications. The experimental methods discussed include the traditional assignment methods as expected, with a much needed discussion of more advanced methods including polarisation transfer and two-dimensional methods. Some mention is also made of computational enhancement methods. The majority of the book is given to a very full discussion of chemical shifts in organic compounds with a good range of assigned structures. Coupling to hydrogen and a selection of other elements

is covered. I was pleased to see an introductory mention of carbon-13 NMR in solids, including some spectra of solid polymers. Each chapter has an extensive bibliography, and the subject index, glossary of acronyms and compound index are extensive.

This book is an up to date general reference text of a high standard. As such, it can be recommended without reservation.

S. Ellison

Two-Dimensional NMR Spectroscopy. Applications for Chemists and Biochemists
Edited by W. R. Croasmun and R. M. K. Carlson. Pp. 490. VCH. 1987. Price $104.50; DM210. ISBN 3 527 26528 7.

Two-dimensional NMR (2D-NMR) methods show NMR signal intensity as a function of two independent frequency variables, rather than a single frequency axis. The practical advantages arise both from increased signal dispersion, that is, spreading signals over a two-dimensional area rather than in a line, and from access to information which is difficult to obtain by single-dimensional methods. The difficulty facing the practicing chemist or biochemist is that 2D-NMR methods have proliferated to a remarkable extent, with the consequence that it is both difficult to choose the method best suited to the problem in hand and, once chosen, to set critical parameters for optimum results. This book appears to be aimed towards assisting the chemist or biochemist.

The book consists of nine separate sections, the first three forming an introduction to 2D-NMR methods and experimental aspects, the remainder being a discussion of applications of 2D-NMR methods to particular fields in chemistry and biochemistry, including one section on biological and geochemical applications. Each section is well written and gives very complete details of many useful methods. Indeed, the detail given often goes well beyond the requirements of most 2D-NMR users; most chemists and biochemists need only optimise a small number of parameters relating to a particular pulse sequence, whereas this book tells them how to write the whole sequence. The approach taken has also resulted in a good deal of repetition of information on the more frequently used methods from one section to the next; on the other hand, one need not look beyond, for example, the Cyclosporin chapter to find details of the pulse sequences used in this instance.

Overall, the book gives a broad and detailed description of 2D-NMR methods in several fields, and will be of interest to any NMR spectroscopist considering new areas of application.

S. Ellison

CUMULATIVE AUTHOR INDEX

JANUARY–JULY 1989

ROYAL SOCIETY OF CHEMISTRY

NUCLEAR MAGNETIC RESONANCE

Volume 17

Senior Reporter: G. A. Webb, *University of Surrey*

Nuclear Magnetic Resonance Volume 17 provides a review of the literature published between June 1986 and May 1987.

Brief Contents:
N.M.R. Books and Reviews; Theoretical and Physical Aspects of Nuclear Shielding; Applications of Nuclear Shielding; Theoretical Aspects of Spin-Spin Couplings; Nuclear Spin Relaxation in Liquids; Solid State N.M.R.; Multiple Pulse N.M.R.; Natural Macromolecules; Synthetic Macromolecules; Conformational Analysis; Nuclear Magnetic Resonance of Living Systems; Oriented Molecules; Heterogeneous Systems.

Nuclear Magnetic Resonance Volume 17 contains a foreword by the Senior Reporter, and a detailed contents list. Each chapter includes extensive references.

ISBN 0 85186 402 3
Hardcover 546 pages

Specialist Periodical Report (1988)
Price £110.00 ($220.00)

PHOTOCHEMISTRY

Volume 19

Senior Reporters: D. Bryce-Smith and A. Gilbert, *University of Reading*

Photochemistry Volume 19 provides a review of the literature published between July 1986 and June 1987.

Brief Contents:
Part I Physical Aspects of Photochemistry: Photophysical Processes in Condensed Phases.
Part II Photochemistry of Inorganic and Organometallic Compounds: The Photochemistry of Transition-metal Complexes; The Photochemistry of Transition-metal Organometallic Compounds; The Photochemistry of Compounds of the Main Group Elements.
Part III Organic Aspects of Photochemistry: Photolysis of Carbonyl Compounds; Enone Cycloadditions and Rearrangements: Photoreactions of Dienones and Quinones; Photochemistry of Alkenes, Alkynes and Related Compounds; Photochemistry of Aromatic Compounds; Photo-reduction and -oxidation; Photoreactions of Compounds containing Heteroatoms other than Oxygen; Photoelimination.
Part IV Polymer Photochemistry
Part V Photochemical Aspects of Solar Energy Conversion

Photochemistry Volume 19 has an author index and each chapter includes extensive references.

"All photochemists remain in the debt of the hard-working crew of scientists who generate these reviews and the production editors who maintain very high standards of presentation." *IAPS Newsletter, reviewing Volume 15.*

ISBN 0 85186 175 X
Hardcover 598 pages

Specialist Periodical Report (1988)
Price £110.00 ($220.00)

GENERAL AND SYNTHETIC METHODS

Volume 10

Senior Reporter: G. Pattenden, *University of Nottingham*

General and Synthetic Methods Volume 10 provides a critical and comprehensive summary and assessment of the literature published from January to December 1985.

Brief Contents:
Saturated and Unsaturated Hydrocarbons; Aldehydes and Ketones; Carboxylic Acids and Derivatives; Alcohols, Halogeno-Compounds and Ethers; Amines, Nitriles, and other Nitrogen-containing Functional Groups; Organometallics in Synthesis; Saturated Carbocyclic Ring Synthesis; Saturated Heterocyclic Ring Synthesis; Highlights in Total Synthesis of Natural Products; Reviews on General Synthetic Methods.

General and Synthetic Methods Volume 10 contains an introduction by the Senior Reporter and is indexed by author.

ISBN 0 85186 914 9
Hardcover 648 pages

Specialist Periodical Report (1988)
Price £125.00 ($250.00)

ROYAL
SOCIETY OF
CHEMISTRY

Information
Services

For further information,
please write to:
Royal Society of Chemistry,
Sales and Promotion department,
Thomas Graham House,
Science Park,
Milton Road,
Cambridge CB4 4WF. U.K.

To Order, please write to:
Royal Society of Chemistry, Distribution
Centre, Blackhorse Road, Letchworth,
Herts SG6 1HN. U.K.
or telephone (0462) 672555 quoting
your credit card details.
We can now accept Access/Visa/
MasterCard/Eurocard.

RSC Members are entitled to a
discount on most RSC publications and
should write to:
The Membership Manager,
Royal Society of Chemistry,
Thomas Graham House,
Science Park, Milton Road,
Cambridge CB4 4WF. U.K.

FOLD HERE

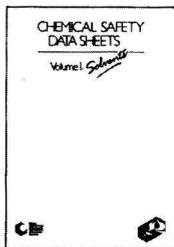# THE ANALYST READER ENQUIRY SERVICE

JULY'89

For further information about any of the products featured in the advertisements in this issue, please write the appropriate number in one of the boxes below.

Postage paid if posted in the British Isles but overseas readers must affix a stamp.

PLEASE USE BLOCK CAPITALS LEAVING A SPACE BETWEEN WORDS   *Valid 12 months*

1 NAME

2 COMPANY

PLEASE GIVE YOUR BUSINESS ADDRESS IF POSSIBLE. IF NOT, PLEASE TICK HERE

3 STREET

4 TOWN

5 COUNTY
POST CODE

6 COUNTRY

7 DEPARTMENT/
DIVISION

8 YOUR JOB TITLE
POSITION

9 TELEPHONE NO

OFFICE USE ONLY   REC'D   PROC'D

FOLD HERE

Postage will be paid by Licensee

Do not affix Postage Stamps if posted in Gt. Britain, Channel Islands, N. Ireland or the Isle of Man

2

BUSINESS REPLY SERVICE
Licence No. WD 106

Reader Enquiry Service
The Analyst
The Royal Society of Chemistry
Burlington House, Piccadilly
LONDON
W1E 6WF
England

ROYAL SOCIETY OF CHEMISTRY

CHEMICAL SAFETY DATA SHEETS
Volume 1 – Solvents

All solvents have hazardous properties, yet find ubiquitous use in industry and are among the most widely used chemicals in society.

This important new book aims to cover every aspect of the hazards of these solvents, providing invaluable information in a concise but readable format, with full references for further investigation if required.

Chemical Safety Data Sheets Volume 1 – Solvents provides up-to-date information on over 100 representative solvents. Included will be the full range of CHEMICAL, PHYSICAL AND BIOLOGICAL hazards likely to be encountered by their use, as well as safe handling, emergency precautions, safe disposal procedures and legislation governing their use regarding exposure, transportation and labelling, plus much more.

It provides a concise overview of the related hazards of compounds, in a uniform style and is fully indexed by chemical names, synonyms, class name, trade names and CAS Registry No., with a special 'flash point' index.

Brief Contents:
The data sheets are arranged in alphabetical order, and cover the following class headings: Glycols; Alcohols; Esters; Amines (including Nitro Compounds); Ethers; Chlorinated Hydrocarbons; Aromatic Hydrocarbons; Ketones.

ISBN 0 85186 903 3   **Published 1989**
Softcover 300 pages   **Price £39.95 ($89.00)**

Volume 2 is scheduled for publication mid 1989 and will be entitled *Main Group Metals and their Compounds*.

SOLVENTS IN COMMON USE: HEALTH RISKS TO WORKERS
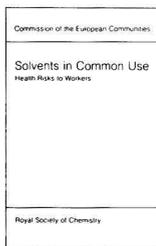
This key handbook contains essential information on ten of the most commonly used solvents and is a must for safety officers and all workers in the EEC at risk from exposure to these solvents.

The following information is given for every solvent covered: Chemical Abstracts name; synonyms and trade names; CAS Registry Number; NIOSH number; chemical and structural formulae; occurrence; spectroscopic data; measurement techniques; conditions under which the solvent is put on the market; storage, handling and use precautions; fire hazards; hazardous reactions; emergency measures in the case of accidental spillage; first aid; physio-chemical properties; toxicity; medical/health surveillance; occupational exposure limits.

The ten solvents covered are:
Acetone; Carbon Disulphide; Diethyl Ether; 1,4-Dioxane; Ethyl Acetate; Methanol; Nitrobenzene; Pyridine; Toluene; Xylene.

The information contained in this extremely useful book was compiled by an expert committee of the Royal Society of Chemistry for the Commission of European Communities.

ISBN 0 85186 088 5   **Published 1988**
Hardcover 308pp   **Price £60.00 ($120.00)**

For further information,
please write to:
Royal Society of Chemistry,
Sales and Promotion department,
Thomas Graham House,
Science Park,
Milton Road,
Cambridge CB4 4WF. U.K.

To Order, please write to:
Royal Society of Chemistry, Distribution Centre, Blackhorse Road, Letchworth, Herts SG6 1HN. U.K.
or telephone (0462) 672555 quoting your credit card details.
We can now accept Access/Visa/ MasterCard/Eurocard.

RSC Members are entitled to a discount on most RSC publications and should write to:
The Membership Manager,
Royal Society of Chemistry,
Thomas Graham House,
Science Park, Milton Road,
Cambridge CB4 4WF. U.K.

ROYAL
SOCIETY OF
CHEMISTRY

Information
Services

Circle 003 for further information

The Analyst

The Analytical Journal of The Royal Society of Chemistry

CONTENTS